CONCEPTUS AND UTERINE FACTORS CONTRIBUTING TO THE ESTABLISHMENT OF PREGNANCY IN PIGS

By

JASON WAYNE ROSS

Bachelor of Science in Animal Science
Iowa State University
Ames, Iowa
2000

Master of Science in Animal Science
Oklahoma State University
Stillwater, Oklahoma
2003

Submitted to the Faculty of the
Graduate College of the
Oklahoma State University
in partial fulfillment of
the requirements for
the Degree of
DOCTOR OF PHILOSOPHY
December, 2006

CONCEPTUS AND UTERINE FACTORS CONTRIBUTING

TO THE ESTABLISHMENT OF PREGNANCY IN PIGS

Dissertation Approved:

Rodney D. Geisert
Dissertation Adviser

Jerry R. Malayer

Patricia J. Ayoubi

Udaya E. DeSilva

A. Gordon Emslie
Dean of the Graduate College

ACKNOWLEDGEMENTS

The most important people in my life are those who have sacrificed the most for me to be able to complete this degree. To Rose Mary, you have been so patient and supportive during graduate school. You are the most important person to me. I could not have done it without you, thank you for being such a loving and caring wife and mother. Abbey, Jake and Gracie, I am more proud to be your Dad than anything else in the world. Thank you for loving me so unconditionally and bringing so much joy to my life. Thank you also to the rest of my family for encouragement and support and for believing in me.

Dr. Geisert, thank you for the opportunity to pursue this degree under your guidance and leadership. The freedom that you have allowed Morgan and myself to think independently and pursue questions in the lab over the past 5 years is not common practice but has been a key component to developing the abilities to be creative in research which will have significant impact on my future success. You have many qualities that I also want to exemplify throughout my career. Thank you for leadership by example. It has not always been just about science, as life is more than just people, it is also relationships. Thank you for your mentoring and friendship over the past six years.

Dr. Ayoubi, Dr. DeSilva, Dr. Malayer and Dr. Ritchey. Thank you all for your service on my PhD committee. You all have excellent qualities that I admire and think have contributed greatly to your successes. My interaction with you during my education at Oklahoma State University has been valuable at both a personal and scientific level. I have enjoyed the time that I have got to spend with you in both scientific and nonscientific settings. Thank you all for your service.

Morgan and Dan, you guys have made going to graduate school much more enjoyable than it could have ever been otherwise. Many of my memories of this era in my life will involve the three of us. Your friendships are far more valuable than the degree.

I would also like to express my gratefulness to God, who is above all. The past five years, through coursework and research, have given me the ability to recognize the intricacies of life that can never be fully comprehended have solidified my faith as a Christian. While I am far from perfect, I am forgiven, and that is the most important gift in life.

TABLE OF CONTENTS

LIST OF TABLES

LIST OF FIGURES

Figure Page

NOMENCLATURE

ACTN4	Actinin α4
AR	Aldose Reductase
ATP	Adenosine Triphosphate
BLAST	Basic Local Alignment Search Tool
CD24a	CD24 Antigen
cDNA	Complimentary Deoxyribonucleic Acid
CL	Corpora Lutea
CSF-1	Colony Stimulating Factor-1
CO	Corn Oil
C_T	Cycle Threshold
CXCL14	Chemokine Ligand 14
D12F	Day 12 Filamentous
D14F	Day 14 Filamentous
DAVID	Database for Annotation, Visualization and Integrated Discovery
dChip	DNA-Chip Analyzer
ddPCR	Differential Display Polymerase Chain Reaction
DNA	Deoxyribonucleic Acid
DTT	Dithiothreitol
EC	Estradiol Cypionate
ECM	Extracellular Matrix
EGF	Epidermal Growth Factor
EGFR	Epidermal Growth Factor Receptor
ELISA	Enzyme-Linked Immunosorbent Assay
EMSA	Electrophoretic Mobility Shift Assay
EPC	Ectoplacental Cone
ERα	Estrogen Receptor α
ERβ	Estrogen Receptor β
ERKO	Estrogen Receptor Knock Out
EST	Expressed Sequence Tag
EV	Estradiol Valerate
F-actin	Filamentous Actin
FDR	False Discovery Rate
FSH	Follicle Stimulating Hormone
GCOS	GeneChip Operating Software
GE	Glandular Epithelium
GnRH	Gonadotropin Releasing Hormone
GO	Gene Ontology
GPAP3.0	GenePix Auto Processor 3.0

HA	Hyaluronic Acid
HSP27	Heat Shock Protein 27
ICM	Inner Cell Mass
IFN-γ	Interferon-γ
IGF	Insulin-like Growth Factor
IGFBP	Insulin-like Growth Factor Binding Proteins
IL-1RAP	Interleukin-1 Receptor Accessory Protein
IL-1RT1	Interleukin-1 Receptor Type 1
IL-1β	Interleukin-1β
IL-6	Interleukin-6
ITI	Inter-α-trypsin Inhibitor
IκBs	Inhibitors of Nuclear Factor κB
IκBβ	Inhibitor of κBβ
JAK-STAT	Janus Kinase- Signal Transducer and Activator of Transcription
LE	Luminal Epithelium
LH	Luteinizing Hormone
LIF	Leukaemia Inhibitory Factor
LPS	Lipopolysaccharide
MBEI	Model-Based Expression Indices
mRNA	Messenger Ribonucleic Acid
NADPH	Nicotinamide Adenine Dinucleotide Phosphate
NBA	Number Born Alive
NFκB	Nuclear Factor κB
NK	Natural-Killer
NMB	Neuromedin B
NMB-R	Neuromedin B Receptor
OD	Optical Density
P45017α	P45017α-hydroxylase
P450arom	Aromatase
PCOS	Polycystic Ovarian Syndrome
PCR	Polymerase Chain Reaction
PG	Prostaglandin
PGE	Prostaglandin E
PGF	Prostaglandin F
$PGF_2\alpha$	Prostaglandin $F_2\alpha$
PLA2	Phospholipase A2
PLAZ	Phospholipase AZ
PM	Perfect-Match
PR	Progesterone Receptor
PTGS1	Prostaglandin Synthetase-1 (also referred to as cyclooxygenase-1)
PTGS2	Prostaglandin Synthetase-2 (also referred to as cyclooxygenase-2)
PTHrP	Parathyroid Hormone Like Hormone
QT-RT-PCR	Quantitative Reverse-Transcriptase Polymerase Chain Reaction
RANK	Receptor Activator of NFκB
RANKL	Receptor Activator of NFκB Ligand
RAR	Retinoic Acid Receptors

RBP	Retinol Binding Protein
RNA	Ribonucleic Acid
rRNA	Ribosomal Ribonucleic Acid
RT-PCR	Reverse Transcriptase Polymerase Chain Reaction
SAGE	Serial Analysis of Gene Expression
SPP1	Secreted Phosphoprotein 1
sqPCR	Semi-quantitative Polymerase Chain Reaction
ST	Stromal Cells
STAR	Steroidogenic Acute Regulatory Protein
STAT	Signal Transducer and Activator of Transcription
TGC	Trophoblast Giant Cells
TGFα	Transforming Growth Factor-Alpha
TGFβ	Transforming Growth Factor-Beta
TH	T-Helper
TLR-4	Toll-like Receptor-4
TNF-α	Tumor Necrosis Factor α
TSG6	Tumor Necrosis Factor Stimulated Gene 6
UG	Uterine Glycocalyx

Chapter I

Introduction

The average pig ovulates 16-18 oocytes per estrus, of which the majority are fertilized and initiate development. However, reproductive efficacy in the swine industry is limited by a prenatal mortality rate ranging from 20-46% [Pope et al., 1990]. According to the National Agriculture Statistics Service (http://www.nass.usda.gov/) the current breeding inventory in the United States is 6.06 million sows, suggesting that even a slight increase in survivability during *in utero* development would make a dramatic impact on the production capability of the swine industry in the United States.

It is not uncommon to have females that can consistently give birth to above average litter sizes and provide ample milk production to wean litters significantly larger than other sows. Unfortunately, the genetic parameters that regulate this unique ability of only a few females is not known. It is likely that numerous factors, both genetic and environmental, impact the variability between the reproductive prolificacy of female pigs making the objective of obtaining a predictable, substantial increase in littersize difficult to obtain. Biologically speaking, multiple mammalian species contain the propensity to regulate their reproductive success with consistent progeny per pregnancy despite other reproductive limitations or superfluities. For example, following fertilization and the formation of a single blastocyst, and an approximate 14-week arrest in development, the nine-banded armadillo (*Dasypus novemcinctus*) consistently gives birth to genetically

identical quadruplets [Enders, 2002]. This occurs by the ability of the inner cell mass within the blastocoele to divide into four separate areas, each giving rise to a single individual while all four utilizing the same placenta [Enders, 2002]. By contrast, different species of elephant shrews exhibit a distinct ability to regulate the quantity of embryos developing *in utero* despite differences in ovulation rate. While some species (E. *rozeti*) consistently ovulate on average 1.2 follicles per ovary and others (E. *edwardi* and E. *myurus*) ovulate 44 – 49 oocyte per ovary, all three of these species appear to limit extended development to an average of only two embryos [Tripp, 1971]. Littersize among female pigs that are of similar lines of selection is still variable. However, the larger litter consistency of some females suggest that some endogenous mechanisms do exist that allow the control of producing consistently large litters.

The following review of literature will focus on the areas of early gestation which represent a significant amount of embryonic mortality, the potential mechanisms involved in those areas, and how disruptions within those mechanisms may lead to reduced littersize in production swine in the United States.

Chapter II

LITERATURE REVIEW

Porcine Estrous Cycle

Once the female pig attains puberty, typically 5-7 months of age, the estrous cycle remains unaffected by season and is halted by anestrous only during pregnancy or postpartum piglet suckling. The porcine estrous cycle is 21 days in length and consists of four distinct phases (proestrous, estrus, metestrus and diestrus) which are under precise regulation of the steroid hormones estrogen and progesterone. Proestrus (Days 17-20) is a result of corpora lutea (CL) regression concomitant with the selection and growth of a cohort of tertiary follicles. Together, the loss of the CL results in rapidly reduced plasma progesterone while estradiol-17β increases steadily as the growing follicles reach maturity and become Graafian follicles. Increasing plasma concentrations of estradiol-17β occur around Day 18 of the estrous cycle and the reduced negative feedback effect of estrogen on the basal medial nuclei of the hypothalamus allows the chronic release of gonadotropin releasing hormone (GnRH) into the hypophyseal portal system causing the pulsitile release of follicle stimulating hormone (FSH). Estrus is the result of mature Graafian follicles producing peak plasma concentrations (~ 45 pg/mL) of estradiol-17β. These elevated levels of circulating estrogen result in the behavior modification of the gilt or sow causing her to be receptive to the boar. This behavior is directly associated with estrus, which typically lasts from 48 to 72 hours in the pig with ovulation occurring

about 36 hours after the onset of estrus. Peak estadiol-17β levels result in positive feedback regulation on the pre-optic nuclei of the hypothalamus resulting in the surge release of luteinizing hormone (LH). The LH surge causes the luteinization of the theca interna and granulosa cells resulting in the degradation of the junctional complexes holding the granulosa cells together as well as the oocyte's resumption of meiosis and the expulsion of a polar body. Continued proteasomal degradation of the theca interna outward near the apex of the follicle results in the formation of a hole and the expulsion of the oocyte. The ovulation of 16-18 oocytes are representative of a follicular pool of as many as 85 tertiary follicles present on the surface of the ovary during the mid-luteal phase of the estrous cycle [Guthrie et al., 1995]. Metestrus lasts only a few days in pig and is characterized by declining plasma estrogen concentrations with the initiation of progesterone production by the conversion of the corpora hemorrhagica to corpora lutea (CL). Diestrus (Days 5-16) is the longest phase of the estrous cycle in the pig. High plasma progesterone concentrations maintain myometrial quiescence and induce endometrial glandular secretions (histotroph) providing an environment for initial conceptus development in the event that fertilization has occurred. The absence of viable conceptuses allows the uterine synthesis and endocrine release of prostaglandin $F_{2\alpha}$ ($PGF_{2\alpha}$) resulting in CL regression and reduction of plasma progesterone by Day 16 of the estrous cycle allowing the recruitment and maturation of the next group of developing tertiary follicles.

Factors Affecting Litter Size in Pigs

Prior to parturition there are four different factors that can affect litter size in pigs; 1) ovulation rate, 2) fertilization rate, 3) early embryonic survival, and 4) uterine capacity. Fertilization rate in the pig is extremely efficient, estimated to be at least 95% [Polge, 1978], suggesting that it is unlikely to be the limiting factor with respect to number of piglets born alive (NBA) at term. However, multiple attempts to increase litter size through superovulation have been unsuccessful (Longenecker and Day, 1968; Dziuk, 1968). While superovulation of gilts increases the number of CL, and thereby the number of viable conceptuses initiating development, the number of conceptuses developing past Day 40 of gestation was not different between superovulated gilts and non-superovulated gilts serviced naturally by a boar [Longenecker and Day, 1968]. The inability of superovulation to significantly impact litter size indicates the importance of early embryonic survival and uterine capacity on litter size at term in the pig. In 1923, Corner established that the number of corpora lutea present on the ovaries is an accurate estimate of ovulation rate and could be utilized to estimate embryonic mortality. Utilizing this method, embryonic mortality has been determined throughout multiple stages of gestation and several assessments of mortality during pregnancy in the pig suggest that the overall embryonic mortality rate is between 20 and 46% [Pope, 1994]. The occurrence of embryonic mortality can be broadly broken into two phases; the peri-implantation stage of development, Days 10-18 of gestation; and post-implantation development, between Day 18 and 114 of gestation.

Early Embryonic Mortality

Not only is early embryonic development critical for the establishment of subsequent placental size but this peri-implantation period (Days 10-18) is also vital for a variety of developmental landmarks that are indicative of conceptus viability and establishment of conceptus uterine cross-talk resulting in the adhesion of the conceptus trophectoderm to the uterine glycocalyx and the initial formation of a diffuse epitheliochorial placenta. Anderson et al. [1978] estimated that 17% of conceptuses are lost during Days 9-18 of gestation, the peri-implantation stage of development. Numerous factors contribute to the significant loss of viable conceptuses during this stage of development. Specifically, conceptus rapid trophoblastic elongation and successful implantation are the two major components of this developmental stage in the pig which represent processes where conceptus loss is recognized.

Incompatibility between the developing conceptus and the rapidly changing uterine environment can result is a major constraint to conceptus survival. Asynchrony greater than 24 h between potentially viable conceptuses and the uterine environment has been established to cause conceptus death as early as Day 8 of gestation [Polge, 1982; Geisert et al., 1991]. Conceptus-uterine asynchrony is less tolerant when the uterine environment is further advanced than conceptus development. Pope et al. [1990] demonstrated this when gestation Day 6 conceptuses transferred to a gestation Day 7 uteri exhibited greater mortality than Day 7 conceptuses transferred to a Day 6 uteri. Moreover, while both Day 5 and 7 conceptuses exhibit viability to at least day 60 when transferred to a gestation Day 6 uteri (24 h asynchrony), the older conceptuses exhibit greater viability when they are both transferred to the same uteri [Pope et al., 1990].

In addition to the developmental limitations caused by conceptus-uterine asynchrony, asynchrony between littermates may represent a significant amount of conceptus mortality realized during the peri-implantation period. Duration of ovulation in the pig requires an average of 1.8 h and ranges from 0.75 to 3.6 hs [Soede et al., 1992], although the authors found no correlation between embryonic diversity with respect to duration of ovulation. Contrary to this finding, Pope et al. [1988a] determined that destroying Day-1 non-ovulated follicles via cauterization resulted in a significant reduction in morphological diversity among pig conceptuses on Day 11 of gestation, with the difference being primarily a reduction of small spherical conceptuses (1-5 mm diameter). Because multiple assessments suggest the timing of ovulation occurs approximately 35-48 h after the onset of estrus behavior [Soede and Kemp, 1997], it seems plausible that insemination and capacitation would not be the limiting factor regarding variation in fertilization and initiation of development but rather would be more directly associated with the variation in ovulation, supporting the data provided by Pope et al. [1988a].

Variation in the duration of ovulation and the subsequent diversity associated with the embryonic morphology could be paramount with respect to the microenvironment asynchrony within the uterus as described by Pope [1988b]. Because of differences in the timing for initiation of trophoblastic elongation and the rapid rate of elongation (less than 2 hours) during the transition from spherical to filamentous morphology, variation in the duration of ovulation may be a very valid cause of multiple morphologies observed between conceptuses within a litter [Anderson et al., 1979]. Primarily, the variation within littermates with respect to the onset of elongation may be related to the lack of

uniform placental size which results in the lesser developed conceptuses acquiring insufficient uterine space for placentation. A secondary consequence of variable onset of trophoblast elongation within a litter may be the endometrial changes stimulated by estrogen release from the advanced conceptuses resulting in endometrial modifications that are difficult for less developed conceptuses to overcome. Administration of exogenous estradiol following progesterone priming results in specific alteration of uterine secretions [Basha et al., 1980; Geisert et al., 1982a]. Moreover, both conceptus aromatase expression and estrogen synthesis and release is directly related to morphological stage of development [Yelich et al., 1997a; Wilde and Pope, 1987]. This would suggest that while conceptuses equidistantly space themselves from one another prior to elongation, endometrial secretions induced by elongating, estradiol-17β secreting conceptuses may generate a uterine environment unsuitable for conceptuses lagging in development, or the additional uterine space acquired by the more advanced conceptuses limits available surface endometrium for placentation by conceptuses tardy in their initiation of conceptus elongation.

Uterine Capacity

Uterine capacity is defined as the maximum number of piglets carried to term when potentially viable conceptuses are not limiting [Christenson et al., 1987]. By applying ligatures to the uterine horn varying lengths (5 cm for each CL) from the uterotubal-junction, Wu et al., (1989) were able to show that a dramatic loss of viable conceptuses occurs between Days 20 and 50 of gestation when uterine space is limited, suggesting that pig conceptuses are vulnerable during uterine crowding. To more

specifically determine the effects of uterine crowding, Vallet and Christenson [1993] double ligated uterine horns ipsilateral to the ovary with the most CL midway between the uterine bifurcation and the utero-tubal junction producing both a crowded and roomy environment for the developing conceptuses. On both Days 25 and 35 of gestation, there was a significant affect of uterine space reducing both placental weight and fetal weight of the conceptuses developing in the crowded uterine environment compared to those developing in the roomy uterine environment. Agreeably, methods to reduce uterine space; unilateral hysterectomy and uterine ligature, and methods to increase embryo numbers; ovulation rate selection, superovulation, and embryo transfer all tend to indicate the capacity of the uterus becomes limiting around Day 40 of gestation [Vallet, 2000].

The Meishan breed of swine originating from China is well known for their reproductive prolificacy. While having similar uterine space and ovulation rate, the Chinese breed consistently produces over 3 pigs per litter more than the less prolific European swine breeds [Ford, 1997]. Ford speculated that this is due to the Meishan conceptuses ability to develop a smaller, more vascular placenta, enabling adequate downstream nutrient exchange while requiring less uterine space. This thought process resulted in the hypothesis that placental efficiency, used as a selection tool may have an impact on litter size in the European breeds. Placental efficiency (fetal weight/placental weight) is highly variable between littermates; however, after one generation of selection of individual littermates in a small research study, Wilson et al. [1999] reported a significant increase in litter size. In a larger study, utilizing swine from a commercial herd, Vonnahme et al. [2002] identified a positive correlation between ovulation rate and the number of viable conceptuses at Day 25 of gestation, however, this correlation was

not present at Days 36 or 44 of gestation. Alternatively, a significant correlation did exist between uterine length and the number of viable conceptuses at Days 36 and 44 but not at Day 25 suggesting that uterine capacity is defined between Days 25 and 36 of gestation. Additionally, placental efficiency was found to be significantly positively correlated to the number of viable conceptuses on Days 25, 36 and 44 [Vonnahme et al., 2002]. While these data support the work done by Wilson et al. [2001] up to Day 44 of gestation, an additional study on using in a much larger population suggested that placental efficiency has a negative correlation to littersize in pigs [Mesa et al., 2003]. It should not be overlooked however, that if placental efficiency truly contributes to increased litter size, these data further indicate the underlying importance of the initial establishment of placenta size which occurs on Day 12 of gestation during trophoblastic elongation.

Porcine Embryonic Development

Early Conceptus Development (first 30 days of gestation)

In 1929, after collecting porcine reproductive tracts from an abattoir, Heuser and Streeter described many of the morphological changes that occur during early porcine embryonic development. Following fertilization and the fusion of the male and female pronuclei to produce a single cell zygote, holoblastic cleavage occurs shortly after nuclear division. Because the holoblastic cleavage plane spans completely through the zygote; thus enabling cytokinesis, the process of equally dividing; each cleavage division results in a reduction of cell size. The initial two divisions occur early, allowing the porcine embryo to reach the 4-cell stage within 24 h following fertilization. Divisions occur less frequently after the 4-cell stage albeit still occurring approximately 24-26 h

until the embryos reach the 8-16 cell stage. Blastomeres from 4-cell stage porcine embryos readily take-up radiolabeled uridine and incorporate it into synthesized RNA suggesting the depletion of the maternal mRNA stored in the oocyte and the activation of the embryonic genome [Tomanek et al., 1989]. Morulation and subsequent blastulation occur by Day 6 following fertilization and the embryos, now migrating into the uterine horns, are defined by having a distinct outside trophectodermal cell layer and a rapidly growing inner cell mass within the blastocoele. Hatching from the zona pellucida on Day 7 to 8 of gestation allows the embryo to expand in diameter concurrent with trophoblast expansion and differentiation of the inner cell mass. By Day 10 of gestation, the conceptus reaches a spherical diameter of 2-3 mm. During their collection of porcine conceptuses, Heuser and Streeter [1929] reported distinct variation in conceptus morphologies present between Days 11 to 12 of gestation, and presented photographs of spherical, tubular and filamentous conceptuses. The morphological transition is followed by the initial attachment of the elongated trophectoderm to the uterine epithelium on Day 13 of gestation [Perry et al., 1981; Dantzer, 1985]. Formation of the extraembryonic membranes occurs after elongation as the allantois is formed, from the expanding embryonic hindgut by Day 14 of gestation and is as long as the expanded trophoblast chorion by Day 17 [Friess et al., 1980]. Allantois expansion continues reaching nearly full contact with the meter long chorion by Day 19 of gestation. By Day 30, allantoic blood vessels completely vascularize the chorion [Wislocky and Dempsy, 1946]. Essentially, Day 12 to 30 of gestation is a critical developmental period in which the conceptuses expand throughout the uterus and establish a nutrient exchange interface with the dam. The extent to which each individual conceptus placenta attains uterine

space for downstream nutrient exchange is directly regulated by the extent at which conceptus trophectoderm is allowed to elongate initially on Day 12 of gestation. In general, conceptuses with the most extensive trophoblastic elongation develop the largest placenta and acquire the greatest uterine surface contact resulting in the highest chance of survival to term; indicating the critical importance of gestational Days 10 to 12, when trophoblastic elongation is initiated.

Conceptus Trophoblastic Elongation

On approximately Day 10 of gestation, 2-3 mm spherical porcine conceptuses will grow in diameter at a rate of 1 mm/4 h through cellular hyperplasia [Geisert et al., 1982b]. The conceptuses continue to expand until they reach an approximate 9-10 mm diameter within 24-36 h [Geisert et al., 1982b; Pusateri et al., 1990]. Upon reaching 9-10 mm in diameter, the spherical conceptus initiates the process of rapid trophoblastic elongation usually between Days 11 to 12 of gestation [Geisert et al., 1982b]. This rapid trophoblastic elongation occurs at the rate of approximately 45 mm / h [Ross, Ashworth and Geisert; unpublished data] throughout the uterine lumen concomitantly with the synthesis and release of the conceptus maternal recognition signal, estrogen [Geisert et al., 1982b; Bazer et al., 1986] and the proinflammatory cytokine, interleukin-1β (IL-1β) [Ross et al., 2003a]. Trophoblastic elongation in the pig is characterized by a series of unique events and the transformation through transient morphological stages. Initially, a 10 mm spherical conceptus transforms into a transient ovoid shape (10-14 mm length), quickly becomes tubular (15-25 mm length), and then rapidly elongating until the conceptus becomes a thin filamentous thread that is 150-200 mm in length within 2 to 4

h. The transformation of the spherical to the elongating conceptus is not the result of cellular hyperplasia, but is rather a process of cellular migration causing trophectodermal migration [Geisert et al., 1982c; Mattson et al., 1990; Pusateri et al., 1990]. Trophoblastic elongation is likely to be very dependent on the uterine three dimensional architecture surrounding the conceptus as these unique morphological transformation events to date has not been accomplished *in vitro*. Perry [1981] likens the process of trophoblastic elongation to rolling a ball a plasticene between two hands, forcing the expansion of the ends while reducing the diameter of the trophectoderm. Mattson et al. [1990] later suggested that the rapid and ephemeral trophectoderm changes were a result of cytoskeletal rearrangements of filamentous actin (f-actin).

The process of trophoblastic elongation serves several fundamental roles. The primary role is that conceptus expansion within the length of the uterine horns allows individual porcine littermates the ability to garner sufficient uterine space for placentation to ensure adequate nutrient exchange throughout gestation [Stroband and Van der Lende, 1990; Geisert and Yelich, 1997]. Another essential role that trophoblastic elongation serves is the delivery of the maternal recognition signal, estrogen, throughout the uterine lumen resulting in the prevention of luteolysis. Evidence for the necessity of this mechanism to deliver the conceptus derived signaling molecules throughout the uterus relies on the demonstration that at least two viable conceptuses are required in each horn to sufficiently prevent luteolysis during the establishment of pregnancy [Polge et al., 1966; Dziuk, 1968].

How the induction of trophoblastic elongation is regulated is not well defined although it has been hypothesized to be either conceptus self regulation or regulated

through maternal signaling. Administration of exogenous progesterone in pregnant gilts on Days 2 and 3 of gestation resulted in an increase in both endometrial protein secretions and an increase in conceptus synthesis and secretion of estrogen on Day 11 of gestation [Vallet et al., 1998]. While this suggests that conceptus development rate can be affected by steroid hormones, the synchrony within littermates seems unaffected. Even though the synthesis and secretion of estrogen occurs simultaneous with trophoblastic elongation, it is unlikely that estrogen is involved with the induction of the morphological transformation. Morgan et al. [1987a] demonstrated that small spherical conceptuses in uteri stimulated with exogenous estrogen fail to commence trophoblastic elongation until they reach at least 10 mm in diameter, the size when normal induction occurs. Furthermore, it seems conceivable that if elongation is under the regulation of maternal sources, it would be synchronous between conceptuses. However, it is not uncommon for littermates that are spherical, tubular and filamentous to exist simultaneously within the same uteri [Anderson et al., 1978; Geisert et al., 1982b]. The presence of multiple morphologies within littermates suggests the maternal system is unable to stimulate uniformity during trophoblastic elongation and that this is rather a process regulated by the conceptuses themselves.

Interleukin-1 receptor type 1 (IL-1RT1) and IL-1 receptor accessory protein are both required for IL-1β signaling to occur. The expression of both receptors in the conceptus while IL-1β levels are elevated suggests that the secretion of IL-1β may have an autocrine effect on the conceptuses themselves [Ross et al., 2003a]. Ross et al. [2003a] also hypothesized that due to the potential autocrine signaling, conceptus synthesis and release of IL-1β may be a potential contributor to trophoblastic elongation.

Interleukin-1β is known to induce gene expression for both phospholipase A2 (PLA2) [Kol et al., 2002] and prostaglandin synthase-2 (PTGS2) [Huang et al., 1998] in reproductive tissues of various species. Activity of phospholipase A2 [Davis et al., 1983] and PTGS2 [Wilson et al., 2002] both increase in the Day 12 filamentous porcine conceptus initiating the subsequent increase of prostaglandin E in the uterine lumen. Phospholipase A2 enzyme activity is responsible for the cleavage and release of free arachidonic acid used in the synthesis of prostaglandins through prostaglandin synthase activity. The release of arachidonic acid from the phospholipid bilayer may contribute to the increased cell membrane fluidity necessary for trophectoderm remodeling [Davis and Blair, 1993; Geisert and Yelich, 1997].

Conceptus Apposition and Attachment to the Uterine Luminal Epithelium

Following trophoblastic elongation and secretion of the maternal recognition of pregnancy signal, estrogen, placental attachment to the uterine luminal epithelium occurs between Days 13 and 18 of gestation [Perry et al., 1981; Dantzer, 1985]. Underlying the importance of trophoblastic elongation as a means to acquire uterine space for placentation is that porcine conceptuses are very non-invasive *in vivo* and develop an epitheliochorial type of placenta [King et al., 1982; Keys and King, 1990], an inefficient transporter of nutrients compared to alternative placental types in other mammals. The pig is unique in that the formation of the diffuse, epitheliochorial placenta preserves the life of the uterine luminal epithelial cells and are not destroyed during placental invasion as in other species, but contribute to the apposition and attachment of the trophectoderm [Burghardt et al., 1997].

The attachment of the conceptus trophectoderm to the extracellular matrix in the uterus involves factors regulating tissue cohesion, cell migration and cell-cell communication. Similar to the formation of a cumulus oocyte complex, extracellular matrix formation and its stabilization is a result of the interactions between hyaluronic acid (HA), the members of the inter-α-trypsin inhibitor (ITI) protein family, CD44, and tumor necrosis factor stimulated gene 6 (TSG6) [Richards et al., 2002; Bost et al., 1998]. The detection of bikunin, the light chain of the ITI protein family, as well as ITI heavy chain 4 are expressed in uterine endometrium during the establishment of pregnancy [Hettinger et al., 2001; Geisert et al., 1998]. Collectively, ITI family members, hyaluronic acid, bikunin, CD44 and TSG6 can function to form an adhesion matrix on the surface of the uterine luminal epithelium as proposed by Ashworth [2005].

Other specific alterations in the uterine epithelium are required for the reorganization and remodeling of the extracellular matrix (ECM), expressing specific ligands and receptors necessary for uterine receptivity and conceptus attachment. Integrins are a family of cell transmembrane glycoproteins that are known to contribute to cell-cell communications and linkage [Hynes, 1992; Lessey, 1995] and are well established in their roles regulating conceptus attachment in the pig [see reviews Jaeger et al., 2001; Burghart et al., 1997]. Integrins consist of numerous α and β subunits, and when forming an αβ heterodimer, results in the formation of a membrane bound receptor whose ligand specificity is dependant on the subunits comprising the heterodimer. In the pig, at least five α (α_1, α_2, α_3, α_4, α_v) and three β (β_1, β_3, β_5) subunits exist in the uterine epithelium while three α (α_1, α_4, α_5) and 2 β (β_1, β_3) have been detected in the conceptus [Bowen et al., 1996]. During conceptus estrogen secretion and initial trophectoderm

attachment, the expression of α_4, α_5, and β_1 is elevated in the uterine endometrium, whereas the expression of α_v and β_3 are constitutive and α_1 and α_3 remain low [Bowen et al., 1996]. Bowen et al. [1996, 1997] further demonstrated that the elevation of α_4, α_5, and β_1 is regulated through progesterone. The potential integrin heterodimers capable of forming in either the pig conceptus, uterine epithelium, or both, include; $\alpha_4\beta_1$, $\alpha_5\beta_1$, $\alpha_v\beta_1$ and $\alpha_v\beta_3$, all of which are members of the fibronectin/vitronectin family of receptors [Bowen and Hunt, 2000]. Vitronectin has been demonstrated to be expressed by both the trophectoderm and the uterine luminal epithelium [Bowen et al., 1996] while fibronectin has been identified in the trophectoderm of conceptuses collected from Day 12 to 15 of gestation [Tou and Bazer, 1996a]. Other potential integrin heterodimer ligands include the transforming growth factor β latency-associated peptide and osteopontin [review, Jaeger et al., 2001]. Osteopontin, also referred to as secreted phosphoprotein 1 (SPP1), is expressed in the uterine luminal epithelium as early as Day 15 of gestation, with expression being much greater by Day 25 of gestation [Garlow et al., 2002]. White et al., [2005] have more recently demonstrated that luminal epithelial expression during early pregnancy is regulated by conceptus estrogen and the prolonged expression throughout late gestation in the uterine glandular epithelium is driven by progesterone.

While the ligand-receptor interaction between the conceptus trophectoderm and the uterine luminal epithelium are critical for attachment to occur, other factors, such as cell surface mucins can also impact trophectoderm adhesion to the luminal epithelium in the pig. The cell surface mucin, MUC-1 has been reported to be a likely regulator of uterine receptivity through its ability to prevent integrin binding between the trophectoderm and uterine epithelium [Surveyor et al., 1995]. With respect to expression

during the estrous cycle, MUC-1 has a similar expression pattern in the mouse [Braga and Gendler, 1993] and pig [Bowen et al., 1996]. Ovarian hormones are likely the key regulators of MUC-1 expression in the pig as expression is greatest following high estrogen and low progesterone plasma concentrations on Days 0 to 4 of the estrous cycle but is nearly undetectable in the by Day 10 in both cyclic and pregnant gilts, when progesterone levels are elevated [Bowen et al., 1996]. The loss of progesterone stimulation is a possible mechanism for MUC-1 depletion in the pig as progesterone receptor is dramatically reduced in the luminal epithelium on Day 10 of gestation after being the greatest on Day 0 [Geisert el al., 1994].

The expression of another cell surface mucin, MUC-4, is also reduced in the uterine epithelium during implantation in rodents [McNeer et al., 1998; Carraway and Idris, 2001]. Interestingly, Ferrel et al. [2003] demonstrated an increased expression of MUC-4 protein expression during placental attachment in the pig. While placentation in the pig is non-invasive, porcine conceptuses themselves are highly invasive *ex utero* [Samuel and Perry, 1972]. Perhaps the coordinated expression of mucins such as MUC-1 and MUC-4 is required to be both permissive for attachment yet regulatory of conceptus proteolytic activity. In rodents, however, the down-regulation of both MUC-1 and MUC-4 may be necessary for a more invasive placentation.

Porcine Conceptus Gene Expression

Because of the substantial impact the events during early porcine conceptus development have on subsequent placental expansion, a significant amount of research has been targeted to identify gene expression changes during early development that may be linked

to critical events. Niemann and Wrenzycki [2000] made the general estimation that following the activation of the embryonic genome, the appropriate expression of approximately 10, 000 genes are involved in successful embryogenesis. Gene expression in the pig following fertilization is predominately under maternal regulation until the activation of the porcine embryonic genome occurs, specifically during the 4 to 8-cell stage of development [Tomanek et al., 1989]. Numerous genes and factors contribute to the transition from maternal to embryonic control, pre-zona pellucida hatching development, and nucleoulus development [see review, Maddox-Hytell et al., 2001]. Why these early developmental events are biologically necessary for subsequent development, most research efforts have focused on the factors regulating conceptus trophoblastic elongation due to the impact this developmental phenomena has on placental expansion, uterine capacity, and ultimate survivability of littermates. Therefore, the remainder of this section will focus on the genes and factors described to be involved with conceptus development on Days 10 to 13 of gestation, when the initiation of both trophoblastic elongation [Geisert et al., 1982b] and conceptus attachment to the uterine epithelium occur [Perry et al., 1981; Dantzer, 1985].

Multiple approaches have been utilized to identify differentially expressed genes during trophoblastic elongation. Numerous strategies have been utilized to identify major regulators of trophoblastic elongation and attachment to the uterine luminal epithelium through utilization of semi-quantitative polymerase chain reaction (sqPCR) [Green et al., 1995; Yelich et al., 1997a; Yelich et al., 1997b; Kowalski et al., 2002], differential display PCR (ddPCR) [Wilson et al, 2000; Wilson et al., 2002], suppression subtractive hybridization (SSH) [Ross et al., 2003b], expressed sequence tag (EST) library

construction and analysis [Smith et al., 2001], utilization of embryonic based cDNA array [Lee et al., 2005] and serial analysis of gene expression (SAGE) [Blomberg et al., 2005].

Activation of conceptus estrogen synthesis during the first signs of mesodermal differentiation in 5 mm spherical conceptuses suggests that the programming for trophoblastic elongation may occur up to 24 h in advance [Geisert and Yelich, 1997]. In mice, mesodermal outgrowth is dependent on the temporally correct expression of the transcription factor, brachyury [Herrman et al., 1990]. Porcine conceptus brachyury gene expression occurs concomitantly with mesodermal outgrowth of 5 mm spherical conceptuses and is temporally associated with $P450_{arom}$ expression [Yelich et al., 1997a]. Cytochromes P450 17α-hydroxylase ($P450_{17\alpha}$) and aromatase ($P450_{arom}$) are two required enzymes for estrogen synthesis. Three distinct isoforms have been identified in the pig for $P450_{arom}$, each encoded by a unique gene [Graddy et al., 2000]. The isoforms, $P450_{arom}$ type I, II and III are expressed specific to the ovary, late gestation placental tissue [Corbin et al., 1995] and conceptus [Choi et al., 1996], respectively. Gene expression for both $P450_{17\alpha}$ and $P450_{arom}$ increase during Day 11 to 12 of gestation concurrent with the initiation of trophoblastic elongation and the formation of filamentous conceptuses [Yelich et al., 1997a]. Another critical enzyme regulating estrogen synthesis is steroidogenic acute regulatory protein (STAR), which is involved with the cleavage of cholesterol resulting in the accumulation of substrates necessary for steroid hormone biosynthesis. The differential expression of STAR during rapid trophoblastic elongation was identified through SAGE [Blomberg et al., 2005]. Interestingly, while the gene expression for STAR increases during the morphological transition from spherical to filamentous; protein expression, as revealed by western

blotting, is significantly less in filamentous conceptuses [Blomberg and Zuelke, 2005]. This translational control of enzyme activity during trophoblastic elongation is indicative of the tight regulation of estrogen biosynthesis and alludes to the mechanism by which estrogen secretion by the pig conceptus remains transient. Increasing amounts of estrogen in uterine luminal flushings has largely been associated with trophoblastic elongation of pig conceptuses [Geisert et al., 1982b; Fischer et al., 1985]. Wilde and Pope [1987] demonstrated that the morphological stage of pig conceptus development directly affects their ability to produce estrogen in vitro during a 6 h incubation. Essentially, while detectable amounts of estrogen are synthesized by spherical conceptuses, filamentous conceptuses from the same litter produce significantly more. In Meishan conceptuses, increased estrogen production is associated with the days in which elongating conceptuses are present; however, the proportion of spherical conceptuses capable of producing estrogen on Day 12 of gestation is much greater than the proportion of spherical conceptuses capable of producing estrogen on Day 11 [Pickard et al., 2003]. This suggests the mechanisms regulating estrogen secretion in Meishan conceptuses is regulated through a time dependent mechanism separate from conceptus morphology.

As production of progesterone from the corpora lutea is greatly elevated it seems plausible that progesterone may also affect conceptus development. Plasma concentration of progesterone peaks by Day 10 of gestation or the estrous cycle. Conflicting evidence exists on the expression progesterone receptor (PR) mRNA by pig conceptuses. Ying et al. [2000] were not able to identify PR protein in Day 6 conceptuses whereas two abstracts presented at annual research symposiums reported RT-PCR revealed PR gene expression in filamentous conceptuses [Dekaney et al., 1998;

Kowalski et al., 2000]. However, Yelich et al. [1997a] were unable to amplify PR mRNA through RT-PCR in Day 11 to 12 conceptuses ranging from 2 mm spheres to filamentous morphology. The occurrence of PR mRNA expression by the pig conceptus would suggest that maternal progesterone may induce responses by developing conceptuses resulting in the establishment of a communication pathway.

The possibility of the synthesis and release of conceptus estrogen to function in an autocrine/paracrine fashion has been suggested due to estrogen receptor β (ERβ) expression in elongating conceptuses [Kowalski et al., 2002] while estrogen receptor α (ERα) was not detected in elongating conceptuses using RT-PCR [Yelich et al., 1997a]. However, ERα has been immunohistochemically detected in the uterine endometrium of gilts from Days 0 to 12 of the estrous cycle and pregnancy [Geisert et al., 1993]. Collectively, this would suggest the mechanisms of conceptus estrogen secretion could be two-fold, operating through each receptor isoform within the conceptus and uterus.

Prostaglandin (PG) production by the developing conceptus is also temporally associated with trophoblastic elongation and conceptus production of estrogen. Both $PGF_{2\alpha}$ and PGE_2 in uterine flushings significantly increase during Days 11 to 12 of gestation [Geisert et al., 1982b]. Prostaglandin production is dependant on the availability of arachidonic acid and the enzymatic activity of both phospholipase A2 (PLA2) and cyclooxygenases-1 (PTGS1) and -2 (PTGS2). Phospholipase A2 functions to enzymatically free arachidonic acid from the phospholipid bilayer which is then utilized as a substrate for prostaglandin synthesis. Guthrie and Lewis [1986] indicated that during elongation, porcine conceptuses increase the synthesis and release of prostaglandins. As expected, the activity of PLA2 and expression of PTGS2 both

increase in filamentous conceptuses [Davis et al., 1983; Wilson et al., 2002]. The relationship between prostaglandin release and trophoblastic elongation is not known other than the temporal and spatial association between the two. However, prostaglandin production may be related to the remodeling of the trophoblast through the release of arachidonic acid, which permits membrane fluidity in the cell membrane phosholipid bilayer necessary for remodeling of the trophectoderm [Davis and Blair, 1993; Geisert and Yelich, 1997]. The induction of prostaglandin synthesis may be related to the conceptus synthesis and production of interleukin-1β (IL-1β) which is transiently expressed during rapid trophoblastic elongation [Tou et al., 1996b; Ross et al., 2003a]. Interleukin-1β is capable of inducing phospholipase A2 gene expression [Kol et al., 2002] and cycoloxygenase-2 gene expression [Huang et al., 1998] in reproductive tissues of various species. The presence of both receptors required for IL-1β signaling in the elongating pig conceptuses [Ross et al., 2003a] suggest that this may be a valid role of conceptus synthesized and released IL-1β. However, the transient, pregnancy specific up-regulation of both receptors in the uterine endometrium suggests a role for the cytokine with respect to induction of a uterine response as well.

Insulin-like growth factors (IGFs), particularly IGF-I and IGF-II, which may have significant impact on the growth and development of the pig conceptus, have been well characterized throughout early gestation in the pig. Endometrial secretion of IGF-I is elevated during the time of trophoblastic elongation and declines shortly thereafter [Simmen et al., 1992] while conceptus gene expression for IGF-I increases steadily during pre-elongation stages peaking at Day 12 of gestation [Letcher et al., 1989]. IGF-I receptor gene expression is present throughout peri-implantation conceptus development;

however there is no variation in expression throughout early development [Green et al., 1995]. The enhanced release of IGF-I by the endometrium is correlated with an increase in conceptus $P450_{arom}$ gene expression [Ko et al., 1994; Green et al., 1995] and has been suggested to regulate conceptus ability to produce estrogen [Hofig et al., 1991]. Uterine IGF-I secretion, which is significantly greater in the uterine lumen of pregnant gilts on Day 12 of gestation compared to Day 12 of the estrous cycle, may act in an autocrine/paracrine fashion to regulate uterine changes [Geisert et al., 2001]. Uterine receptivity to IGF-I occurs through the IGF-1 receptor that is copiously expressed in the uterine endometrium [Simmen et al., 1992]. Pig conceptuses also express IGF-II receptor [Chastant et al., 1994] and its stimulation is likely associated with growth and development before and during the time of conceptus elongation. Endometrial release of IGF-II into the uterine lumen significantly increases from Day 10 to 12 of gestation and is much greater on Day 12 of pregnancy compared to the equivalent day of the estrous cycle [Geisert et al., 2001]. Both IGF-I and -II can stimulate conceptus growth and development by acting through the IGF- II receptor in the conceptus [Czech, 1986]. IGF binding proteins (IGFBP) function to bind IGF thereby regulating the degree to which IGF is capable of biologically stimulating a target cell [Rechler, 1993]. Lee et al. [1998] demonstrated that IGFBPs were present in the pig uterine lumen before Day 11 of gestation and became absent in the lumen after Day 11 of gestation. The loss of IGFBP-2 and -3 was not caused by a decrease in endometrial gene expression but rather through cleavage of IGFBP-2 and -3. Since the loss of IGFBPs correlated with the time of trophoblastic elongation, Lee et al [1998] suggested conceptus regulation of IGFBP cleavage. However, Geisert et al. [2001] have indicated that the cleavage of IGFBP-2

and -3 in the uterine lumen on Day 12 occurs in both pregnant and cyclic gilts likely through the protease activity of kallikrein and/or matrix metalloproteinases. Cleavage of IGFBP-2 and -3 increases the bioavailability of IGF-I and -II at a time period when conceptus growth and steroid production is peaking.

Epidermal growth factor (EGF) and transforming growth factor-alpha (TGFα) are additional growth factors that can affect conceptus development. Interestingly, EGF and TGFα serve as ligands for the same receptor, EGF receptor (EGF-R) [Burgress, 1989]. Porcine conceptus TGFα gene expression is detected briefly during peri-implantation development from Days 8 through 12 of gestation with maximal expression occurring on Day 10. In contrast, conceptus EGF gene expression commences on Day 15 of gestation and continues to increase into early organogenesis [Vaughan et al., 1992]. EGF-R is constitutively expressed in the conceptus from Day 7 until at least Day 22 of gestation [Vaughan et al., 1992]. While the gene expression profiles of TGFα and EGF differ drastically, it is likely that they both act via EGF-R and serve unique stimulatory roles affecting early conceptus development in the pig. In mouse conceptus development, TGFα stimulates fluid uptake thereby regulating blastocoele expansion [Dardik and Schultz, 1991]. Blastocyst formation in the pig occurs on Day 8 of gestation and may be under the partial regulation of TGFα as the receptor is expressed as early as Day 7. It is also highly possible that TGFα could illicit similar effects in porcine conceptuses regulating membrane fluidity, which is necessary for commencement of trophoblastic elongation [Geisert and Yelich, 1997]. However, EGF probably contributes most to early organ and placental development occurring from Day 14 to 22 of gestation as indicated by its temporally associated gene expression.

Another family of growth factors that have been extensively investigated during conceptus-maternal interfacing that occurs between Days 10 and 14 of gestation are the three transforming growth factor β isoforms (TGFβ-1, -2 and -3). *In situ* hybridization analysis indicated gene expression for all three TGFβ isoforms tends to increase in the porcine conceptus trophectoderm and endoderm from Days 10 to 14 of gestation while only TGFβ-2 increased in the embryonic ectoderm and mesoderm during Days 12 to 14 [Gupta et al., 1998]. Gene expression for all three TGFβ isoforms increases in uterine luminal epithelium on Days 10 to 14 of gestation [Gupta et al., 1998], which coincides with increasing estrogen synthesis and release into the uterine lumen during conceptus elongation [Geisert et al., 1982b]. Yelich et al. [1997b] evaluated conceptus TGFβ-2 and -3 gene expression during trophoblastic elongation and reported that TGFβ-2 was not detectable through RT-PCR. However, Yelich and coworkers [1997b] confirmed that TGFβ-3 gene expression increased during the period of rapid morphological change in conceptus development during Days 10 to 12 of gestation. Immunostaining for TGFβ receptors revealed both TGFβ receptor type I and II are expressed in the peri-implantation pig conceptus during Days 10-14 of gestation [Gupta et al., 1996]. Presence of the TGFβ receptors indicates the ability of the conceptus to respond to TGFβ stimulation from conceptus or endometrial origin.

Throughout the last decade retinol, the common form of vitamin A, has received thorough investigation regarding the effects it may have on conceptus development in pigs, particularly during Days 10-18 of gestation. Retinol likely plays integral roles orchestrating cell division, organogenesis and placental growth in all mammals [Roberts et al., 1993], however, when excessive, retinol can be embryotoxic [Thompson et al.,

1964]. Retinol, retinal, and retinoic acid, collectively termed retinoids, induce biological actions via retinoic acid receptors (RAR) α, β, and γ. Yelich et al. [1997b] revealed that all three RAR isoforms are expressed before, during and after rapid trophoblastic elongation. Both RARα and RARγ continue to be expressed in Day 15 porcine conceptuses [Harney et al., 1994]. Roberts et al. [1993] reviewed the changes in uterine retinol and indicated its concentration in uterine flushings containing filamentous conceptuses during Days 10-13 of gestation is 10-50 fold greater than uterine flushings during the same time frame only containing spherical conceptuses. Flushings containing spherical conceptuses had a concentration of retinol that was similar to that of uterine flushings from non-pregnant animals on Day 11 to 12 of the estrous cycle. Vallet et al. [1996] published similar data indicating significantly higher retinol binding protein (RBP) in the uterine lumen on Day 13 compared to Day 10 of gestation. Retinol transport from the uterine lumen to the conceptus is primarily under the regulation of RBP. RBP is a secretory product of the pig conceptus [Harney et al., 1990] whose gene expression increases steadily as conceptuses develop from 4 mm spheres into more advanced filamentous conceptuses [Yelich et al., 1997b]. Furthermore, gene expression of RBP by the uterine endometrium of Day 12 pregnant gilts is highly dependent on morphological stage of conceptus development [Trout et al., 1992]. Endometrium from gilts bearing Day 12 filamentous conceptuses had dramatically greater RBP gene expression than Day 12 endometrium in the presence of spherical conceptuses. Synchronization and timing of the gene expression for both RAR's and RBP in the conceptus and endometrium suggests a significant dependency of conceptus development on retinol availability. Geisert and Yelich [1997] proposed that conceptus secreted

estrogen stimulates the endometrial release of RBP resulting in the transport of retinol to the conceptus cytoplasm where it is converted to retinoic acid (RA). Available RA stimulates conceptus RAR's inducing extracellular matrix (ECM) remodeling, needed for trophoblastic elongation to occur, both directly, and indirectly through downstream stimulation of morphogens such as TGFβ's.

During the past decade, cytokines are proving to be intimately involved with the regulation of conceptus development and the establishment of pregnancy in many species. Mathialagan et al. [1992] evaluated interleukin-6 (IL-6) gene expression in pig conceptuses and indicated that greatest expression occurred during the period of attachment and early placentation. A later study by Modric et al. [2000] reported that IL-6 gene expression in the preimplantation conceptus peaked in Day 12 filamentous conceptuses but gene expression was not detectable in Day 14 conceptuses. The ability of IL-6 to induce an acute phase pro-inflammatory response is imitated, albeit to a lesser degree, by interleukin-1 (IL-1) [Mantovani et al., 1998]. Using northern blotting, Tou et al. [1996b] demonstrated that IL-1β is transiently expressed by porcine conceptuses between 11 and 13 days of gestation. Ross et al. [2003a] further demonstrated the increased mRNA abundance associated with trophoblastic elongation is temporally associated with significant increased IL-1β concentrations in uterine lumen flushings. Both receptors for IL-1β, IL-1RT1 and IL-1RAP, increase in gene expression in the uterine endometrium and conceptus while IL-1β protein levels are elevated in the uterine flushings on days 12-15 of gestation [Ross et al., 2003a]. Peri-implantation IL-1β gene expression has also been documented to increase prior to initiation of blastocyst implantation in the mouse [Takacs and Kauma, 1996; Kruessel et al., 1997] and has been

suggested as the initiator of conceptus-uterine cross-talk during early pregnancy in the human [Lindhard et al., 2002]. The importance of a conceptus induced acute phase inflammatory response in the pig uterus is not well understood although its occurrence has been described by Geisert and Yelich [1997]. Inflammation is generally associated with the recruitment of immune cells. During pregnancy in the pig, stromal leukocyte populations are significantly greater at attachment sites opposed to between attachment sites [Engelhardt et al., 2002]. The majority of these leukocytes morphologically resembled lymphocytes suggesting they were predominately T, B and/or natural killer (NK) cells. This initial contact, coupled with embryonic signals, invokes an acute phase inflammatory response by the uterus and likely results in the differentiation of undifferentiated T-helper (Th0) cells to either type 1 (Th1) or type 2 (Th2) cells. Th1 mediated immunity is referred to as cell-mediated immunity and is generally associated with pregnancy failure [Raghupathy, 1997] while humoral immunity mediated by Th2 is thought to be required for the successful establishment of pregnancy [Wegmann et al., 1993]. However, the TH1/TH2 paradigm is challenged in that numerous factors such as IL-1β [Ross et al., 2003a] and interferon γ (IFN-γ) [Lefevre et al., 1990]; which are generally considered to be stimulators of TH1 immunity, are both expressed by the conceptus during the early attachment phase. Immunological stimulation of the uterine milieu is unavoidable; however, the induced inflammation is necessary and not necessarily devastating to the conceptus as it stimulates counter regulatory responses limiting induced damage while encouraging shifts in the maternal T cell repertoire more suitable for a successful pregnancy [Mellor and Munn, 2000].

Colony stimulating factor-1 (CSF-1) is an additional factor produced by the conceptus that is suspected to accentuate growth and differentiation. CSF-1 gene expression is present in conceptuses as early as Days 10 to 12 of gestation. However, CSF-1 expression peaks at Day 30 and continues to be expressed in fetal tissues throughout gestation [Tuo et al., 1995]. CSF-1 is thought to be responsible for the recruitment of macrophages to the site of implantation and involved in regulating placental development [Wood et al., 1997]. Osteopetrotic (*op/op*) mice lack the CSF-1 gene [Wiktor-Jedrzejczak et al., 1990], which is required for successful female fertility. Pollard and coworkers [1991] demonstrated that while *op/op* x *op/op* crosses resulted in consistent infertility, pregnancies created by crossing heterozygous males (*+/op*) with *op/op* females were partially salvaged. This indicates that the necessity for conceptus produced CSF-1 to either compensate or attenuate the CSF-1 production in the uterine endometrium.

Leukaemia inhibitory factor (LIF) is a cytokine that has been proposed to regulate conceptus growth and development. Anegon et al. [1994] indicated that LIF is present in porcine uterine luminal flushings on Days 7-13 of the estrous cycle and peaks on Day 12 of gestation. LIF likely has direct effects on the conceptus as both pre- and post-elongation conceptuses express LIF receptor β [Modric et al., 2000]. Pregnancy specific endometrial gene expression of LIF is detected in pregnant animals during the approximate time rapid trophoblastic elongation is initiated and could serve as a pathway for possible conceptus-uterine communication [Anegon et al., 1994]. LIF receptor is also expressed in the mouse uterus on Day 4, the time of blastocyst implantation [Ni et al., 2002]. Interestingly, LIF receptor was not expressed in the uterus following progesterone

priming although it was greatly increased following estrogen-mediated termination of delayed implantation [Ni et al., 2002]. Estrogen likely mediates similar effects in pigs as the transient increase in expression of LIF in the uterus occurs concurrently with increased conceptus estrogen production and LIF receptor expression.

While the information presented in this section provides valuable information regarding gene expression during early porcine conceptus development. Genes controlling trophoblastic elongation remain largely unknown.

Role of Estrogen During Early Pregnancy in the Pig

Estrogen as the Maternal Recognition of Pregnancy Signal

In 1969, Short coined the term "maternal recognition of pregnancy" when describing the process resulting in the extension of the CL life beyond that which occurs during a normal estrous cycle. Maternal recognition of pregnancy is the process by which the developing conceptus(es) synthesize and release a chemical signal, that modifies a molecular cascade of events prolonging the lifespan of the CL beyond the length of a normal estrous cycle [Geisert et al., 1990]. Protection of the CL promotes continued progesterone production thereby allowing maintenance of myometrial quiescence and endometrial histotroph production. In pigs, progesterone production by the CL is required throughout pregnancy as ovariectomy at any stage of pregnancy results in abortion [Nara et al., 1981]. Perry et al. [1973, 1976] demonstrated that porcine conceptuses possess the metabolic ability to convert steroid precursor molecules into estrogens. Later, Bazer et al. [1982] established that the conceptus synthesis and secretion of estrogen did in fact serve as the maternal recognition signal. Conceptus

synthesis and release of estrogen during early pregnancy in the pig is biphasic; first transiently peaking on Day 11 to 12 during trophoblastic elongation trailed by a more sustained period of secretion initiated on Day 15-16 of gestation [Geisert et al., 1990]. A variety of studies have coordinately established that estrogen alone is capable of functioning as a luteotrophin. While responses were highly variable, injections of estradiol valerate on Days 11 to 15 of the estrous cycle induced psuedopregnancy in gilts for an average of 146 days [Frank et al., 1977]. Even single injections of exogenous estrogen given to gilts after Day 9 of the estrous cycle extended the corpora lutea lifespan [Kidder et al., 1955]. In 1963, Gardner et al. demonstrated the ability to lengthen the interestrous interval by administration of exogenous estrogen on Day 11-12 of the estrous cycle. Similarly, Geisert et al. [1987] demonstrated a 7 day extension to the CL lifespan in response to exogenous estrogen administered on Day 12 of the estrous cycle. These data are further supported by estradiol valerate extending CL survival following infusions directly into the uterine lumen between Days 11-15 of the estrous cycle [Ford et al., 1982a]. King and Rajamahendran [1988] also demonstrated the ability of estrogen impregnated sialastic beads implanted into the uterine lumen on Day 10 of the estrous cycle induced psuedopregnancy. In an effort to mimic the physiological release of estrogen by the conceptus as described by Geisert et al. [1982b], an initial injection of estrogen on Day 11 to 12 followed by an additional 2nd dose of estrogen on Days 14-16 of the estrous cycle prolonged the life of the corpora lutea greater than 60 days [Geisert et al., 1987]. The impersonation of the biphasic estrogen synthesis and release establishing a prolonged psuedopregnancy indicates the critical temporal nature of conceptus estrogen secretions as injections mimicking conceptus estrogen release at either phase only did not

induce psuedopregnancy beyond 35 days [Geisert et al., 1987]. Clearly, the extensive, confirming reports of exogenous estrogen, when given at time points temporally associated with the endogenous conceptus synthesis and release of estrogen, having the ability to induce psuedopregnancy has resulted in its acceptance as the maternal recognition of pregnancy signal in the pig.

Temporally associated with increased uterine lumen estrogen concentrations during early pregnancy is the augmentation of uterine blood flow [Ford and Christenson, 1979; Ford et al., 1982b] as well as the production and secretion of PGE_2 into the uterine lumen [Geisert et al., 1982b]. The association of PGE_2 production was later determined to be a result of conceptus phospholipase A2 activity and prostaglandin production between Days 7 and 14 of gestation [Davis et al., 1983]. PGE_2 has been shown to enhance CL performance through increased weight and progesterone production [Ford and Christenson, 1991] and is considered a luteotrophic agent during pregnancy in the pig [Ziecik, 2002]. Production of prostaglandins is critical for the establishment of pregnancy in pigs as inhibition results in pregnancy failure during early gestation [Kraeling et al., 1985]. Interestingly, gene and protein expression of both prostaglandin synthase-1 (PTGS1) and -2 (PTGS2) have been detected in the uterine endometrium during the estrous cycle and early pregnancy [Ashworth et al., 2006; Blitek et al., 2006]. Both PTGS1 and -2 are principal enzymes that convert arachidonic acid to prostaglandin H2 (PGH_2). While PTGS1 appears to be constitutively expressed, PTGS2 may have a more prominent role with respect to prostaglandin production as its gene and protein expression increases during the luteal phase of the estrous cycle and early pregnancy in the pig [Ashworth et al., 2006; Blitek et al., 2006]. Subsequently, two terminal enzymes,

PGE synthase and PGF synthase catalyze the conversion of PGH_2 to PGE_2 and $PGF_{2\alpha}$, respectively [Smith and Dewitt, 1996]. Both PGE_2 and $PGF_{2\alpha}$ are intricately involved in the establishment of pregnancy in the pig. PGE_2 is a vasodilator that, in addition to estrogen, dramatically increases in concentration in the uterine flushings during the time of trophoblastic elongation and maternal recognition of pregnancy in the pig [Geisert et al., 1982b], while $PGF_{2\alpha}$ is a vasoconstrictor synthesized and released by the uterine endometrium that is responsible for corpora lutea death around Day 15 of the estrous cycle in the pig [Moeljono et al., 1976].

Control of Luteolysis

Luteolysis in pigs is dependant on the uterine endometrial secretion of the luteolysin, $PGF_{2\alpha}$, into the vasculature through an endocrine mechanism resulting in the delivery to and subsequent lysis of the CL. The response of the CL in the pig to the luteolysin varies dramatically during the estrous cycle and early pregnancy and is a tightly regulated process. Gadsby et al. [1990] demonstrated that the CL refractory period to luteolysis is most likely in response to the low abundance of luteal receptors for $PGF_{2\alpha}$ prior to Day 12 of the estrous cycle or early pregnancy. On Day 13, there is a dramatic increase in luteal $PGF_{2\alpha}$ receptor expression that remains elevated on Day 14 to 17 resulting in the susceptibility of the CL to $PGF_{2\alpha}$. A more comprehensive review outlining the involvement of other factors such as endothelin-1, tumor necrosis factor-α and insulin like growth factor-1 during the acquisition of luteolytic sensitivity and luteolysis is available [Gadsby et al., 2006]. While specific mechanisms regulating endometrial prostaglandin production are not well elucidated, McCracken et al. [1999]

have hypothesized that the hypothalamic production of oxytocin subsequently binding to its receptor in the uterine endometrium as an initiator and/or potentiator of endometrial production of prostaglandins in the ewe. It also seems plausible that activation of the transcription factor, nuclear factor κ B (NFκB), may occur as the PTGS2 gene contains the κB site [Ali and Mann, 2004]; and that PTGS2 expression increases are specific to the luminal epithelium and temporally associated with $PGF_{2\alpha}$ production [Ashworth et al., 2006].

Because prostaglandin synthesis and secretion is required for pregnancy establishment and $PGF_{2\alpha}$ is also the luteolysin in the pigs, the mechanisms by which $PGF_{2\alpha}$ is capable of communicating with the CL is tightly regulated. Frank et al. [1977] demonstrated that i.m. delivery of 5 mg of estradiol valerate on Days 11 to 15 of the estrous cycle reduced $PGF_{2\alpha}$ concentrations in the utero-ovarian vein. This mechanism of action was further confirmed when infusion of 375 ng of estradiol-17β into the uterine lumen of gilts every 6 h on Days 11 to 15 of the estrous cycle also had lower $PGF_{2\alpha}$ concentrations in the utero-ovarian vein compared to control gilts [Ford et al., 1982a].

The conceptuses are the main instigators preventing luteolysis during early pregnancy in the pig. Dziuk [1968] demonstrated that prior to Day 18 of gestation, at least two conceptuses must be present in each uterine horn to prevent luteolysis and establish pregnancy in the pig. This is largely due to the expansive nature of the pig uterine endometrium that is capable of producing prostaglandins and the necessity of local communication of conceptuses with the maternal endometrium during pregnancy establishment. As the synthesis and secretion of $PGF_{2\alpha}$ from endometrium of both cyclic and pregnant gilts occurs, specific mechanisms are required to prevent luteolysis in

pregnant gilts while allowing it to occur in cyclic gilts. The most accepted theory describing the mechanisms by which pregnant gilts overcome luteolysis is described by the endocrine/exocrine theory of maternal recognition [Bazer and Thatcher, 1977]. During the estrous cycle and normal CL regression, the uterine endometrium functions as an endocrine tissue capable of releasing $PGF_{2\alpha}$. Bazer and Thatcher suggested that the conceptus estrogen secretion redirects movement of endometrial $PGF_{2\alpha}$ release toward the uterine lumen (exocrine) rather than being directed through the underlying endometrial stroma and secreted into uterine vasculature network (endocrine). This is supported in that both pregnant and estrogen induced psuedopregnant gilts have elevated $PGF_{2\alpha}$ in their uterine flushings [Zavy et al., 1982]. Failure to redirect endometrial $PGF_{2\alpha}$ can result in release of $PGF_{2\alpha}$ directly into the utero-ovarian portal vessels allowing the transportation of the luteolysin directly to the CL. Also, because the pig lungs are capable of reducing only 18% of the systemic $PGF_{2\alpha}$ to its metabolite, 15 keto-13,14 dihydro-prostaglandin $F_{2\alpha}$, through one circulatory passage, systemic as well as local delivery of $PGF_{2\alpha}$ from the uterus is capable of initiating luteolysis [Davis et al., 1979]. While increased $PGF_{2\alpha}$ concentrations have been detected in the utero-ovarian vein just prior to and during luteolysis [Bazer et al., 1982], systemic delivery also appears to contribute to corpora lutea death as Dhindsa and Dziuk [1968] demonstrated that conceptuses were required in both uterine horns to prevent luteolysis and extend gestation past 30 days. Once the CL becomes sensitive to the luteolysin, endometrial $PGF_{2\alpha}$ induces intra-luteal production of $PGF_{2\alpha}$ through the activation of PTGS2 in the CL [Diaz et al., 2002]. Ultimately, maternal recognition of pregnancy in the pig requires a sufficient number of embryos equidistantly spaced to deliver the maternal recognition of

pregnancy signal, estrogen. Adequate and synchronized trophoblastic elongation throughout the uterine lumen during estrogen secretion redirects endometrial $PGF_{2\alpha}$ production from systemic venous drainage to exocrine secretion thereby protecting the integrity of the corpora lutea and enabling the establishment of pregnancy.

Endocrine Disruption of Pregnancy

In general, a thickening of the uterine glycocalyx (UG) occurs between Days 13 and 18 of gestation in the pig [Perry et al., 1981; Dantzer, 1985; Geisert et al., 1991] and ultimately provides an essential adhesion matrix necessary for the attachment of the conceptus trophectoderm to the uterine epithelium. Premature administration of estrogen (Days 9 and 10) impairs the thickening of the UG, actually causing it to completely slough off by Day 16 of gestation preventing the necessary cell-cell interactions for conceptus attachment resulting in conceptus mortality and loss of pregnancy [Morgan et al., 1987a; Blair et al., 1991; Geisert et al., 1991]. This disruption of the UG formation is closely associated with embryonic mortality on Days 15 to 18 of gestation in gilts [Blair et al., 1991]. While adverse timing of estrogen exposure via i.m. administration of estrogen to the dam on Days 9 and 10 of gestation results in a total pregnancy loss, the same dosage given on Days 11 and 12, in sync with conceptus synthesis and release of estrogen, has no adverse affect on pregnancy establishment [Pope et al., 1994]. Ill-timed ingestion of naturally occurring estrogenic alfatoxins, such as zearalenone, found in moldy corn, also results in total litter loss [Long and Diekman, 1984]. The effects of early estrogen exposure do not affect the ability for the conceptuses to elongate or equidistantly space themselves, but is rather a result of endometrial modification.

The negative effects estrogen bears on early pregnancy establishment appears to be paralogous. Estrogen stimulation, albeit of ovarian origin, appears necessary for pregnancy in mice as estrogen receptor alpha null (αERKO) mice are infertile [Couse and Kourach, 1999]. The infertility in αERKO mice is thought to occur in part to dysfunctional ovarian events; however, uterine hormone insensitivity is thought to contribute as well. Indeed, transferred embryos into uteri of αERKO mice failed to implant successfully, however, decidualization associated markers were still expressed [Hewitt et al., 2002]. Estrogen may also affect implantation in humans as recurrence of spontaneous miscarriage in individuals with polycystic ovarian syndrome (PCOS) may be related to the greater amounts of serum estrogen and increased endometrial estrogen receptor alpha (ERα). While the estrogen source varies between mice and pigs (ovarian in mice, conceptus in pigs), the timing and dosage of estrogen stimulation has been shown to dramatically affect the ability of the conceptus to attach to the uterine epithelium and initiate implantation in both species.

Critical parameters exist with regards to the specific timing and amount of estrogen released during this stage of pregnancy in the pig. Insufficient estrogen production, as seen in litters with less than two piglets per uterine horn at the time of implantation, results in the failure to prevent luteolysis and subsequent pregnancy loss [Polge et al., 1966; Dziuk, 1968]. While estrogen is required as a maternal recognition of pregnancy signal and thought to be involved with the opening of the "implantation window" in the pig, timing and extent of estrogen exposure can have dramatic effects on conceptus development and survival. While estrogen exposure to the uterine endometrium has a huge impact with regard to endometrial function and the ability to

regulate the outcome of pregnancy, little is known considering the mechanisms of estrogen during the establishment of pregnancy in the pig. Moreover, this underlines the physiological importance of conceptus trophoblastic elongation to deliver estrogen throughout the uterine lumen and also the synchrony by which it happens between conceptuses. As it is evident that estrogen modification of the uterine microenvironment can be destructive to conceptuses still in early spherical development; the production and secretion of estrogen by developmentally advanced conceptuses may alter the micro-environment surrounding conceptuses that are lagging in development and ensure their demise.

The Opening of the Implantation Window

The opening of the implantation window is the initiating point of the period during gestation at which specific endometrial alterations occur to allow the attachment of the conceptus trophectoderm and subsequent development. It is this period of development that requires the formation of a communication network between the developing conceptus and the maternal endometrium; dysfunction on the part of either the conceptus or the uterine endometrium will result in the inability to establish pregnancy. Steroid hormones, progesterone and estrogen, no doubt serve a fundamental responsibility in the pattern of endometrial secretions and the induction of uterine receptivity. While progesterone serves more of a conceptus nurturing role through regulating myometrial quiescence and endometrial histotroph secretion, estrogen stimulation is critical for uterine receptivity through its protective mechanisms regarding the corpora lutea and endometrial alterations necessary for conceptus attachment.

Progesterone and progesterone receptor expression are thought to play a dramatic role in regulating uterine receptivity in many species, including the pig. Corpora lutea production of progesterone during early pregnancy is chiefly responsible for regulating the production of uterine histotroph and prevention of myometrial contractions. Recently, Geisert et al. [2006] described the potential role of progesterone and progesterone receptor as regulators of the estrous cycle through its potential to interact with the transcription factor, NFκB, during the opening of the implantation window. Progesterone supplementation to sheep and cattle prior to endogenous production via the corpora lutea results in shortened estrous cycle [Ottobre et al., 1980; Garrett et al., 1988]. Mifepristone, a progesterone receptor antagonist, administered to sheep during days 3-5 of the estrous cycle results in a delay of luteolysis [Morgan et al., 1993]. Collectively, these data suggest that the duration of progesterone exposure is directly related to endometrial events necessary for luteolysis. Progesterone signaling requires the expression of progesterone receptor. The down-regulation of progesterone receptor in the uterine luminal epithelium is generally associated with the opening of the implantation window in the human [Lessey et al., 1988, 1996], baboon [Fazleabas et al., 1999], sheep [Spencer and Bazer, 1995], cattle [Meikle et al., 2001], pigs [Geisert et al., 1994] and horses [Hartt et al., 2005]. While the down-regulation of progesterone receptor in the luminal epithelium limits progesterone signaling, it is not obsolete as expression persists in the underlying stroma during the time of implantation in the pig [Geisert et al., 1994].

Recently, data has provided insight into progesterone receptor regulation of transcription of genes through its interactions with the transcription factor, NFκB [Kalkoven et al., 1996]. The data suggest that the p65 sub-unit of NFκB and

progesterone receptor are mutually repressive of each other and the authors hypothesize that this is through interaction with the transcription factors themselves or binding to genomic DNA in regions preventing transcriptional machinery necessary for gene transcription to occur [Kalkoven et al., 1996]. Thus the down-regulation of progesterone receptor just prior to the opening of the implantation window may be associated with endometrial transcriptional changes necessary for uterine receptivity leading to implantation. In mice, NFκB activity has been assessed via electrophoretic mobility shift assay and increased activity is associated with the period of implantation [Nakamura et al., 2004a]. Viral delivery of inhibitor of NFκB α (IκBα) into the uterus in mice delays implantation by suppressing NFκB activity and subsequent leukemia inhibitory factor expression [Nakmura et al., 2004b]. Interestingly, the authors were capable of partially restoring uterine receptivity when LIF was administered with the in vivo delivery of IκBα.

The pig also expresses numerous NFκB regulated genes in the uterine epithelium such as interleukin-6, LIF, and others [see review; Geisert and Yelich, 1997]. Prostaglandin synthase-2, also an NFκB regulated gene increases expression in the uterine luminal epithelium in both cyclic and pregnant gilts coordinately with progesterone receptor down-regulation and uterine receptivity and associated with the significant production of $PGF_{2\alpha}$ secreted into the uterine lumen [Ashworth et al., 2006]. Interestingly, the administration of indomethacin during the period of uterine receptivity in pigs dramatically reduced prostaglandin production in the uterine lumen and resulted in a total pregnancy loss [Kraeling et al., 1985]. Notably, indomethacin is an inhibitor of

IκBα kinase activity which thereby functions to prevent IκBα degradation and the freeing of the nuclear localization signal on the NFκB dimers.

What regulates this activation of NFκB, or the down-regulation of progesterone receptor in the uterine endometrium remains unclear. One potential regulator of NFκB activation is receptor activator of nuclear factor κB (RANK) and its ligand (RANKL) which are both involved in bone remodeling and mammary gland development [Jones et al., 2002; Cao and Karin, 2003]. Because expression of RANKL can be stimulated by progesterone [Srivastava et al., 2003] may suggest the potential of RANK mediated NFκB activation in the pig endometrium if RANKL is capable of signaling through endometrial stromal cells which still express progesterone receptor during the implantation window in the pig [Geisert et al., 1994].

Another critical component of NFκB activation during implantation in the pig during the period of conceptus elongation and secretion of both estrogen and IL-1β secretion is the potentiation and/or regulation of NFκB activation in the uterine endometrium provided by the conceptus. While both receptors for IL-1β, an inducer of NFκB activity, are expressed in the uterine endometrium [Ross et al., 2003a], the production and secretion of conceptus estrogen may also regulate activity of NFκB. Ghilsetti et al. [2005] demonstrated the *in vitro* ability of estrogen, signaling through ERα and not ERβ, of preventing activated NFκB in the cytoplasm from being translocated into the nucleus of the cell and inducing transcription. The progesterone receptor down-regulation in the luminal epithelium concurrent with conceptus secretion of both IL-1β and estrogen, all potential modulators of NFκB activity suggests the molecular mechanisms by which uterine receptivity, and subsequent attachment and

implantation in the pig, remain unclear. Perhaps the down-regulation of the luminal epithelial progesterone receptor just prior to implantation is merely a default mechanism by the uterine endometrium during cyclicity following progesterone "priming". By omission, the uterine endometrium is "putting the ball in the conceptus' court", allowing the default activation of NFκB by progesterone driven progesterone receptor withdrawal. Then requiring progressive stimulation by the conceptuses to prevent or redirect endometrial $PGF_{2\alpha}$ secretion as well as provoke the appropriate endometrial response necessary for conceptus-endometrial cross-talk. Nonetheless, the biological understanding of this process is critical due to the implications regarding agricultural farm animal production and the reproductive health of humans.

Statement of the Problem

There are numerous conceptus and endometrial factors that contribute to the establishment of a successful pregnancy yielding large litter size in pigs. Unfortunately, pig production from a reproductive standpoint in the United States is far from optimal. Of the 20 to 46 % conceptus mortality rate realized throughout gestation in the pig, a majority is directly related to the events during the peri-implantation stage of development. Three extremely critical events occur during this time period: 1) the rapid elongation of the conceptus trophoblast and delivery of the maternal recognition signal, estrogen; 2) the uterine response to conceptus secreted estrogen, and 3) the down-regulation of the luminal epithelial progesterone receptor and the uterine receptivity associated with it. Temporally, these three biological processes all occur coordinately within a very narrow time frame (Days 10 to 13 of gestation). As important as they are

regarding the establishment of pregnancy in the pig, little biological information is available delineating the mechanisms that regulate these events.

Ford [1997] attributes the larger litter size of the Meishan sows to the ability of the conceptuses to regulate the uniformity and the extent to which they expand their trophoblast. Geisert and Schmitt [2000] suggested that the ability to regulate the simultaneous initiation of trophoblastic elongation would result in more consistent placental size and uterine space among littermates potentially increasing litter size. While multiple attempts to identify mechanisms critical for this stage of development have provided much data, there remains a void as to what exactly regulates rapid trophoblastic elongation in the pig.

Estrogen, while a required component of pregnancy establishment in the pig also plays integral roles during pregnancy establishment. Copious amounts of estrogen delivered by the conceptus during Days 11 to 12 of gestation appear to be required as too few conceptuses are incapable of establishing pregnancy. While amount of estrogen stimulation appears to have a requirement, the timing of the estrogen stimulation is also critical as ill-timed administration or ingestion of estrogen has been shown to cause a total loss of pregnancy in the pig. While certain events such as the redirecting of endometrial $PGF_{2\alpha}$ secretion are attributed to conceptus estrogen stimulation, very little is known regarding the endometrial molecular mechanisms and events following estrogen exposure. A deeper understanding the regulatory roles that estrogen serves during pregnancy establishment in the pig will lend insight to steroidogenic factors affecting pregnancy outcome in pigs. Also the biological understanding of estrogen's impact on endometrial function may also be applicable to women who suffer from polycystic

ovarian syndrome that is associated with elevated estrogen circulation and early recurrent spontaneous miscarriage.

Finally, the critical molecular events associated with the opening of the implantation window and the period of uterine receptivity is vaguely described in any species. While the down-regulation of the progesterone receptor in the luminal epithelium is associated with uterine receptivity in most species, the biological forces driving that phenomenon are not well described. Certainly, the regulation of specific transcription factors and the downstream activation of their regulated genes contribute to the establishment of pregnancy in the pig. Determining if a relationship between the activation of the transcription factor, NFκB, and progesterone receptor down-regulation during exists during the period at which endocrine release of endometrial $PGF_{2\alpha}$ is redirected in the pig will be prudent biological information necessary for understanding the events of pregnancy establishment for many species.

Approach

While biotechnological advancements have been rapid over the past few years, bioinformatics resources have made exceptional progress recently. The ability to link microarray data acquisition platforms to bioinformatics tools has dramatically changed the capability to identify differentially expressed genes in a biological system and then accurately annotate the biological themes associated with the alterations in the system evaluated. Recently, a porcine 15K cDNA microarray representing genes from conceptus, brain, ovarian and uterine tissues has been developed [Whitworth et al., 2005]. Also, the significant amount of expressed sequence tags from the pig deposited into

GenBank has prompted the development of the GeneChip® Porcine Genome Array by Affymetrix®. The 23, 937 probe set interrogates 23, 256 transcripts representing 20, 201 porcine genes. Utilization of these array platforms and modern bioinformatics approaches will help identify the biological processes that are associated with both endometrial response to estrogen stimulation as well as the factors that are involved with rapid trophoblastic elongation during early porcine conceptus development. Identification and characterization of the changes in gene expression that are related to trophoblastic elongation, endometrial estrogen stimulation and uterine receptivity as a result of transcription factor activation will provide a better understanding of the biological events necessary for embryonic survival, implantation and a successful pregnancy in the pig.

Chapter III

ANALYSIS AND CHARACTERIZATION OF DIFFERENTIAL GENE EXPRESSION DURING PORCINE CONCEPTUS RAPID TROPHOBLASTIC ELONGATION AND ATTACHMENT TO THE UTERINE LUMENAL EPITHELIUM

Introduction

As in any mammalian species, successful establishment of pregnancy and embryonic development in the pig follows a specific pattern of temporal and spatial gene expression. It is estimated that successful pre-implantation and early fetal development involves the expression of approximately 10,000 genes [Niemann and Wrenzycki, 2000]. During early pregnancy in the pig, the peri-implantation period is one of the most critical stages of conceptus development. After ovulation and fertilization, prenatal mortality in the pig ranges from 20% to 46% by term [Pope, 1994] with the majority of the loss occurring during the peri-implantation stage of development between Days 12 to 18 of gestation [Stroband and Van der Lende, 1990]. This significant period of elevated conceptus mortality during the peri-implantation stage of development coincides with conceptus rapid trophoblastic elongation [Geisert et al., 1982b], neurulation of the inner cell mass, the transient synthesis and release of the maternal recognition of pregnancy signal, estrogen [Geisert et al., 1982b]; and finally, trophectoderm differentiation followed by adhesion and attachment to the uterine surface epithelium [Burghardt et el.,

1997]. The disruption of any of these critical biological processes can result in conceptus mortality and a reduction in litter size.

Conceptus trophoblastic elongation, which occurs between Days 11 to 12 of gestation, is characterized by transition through four distinct morphological stages (spherical, ovoid, tubular and filamentous). The cellular remodeling and migration of the trophectoderm is initiated when a conceptus reaches a 9-10 mm spherical morphology, rapidly transforming from a ovoid shape into a tubular morphology which rapidly expands into a long filamentous thread greater than 150 mm in length within 2-3 h [Geisert et al., 1982b]. Secretion of the conceptus produced maternal recognition signal, estrogen [Geisert et al., 1990, Bazer and Thatcher, 1977], and IL-1β [Ross et al., 2003a] occurs concomitantly with elongation of the trophoblastic membrane. Trophoblastic elongation and expansion through the uterine horns provides the biological function of maximizing nutrient exchange throughout gestation through increased placental-uterine contact during the formation of a diffuse epitheliochorial type of placenta [Stroband and Van der Lende, 1990]. The associated release of estrogen induces alterations in the endometrium, shifting the uterine environment, which may be unfavorable for less developed littermates [Pope, 1994; Geisert and Yelich, 1997]. Litter variation in conceptus morphological stage of development around Day 12 of gestation is not uncommon [Anderson et al., 1978]. Given that the amount of estrogen production by individual conceptuses is directly proportional to the morphological stage of development [Pope et al., 1988], it is plausible to conclude that variation within the onset of trophoblastic elongation and estrogen production between littermates can reduce survivability of the lesser developed conceptuses as the uterine microenvironment is

altered. While conceptus trophoblastic elongation is a required phenomenon for the establishment of pregnancy in the pig, the subsequent adhesion of the trophectoderm to the uterine surface epithelium is also critical for continued conceptus development.

Numerous conceptus products have been hypothesized to be important in porcine conceptus development following detection of its mRNA expression in the various conceptus morphological stages using techniques such as semi-quantitative RT-PCR [Green et al., 1995; Yelich et al., 1997a; Yelich et al., 1997b; Kowalski et al., 2002], differential display RT-PCR [Wilson et al, 2000], suppression subtractive hybridization (SSH) [Ross et al., 2003b], expressed sequence tag (EST) library construction and analysis [Smith et al., 2001], utilization of embryonic based cDNA array [Lee et al., 2005] and serial analysis of gene expression (SAGE) [Blomberg et al., 2005]. While these techniques have compiled complementary data representing potential regulators of trophoblastic elongation, most studies have only compared the expression of Day 12 filamentous conceptuses to those of earlier morphological stages of development and not post-elongated conceptuses which are initiating attachment to the uterine epithelial surface. At present, little information is available regarding the large number of genes that may be responsible for initiating rapid trophoblastic elongation as well as those involved with the initial attachment to the uterine lumenal epithelium. The objective of the present investigation was to utilize the GeneChip® Porcine Genome Array from Affymetrix representing 20, 201 genes to identify differentially expressed genes during rapid trophoblastic elongation and attachment to the uterine surface in the pig. Identification and characterization of conceptus gene expression patterns during rapid

trophoblastic elongation and attachment in the pig will provide a better understanding of the events required for successful implantation and embryonic survival.

Materials and Methods

Conceptus Collection

Research was conducted in accordance with and approved by the Oklahoma State Institutional Animal Care and Use Committee. Twenty crossbred, cyclic gilts were checked for expression of estrus twice daily in the presence of an intact boar and naturally mated at the onset of the second estrus and again 24 h later. Gilts were hysterectomized between Days 11 and 12 of gestation to collect spherical and tubular conceptuses while filamentous conceptuses were collected on Days 12 and 14 of gestation. Hysterectomies were conducted as previously described for our laboratory [Gries et al., 1989]. After removal of the uterine horns, conceptuses from each uterine horn were flushed into a sterile petri dish with 20 mL of physiological saline. Due to the limited time frame when conceptuses are in tubular transitional development (2-3 h) and difficulty in determining when tubular conceptuses are in the uterus following mating, one uterine horn was removed on Day 11.5 of gestation in a subset of gilts. Conceptuses were evaluated to determine an appropriate time-delayed removal of the second horn corresponding to a predicted time conceptuses would be in a tubular morphology per the rate of development described by Geisert et al. [1982c]. Following collection from the uterine horns, conceptuses of identical morphologies were transferred to cryogenic vials, snap-frozen in liquid nitrogen, and stored at -80^{o}C until RNA was extracted.

RNA Isolation

Total RNA was isolated from conceptus pools, each representing multiple individuals (4-8) of identical morphologies. Total RNA was isolated using RNAwiz (Ambion, Austin, TX) according to the manufacturer's recommendations. The RNA pellet was dried at 22-25^{o}C and re-suspended in 30 µl of nuclease-free H_2O. RNA concentrations were calculated based on absorbance at the 260 nm wavelength. Purity and integrity of the RNA was determined from the 260:280 ratio and agarose gel electrophoresis.

Microarray Analysis

Affymetrix Porcine Chip

The GeneChip® Porcine Genome Array (Affymetrix, Santa Clara, CA) contains 23, 937 probe sets interrogating 23, 256 transcripts, representing 20, 201 genes. Four chips were used for each morphological stage of development (spherical, tubular, Day 12 filamentous (D12F) and Day 14 filamentous (D14F)). RNA utilized for each chip represented a unique pool of conceptus total RNA for the respective morphological stage of development. Prior to target labeling, RNA was further purified (RNeasy MinElute Cleanup, Qiagen, Valencia, CA). Target labeling, GeneChip® hybridization, scanning and quantitation were conducted by The University of Tulsa Microarray Core Facility. Affymetrix GeneChip Operating Software (GCOS version 1.1.1, Affymetrix, Santa Clara, CA) was used to quantitate each GeneChip®. The summary intensities for each probe were loaded into DNA-Chip Analyzer (dChip), version 1.3 for normalization, standardization, and analysis.

Normalization and Standardization

For normalization, dChip's method of invariant set normalization in which the chip with the median intensity value was used as the baseline against which the brightness of the remaining chips were adjusted in order to be of a comparable level. To reduce variance of expression level estimates by accounting for probe differences, standardization was conducted by calculating model-based expression indices (MBEI) using dChip's Perfect-Match (PM)-only model.

Log Transformation and Statistical Analysis

The MBEI were log base 2 transformed to approximate a normal distribution for each gene and provide measures by which to conduct the statistical analysis. Unpaired t-tests were calculated using dChip to evaluate differences between two groups. Analysis of gene expression was done to compare expression changes between all morphological stages of development utilized in the study. The false discovery rate (FDR) utilized to restrict the list of candidate genes was a *P* value less than 0.001 as determined by the unpaired t-test and a numerical change in expression of at least 2-fold for each morphological comparison evaluated.

GeneChip® Porcine Genome Array Re-annotation

The annotation was updated by utilizing the provided sequence from Affymetrix that was utilized in probe development. Through the utilization of BLAST [Altschul et al., 1990], a human accession number, based on homology, was assigned to each Affymetrix ID already correlated to each probe on the chip. The assignment of a human

accession number allowed a more elaborate analysis of the biological processes being regulated during this transition, by enabling the more effective use of software such as the Database for Annotation, Visualization and Integrated Discovery (DAVID).

Clustering Analysis

All genes determined to be significantly different based on the FDR indicated for at least one comparison between morphological stages of development (n = 1473) were utilized for analysis in Cluster 3.0 [Eisen et al., 1998]. We chose to sort the 1473 genes that were both statistically ($P < 0.001$) and numerically (± 2-fold change) different into 25 clusters. The 25 clusters were identified using the k-means learning algorithm following 1000 replications.

Database for Annotation, Visualization and Integrated Discovery

Database for Annotation, Visualization and Integrated Discovery (DAVID) version 2.0 (http://david.niaid.nih.gov/david/version2/index.htm) is a program that enables the utilization of microarray gene lists to generate specific functional annotations of the biological processes affected by the treatment as determined through microarray experiments [Glynn et al., 2003]. DAVID was utilized to annotate biological themes occurring during the two major developmental transitions during pig conceptus development; spherical to D12F and D12F to D14F. These two transitional stages are characteristic of trophoblastic elongation induction and initial conceptus-uterine attachment. All genes identified to be both significantly different ($P < 0.001$) and biologically different (± 2-fold change) for the spherical vs. D12F and D12F vs. D14F

comparisons, and also successfully assigned a human accession number, were used in the analysis via DAVID. Utilizing gene ontology (GO) terms as identified through biological process, cellular component and molecular function; as well as protein domain, and biochemical pathway membership; biological themes were generated by grouping like terms thereby creating annotation clusters associated with each developmental transition.

Quantitative One-Step RT-PCR

Quantitative RT-PCR analysis of transcripts of interest was conducted as previously described by our laboratory [Ashworth et al., 2006]. RNA from the same conceptus pools utilized for affymetrix analysis was aliquoted to be used for PCR analysis. Genomic DNA removal and the synthesis of cDNA to be used for quantitative analysis were done using the QuantiTect Reverse Transcription kit according to manufacturer's recommendations (Qiagen, Valencia, CA). Briefly, 0.8 μg of each embryo pool (n = 4 pools for each conceptus developmental stage) was added to a genomic DNA wipeout buffer for 5 min at 37^{o}C, followed by a 2 min incubation on ice, then proceeding to the addition of reverse transcription buffer, RT primer mix and reverse transcriptase; and incubated at 42^{o}C for 30 min. Individual and small pools of conceptuses were evaluated at the four morphologically distinct stages (spherical, tubular, D12F and D14F). The PCR amplification was conducted using the ABI PRISM 7700 Sequence Detection System (PE Applied Biosystems). The real-time detection during each amplification cycle was done by using either a sequence specific dual-labeled fluorescent probe designed to have a 5' reporter dye (6-FAM) and a 3' quenching dye (TAMRA) nested

between the forward and reverse sequence specific primers or the intercalating dye, SYBR green. All primers and probes utilized for quantitative analysis for each target gene are presented in Table 3.1. One hundred nanograms of synthesized cDNA were assayed for each sample in duplicate. Thermal cycling conditions using the dual labeled probe were 50^{o}C for 30 min, 95^{o}C for 15 min, followed by 40 repetitive cycles of 95^{o}C for 15 sec and a combined annealing/extension stage, 59^{o}C for 1 min. Fluorescent data acquisition was done during the annealing/extension phase when using the dual-labeled probes. Cycling conditions for SYBR green detection were 50^{o}C for 30 min and 95^{o}C for 15 min, followed by 40 repetitive cycles of 95 for 15^{o}C sec and variable annealing temperature for 30 sec, 72^{o}C for 33 sec and a variable temperature during fluorescent detection for 33 sec. Fluorescence detection temperature was determined by evaluating melting curve analysis for the samples and the no template control amplification plot. Detection temperatures were set at a temperature when the intended target was the only contributing factor to fluorescence. 18S ribosomal RNA was assayed as a normalization control to correct for loading discrepancies. Following RT-PCR, quantitation of gene amplification was made by determining the cycle threshold (C_T) based on the fluorescence detected within the geometric region of the semilog view of the amplification plot. Relative quantitation of target gene expression was evaluated using the comparative C_T method as previously described [Hettinger et al. 2001; Ashworth et al., 2006]. The ΔC_T value was determined by subtracting the target C_T of each sample from its respective ribosomal 18S C_T value. Calculation of $\Delta\Delta C_T$ involves using the single greatest sample ΔC_T value (the sample with the lowest expression) as an arbitrary constant to subtract from all other sample ΔC_T values. Relative mRNA units for each

sample were calculated assuming an amplification efficiency of 2 during the geometric region of amplification, and applying the equation, $2^{\Delta\Delta Ct}$. Relative units in figures 3.2A-3.2J are presented as mean ± SEM. To compare the expression patterns determined through QT-RT-PCR with that determined using microarray analysis, the mean relative mRNA units for tubular, D12F and D14F, as determined for each gene, were divided by the mean relative mRNA units for the spherical morphology to produce fold differences presented in Table 3.6.

Quantitation and Statistical Analysis

Normalized QT-RT-PCR ΔC_T values were analyzed using the PROC MIXED of the Statistical Analysis System. The statistical model used in the analysis tested the fixed effect of morphology (spherical, tubular**,** D12F and D14F). Significance ($P < 0.05$) was determined by probability differences of least squares means between morphological stages of development on normalized gene expression.

Table 3.1. Primer and probe sequence information for the quantitative amplification of each target gene.

Affymetrix ID[a]	Target[b]	Primers (Forward/Reverse)[c]	Fluorescent Reporter[d]	Amplicon Size[e]
Ssc.4093.1.A1_at	IFNγ	GGTAGCTCTGGGAAACTGAATGACTTCG TGCTCTCTGGCCTTGGAACATAGT	TCTGCAGATCCAGCGCAAAGCCATCAGTGA	174 bp
Ssc.11197.1.S1_at	HSP27	AAAGAGCACAGAGAGTTGGCAGGT GGCTTCATTTCCCGGTGTTTCACT	AGCAGCAGGGCGAAGGCCTTTACTTGGTT	304 bp
Ssc.13805.1.S1_at	Angiomotin	TTCCAGATCACACAGCACAGCGTT ACCCTGGACAAACTATGCAAGCCA	AGCGACATGGCCCAGGGCACATGCATTT	159 bp
Ssc.55.1.S1_at	Epidermal Growth Factor Receptor	ACACTTGATTCCACTGGCTCTGCT TGGCTTATCCTCTTGCACCTGACA	TGTCCCAGGCAGGCCCGATTGGTACTCTGT	132 bp
Ssc.27214.2.S1_at	Actinin α4	CCCTCACACATACACACACAA GGGCAAATCAGCTATGTCTTCA	ACATATCTCTGCCGCCTCTTGCTCCCGT	196 bp
Ssc.8594.1.A1_at	B-Cell Linker	CCTGCGCAGAAACCAATCCATCAA ATACAGCCTCTTCAGCTGACTTCCGA	SYBR Green	190 bp
Ssc.4984.1.S1_at	Chemokine Ligand 14	TCATCACCACCAAGAGCATGTCCA TCCAGGCGTTGTACCACTTGATGA	SYBR Green	102 bp
Ssc.9991.1.S1_at	Parathyroid Hormone Like Hormone	TGGCTGAACTGCAGCATGG ATACGTCCTCTGAAGGTCTCTGCT	SYBR Green	200 bp
Ssc.26693.1.S1_at	Maspin	TCCTTGGGTAGCAGGATGAGCATA ACCAAAGAATGCCCTTTCAGGGTC	SYBR Green	127 bp

[a]The Affymetrix ID refers to the ID given by Affymetrix for which the probe set was designed.
[b]The target gene name was determined through manual annotation of the EST sequence used by Affymetrix during the generation of the probe set.
[c]Forward and reverse primers for each target gene. The forward primer sequence is above the reverse for each target gene. Forward and reverse do not necessarily indicate the *in vivo* direction of transctiption.
[d]Either a dual-labeled probe (FAM-TAMRA) or the intercalating dye, SYBR Green was used to measure amount of amplified target during each cycle of quantitative RT-PCR.
[e]Amplicon size refers to the product size of the amplified PCR product.

Results

Affymetrix Analysis

Chips with more than 5% of probe sets flagged as array outliers are of suspect quality. dChip did not flag any of the arrays as an outlier (when fitted expression for the entire probe set has a standard error greater than 3 standard deviations from the mean when compared to the other chips). Accordingly, no tissue was re-hybridized to a new array nor was any array dropped from analysis. Single outliers are lone probes of unusual intensity within a chip. In this set of samples, outlier percentages ranged from 0.02% to 0.13%. Single outliers were treated as missing values in subsequent analyses. The percentage of genes called "present" by the GCOS software ranged from 65.49% to 70.37%. Table 3.2 lists the intensities, presence call percentages, and outlier percentages for each gene chip as produced by dChip. When the results from the six comparisons were combined, there were 3850 significantly altered probe sets of which 3759 remained after deleting those with an "absent" detection call across all chips in both comparison groups. When the results were restricted to unique GenBank Accession numbers, 3736 were found to differ significantly in their expression in one or more of the six comparisons. The number of statistically, as well as statistically and biologically different for each comparison between morphologies is present in Table 3.3.

GeneChip® Porcine Genome Array Re-annotation

Two comparisons, spherical vs. D12F and D12F vs. D14F were further analyzed due to their biological importance with respect to this stage of pregnancy. For the specific biological comparisons of interest, spherical vs. D12F and D12F vs. D14F, 280

Table 3.2. Intensities, percent present, and outliers for each AffyChip utilized during microarray analysis.

Array[a]	Median Intensity (unnormalized)[b]	"Present" Detection Call %[c]	Single Outlier %[d]
Spherical, Chip 1	129	66.64	0.02
Spherical, Chip 2	94	65.96	0.06
Spherical, Chip 3	95	65.83	0.04
Spherical, Chip 4	97	66.51	0.05
Tubular, Chip 5	100	67.48	0.04
Tubular, Chip 6	118	68.38	0.04
Tubular, Chip 7	114	65.49	0.06
Tubular, Chip 8	118	65.75	0.04
Day 12, Chip 9	99	68.45	0.03
Day 12, Chip 10	126	67.93	0.02
Day 12, Chip 11	127	66.10	0.10
Day 12, Chip 12	114	66.93	0.05
Day 14, Chip 13	98	69.14	0.13
Day 14, Chip 14	94	68.08	0.13
Day 14, Chip 15	93	67.20	0.08
Day 14, Chip 16	113	70.37	0.05

[a]Each morphological stage of development was hybridized to four chips.
[b]Unnormalized median target intensity for each chip. Prior to analysis in dChip, intensity for each chip was normalized by adjusting the brightness of each chip to be comparable to the median intensity; Day 14, Chip 16.
[c]Detection call percentage refers to the percentage of targets that were identified present for each chip.
[d]This column represents the percentage of individual outliers for each chip. Five percent or greater of individual probe set outliers would indicate an array of poor quality.

Table 3.3. Numbers of statistically different mRNA abundance for genes identified between morphological comparisons

Comparison[a]	N unique Genes[b]	N unique, ≥ 2-Fold Difference[c]	N unique, ↑ ≥ 2-Fold Difference[d]	N unique, ↓ ≥ 2-Fold Difference[d]
Spherical v Tubular	12	0	0	0
Spherical v Day 12	1367	482	177	305
Spherical v Day 14	1522	915	465	450
Tubular v Day 12	1048	433	127	306
Tubular v Day 14	1565	997	420	577
Day 12 v Day 14	708	232	152	80

[a]Represents the morphological comparison for each row.
[b]The number of genes with a unique identity based on the accession number utilized for the creation
[c]The number of unique genes that have at least a 2-fold difference in mRNA abundance between the two morphologies.
[d]The number of genes increasing or decreasing in mRNA abundance for a given comparison.

of 482 and 157 of 232 genes were successfully assigned a GenBank accession number for a homologous human gene, respectively. The human accession numbers assigned to each Affy ID representing a gene with statistical and biological differences are presented in the Appendix, Tables 7.1 and 7.2.

Database for Annotation, Visualization and Integrated Discovery

Analysis through Database for Annotation, Visualization and Integrated Discovery was conducted to allow detection of biological processes affected during the two major transitions; spherical vs. D12F and D12F vs. D14F. Several processes were consistent throughout this overall period of development but distinct differences were also notable. During the transition from spherical to D12F morphology, genes associated with lipid metabolism, phospholipid metabolism, localization/transport, locomotion/cell motility, ATP activity and binding, regulation of cell growth, amino acid utilization/metabolism, metal ion binding, and regulation of apoptosis were detected (Table 3.4). Transition of D12F to D14F morphology revealed that several biological themes were still persistent from the spherical to D12F transition. The regulation of apoptosis was the most prominent biological theme during the transition for D12F to D14F as three annotation clusters represented terms associated with apoptosis. Other critical processes appear to be those involved with protein kinase activity, regulation of cell cycle progression and other cell physiological processes, and chromosome organization (Table 3.5). The processes that appeared to be involved in both developmental transitions did differ in their significance ranking as determined through

Table 3.4. Functional annotation clusters of biological terms representing processes affected during the conceptus transition from spherical to D12F.

Annotation Cluster[a]	Enrichment Score[b]	Biological Terms[c]
1	2.81	phospholipid dephosphorylation(4), inositol or phosphatidylinositol phosphatase activity (5), lipid modification (4)
2	2.68	metal ion binding (68), ion binding (68), cation binding (63)
3	2.10	localization (9), establishment of localization (9), transport (9)
4	1.88	membrane lipid biosynthesis (6), phospholipid biosynthesis (5), phospholipid metabolism (5), membrane lipid metabolism (6)
5	1.68	locomotion (9), cell motility (9), localization of cell (9)
6	1.59	positive regulation of cellular process (16), positive regulation of cellular physiological process (13), positive regulation of biological process (16), positive regulation of physiological process (13)
7	1.50	adenyl nucleotide binding (29), ATP binding (28), purine nucleotide binding (34), nucleotide binding (36)
8	1.45	ATPase activity, coupled to movement of substances (8), ATPase activity, coupled to transmembrane movement of substances (8), hydrolase activity, acting on acid anhydrides, catalyzing transmembrane movement of substances (8), ATPase activity, coupled (10), ATPase activity (10), pyrophosphatase activity(12), hydrolase activity, acting on acid anhydrides, in phosphorus-containing anhydrides (12), hydrolase activity, acting on acid anhydrides (12), nucleoside-triphosphatase activity (10)
9	1.38	growth (8), regulation of cell growth (6), regulation of growth (6), cell growth (6), regulation of cell size (6)
10	1.32	amino acid transport (5), amine transport (5), carboxylic acid transport (5), organic acid transport (5), amino acid transporter activity (4), amine transporter activity (4), carboxylic acid transporter activity (4), organic acid transporter activity (4), polyamine transporter activity (3)
11	1.28	amino acid and derivative metabolism (10), amino acid metabolism (9), amine metabolism (10), nitrogen compound metabolism (10)
12	1.23	acyltransferase activity (6), transferase activity, transferring groups other than amino-acyl groups (6), transferase activity, transferring acyl groups (6)
13	1.11	calcium ion transporter activity (3), di-, tri-valent inorganic cation transporter activity (3), metal ion transporter activity (4)
14	1.06	channel or pore class transporter activity (11), alpha-type channel activity (10), ion channel activity (9)
15	0.86	regulation of apoptosis (10), regulation of programmed cell death (10), apoptosis (12), programmed cell death (12), cell death (12), death (12)

[a]The fifteen most significant annotation clusters identified based on the gene list submitted for analysis through DAVID.

[b]The enrichment score is determined through DAVID and ranks the significance of each annotation cluster based on the relatedness of the terms and the genes associated with them.

[c]This column represents terms in the annotation clusters. The gene ontology (GO) terms were gathered based on the known annotation of the submitted genes with respect to biological process, cellular component, and molecular function; as well as biological pathway membership and protein domains.

Table 3.5. Functional annotation clusters of biological terms representing processes affected during the conceptus transition from D12F to D14F.

Annotation Cluster[a]	Enrichment Score[b]	Biological Terms[c]
1	2.79	apoptosis (12), programmed cell death (12), cell death (12), death (12)
2	1.75	regulation of cellular process (36), regulation of cellular physiological process (33), regulation of biological process (36), regulation of physiological process (33)
3	1.62	negative regulation of biological process (12), negative regulation of cellular process (11), negative regulation of cellular physiological process (10), negative regulation of physiological process (10)
4	1.60	positive regulation of cellular process (10), positive regulation of biological process (10), positive regulation of cellular physiological process (8), positive regulation of physiological process (8)
5	1.43	protein kinase inhibitor activity (3), kinase inhibitor activity (3), protein kinase regulator activity (3), kinase regulator activity (3)
6	1.37	regulation of progression through cell cycle (8), regulation of cell cycle (8), cell cycle (10)
7	1.07	cellular physiological process (85), physiological process (91), cellular process (91)
8	1.07	induction of apoptosis (4), induction of programmed cell death (4), positive regulation of apoptosis (4), positive regulation of programmed cell death (4)
9	0.99	negative regulation of apoptosis (4), negative regulation of programmed cell death (4), anti-apoptosis (3)
10	0.77	intracellular membrane-bound organelle (52), membrane-bound organelle (52), intracellular organelle (59), organelle (59), intracellular (69)
11	0.73	heparin binding (3), glycosaminoglycan binding (3), polysaccharide binding (3), pattern binding (3), carbohydrate binding (3)
12	0.72	chromosome organization and biogenesis (sensu Eukaryota) (5), establishment and/or maintenance of chromatin architecture (4), DNA packaging (4)
13	0.66	locomotion (4), cell motility (4), localization of cell (4)
14	0.64	metal ion binding (30), ion binding (30), cation binding (28)
15	0.63	regulation of kinase activity (3), regulation of protein kinase activity (3), regulation of transferase activity (3), regulation of enzyme activity (4)

[a]The fifteen most significant annotation clusters identified based on the gene list submitted for analysis through DAVID.

[b]The enrichment score is determined through DAVID and ranks the significance of each annotation cluster based on the relatedness of the terms and the genes associated with them.

[c]This column represents terms in the annotation clusters. The gene ontology (GO) terms were gathered based on the known annotation of the submitted genes with respect to biological process, cellular component, and molecular function; as well as biological pathway membership and protein domains.

DAVID. While cell motility/locomotion ranked high and apoptosis regulation ranked low during the spherical to D12F transition, apoptosis was of the most prominent themes during the D12F to D14F transition while cell motility/locomotion was much less distinguished (Tables 3.4 and 3.5).

Clustering Analysis

The 25 clusters generated utilizing the K-means clustering algorithm were distinguishable by their expression patterns and represented the 1473 genes that were determined to meet the FDR threshold for one or more of the comparisons between the morphological stages of development. The smallest cluster contained 3 genes while the largest contained 364 genes. The mean cluster size was nearly 59 genes; however, the median cluster size was 19 genes suggesting that most of the clusters represented unique expression patterns and a few larger clusters represented general trends (Figure 3.1). Expression patterns that displayed a transient shift in expression during the spherical to D12F transition are represented by clusters 4, 7, 14, 21, 24. Clusters 4, 14, 21, and 24 represent 17, 10, 3 and 76 genes, respectively, whose expression was greatest in the elongating D12F conceptuses; while cluster 7 represented 88 genes whose expression was at a transient nadir in D12F conceptuses. The affymetrix ID, associated human GenBank accession number, putative identity for each gene and expression profile is listed for each gene that was significantly ($P < 0.001$) and biologically different (> 2-fold change) between any two developmental stages are listed in association with their k-means cluster in the Appendix, Table 7.3.

Figure 3.1. Twenty-five clusters were generated using the k-means clustering algorithm to associate genes with similar expression patterns from the transition from spherical to D14F. The 1473 genes determined to be both significantly and biologically different between at least one of the comparisons of morphological stage of development produced an average cluster size of 59 genes and a median cluster of 19 genes. Note that five clusters indicate genes whose peak or nadir expression occurs during the D12F morphological stage of development (clusters 4, 7, 14, 21 and 24). The number of genes associated with each cluster is indicated in the title of each chart.

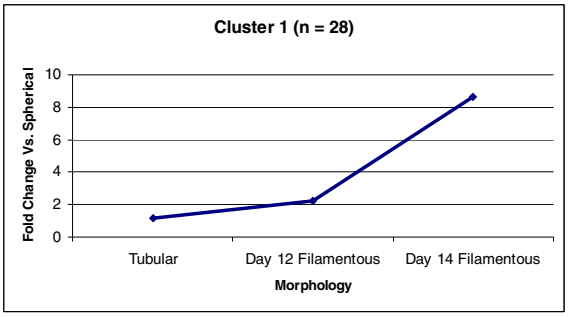
Cluster 1 (n = 28)
Fold Change Vs. Spherical
10
8
6
4
2
0
Tubular
Day 12 Filamentous
Day 14 Filamentous
Morphology

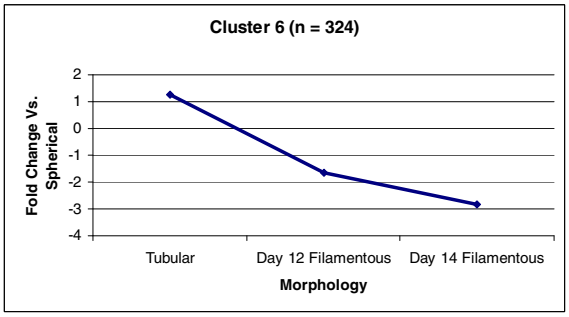
Cluster 6 (n = 324)
Fold Change Vs. Spherical
2
1
0
-1
-2
-3
-4
Tubular
Day 12 Filamentous
Day 14 Filamentous
Morphology

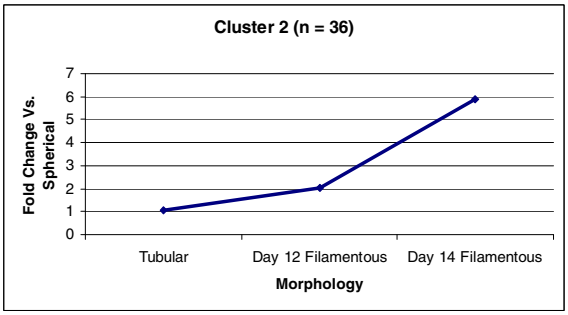
Cluster 2 (n = 36)
Fold Change Vs. Spherical
7
6
5
4
3
2
1
0
Tubular
Day 12 Filamentous
Day 14 Filamentous
Morphology

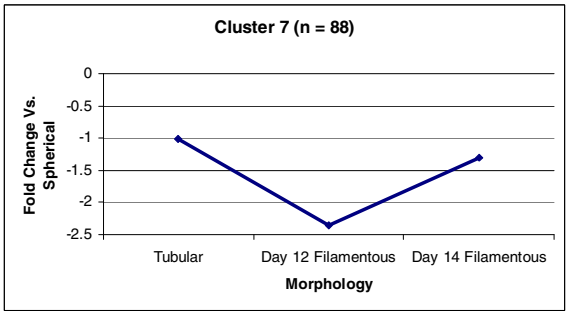
Cluster 7 (n = 88)
Fold Change Vs. Spherical
0
-0.5
-1
-1.5
-2
-2.5
Tubular
Day 12 Filamentous
Day 14 Filamentous
Morphology

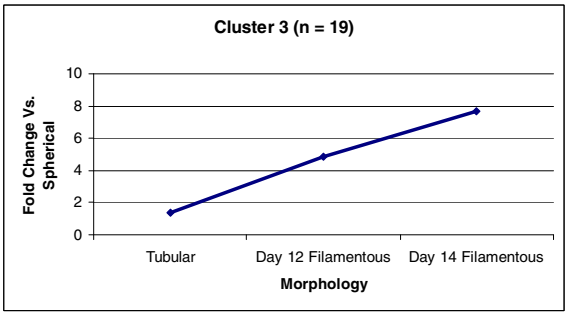
Cluster 3 (n = 19)
Fold Change Vs. Spherical
10
8
6
4
2
0
Tubular
Day 12 Filamentous
Day 14 Filamentous
Morphology

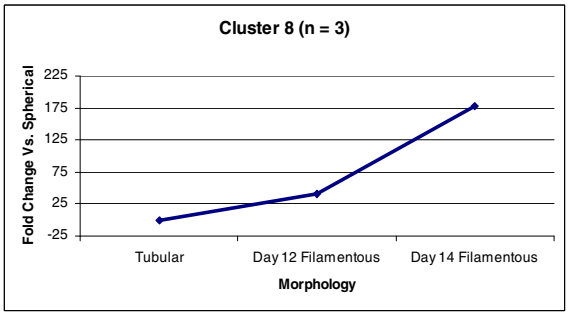
Cluster 8 (n = 3)
Fold Change Vs. Spherical
225
175
125
75
25
-25
Tubular
Day 12 Filamentous
Day 14 Filamentous
Morphology

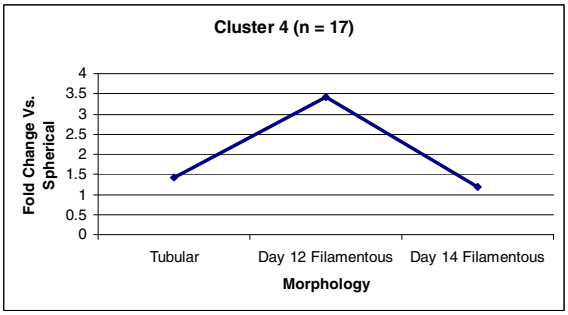
Cluster 4 (n = 17)
Fold Change Vs. Spherical
4
3.5
3
2.5
2
1.5
1
0.5
0
Tubular
Day 12 Filamentous
Day 14 Filamentous
Morphology

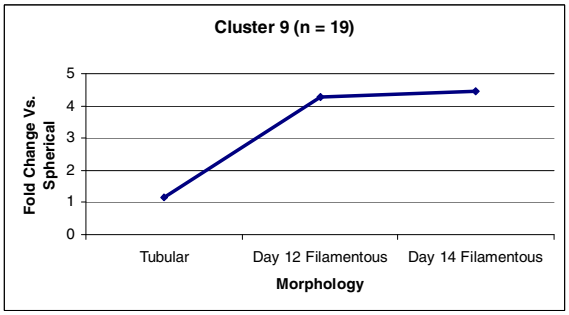
Cluster 9 (n = 19)
Fold Change Vs. Spherical
5
4
3
2
1
0
Tubular
Day 12 Filamentous
Day 14 Filamentous
Morphology

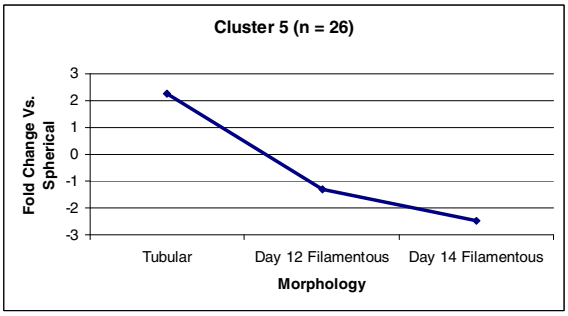
Cluster 5 (n = 26)
Fold Change Vs. Spherical
3
2
1
0
-1
-2
-3
Tubular
Day 12 Filamentous
Day 14 Filamentous
Morphology

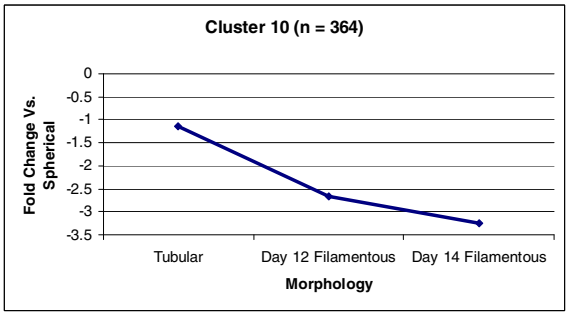
Cluster 10 (n = 364)
Fold Change Vs. Spherical
0
-0.5
-1
-1.5
-2
-2.5
-3
-3.5
Tubular
Day 12 Filamentous
Day 14 Filamentous
Morphology

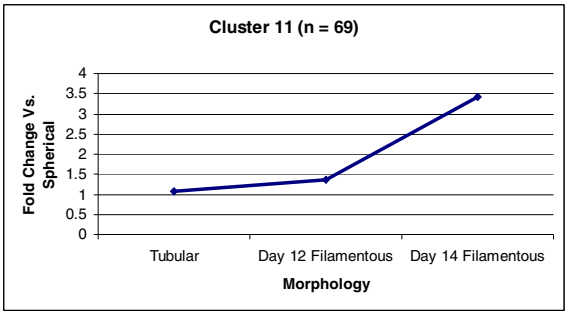
Cluster 11 (n = 69)
Fold Change Vs. Spherical
4
3.5
3
2.5
2
1.5
1
0.5
0
Tubular
Day 12 Filamentous
Day 14 Filamentous
Morphology

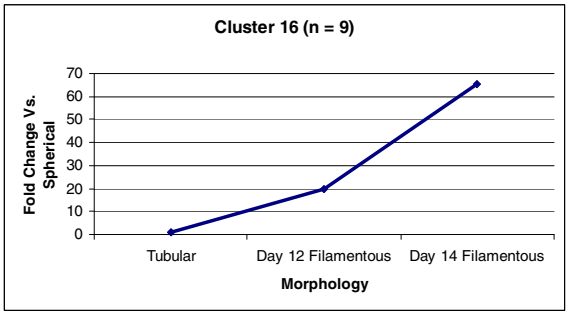
Cluster 16 (n = 9)
Fold Change Vs. Spherical
70
60
50
40
30
20
10
0
Tubular
Day 12 Filamentous
Day 14 Filamentous
Morphology

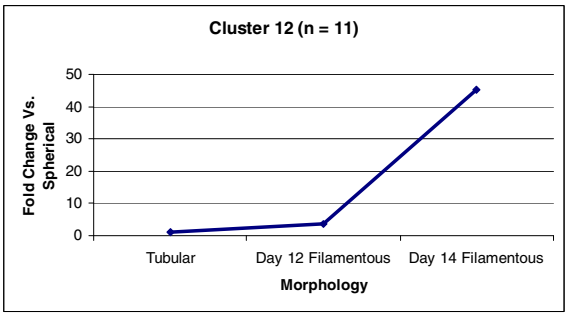
Cluster 12 (n = 11)
Fold Change Vs. Spherical
50
40
30
20
10
0
Tubular
Day 12 Filamentous
Day 14 Filamentous
Morphology

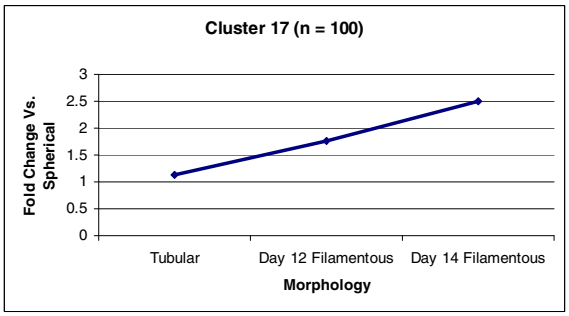
Cluster 17 (n = 100)
Fold Change Vs. Spherical
3
2.5
2
1.5
1
0.5
0
Tubular
Day 12 Filamentous
Day 14 Filamentous
Morphology

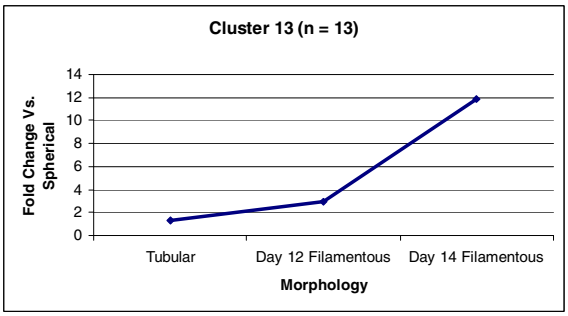
Cluster 13 (n = 13)
Fold Change Vs. Spherical
14
12
10
8
6
4
2
0
Tubular
Day 12 Filamentous
Day 14 Filamentous
Morphology

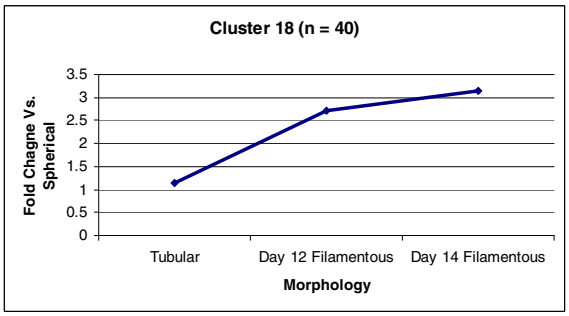
Cluster 18 (n = 40)
Fold Chagne Vs. Spherical
3.5
3
2.5
2
1.5
1
0.5
0
Tubular
Day 12 Filamentous
Day 14 Filamentous
Morphology

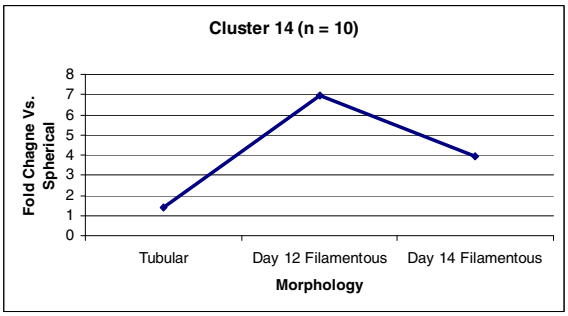
Cluster 14 (n = 10)
Fold Chagne Vs. Spherical
8
7
6
5
4
3
2
1
0
Tubular
Day 12 Filamentous
Day 14 Filamentous
Morphology

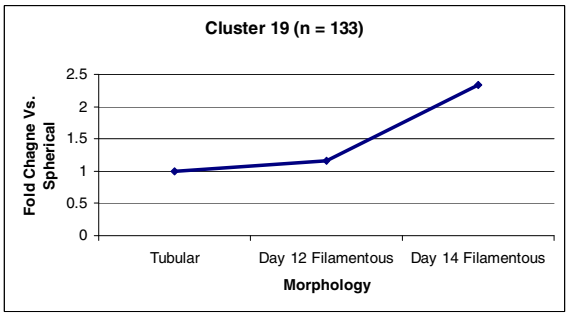
Cluster 19 (n = 133)
Fold Chagne Vs. Spherical
2.5
2
1.5
1
0.5
0
Tubular
Day 12 Filamentous
Day 14 Filamentous
Morphology

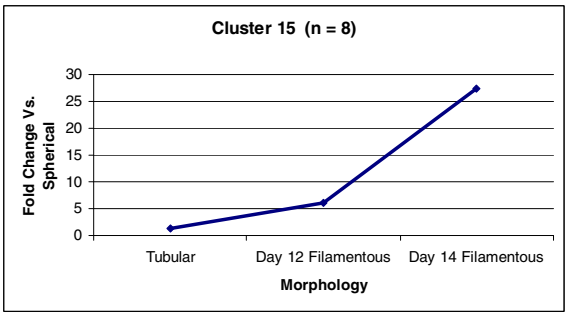
Cluster 15 (n = 8)
Fold Change Vs. Spherical
30
25
20
15
10
5
0
Tubular
Day 12 Filamentous
Day 14 Filamentous
Morphology

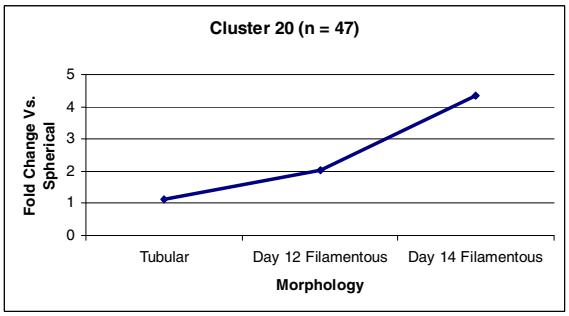
Cluster 20 (n = 47)
Fold Change Vs. Spherical
5
4
3
2
1
0
Tubular
Day 12 Filamentous
Day 14 Filamentous
Morphology

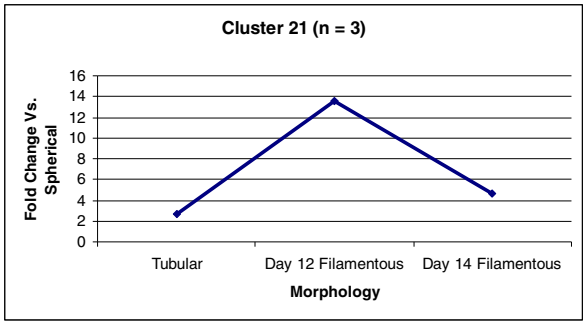
Cluster 21 (n = 3)
Fold Change Vs. Spherical
16
14
12
10
8
6
4
2
0
Tubular
Day 12 Filamentous
Day 14 Filamentous
Morphology

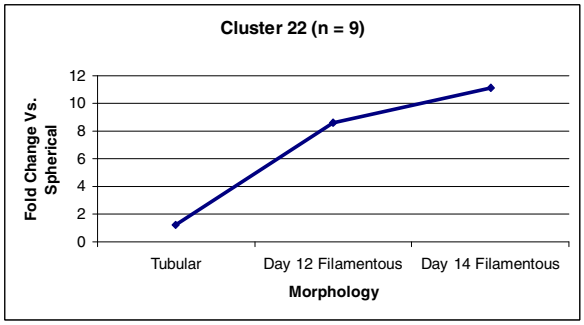
Cluster 22 (n = 9)
Fold Change Vs. Spherical
12
10
8
6
4
2
0
Tubular
Day 12 Filamentous
Day 14 Filamentous
Morphology

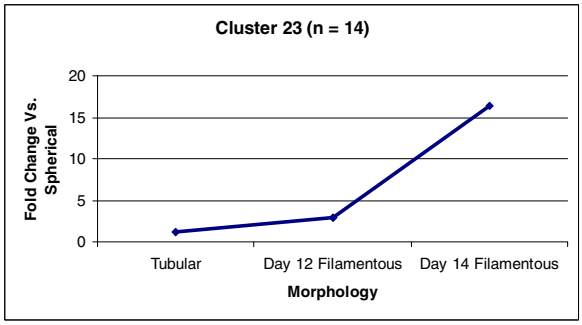
Cluster 23 (n = 14)
Fold Change Vs. Spherical
20
15
10
5
0
Tubular
Day 12 Filamentous
Day 14 Filamentous
Morphology

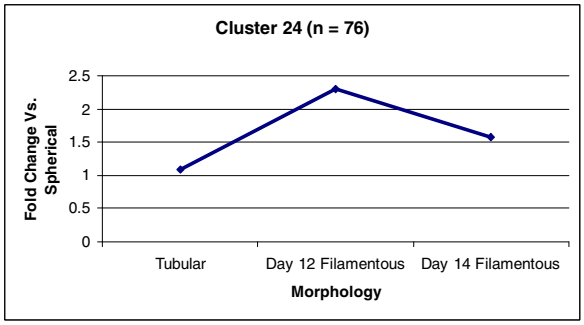
Cluster 24 (n = 76)
Fold Change Vs. Spherical
2.5
2
1.5
1
0.5
0
Tubular
Day 12 Filamentous
Day 14 Filamentous
Morphology

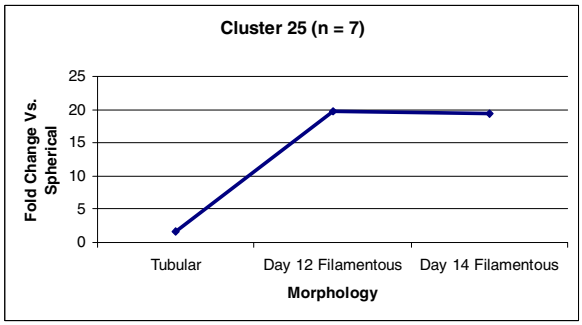
Cluster 25 (n = 7)
Fold Change Vs. Spherical
25
20
15
10
5
0
Tubular
Day 12 Filamentous
Day 14 Filamentous
Morphology

Quantitative Two-Step RT-PCR

Based on the evaluation through DAVID and k-means clustering, differences in mRNA abundances between the four conceptus developmental stages were further quantified using the two-step method for QT-RT-PCR. Messenger RNA's that were evaluated using this method are listed in association with the primer/probe sequences used for detection (Table 3.1). Quantitative gene expression was done to analyze expression of interferon-γ (IFNγ), heat shock protein 27 kDa (HSP27), angiomotin, epidermal growth factor receptor (EGFR), and actinin α4 (ACTN4), B-cell linker (BLNK), chemokine ligand 14 (CXCL14), parathyroid hormone like hormone (PTHrP) and maspin. The expression patterns for IFNγ, HSP27, and angiomotin, BLNK, CXCL14, PTHrP and maspin mRNA, as determined by quantitative RT-PCR, were similar to that determined by microarray analysis while expression patterns for EGFR and ACTN4 differed slightly between the two techniques (Table 3.6).

Interferon-γ

An effect of morphology ($P < 0.001$) was observed regarding IFNγ mRNA abundance during early conceptus development. The expression was not different between spherical and tubular morphologies. However, there was an approximate 150- and 570-fold increase in gene expression in D12F and D14F conceptuses, respectively, when compared to spherical development (Figure 3.2A).

Table 3.6. Results from quantitative RT-PCR in comparison with Affymetrix Results.

		Fold Change[§]				
Target[¶]	**Method[#]**	**Spherical**	**Tubular**	**D 12 Filamentous**	**D 14 Filamentous**	**P Value[*]**
IFNγ	QT-RT-PCR	1.0[a]	2.6[a]	143.2[b]	566.8[b]	< 0.001
	AffyChip	1.0[a]	1.0[ab]	4.3[b]	4.8[b]	< 0.001
HSP27	QT-RT-PCR	1.0[a]	8.4[b]	30.8[c]	31.2[c]	< 0.002
	AffyChip	1.0[a]	1.2[a]	4.1[b]	4.8[b]	< 0.002
Angiomotin	QT-RT-PCR	1.0[a]	4.1[b]	15.8[c]	23.6[c]	< 0.001
	AffyChip	1.0[a]	1.1[a]	4.4[b]	4.7[b]	< 0.001
Epidermal Growth Factor Receptor	QT-RT-PCR	1.0[a]	3.5[b]	1.5[ab]	3.3[b]	0.026
	AffyChip	1.0[a]	1.1[a]	-2.2[b]	1.1[a]	< 0.001
Actinin α4	QT-RT-PCR	1.0[a]	3.4[ab]	2.5[ab]	6.6[b]	0.045
	AffyChip	1.0[a]	-1.2[ab]	-2.0[b]	-1.3[ab]	< 0.001
B-Cell Linker	QT-RT-PCR	1.0[a]	1.4[a]	-9.8[b]	-2.8[b]	0.002
	AffyChip	1.0[a]	-2.0[a]	-28.8[b]	-17.3[b]	< 0.001
Chemokine Ligand 14	QT-RT-PCR	1.0[a]	4.2[ab]	27.4[b]	1285.1[c]	< 0.001
	AffyChip	1.0[a]	-1.0[a]	1.9[a]	36.7[b]	< 0.001
Parathyroid Hormone Like Hormone	QT-RT-PCR	1.0[a]	3.4[a]	54.6[b]	140.4[b]	< 0.001
	AffyChip	1.0[a]	1.2[ab]	16.9[bc]	20.3[c]	< 0.001
Maspin (Serpin Peptidase Inhibitor)	QT-RT-PCR	1.0[a]	3.6[b]	-1.7[ac]	-2.3[c]	0.004
	AffyChip	1.0[a]	-1.1[a]	-5.2[b]	-5.9[b]	< 0.001

[¶]Primer and probe sets were designed to specifically assay each of the targets using fluorescent probes.
[#]The method for which the data was generated to determine fold differences in gene expression.
[§]Fold differences were determined by using dChip for Affymetrix analysis while the comparative C_T method was utilized for determining fold differences from the QT-RT-PCR. Fold differences within a row without a common superscript differ significantly ($P < 0.05$).
[*]Statistical analysis was performed in dChip for Affymetrix analysis and LS Means of PROC MIXED in SAS for quantitative RT-PCR as described in the *Materials and Methods*

Heat Shock Protein 27 kDa

HSP27 mRNA abundance was affected by morphological stage of development ($P < 0.002$). Expression increased about 8-fold in tubular conceptuses compared to those in spherical morphology (Table 3.6, Figure 3.2B). Messenger RNA abundance continued to increase with concetpus development as expression was approximately 5-fold greater in D12F and D14F compared to tubular conceptuses (Figure 3.2B)

Angiomotin

The expression of angiomotin was affected by morphological stage of development ($P < 0.001$). Messenger RNA abundance increased steadily with a 3.8-, 15.8-, and 28.0-fold greater expression in tubular, D12F and D14F compared to spherical stage of development (Table 3.6, Figure 3.2C).

Epidermal Growth Factor Receptor

Gene expression of EGFR was affected by morphological stage of development ($P < 0.026$). Conceptus EGFR expression was greatest in tubular and D14F conceptuses, with a 3.5- and 3.3-fold greater mRNA abundance compared to spherical conceptuses. However, expression in D12F conceptuses was not different from any other morphological stage of development (Table 3.6, Figure 3.2D).

Actinin α4

The ACTNα4 gene expression profile was inversed compared to the expression profile generated by microarray hybridizations (Table 3.6). While a significant

morphological effect ($P < 0.045$) was detected, there were no differences between spherical, tubular and D12F conceptuses while D14F was significantly (5.9-fold) greater in D14F conceptuses compared to spherical (Figure 3.2E).

B-cell Linker

Expression of BLNK was affected by morphological stage of development ($P < 0.002$). While mRNA abundance was not different between spherical and tubular conceptuses, there as a significant 9.8 and 2.8-fold reduction in D12F and D14F conceptuses in comparison to those spherical in morphology (Table 3.6, Figure 3.2F).

Chemokine Ligand 14

There was a morphological affect ($P < 0.001$) on CXCL14 mRNA abundance during trophoblastic elongation and attachment to the uterine LE. Expression was not different between spherical and tubular conceptuses. However, mRNA expression increased 27- and 1285-fold in D12F and D14F conceptuses in comparison to those morphologically spherical, respectively (Table 3.6, Figure 3.2G).

Parathyroid Hormone Like Hormone

PTHrP was significantly different between morphological stages of development ($P < 0.001$). While expression was not different between spherical and tubular morphologies or D12F and D14F conceptuses, there was an approximate 16-fold increase during the tubular to D12F transition ($P < 0.003$) and remaining elevated in the D14F conceptuses (Table 3.6, Figure 3.2H).

Maspin

Maspin mRNA abundance was affected by morphology ($P < 0.004$). While the expression pattern was consistent with the microarray data in that mRNA abundance was lower ($P < 0.05$) in D14F conceptuses compared to their spherical counterparts, QT-RT-PCR demonstrated that tubular conceptuses had the greatest maspin expression ($P < 0.04$), being at least 3.6-fold greater compared to all other morphological stages of development (Table 3.6, Figure 3.2I).

Discussion

Conceptus and endometrial changes during the peri-implantation development in the pig are critical for successfully establishing pregnancy and minimizing prenatal mortality throughout the gestation period [Pope et al., 1994]. Trophoblastic elongation is among the most critical events during early gestation in the pig. Conceptus expansion throughout the extensive uterine horns of the pig is essential for delivery of the maternal recognition signal, estrogen, which stages the uterine surface area that each individual conceptus is allowed to attach and develop within throughout gestation. The extent of initial trophoblastic elongation establishes whether adequate downstream nutrient flow between the dam and the conceptuses can occur throughout gestation, impacting conceptus survivability [Stroband and Van der Lende, 1990].

Utilization of the Affymetrix GeneChip® Porcine Genome Array allowed the identification of numerous factors that are differentially expressed during the transition through the multiple developmental stages during early pregnancy in the pig.

Figure 3.2 A significant morphological effect on relative mRNA units (mean ± SEM) was detected for IFNγ (A, $P < 0.001$), HSP27 (B, $P = 0.002$), angiomotin (C, $P < 0.001$), EGFR (D, $P = 0.026$), ACTN4 (E, $P = 0.045$), BLNK (F, $P = 0.002$), CXCL14 (G, $P < 0.001$), PTHrP (H, $P < 0.001$), and maspin (I, $P < 0.004$) during the porcine conceptus trophoblastic elongation and trophectoderm attachment to the uterine luminal epithelium. Abundance of mRNA was calculated from the real-time PCR analysis as described in *Materials and Methods*. Relative mRNA abundance is presented as mean ± SEM. Bars with without a common superscript represent a statistical difference between morphological stages of development ($P < 0.05$).

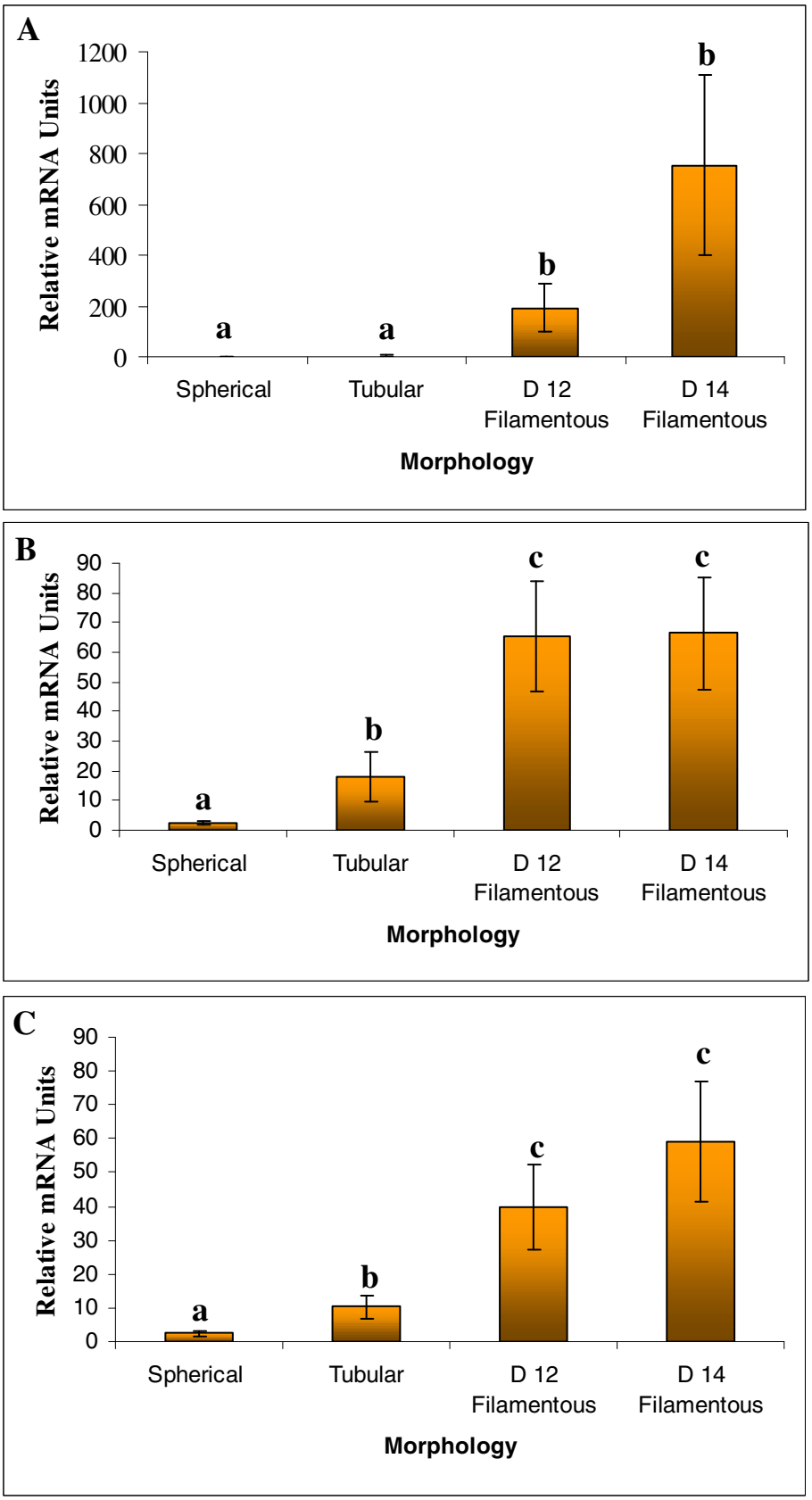
A
Relative mRNA Units
1200
1000
800
600
400
200
0
a
a
b
b
Spherical
Tubular
D 12 Filamentous
D 14 Filamentous
Morphology
B
Relative mRNA Units
90
80
70
60
50
40
30
20
10
0
a
b
c
c
Spherical
Tubular
D 12 Filamentous
D 14 Filamentous
Morphology
C
Relative mRNA Units
90
80
70
60
50
40
30
20
10
0
a
b
c
c
Spherical
Tubular
D 12 Filamentous
D 14 Filamentous
Morphology

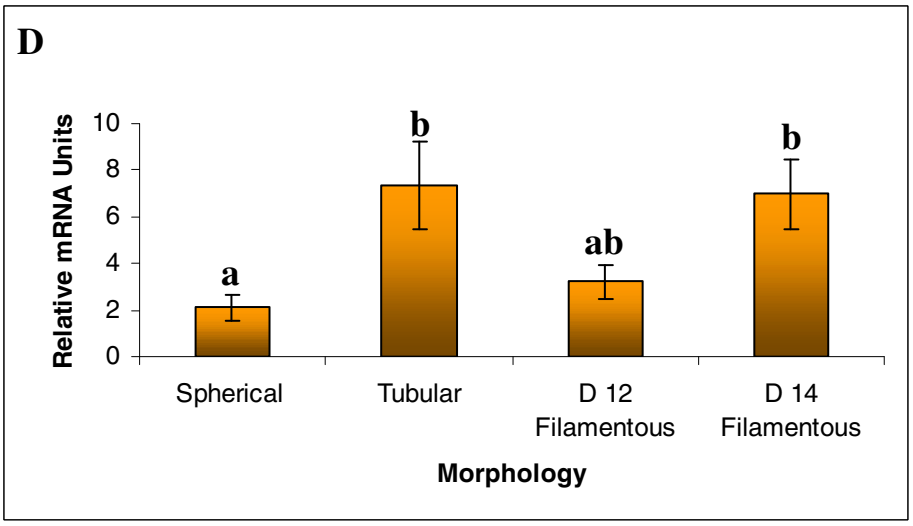
D
Relative mRNA Units
10
8
6
4
2
0
a
b
ab
b
Spherical
Tubular
D 12 Filamentous
D 14 Filamentous
Morphology

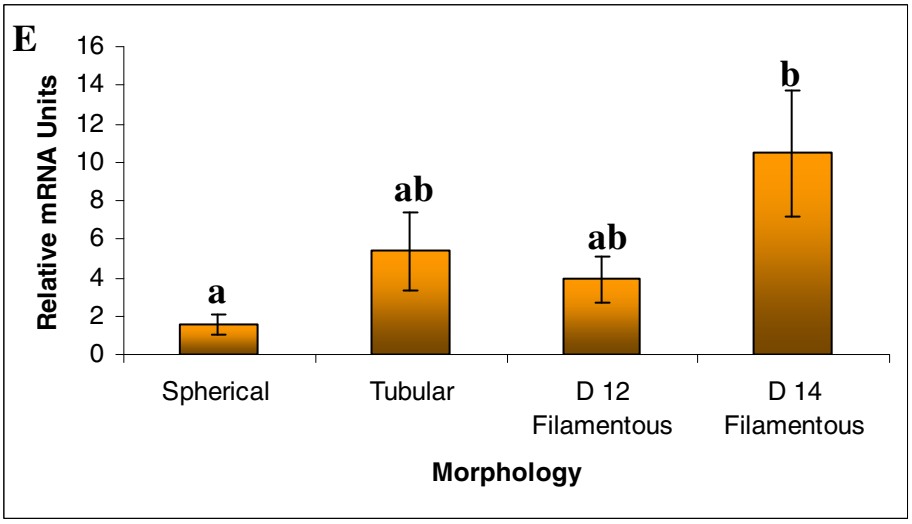
E
Relative mRNA Units
16
14
12
10
8
6
4
2
0
a
ab
ab
b
Spherical
Tubular
D 12 Filamentous
D 14 Filamentous
Morphology

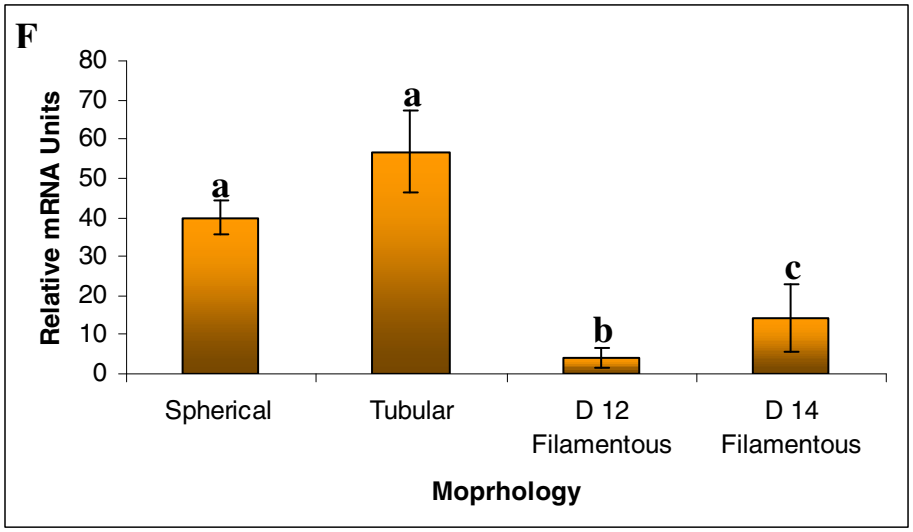
F
Relative mRNA Units
80
70
60
50
40
30
20
10
0
a
a
b
c
Spherical
Tubular
D 12 Filamentous
D 14 Filamentous
Moprhology

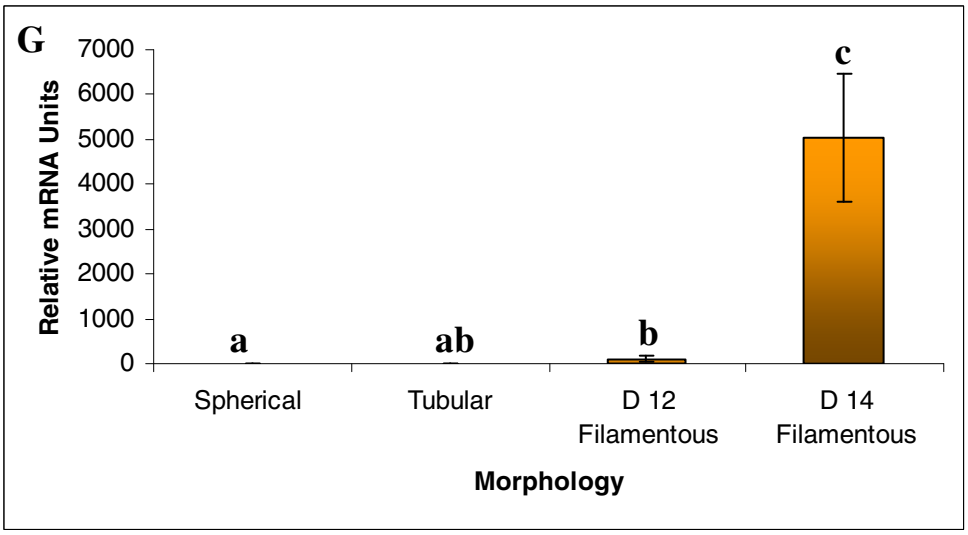
G
Relative mRNA Units
7000
6000
5000
4000
3000
2000
1000
0
a
ab
b
c
Spherical
Tubular
D 12 Filamentous
D 14 Filamentous
Morphology

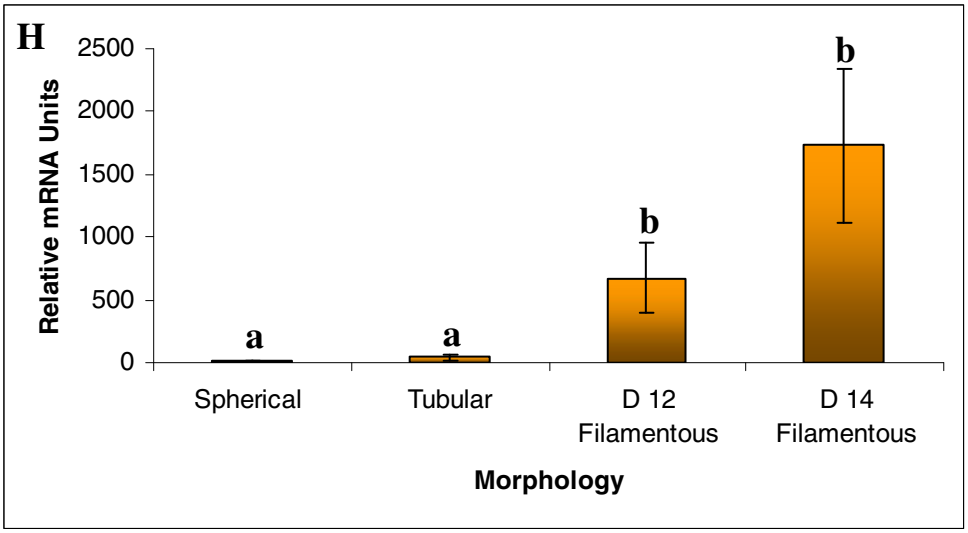
H
Relative mRNA Units
2500
2000
1500
1000
500
0
a
a
b
b
Spherical
Tubular
D 12 Filamentous
D 14 Filamentous
Morphology

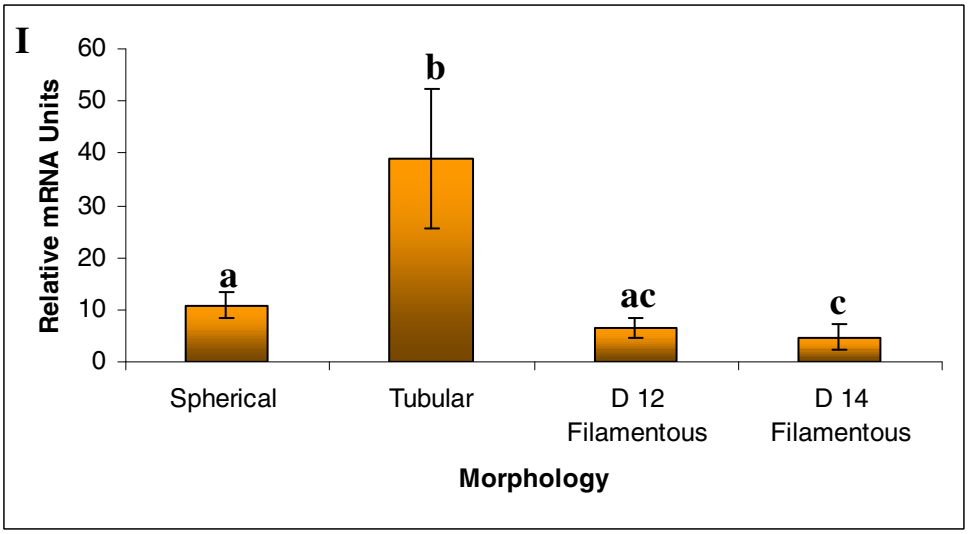
I
Relative mRNA Units
60
50
40
30
20
10
0
a
b
ac
c
Spherical
Tubular
D 12 Filamentous
D 14 Filamentous
Morphology

Interestingly, as determined through the statistical analysis using dChip, there were no genes detected during the transition from spherical to tubular morphology (Table 3.3) that met the FDR criteria, whereas targets for 482 probes had different abundance levels between spherical and D12F morphologies. The lack of significant gene expression changes detected during the spherical to tubular transition while a large transcriptional change is present between D12F versus spherical conceptuses suggests the initial trophectodermal remodeling is not dependant on large transcriptional changes. Also, transcriptional differences between conceptuses being 8, 9 and 10 mm in diameter were not detected as these morphologies were pooled to collectively represent the spherical morphoblogical stage of development. It is possible that changes in gene expression in between 8 mm to 10 mm spherical conceptuses could contribute to the initiation of trophoblastic elongation. It is alsp possible that the initiation of trophoblastic remodeling may be the result of an in place mechanism requiring instigation once specific developmental landmarks are achieved. Perhaps very subtle changes in expression of select genes may be capable of initiating trophectoderm remodeling. While D14F conceptuses are still elongating to some degree, it is not as rapid as the initial several hundred millimeters of the spherical to D12F transition. However, the D14F conceptuses represent the stage of conceptus development which trophoblast attachment to the uterine lumenal epithelia occurs. During this initial attachment to the uterine endometrium, 232 genes had at least a 2-fold change in mRNA abundance. These genes likely represent factors associated with ending elongation, placental differentiation and conceptus-uterine crosstalk.

As no differences between spherical and tubular were detected, the transitions from spherical to D12F and D12F to D14F were the two developmentally critical comparisons whose gene lists were utilized for biological annotation in DAVID. Based on the enrichment score, the most significant processes affected from spherical to D12F were related to lipid and membrane metabolism/biosynthesis as well as cell motility and locomotion. This seems plausible in that visually, conceptuses collected that are in early stages of elongation appear more fluid, with filipodia extending from trophectodermal cells within an elongation zone of the conceptus trophectoderm aiding in the elongation process [Geisert et al., 1982c]. The alterations in genes during the period also suggest the involvement of significant ATP utilization, cell growth factors, amino acid transport and the regulation of apoptosis, (Table 3.4). It is logical that the dramatic increase in conceptus mass from spherical to D12F is a result of energy catabolism and several cell growth factors contribute the morphological change. Interestingly, as DAVID ranks the significance of each cluster, apoptosis related genes were ranked low in the spherical vs. D12F transition but apoptosis represented clusters 1, 8 and 9 in the D12F to D14F transition suggesting the critical nature apoptosis may play regarding conceptus development during attachment to the uterine epithelium. However, it is difficult to ascertain whether gene expression changes are specific to the trophectoderm or inner cell mass or both. Overall, the processes identified in the transition of D12F to D14F compared to spherical to D12F involved more complicated processes, which is expected as conceptus complexity is greatly increased during these two days of development; such as the attachment to the uterine epithelium, neurulation of the inner cell mass, as well as

cell lineage branching in preparation for early organ development of the ICM and the differentiation of placental layers from the single trophectoderm.

Clustering analysis is critical in the ability to identify expression patterns for specific genes allowing the identification of associations between genes that may be regulated by a similar mechanism. This transient expression pattern associated with the rapid stage of trophectoderm remodeling (clusters 4, 7, 14, 21 and 24) would indicate those genes that could be considered as putative markers of trophoblastic elongation. Thus, these markers of trophoblastic elongation are targets for exploration regarding biological function during this stage of conceptus development to determine their effect during the establishment of pregnancy.

Quantitative RT-PCR was utilized to evaluate gene expression differences and confirm the expression patterns of multiple genes associated with DAVID annotation clusters of interests, k-means clusters suggestive of particular biological importance and genes that are of interest based on their potential roles in early porcine conceptus development according to literature. To name a few; PTGS2 [Wilson et al., 2002], steroidogenic acute regulatory factor [Blomberg et al., 2005], transforming growth factor β [Gupta et al., 1996], epidermal growth factor receptor [Vaughn et al., 1992], interferon-γ [La Bonnardiere et al., 2002], and retinol binding protein [Yelich et al., 1997a] are among the many genes previously identified to be differentially regulated during early peri-implantation conceptus development in the pig that have also been identified as differentially expressed during or after trophoblastic elongation in this communication. However, this approach to the analysis of gene expression during trophoblastic

elongation has allowed a tremendous amount of new information regarding this developmental phenomenon.

PDZ-LIM binding proteins are capable of linking LIM binding proteins to the cytoskeleton. Numerous genes identified in this communication possess intact PDZ-LIM domains (Appendix, Table A.3). Intact PDZ and LIM domains allow colocalization with β1-integrins and α-actinin, and attachment to collagen and fibrinogen; all components of the uterine epithelium extracellular matrix [Burghardt et al., 1997; Jaeger et al., 2001], potentially regulating epithelial cell motility [Loughran et al., 2005]. Collectively, the association of so many genes that are differentially regulated during the transition of spherical to D12F that are related to and have the ability to interact with F-actin through PDZ-LIM domains is suggestive to their contribution to trophoblastic cellular remodeling.

Prostaglandin synthase-2 (PTGS-2) gene expression has been previously reported to increase in pig conceptuses once reaching the D12F morphology [Wilson et al., 2002] and is temporally associated with increased prostaglandin $F_{2\alpha}$ and E_2 concentrations in the uterine lumen [Geisert et al. 1982b], which is required for pregnancy establishment in the pig [Kraeling et al., 1985]. While prostaglandins have predominately been linked to uterine angiogenesis and luteolysis, these data suggest prostaglandin signaling may also affect conceptus development as prostaglandin F receptor is much greater (14-fold) in D14F conceptuses compared to the earlier three morphologies evaluated using the array (Table A.3, cluster 23).

Interferon-γ is a significant component of pregnancy in many species and is generally known for its immune related function in non-pregnancy related biology. In

certain B-cell lymphoma cell lines, IFNγ is capable of reducing cell growth through apoptosis sensitivity [Niitsu et al., 2002]. Generally, IFNγ largely elicits its effects through the activation of either signal transducer and activator of transcription (STAT) -1 or -3 JAK-STAT activation pathways, that lead to transcription through the activation of interferon regulatory factors [Darnell, 1997]. The data presented herein demonstrate a temporal down-regulation of interferon regulatory factor 6 (IRF6; Table A.3, Cluster 6) and an up-regulation of STAT-3 (Table A.3, cluster 11) suggesting that STAT3 activation by IFNγ is likely during conceptus development although it is difficult to assess what activation occurs downstream as a result.

By definition, heat shock proteins generally serve protective roles and are involved in protein folding and chaperoning. Using yeast two-hybrid screening, HSP27 has been shown to strongly associate with ERβ, but not ERα, suggesting a role in estrogen modulated signaling [Miller et al., 2005]. Interestingly, the pig conceptuses also express ERβ during trophoblastic elongation [Kowalski et al., 2002] whereas ERα is not [Yelich et al., 1997a]. It is possible that HSP27 may also regulate the ability of conceptus secreted estrogen to function in an autocrine fashion. HSP27 has also been shown to closely associate with F-actin, which may contribute to the maintenance of cell architecture during ATP depletion, as in renal epithelial cells [Van Why et al., 2003]. It is clear that actin stabilization/remodeling is tightly regulated based on the data presented within this manuscript that many of the genes that are differentially expressed during trophoblastic elongation have the ability to attach to actin, particularly those with PDZ-LIM domains. The protective role of HSP27 during ATP deletion may also be critical as the transition from spherical to D12F is associated with 8-12 genes related to ATPase

activity/utilization. Genes related functionally to ATP binding and utilization represented the 7th and 8th most significant biological annotation clusters characterizing the transition from spherical to D12F as determined through DAVID (Table 3.4).

Angiomotin was originally identified through its ability to bind and block the inhibitory effects of angiostatin thereby promoting angiogenesis through endothelial cell migration [Troyanovsky et al., 2001]. While deletion of the C-terminal PDZ binding motif of angiomotin in mouse endothelial cells blocked chemotactic capacity of those cells, the mutant protein was still localized to the lamellipodia of cells, as in migrating cells that contain PDZ intact angiomotin [Levchenko et al., 2003]. More recently, the report of two alternative splice isoforms of angiomotin working coordinately suggest that an 80 kDa (p80-angiomotin) form is primarily responsible for cell migration and a 130 kDa isoform (p130-angiomotin) colocalizes with F-actin regulating cell shape. While both isoforms are expressed in mouse placental tissue the predominant form is p80-angiomotin, which is the exclusive form expressed it the mouse embryo [Ernkvist et al., 2006]. Because the angiomotin sequence information available for the pig is not complete; the region in which the primers for quantitative RT-PCR were developed are homologous to the mouse sequence that codes the C-terminal of angiomotin, present in both the p80 and p130 isoforms of angiomotin, making it difficult to ascertain which isoform is differentially expressed during trophoblastic elongation in the pig. It still seems quite plausible that either angiomotin isoform could be involved with conceptus elongation, due to its ability to localize to the lamellipodia, suggesting it is involved with cellular homing as well as its ability to interact with F-actin, which the rearrangement of has been previously suggested to be involved with rapid trophectoderm changes in the

pig [Mattson et al., 1990]. Interestingly, electron microscopy of elongating tubular conceptuses identifies the extension of filipodia extending from the trophectodermal cells [Geisert et al., 1982c] suggesting that angiomotin may indeed be associated with the cellular remodeling of the trophectoderm cells as it is in endothelial cells during angiogenesis. It may also be suggested that angiomotin is a key component of angiongenic development of the porcine placenta as expression increases 4-fold from spherical to D12F is persistent at D14F (Figure 3.2C).

B-cell linker is a required component of B cell development as progenitor B cells in BLNK -/- mice fail transition into precursor B cells [Pappu et al., 1999]. BLNK may also regulate B cell function through B cell receptor mediated signaling inhibition during conceptus attachment in the pig as conceptus BLNK expression is so dramatically down-regulated (28- and 17-fold in D12F and D14F, respectively, relative to spherical conceptuses; Table 3.6) during adhesion of the trophectoderm to the uterine endometrium. In pregnant mice, maternal B lymphocytes capable of responding to paternal MHC antigens are partially deleted [Ait-Azzouzene et al., 1998], suggesting the importance of B cell regulation during pregnancy. Because BLNK is critical for B cell function, it is likely that the significant reduction in BLNK expression during pig conceptus development involves the regulation of the maternal immune response to the developing conceptus.

In contrast to BLNK, CXCL14 is significantly upregulated (over 27-fold, Table 3.6, Figure 3.2G) following trophoblastic elongation by D14F conceptuses, during the period of trophoblastic elongation. The receptor for CXCL14, CCR1, is abundantly expressed in endometrium at the maternal–fetal interface during implantation; and

CXCL14 promotes the migration of human cytotrophoblast cells [Hannan et al., 2006]. Furthermore, CCR1 is also expressed in human extravillous trophoblast cells but not in cytotrophoblast cells [Sato et al., 2003] suggesting a role in trophoblast differentiation and invasion into the decidua. The significant upregulation of CXCL14 in D14F pig conceptuses may also be part of trophoblast differentiation as placental layers begin to differentiate during the adhesion to the uterine endometrium [Friess et al., 1980].

Parathryroid hormone (PTH) and PTHrP are both involved in the calcium mobilization and homeostatis [Potts, 2005]. Calcium concentrations change significantly in the uterine lumen during this period of pregnancy in the pig [Geisert et al., 1982b]. The temporal increase in conceptus PTHrP production may be associated with the changes in uterine lumenal calcium concentrations. The dramatic upregulation of PTHrP associated with trophoblastic elongation is also suggestive of a regulatory role in trophectoderm remodeling and conceptus growth. Indeed, in mice trophoblast giant cells (TGC), PTHrP has been shown to be involved with the rearrangement and cytoskeleton organization near the ectoplacental cone (EPC) [El-Hashash and Kimber, 2006]. Human cytotrophoblast express PTHrP mRNA while lacking protein expression whereas syncytiotrophoblast and avascular amnion cells express both gene and protein expression for PTHrP suggesting a role regulating migration and differentiation of trophectoderm cells [Dunne et al., 1994]. During pregnancy in the rat, the expression of PTHrP and its receptor are spatially and temporally associated with the differentiation of uterine stromal cells into decidual cells during implantation [Tucci and Beck, 1998]. While the roles of PTHrP during conceptus elongation could be multifaceted, it is important to note that the morphological changes induced by the PTHrP in TGCs of mice near the EPC [El-

Hashash and Kimber, 2006] are similar in nature to those described to occur in trophoblast cells near the elongation zone in pig conceptuses during rapid trophoblastic elongation [Geisert et al., 1982c].

Maspin has been shown in numerous scenarios to function as a suppressor of tumor growth and metastasis [Chen and Yates, 2006]. Its expression during pig conceptus development is significantly down-regulated in D12F and D14F conceptuses compared to those spherical in morphology. Interestingly, the downregulation of maspin also occurs during the transition of non-invasive to invasive prostate carcinomas [Pierson et al., 2002]. While placentation in the pig results in the formation of a non-invasive placenta, pig conceptuses exhibit a highly invasive phenotype *ex utero* [Samuel and Perry, 1972], which could be associated with the loss of maspin expression during the period of conceptus attachment.

The use of the Affymetrix GeneChip® Porcine Genome Array effectively identified hundreds of porcine genes that are differentially expressed during the developmental period consisting of trophoblastic elongation and the initial attachment of the conceptus trophectoderm to the maternal uterine endometrium. While, based on literature, mechanisms of action for the reported lists of genes can be hypothesized; it is also critical to determine what interactions do exist between these proteins and others during pig conceptus elongation and the exact regulatory functions these genes may elicit. Enhanced understanding of this process will allow a more comprehensive approach to select for effective conceptus development resulting in optimal degrees of placentation among conceptuses; promoting similar development between littermates and increased litter size in pigs.

Chapter IV

IDENTIFICATION AND ANALYSIS OF MOLECULAR MARKERS FOLLOWING ENDOCRINE DISRUPTION OF PREGNANCY IN THE PIG

Introduction

Porcine conceptuses initiate attachment to the uterine lumenal surface on Day 13 of pregnancy following a rapid morphological elongation of their trophoblast throughout the uterine lumen [Geisert et al., 1982b]. This dramatic transformation in structural morphology coincides with the elevated conceptus estrogen synthesis and release [Geisert et al., 1982b] which is required for the establishment of pregnancy in the pig.

Critical parameters exist with regards to the specific spatiotemporal release of estrogen during this stage of pregnancy in the pig. Insufficient estrogen production, as seen in litters with less than two piglets per uterine horn at the time of trophoblast elongation, results in the failure to prevent luteolysis and subsequent termination of pregnancy [Polge et al., 1966; Dziuk, 1968]. On the contrary, adverse timing of estrogen exposure to the dam on Days 9 and 10 of gestation results conceptus degeneration during the period of placental attachment to the uterine surface. However, the same dosage of estrogen given on Days 11 and 12, in synchrony with conceptus synthesis and release of estrogen, has no adverse affect on conceptus development and pregnancy establishment [Pope et al., 1987; Pope et al., 1986]. In the commercial swine industry, it is well known that ill-timed ingestion of naturally occurring estrogenic alfatoxins, such as zearalenone, found in moldy corn, also causes total litter loss [Long and Diekman, 1984].

While estrogen is required as a maternal recognition of pregnancy signal and thought to be involved with the opening of the "implantation window" in the pig, timing and extent of estrogen exposure can have dramatic effects on conceptus development and survival as described. In general, the diffuse type of porcine placental attachment occurs between Days 13 and 18 of gestation and is associated with a thickening of the uterine glycocalyx (UG) [Perry et al., 1981; Dantzer, 1985; Geisert et al., 1991]. Disruption of the UG is closely associated with embryonic mortality that occurs in gilts treated with estrogen on Days 9 and 10 of gestation [Morgan et al., 1987a; Blair et al., 1991; Geisert et al., 1991]. The ability for estrogen to regulate implantation success or failure also occurs in mice, where high concentrations of endogenous estrogen shortens the implantation window and alters the gene expression profile in the uterine endometrium around the time of blastocyst attachment [Ma et al., 2003]. We propose that the cascade of molecular events induced by normal endogenous conceptus release of estrogen into the uterine lumen is initiated prematurely by exogenous estrogen administered on Days 9 and 10 of gestation.

Identification of endometrial changes in gene expression in response to premature exposure to exogenous estrogen will aid in determining those factors which may also be regulated by conceptus estrogen stimulation that are critically expressed during the initial stages of attachment during pregnancy in the pig.

Materials and Methods

Animals

Research was conducted in accordance with the Guide for Care and Use of Animals promoted by The Endocrine Society and approved by the Oklahoma State Institutional Animal Care and Use Committee. Cyclic, crossbred gilts of similar age (8-10 mo) and weight (100-130 kg) were checked for estrous behavior twice daily in the presence of an intact boar. Onset of estrus was designated Day 0 of the estrous cycle. Gilts were naturally mated with fertile boars at the onset of their second estrus (Day 0 of estrous cycle) and again 24 h later.

Tissue Collection

Pregnant gilts (4 animals/treatment/day) were randomly assigned to one of the following treatment groups: (a) Control (CO), i.m. injection of corn oil (2.5 mL) on Days 9 and 10 of gestation or (b) Estrogen (EC), 5 mg i.m. injection of estradiol cypionate (A.J. Legere, Scottsdale, AZ) on Days 9 and 10 of gestation. Gilts were hysterectomized (n=4 gilts/treatment/day) through midventral laporatomy as previously described by Gries et al. [1989] on either Days 10, 12, 13, 15 and 17 of gestation. Following induction of anesthesia with 1.8 mL of i.m. administration of a cocktail consisting of 2.5 mL (Xylazine: 100 mg/mL: Miles Inc., Shawnee Mission, KS) and 2.5 mL Vetamine (Ketamine HCl 100 mg/mL Molli Krodt Veterinary, Mundelein, IL) in 500 mg of Telazol (Tiletamine HCl and Zolazepum HCl: Fort Dodge, Syracuse, NE), anesthesia was maintained with a closed circuit system of halothane (5%) and oxygen (1.5 liters/min). Immediately following removal, each uterine horn was flushed with 20 mL of a

physiological saline and conceptuses were removed. Uterine flushings were transferred to a 50 mL conical tube and centrifuged at 1000 rpm for 1 min to remove cell debris. Uterine flushings were stored at -80^{o}C until utilized. Following conceptus removal, one uterine horn was cut along its anti-mesometrial border, and endometrium (5-10 g) was removed with sterile scissors. Endometrium was snap-frozen in liquid nitrogen and stored at -80^{o}C until analyzed.

RNA Isolation

Total RNA was extracted from uterine endometrium tissue using the RNAwiz reagent (Ambion, Inc., Austin, TX) according to manufacturer's recommendations. Approximately 500 mg of endometrium was homogenized in 5 mL RNAwiz reagent using a Virtishear homogenizer (Virtis Company Inc., Gardiner, NY). RNA pellets were rehydrated in nuclease-free H_2O and stored at -80^{o}C. RNA content was estimated spectrophotmetrically and purity determined by the 260:280 ratio. RNA quality was assessed through gel electrophoresis.

Microarray Analysis

Microarray analysis was conducted utilizing a spotted cDNA array which represents mRNA transcripts from pig brain, uterine endometrium, early pregnancy conceptuses and ovarian tissues. The array, developed at the University of Missouri, contains 19 968 features, representing 14 970 PCR amplified cDNA transcripts of which 4108 lack useful annotation, meaning approximately 10 800 genes with known identity

can be interrogated. Specific procedures utlizied in the development of the array have been described [Whitworth et al., 2005].

cDNA Synthesis and Hybridization

Total RNA (20 μg) from endometrial tissue collected on Days 10, 13 and 15 of pregnancy representing each day x treatment combination was utilized for reverse transcribed cDNA labeling using the 3DNA Array 50 Expression Array Detection Kit (Genisphere Inc, Hatfield, PA). This method employs the use of a dendrimer ridden with fluor molecules which hybridizes to a "capture" sequence specific to an oligonucleotide utilized in the reverse transcription reaction during cDNA synthesis. Hybridizations were conducted per the manufacturer's recommendations. Four hybridizations were conducted for each day to compare mRNA abundance differences between CO and EC treated gilts on Days 10, 13 and 15. Day 12 tissue samples were not included in the microarray analyses due to morphological variation of conceptus development between the litters and Day 17 was not included in the analysis as conceptus mortality and degradation was conclusive. For each technical replication (n = 4), the total volume from the cDNA synthesis reaction was combined with the cDNA created for the opposite treatment to compare differences using dual-channel analysis. After combining the cDNA synthesis reactions for each treatment (260 μl), the cDNA was concentrated to 3-10 μl volume using Microcon YM-30 centrifugal devices (Millipore, Billerica, MA). Nuclease free water was added to bring the total volume of the concentrated cDNA to 10 μl. Hybridizations were performed according to the manufacturer's recommendations. For the primary hybridization, the hybridization solution (10 μl concentrated cDNA, 25 μl 2X formamide hybridization buffer, 2 μl LNA dT blocker, and 13 μl of nuclease free water)

was denatured at 80°C for 10 min, applied to the array slide utilizing a 22 x 40 mm LifterSlip (Erie Scientific Co., Portsmouth, NH) then incubated at 53°C for 16 h in a humidified hybridization cassette. Following hybridization, coverslips were washed off in 2X SSC, 0.2% SDS at R.T. followed by a series of washes (2X SSC, 0.2% SDS, 65°C, 15 min; 2X SSC, R.T., 15 min; 0.2X SSC, R.T., 15 min). Slides were rinsed in 95% EtOH for 2 min at R.T. to fix cDNA molecules then dried on a slide centrifuge. Secondary hybridizations, the attachment of the fluorescent dendrimer ridden capture sequence to probes bound during the primary hybridization, were conducted at 50°C for 3 h in a humidified hybridization cassette. Post secondary hybridization washes were carried out as followed the primary hybridization. Slides were dried on a slide centrifuge and stored in a light protected box.

Imaging and Microarray Data Acquisition

Each microarray slide was scanned with both the Cy3 and Cy5 channels using the ScanArray Express (Perkin-Elmer, Wellesly, MA). Laser power and PMT gain were adjusted for each slide to minimize variation between wavelengths.

Analysis Using GenePix Auto Processor (GPAP3.0)

GenePix Auto Processor 3.0 software (GPAP3.0; http://darwin.biochem.okstate.edu/gpap3, Weng and Ayoubi, in preparation) was used for data pre-processing, background correction, and Local Loess pin by pin intensity normalization, and microarray statistical analysis. Genes that were determined to change

at least 1.8-fold in response to EC with a *P* value less than 0.1 were included in further analysis using the Database for Annotation, Visualization and Integrated Discovery.

Analysis by the Database for Annotation, Visualization and Integrated Discovery

The Database for Annotation, Visualization and Integrated Discovery (DAVID 2.1; http://niaid.abcc.ncifcrf.gov/) is a program that enables the utilization of microarray gene lists to generate specific functional annotations of the biological processes affected by the treatment as determined through microarray experiments [Glynn et al., 2003]. A gene list containing the GenBank accession numbers for all genes affected by the treatment for all days was compiled to determine the underlying biological themes that were altered due to EC treatment. Accession numbers utilized were those assigned to each gene during annotation as previously described [Whitworth et al., 2005]. Based on the gene ontology (GO) assessment of the biological process, molecular function, and cellular component of each gene altered by the treatment; clusters of functional annotation terms were generated. Not all differentially expressed genes were utilized in the functional annotation as a number of genes differentially expressed were unique or lacked sufficient biological annotation to be useful for functional annotation.

Validation through Quantitative One-Step RT-PCR

Quantitative analysis of secreted phosphoprotein 1 (SPP1), aldose reductase (AR), neuromedin B (NMB), and CD24 antigen (CD24) mRNA were assayed using quantitative real-time RT-PCR and a fluorescent reporter as previously described [Hettinger et al., 2001]. The PCR amplification was conducted using the ABI PRISM

7500 Sequence Detection System (PE Applied Biosystems, Foster City, CA). The samples were evaluated for SPP1 expression differences using a dual-labeled probe designed to have a 5' reporter dye (6-FAM) and a 3' quenching dye (TAMRA) and to anneal between the forward and reverse primers. Thermal cycling conditions were 50°C for 30 min and 95°C for 15 min, followed by 40 repetitive cycles of 95 for 15°C sec and 60°C for 1 min. Amplification differences for AR, CD24, and NMB mRNA were detected using the intercalating dye, SYBR green. Primer and probe sequences are presented in Table 4.1. Cycling conditions for SYBR green detection were 50°C for 30 min and 95°C for 15 min, followed by 40 repetitive cycles of 95 for 15°C sec and variable annealing temperature for 30 sec, 72°C for 33 sec and a variable temperature during fluorescent detection for 33 sec. Fluorescence detection temperature was determined by evaluating melting curve analysis for the samples and the no template control amplification plot. Detection temperatures were set at a temperature when the intended target was the only contributing factor to fluorescence. One hundred nanograms of total RNA were assayed for each sample in duplicate for each target template. 18S ribosomal RNA was assayed as a normalization control to correct for loading discrepancies for all samples assayed. Template amplification was quantified by determining the threshold cycle (C_T) based on the fluorescence detected within the geometric region of the semilog plot. Theoretically, in the geometric region, one cycle is equivalent to the doubling of the PCR target template. A dilution series was made for each assay to determine the dynamic range of amplification for each gene target. To confirm genomic DNA contamination was not contributing to the amplification, pooled samples were assayed in the presence and absence of reverse transcriptase to insure only synthesized cDNA

contributed to the amplification of the target. Relative mRNA abundance was determined using a previously established method [Ashworth et al., 2006]. The ΔC_T value was determined by subtracting the target C_T of each sample from its respective ribosomal 18S C_T value. Target mRNA expression differences were calculated by arbitrarily setting the highest sample ΔC_T (the sample with the least expression) as the standard to subtract all other sample ΔC_T to produce the $\Delta\Delta C_T$. Relative mRNA expression units between sample means was calculated by assuming an amplification efficiency of 2 and applying the equation $2^{\Delta\Delta Ct}$ for each sample mean $\Delta\Delta C_T$.

In Situ Hybridization Analysis

SPP1, AR, CD24, NMB mRNA were localized in porcine uterine cross-sections by *in situ* hybridization using methods previously described [Johnson et al., 1999]. Paraffin embedded cross-sections (~5 µm) were deparaffinized, rehydrated, and deproteinated then hybridized with radiolabeled antisense or sense porcine cRNA probes (5.0×10^6 counts per minute/slide) synthesized by *in vitro* transcription with [α-^{35}S] uridine 5-triphosphate (MP Biomedicals, Irvine, CA). For *in vitro* transcription, appropriate RNA polymerases (T3, T7, SP6) were utilized with the linearized plasmid carrying the transcript printed on the array [Whitworth et al., 2005]. Following hybridization washes, and RNase A digestion, hybridized slides were exposed to Biomax maximum resolution film (Eastman Kodak, New Haven, CT) overnight to determine signal strength. Autoradiography was performed using NTB liquid photographic emulsion (Eastman Kodak). Slides were dipped in emulsion and exposed at 4°C for a period of time relative to signal strength, developed in Kodak D-19 developer,

Table 4.1 Primer and probe sequences used for quantitative RT-PCR analysis.

Target[a]	Forward/Reverse Primers (5'→3')[b]	Fluorescent Reporter[c]	Length of Amplicon[d]	GenBank Accession #[e]
SPP1	TTGGACAGCCAAGAGAAGGACAGT GCTCATTGCTCCCATCATAGGTCTTG	5'-TGGAAACCCGCAGCCAGGAGCAGTCCAAA-3'	121 bp	NM_214023
AR	AAGGAGCACAGTTCCAAGCAGTCA CCCGAAGAGCACTACCTGTAGATT	SYBR Green	166 bp	CO994619
CD24	AGAGATGTACAGCATTCAGGTATGAAAC TCTTTAGAAACCTACACTGGAACAGCC	SYBR Green	105 bp	AJ952935
NMB	CCTGGCAACTCAACCAGAAATCAC AGACTCCACAACATGGCTTAGGCT	SYBR Green	136 bp	CO993274

[a]The amplification target. SPP1, Secreted phosphoprotein 1; AR, Aldose Reductase; CD24, CD24 antigen; and NMB, Neuromedin B.
[b]The forward and reverse DNA oligos used in the amplification of the target. Forward and reverse do not necessarily indicate the *in vivo* direction of transctiption.
[c]Either a dual-labeled probe (FAM-TAMRA; SPP1) or the intercalating dye, SYBR Green (AR, CD24, NMB) was used to measure amount of amplified target during each cycle of quantitative RT-PCR.
[d]The length of the amplicon created during PCR.
[e]The accession number to the porcine sequence that was utilized during primer and probe design.

counterstained with Harris modified hematoxylin (Fisher Scientific, Fairlawn, NJ), dehydrated, and protected with cover slips.

Photomicrography

Digital photomicrographs of *in situ* hybridization, bright-field and dark-field images of liquid emulsion autoradiography, were collected using a Nikon Eclipse E6000 microscope interfaced with the CoolSNAPcf digital camera equipped with a cooled charge-coupled device (Photometrics, Tucson, AZ) and imaging software (MetaVue, Molecular Devices, Downington, PA). Photographic plates were assembled using Adobe Photoshop (version 6.0, Adobe Systems Inc., San Jose, CA).

Statistical Analysis

Quantitative RT-PCR ΔC_T values were analyzed using PROC MIXED of the Statistical Analysis System. Analysis of endometrial gene expression tested for the effect of treatment, day and day x treatment interaction. Significance ($P < 0.05$) was determined by probability differences of least squares means. Figures representing fold differences in gene expression have superscripts above bars depicting significant differences as determined by the ΔC_T values ($P < 0.05$).

Results

Conceptus Growth and Development

The physiological response regarding conceptus development and viability following premature exposure of pregnant gilts to estrogen has been previously reported [Ashworth et al., 2006]. Briefly, conceptuses recovered on Days 10 and 12 of pregnancy

were phenotypically normal. Normal, viable appearing peri-attachment conceptuses were recovered in both CO and EC treated gilts on Day 13 of pregnancy, however, conceptuses from EC treated gilts harvested on Days 15 and 17 of pregnancy were severly fragmented into small pieces. The deterioration of the conceptus trophectoderm indicated the viabliblity of the conceptuses was completely compromised by Day 17.

Microarray Analysis

Microarray hybridizations were conducted to identify differential gene expression between EC and CO treated pigs on Days 10, 13 and 15 of gestation. The specific days for microarray analyses represent three critical periods in the establishment of pregnancy; pre-conceptus estrogen release, post-conceptus estrogen release and initiation of implantation. Following hybridization, scanning and raw data acquisition through GenePix4000, data for each day was processed and analyzed using GenePix Auto Processor 3.0. Following pin-by-pin intensity dependant normalization, 8, 32 and 5 endometrial genes were identified up-regulated at least 1.8-fold ($P < 0.1$) in the EC gilts on Days 10, 13 and 15, respectively. A total of 1, 39, 16 endometrial genes expressed in EC were down-regulated at least 1.8-fold ($P < 0.1$) on Days 10, 13 and 15, respectively (Tables 4.2, 4.3, and 4.4). Twenty-one of the total 77 differentially expressed genes represented unique sequences. The remaining 56 differentially expressed genes assigned a putative annotation based on their associated GenBank accession number representing factors involved with attachment, immunology, transcription regulation, protein regulation and metabolism.

Database for Analysis, Visualization and Integrated Discovery

Utilization of DAVID resulted in identification of 10 functional annotation clusters representing biological systems that were affected by exogenous EC treatment on Days 9 and 10 of gestation (Table 4.5). Collectively, regulation of cellular/physiological processes, biosynthesis, immune response, multiple aspects of metabolism, apoptosis, transport, calcium and metal ion binding are among the general functional themes affected. Not all genes presented in Tables 4.2-4.4 were included in all the functional annotation clusters. Other functional processes identified by DAVID that may also be involved based on the expression differences that were not included in a cluster include response to chemical stimuli, cytoskeleton protein binding, and signal transduction.

Table 4.2. Differentially expressed genes in uterine endometrium on Day 10 following exogenous EC on Day 9 of gestation.

GenBank Accession Number	Clone ID	Putative Annotation	E2/CO Fold Change	P Value	Functional Annotation Cluster Association
NM_006744	Pd12-14end 01-04-P15	Retinol Binding Protein 4	8.25	0.028	8
NM_002970	Pd12-14end 05-08-G21	Spermidine/spermine N1-acetyltransferase	6.82	0.028	2,
NM_002213	Pd12-14end 01-04-A20	Similar to integrin, beta 5 (Human)	4.59	0.031	
UNIQUE	pfubo 45-48-N23	UNIQUE pd6end1-009-H10	3.13	0.100	
UNIQUE	pfubo 49-52-C05	UNIQUE pd6end2-001-e06	2.92	0.100	
NM_003187	pfubo 41-44-P03	TAF9 RNA polymerase II, TATA box binding protein (TBP)-associated factor, 32kDa	2.87	0.031	2, 5, 7, 10
XM_379200	pfu14 57,58,09,10-D12	Similar to Homo sapiens LOC401078 (LOC401078)	2.30	0.031	
XM_370781	puof 21-24-F16	Similarity to Ig alpha-2 chain C region (Human)	1.91	0.028	
CB424794	pfu14 57,58,09,10-N05	Strong similarity to Metastasis-associated protein MTA1 (Human)	-2.18	0.098	

[a]Accession numbers of genes with strong homology to porcine microarray probes identified during annotation of the porcine EST library.
[b]The clone ID assigned during the creation of the microarray.
[c]Putative identity of probe determined during annotation.
[d]Fold difference in gene expression following processing and normalization using GPAP 3.0 as described in materials and methods.
[e]*P* Values determined via GPAP regarding the significance of the detected differences.
[f]Annotation clusters identified through DAVID, presented in Table 4.5, which the probe associates with.

Table 4.3. Differentially expressed genes in uterine endometrium on Day 13 following exogenous EC on Days 9 and 10 of gestation.

GenBank Accession Number[a]	Clone ID[b]	Putative Identity[c]	E2/CO Fold Change[d]	*P* Value[e]	Functional Annotation Cluster Association[f]
UNIQUE	pfubo 53-56-A18	UNIQUE peov3-001-H05	9.65	0.005	
CB169174	pfu14 57,58,09,10-E01	Transcribed sequences	7.18	0.002	
AK095434	pfubo 53-56-B01	Similar to Chromosome 14 open reading frame 43 (Human)	5.98	0.063	5, 10
NM_006135	Pd12-14end 01-04-H08	Capping protein (actin filament) muscle Z-line, alpha 1 (CAPZA1)	4.91	0.010	1, 3, 5, 7, 10
NM_009846	puof 69-72-C19	CD24a antigen	4.55	0.001	3
NM_018955	Pd12-14end 05-08-N12	Ubiquitin B (UBB)	4.43	0.001	7,
BC047028	pfubo 05-08-O23	Fanconi anemia, complementation group F	3.83	0.003	7, 10
NM_000582	pfu14 57,58,09,10-M11	Secreted phosphoprotein 1 (osteopontin)	3.42	0.008	1, 3, 5, 6, 10
BP444412	pfubo 21-24-J13	Weak similarity to hypothetical protein LOC51316 (Human)	3.26	0.015	
NM_199161	pfu14 57,58,09,10-K03	Serum amyloid A1	2.92	0.005	
BF712745	pfubo 09-12-G18	Transcribed sequence	2.88	0.046	
NM_003167	predoch 01-04-H20	Sulfotransferase family, cytosolic, 2A, dehydroepiandrosterone (DHEA) - preferring, member 1	2.85	0.083	4
NM_000067	pfu14 57,58,09,10-I03	Carbonic anhydrase II	2.67	0.033	9
XM_072554	pfu14 57,58,09,10-F02	Similar to RIKEN cDNA 4833436C18 gene (LOC138729), mRNA	2.62	0.062	
NM_006021	puof 33-36-M10	Deleted in lymphocytic leukemia, 2	2.50	0.025	
BQ605000	pfubo 49-52-D15	Strong similarity to phosphoserine aminotransferase, isoform 1 (Human)	2.29	0.007	
NM_016015	peuo 17-20-C20	Leucine carboxyl methyltransferase 1	2.26	0.062	
NM_012332	pfubo 37-40-B01	Likely ortholog of mouse acyl-Coenzyme A thioesterase 2, mitochondrial	2.21	0.065	
AK033438	puof 33-36-I11	Similar to unknown EST (Human)	2.12	0.041	
NM_005627	pfubo 41-44-F20	Serum/glucocorticoid regulated kinase	2.01	0.023	6, 7, 8
NM_145740	puof 33-36-F22	Glutathione S-transferase A1	1.98	0.019	
NM_001614	Pd12-14end 01-04-O20	Actin, gamma 1 (ACTG1)	1.97	0.019	1, 7
BF704319	puof 73-76-I18	Transcribed sequences	1.96	0.056	
NM_020676	pfubo 21-24-H22	Abhydrolase domain containing 6	1.94	0.083	
NM_005827	pfubo 17-20-F12	UGTREL1; UDP-galactose transporter	1.93	0.009	8
BM659101	pfubo 49-52-L23	Transcribed sequences	1.93	0.032	
NM_014579	pfubo 21-24-B18	Solute carrier family 39 (zinc transporter), member 2	1.91	0.008	9

NM_002970	Pd12-14end 01-04-L04	Spermidine/spermine N1-acetyltransferase	1.90	0.021	
NM_014160	pfu14 57,58,09,10-H02	Similar to Makorin (Human)	1.90	0.059	9
NM_005952	pfubo 49-52-D20	Metallothionein 1X	1.87	0.019	8, 9
BF702843	pfubo 09-12-O08	Moderate similarity to AKAP-associated sperm protein (Human)	1.83	0.084	
NM_173630	pfubo 33-36-O07	Rotatin	1.80	0.072	
UNIQUE	pfu14 57,58,09,10-L04	UNIQUE peov3-014-D12	-1.81	0.015	
NM_024911	peuo 17-20-D17	Putative NFkB activating protein 373	-1.81	0.065	5, 10
NM_006623	pfubo 29-32-H20	Phosphoglycerate dehydrogenase	-1.82	0.016	2, 8
BF711640	pfubo 05-08-E24	Transcribed sequences	-1.83	0.068	
NM_014328	pfubo 05-08-H24	RUN and SH3 domain containing 1	-1.83	0.089	
NM_144583	pfu14 57,58,09,10-J15	ATPase, H+ transporting, lysosomal 42kDa, V1 subunit C isoform 2	-1.85	0.056	2, 7, 8, 10
UNIQUE	pfubo 17-20-O17	UNIQUE pd10en3-013-E11	-1.92	0.017	
BQ605109	pfubo 17-20-B18	Transcribed sequences	-1.93	0.053	
UNIQUE	Pd12-14end 01-04-J05	UNIQUE pd12-14end-002-E05	-1.93	0.065	
UNIQUE	pfubo 29-32-L14	UNIQUE pd3end2-003-C10	-1.98	0.041	
NM_004665	pfubo 53-56-K04	Vanin 2	-1.99	0.018	1, 2,
BI402645	pfubo 17-20-B23	Moderate similarity to Neuromedin U-25 precursor (Human)	-2.05	0.100	
NM_001153	Pd12-14end 01-04-N14	Annexin A4	-2.06	0.015	1, 3, 5, 6, 9, 10
BG894507	Pd12-14end 05-08-O10	Transcribed sequences	-2.13	0.014	
UNIQUE	pfubo 37-40-E15	UNIQUE pd3ov2-001-A03	-2.16	0.016	
UNIQUE	peuo 17-20-O11	UNIQUE pblivv4-016-d08	-2.17	0.013	
NM_000245	pfubo 13-16-F21	Hepatocyte growth factor receptor	-2.25	0.006	3, 7
UNIQUE	Pd12-14end 01-04-P23	UNIQUE pd12-14end-004-H11	-2.29	0.005	
UNIQUE	pfubo 49-52-C05	UNIQUE pd6end2-001-e06	-2.34	0.096	
XM_372261	pfubo 17-20-M18	Similar to DKFZP586L0724 protein (Human; LOC389900)	-2.34	0.010	
BF712656	pfubo 09-12-C20	Moderate similarity to alanine-glyoxylate aminotransferase 2-like 1 (Human)	-2.35	0.008	
NM_001623	pfubo 05-08-L09	Allograft inflammatory factor 1	-2.37	0.100	1, 3, 5, 9, 10
NM_001903	Pd12-14end 05-08-M23	Catenin (cadherin-associated protein), alpha 1, 102kDa	-2.48	0.016	7,
BC040077	pfubo 01-04-I06	Mitogen-activated protein kinase kinase kinase kinase 4	-2.51	0.003	7,
NM_002004	puof 13-16-H10	Farnesyl diphosphate synthase	-2.66	0.013	4,
NM_006681	Pd12-14end 05-08-E10	Neuromedin U	-2.69	0.004	
XM_084530	Pd12-14end 05-08-L06	Similarity to mRNA for KIAA0033 protein (Human)	-2.74	0.004	

BQ604324	puof 73-76-E19	Moderate similarity to N-acetylated alpha-linked acidic dipeptidase 2 (Human)	-2.80	0.088	
UNIQUE	pfubo 45-48-N23	UNIQUE pd6end1-009-H10	-2.95	0.015	
NM_174142	Pd12-14end 05-08-O09	Phytanoyl-CoA hydroxylase	-2.95	0.015	
UNIQUE	Pd12-14end 05-08-K21	UNIQUE pd12-14end-007-F09	-3.16	0.056	
BC054832	pfubo 05-08-A14	Zinc finger protein 191	-3.22	0.004	
NM_024315	puof 89-92-N14	Similar to Chromosome 7 open reading frame 23 (Human)	-3.45	0.015	
BQ601110	Pd12-14end 01-04-F13	Transcribed sequences	-3.49	0.030	
NM_021077	predoch 05-08-N17	Neuromedin B	-3.72	0.001	
BM069527	puof 77-80-L13	Programmed cell death 1 ligand 1	-4.07	0.013	3
L20826	puof 85-88-P11	Plastin 1 (I isoform)	-4.40	0.004	9
NM_005563	pfubo 05-08-A23	Stathmin 1	-4.53	0.003	7
NM_001628	Pd12-14end 05-08-K01	Aldose reductase	-13.93	0.001	7

[a]Accession numbers of genes with strong homology to porcine microarray probes identified during annotation of the porcine EST library.
[b]The clone ID assigned during the creation of the microarray.
[c]Putative identity of probe determined during annotation.
[d]Fold difference in gene expression following processing and normalization using GPAP 3.0 as described in materials and methods.
[e]*P* Values determined via GPAP regarding the significance of the detected differences.
[f]Annotation clusters identified through DAVID, presented in Table 4.5, which the probe associates with.

Table 4.4. Differentially expressed genes in uterine endometrium on Day 15 following exogenous EC on Days 9 and 10 of gestation.

GenBank Accession Number[a]	Clone ID[b]	Putative Identity[c]	E2/CO Fold Change[d]	*P* Value[e]	Functional Annotation Cluster Association[f]
BF711640	pfubo 05-08-E24	Transcribed sequences	4.29	0.065	
UNIQUE	pfubo 45-48-N23	UNIQUE pd6end1-009-H10	3.01	0.058	
UNIQUE	pfubo 49-52-P15	UNIQUE peov1-004-A10	2.82	0.073	
UNIQUE	pfubo 49-52-C05	UNIQUE pd6end2-001-e06	2.26	0.099	
UNIQUE	pd12-14end 05-08-P20	UNIQUE pd12-14end-008-H08	1.90	0.065	
BI345641	puof 89-92-C02	Transcribed sequences	-1.81	0.076	
BF711276	puof 73-76-C23	Transcribed sequence	-1.82	0.064	
NM_013758	puof 85-88-G21	Adducin 3 (gamma)	-1.84	0.073	
CB477767	pfubo 33-36-P16	Beta 2-microglobulin	-1.86	0.064	
NM_000582	pfu14 57,58,09,10-M11	Secreted phosphoprotein-1 (osteopontin)	-1.88	0.062	1, 3, 5, 6, 10
AK092773	pfubo 05-08-K21	aarF domain containing kinase 5	-1.88	0.073	
NM_138799	pfubo 33-36-D06	Similar to hypothetical protein BC016005 (Human; LOC129642)	-1.89	0.073	
BF713356	puof 73-76-C06	Signal transducer and activator of transcription 1	-2.07	0.064	
NM_199161	pfu14 57,58,09,10-K03	Serum amyloid A1	-2.07	0.056	1, 3, 5
BC040643	pfubo 49-52-D11	Sortilin-related receptor, L(DLR class) A repeats-containing	-2.15	0.056	4, 8
UNIQUE	pfubo 53-56-K24	UNIQUE peov3-003-H04	-2.17	0.056	
UNIQUE	pfubo 53-56-A18	UNIQUE peov3-001-H05	-2.29	0.062	
AB033044	pfubo 41-44-D02	Similar to mRNA for KIAA1218 protein (Human)	-2.29	0.072	
AF152103	puof 73-76-O08	Interferon stimulated gene 17	-2.29	0.056	
CB169174	pfu14 57,58,09,10-E01	Transcribed sequences	-2.37	0.056	
NM_013285	pfubo 53-56-I17	Nucleolar GTPase	-2.80	0.056	7,

[a]Accession numbers of genes with strong homology to porcine microarray probes identified during annotation of the porcine EST library.
[b]The clone ID assigned during the creation of the microarray.
[c]Putative identity of probe determined during annotation.
[d]Fold difference in gene expression following processing and normalization using GPAP 3.0 as described in materials and methods.
[e]*P* Values determined via GPAP regarding the significance of the detected differences.
[f]Annotation clusters identified through DAVID, presented in Table 4.5, which the probe associates with.

Table 4.5. Functional annotation clusters of Gene Ontology terms representing biological processes affected by exogenous EC treatment on Days 9 and 10 of gestation.

Annotation Cluster #[a]	Functional Annotations Based on GO Biological Process, Cellular Component, and Molecular Function[b]
1	localization of cell, cell motility, negative regulation of physiological process
2	amine biosynthesis, nitrogen compound biosynthesis, nitrogen compound metabolism, amino acid and derivative metabolism, amine metabolism, cellular biosynthesis
3	negative regulation of physiological process, inflammatory response, cell proliferation, response to pest, pathogen or parasite, response to other organism, response to wounding, immune response, defense response
4	steroid metabolism, cellular lipid metabolism, lipid metabolism
5	negative regulation of physiological process, negative regulation of cellular physiological process, negative regulation of cellular process, regulation of cellular physiological process
6	apoptosis, programmed cell death, cell death
7	purine nucleotide binding, ATP binding, adenyl nucleotide binding, phosphorylation, phosphate metabolism, phosphorus metabolism, protein amino acid phosphorylation, protein modification, biopolymer modification, protein metabolism, cellular protein metabolism, macromolecule metabolism, cellular macromolecule metabolism, biopolymer metabolism
8	cation transport, transport, ion transport
9	calcium ion binding, cation binding, metal ion binding, zinc ion binding, transition metal ion binding
10	regulation of cellular physiological process, regulation of metabolism, regulation of transcription; regulation of nucleobase, nucleoside, nucleotide and nucleic acid metabolism; nucleobase, nucleoside, nucleotide and nucleic acid metabolism; transcription, regulation of cellular metabolism

[a]The ten most significant annotation clusters identified based on the gene list submitted for analysis through DAVID.

[b]This column represents terms in the annotation clusters. The gene ontology (GO) terms were gathered based on the known annotation of the submitted genes with respect to biological process, cellular component, and molecular function.

Quantitative RT-PCR

Quantitative RT-PCR was utilized to validate differential expression of candidate genes identified through microarray analysis using all the endometrial tissue samples collected in the study (Days 10, 12, 13, 15, and 17).

A day x treatment interaction ($P < 0.03$) was detected for endometrial AR gene expression. In CO gilts, AR mRNA expression was relatively low on Days 10, 15 and 17 in contrast to a 25- and 45-fold greater expression that occurred on Days 12 and 13, respectively (Figure 4.1A). Although no significant difference in AR mRNA abundance was detected between CO and EC treatments on Days 10, 12, 15, or 17; EC treatment caused a 40-fold reduction in AR expression ($P < 0.001$) on Day 13 (Figure 4.1A).

Expression of CD24 antigen mRNA was affected by a day x treatment interaction ($P < 0.02$). Endometrial CD24 mRNA expression was lowest on Day 10 in both CO and EC treated gilts (Figure 4.1B). In comparison to Day 10, endometrial CD24 expression increased 8, 53, 276 and 353-fold in CO gilts on Days 12, 13, 15 and 17, respectively. EC treatment increased CD24 mRNA abundance on Days 12 (6.7-fold) and 13 (6.5-fold) while expression was similar to CO gilts on Days 10, 15 and 17 (Figure 4.1B).

Quantitative analysis of SPP1 mRNA abundance was affected by day ($P < 0.001$). Gene expression increased from Days 10 to 17 with Day 15 and 17 endometrial SPP1 expression 61 and 115 fold greater, respectively, compared to Day 10 (Figure 4.1C). While not statistically significant, SPP1 expression was numerically greater (7-fold) in EC treated gilts compared to CO treated gilts on Day 13 of pregnancy (Figure 4.1C). No day x treatment interaction was detected ($P = 0.19$).

Figure 4.1. Fold differences of mRNA abundance for endometrial AR (**A;** day x treatment, $P < 0.03$), CD24 (**B;** day effect, $P = 0.02$), SPP1 (**C;** day x treatment, $P < 0.14$) and NMB (**D;** day x treatment, $P < 0.001$) in response to EC (yellow bar) and CO (blue bar). Relative abundance of mRNA was calculated from the quantitative RT-PCR analysis as described in *Materials and Methods.* Bars without common lowercase superscripts represent a statistical difference ($P < 0.05$) between day/treatment combinations whereas differences in uppercase superscripts represent statistical differences between days of gestation.

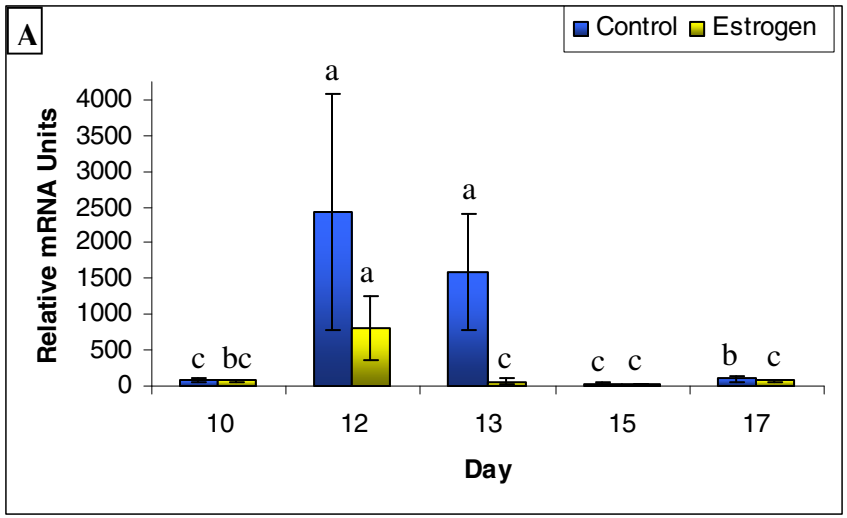
A
Control
Estrogen
Relative mRNA Units
4000
3500
3000
2500
2000
1500
1000
500
0
c bc
a
a
c
c c
b c
10
12
13
15
17
Day

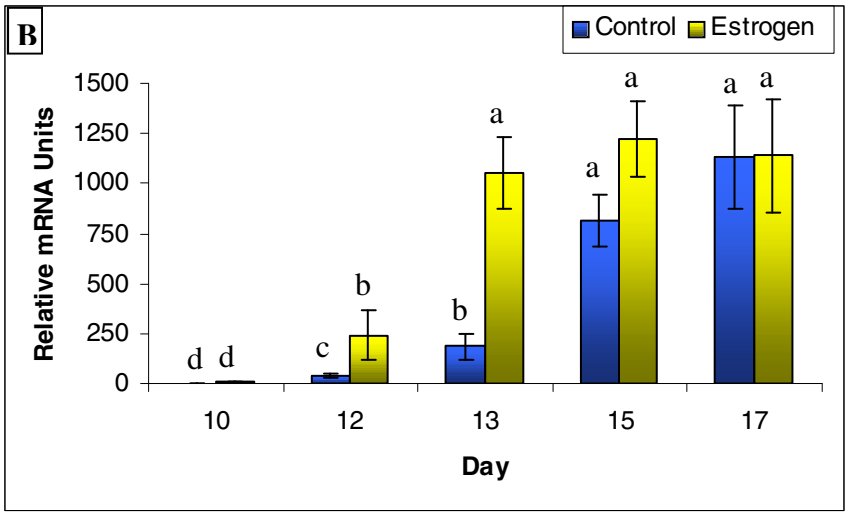
B
Control
Estrogen
Relative mRNA Units
1500
1250
1000
750
500
250
0
d d
c
b
b
a
a
a a
10
12
13
15
17
Day

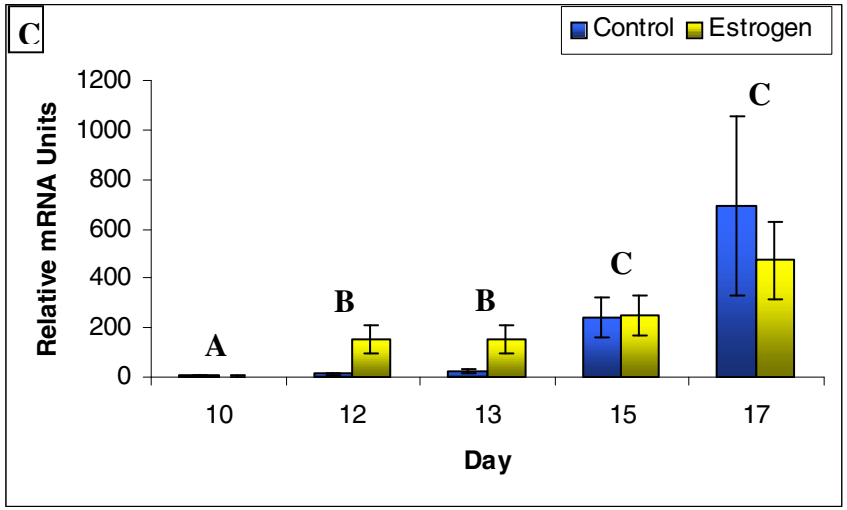
C
Control
Estrogen
Relative mRNA Units
1200
1000
800
600
400
200
0
A
B
B
C
C
10
12
13
15
17
Day

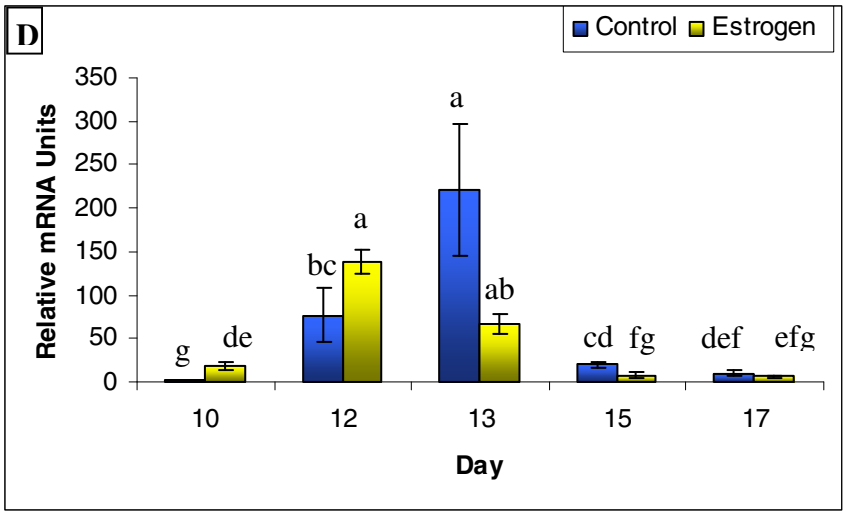
D
Control
Estrogen
Relative mRNA Units
350
300
250
200
150
100
50
0
g de
bc
a
a
ab
cd fg
def efg
10
12
13
15
17
Day

A significant day x treatment interaction ($P < 0.001$) was detected for endometrial NMB mRNA expression (Figure 4.1D). In comparison to CO gilts, expression of NMB mRNA was greater in the EC treated gilts on Days 10 ($P < 0.002$) and 12 ($P < 0.04$) by 6.7- and 2.8-fold, respectively. Alternately, expression tended to be reduced (2.7 fold) in EC treated gilts on Day 13 ($P < 0.07$) and significantly reduced 4.4 fold on Day 15 ($P < 0.01$) when compared to CO gilts.

In Situ Hybridization

Endometrial expression of AR was localized only to the uterine luminal epithelium (LE) of both CO and EC gilts. Expression of AR was detectable in the LE on Days 12 and 13 in CO treated gilts and on Day 12 EC treated gilts (Figure 4.2). Administration of estrogen on Days 9 and 10 of pregnancy completely suppressed the expression of AR in the LE of gilts on Day 13 of pregnancy. Expression of AR mRNA in the LE was low by Days 15 and 17 of gestation in both CO and EC gilts.

Similar to AR mRNA expression, SPP1 was not clearly localized to the LE until Day 15 of pregnancy in CO gilts. Intensity of the signal increased from Days 15 to 17 (Figure 4.3). Expression of SPP1 mRNA was apparent in the LE on Days 12 and 13 of EC treated gilts with a strong signal detectable in the uterine LE on Day 15 (Figure 4.3).

Expression of CD24 was present in the LE of both CO and EC gilts. Uterine LE CD24 expression increased steadily from Days 12 through 17 (Figure 4.4). Slight CD24 expression was detected in the glandular epithelium (GE) on Days 13 through 17 in both CO and EC gilts. Interestingly, the GE CD24 expression appeared to be elevated on Day 10 in EC compared to Day 10 CO gilts.

Figure 4.2. *In Situ* hybridization analysis of AR mRNA expression in porcine endometrium during early gestation in response to estradiol cypionate (EC) or corn oil (CO) given i.m. on Days 9 and 10 of gestation. Protected transcripts in endometrium from Days 10, 12, 13, 15 and 17 of each treatment were visualized by liquid emulsion autoradiography and imaged under bright-field and dark-field illumination. Note during normal gestation (CO) on Days 12 and 13 of gestation, the expression is abundant, but limited to the luminal epithelium (LE) and lacking in the stromal (ST) and glandular epithelium (GE). Following EC treatment, mRNA abundance was dramatically and prematurely reduced in the LE. A representative Day 13 EC section was hybridized with radiolabeled sense cRNA probe (sense) to serve as a negative control. All other images are representative from four biological replications. 4X Objective and 10X eyepiece for original magnification 40X.

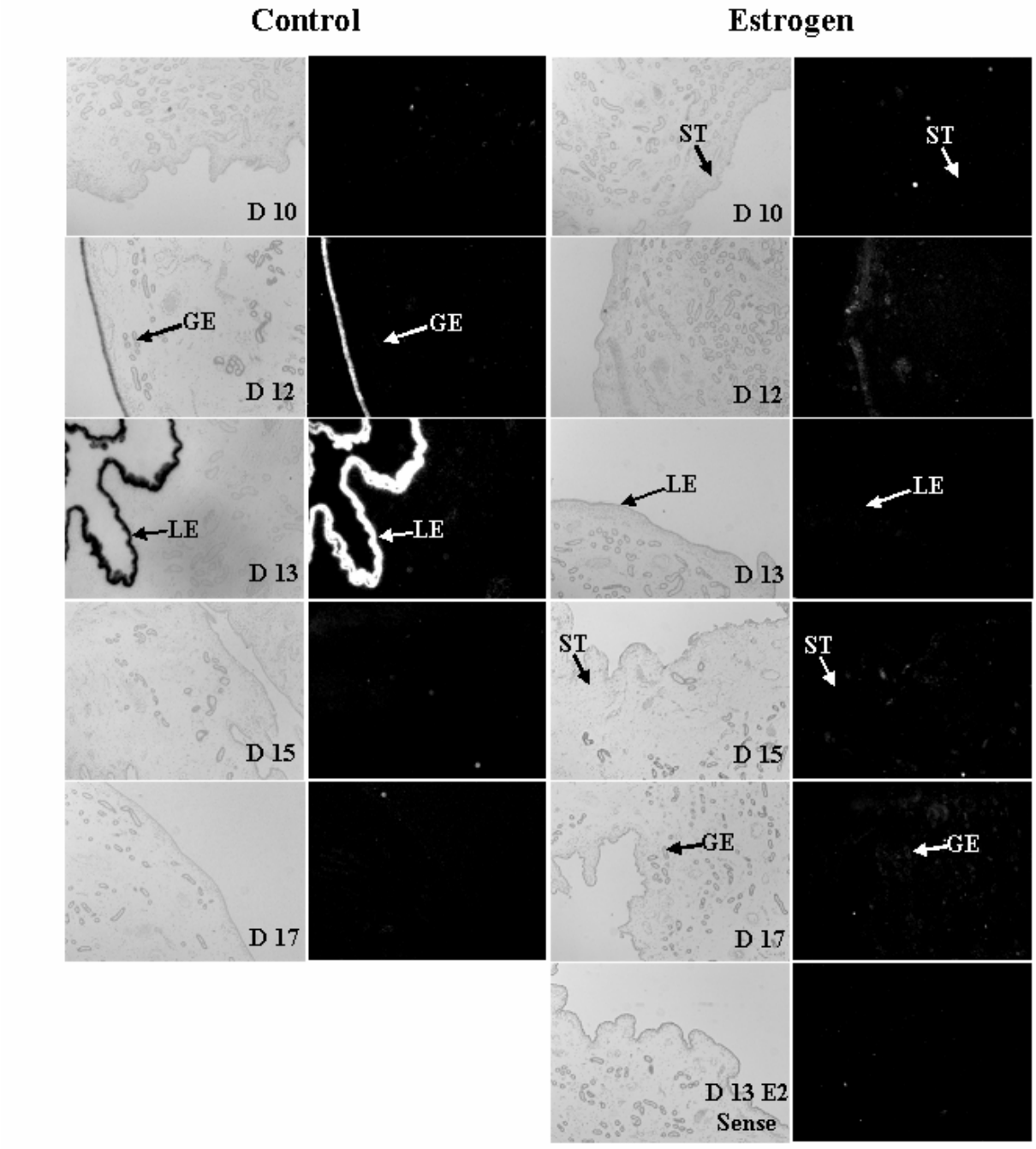
Control
Estrogen
D 10
ST
D 10
ST
GE
D 12
GE
D 12
LE
D 13
LE
LE
D 13
LE
D 15
ST
D 15
ST
D 17
GE
D 17
GE
D 13 E2
Sense

Figure 4.3. *In Situ* hybridization analysis of SPP1 mRNA expression in porcine endometrium during early gestation in response to estradiol cypionate (EC) or corn oil (CO) given i.m. on Days 9 and 10 of gestation. Protected transcripts in endometrium from Days 10, 12, 13, 15 and 17 of each treatment were visualized by liquid emulsion autoradiography for 5 days and imaged under bright-field and dark-field illumination. During normal gestation (CO), expression increases in the luminal epithelium (LE) on Days 15 and 17 while expression is lacking in the stromal (ST) and glandular epithelium (GE). EC treatment, however, visually increased mRNA abundance in the LE on Days 12, 13, 15 and 17 in the LE when compared to the EC. A representative section on Day 15 EC hybridized with radiolabeled sense cRNA probe (sense) served as a negative control. All other images are representative of four biological replications. 4X Objective and 10X eyepiece for original magnification 40X.

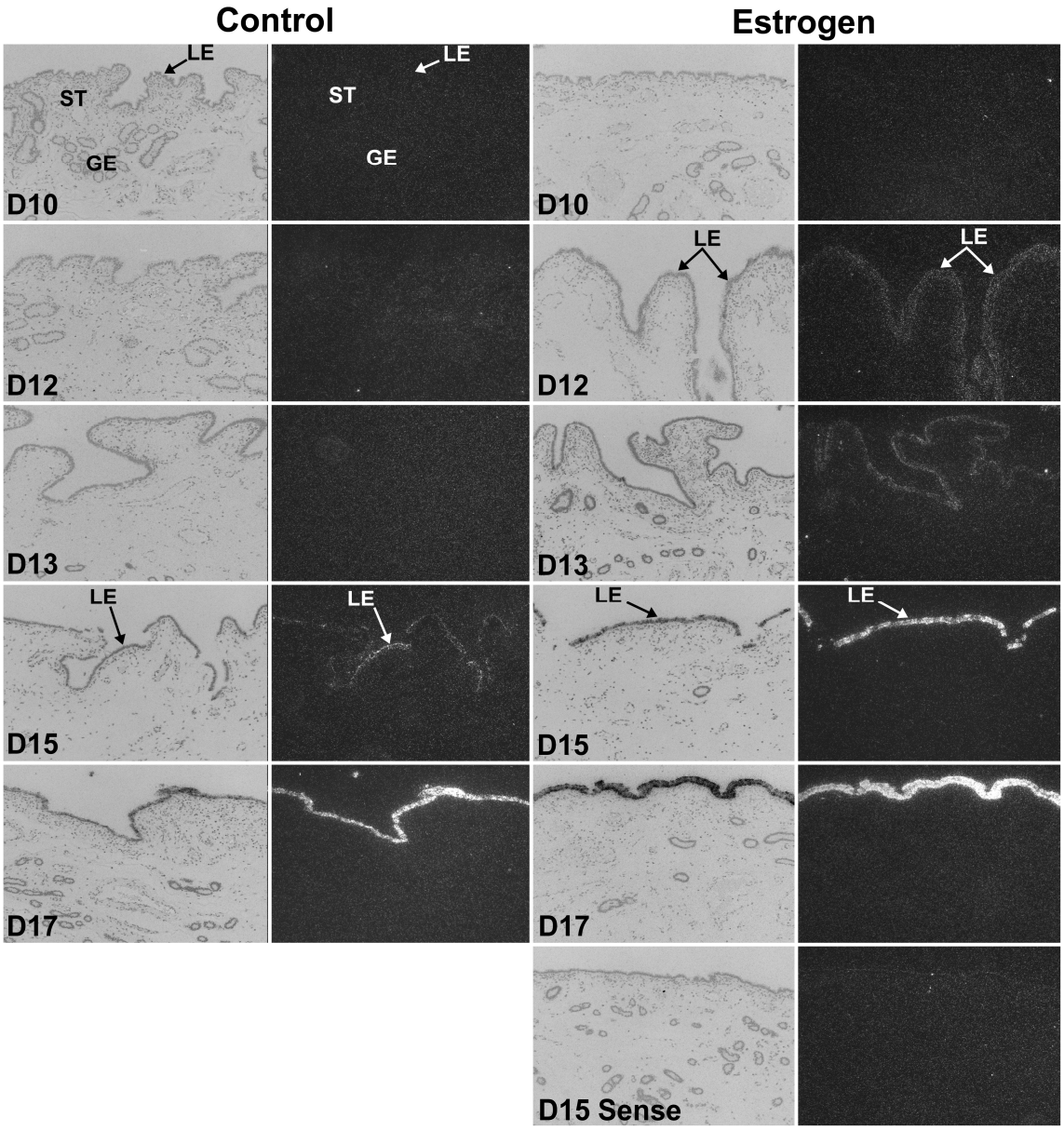
Control
Estrogen
LE
ST
GE
D10
D12
D13
D15
D17
D15 Sense

Figure 4.4. *In Situ* hybridization analysis of CD24 mRNA expression in porcine endometrium during early gestation in response to estradiol cypionate (EC) or corn oil (CO) given i.m. on Days 9 and 10 of gestation. Protected transcripts in endometrium from Days 10, 12, 13, 15 and 17 of each treatment were visualized by liquid emulsion autoradiography for 8 wks and imaged under bright-field and dark-field illumination. CD24 expression seems to occur predominately in the LE although some expression appears present in ST cells on Days 10, 12, and 13 of both CO and EC gilts. Expression is greatest in the LE of endometrium from gilts on Days 13, 15 and 17 in both CO and EC gilts. A representative section on Day 13 CO hybridized with radiolabeled sense cRNA probe (sense) to serve as a negative control. All other images are representative of four biological replications. 4X Objective and 10X eyepiece for original magnification 40X.

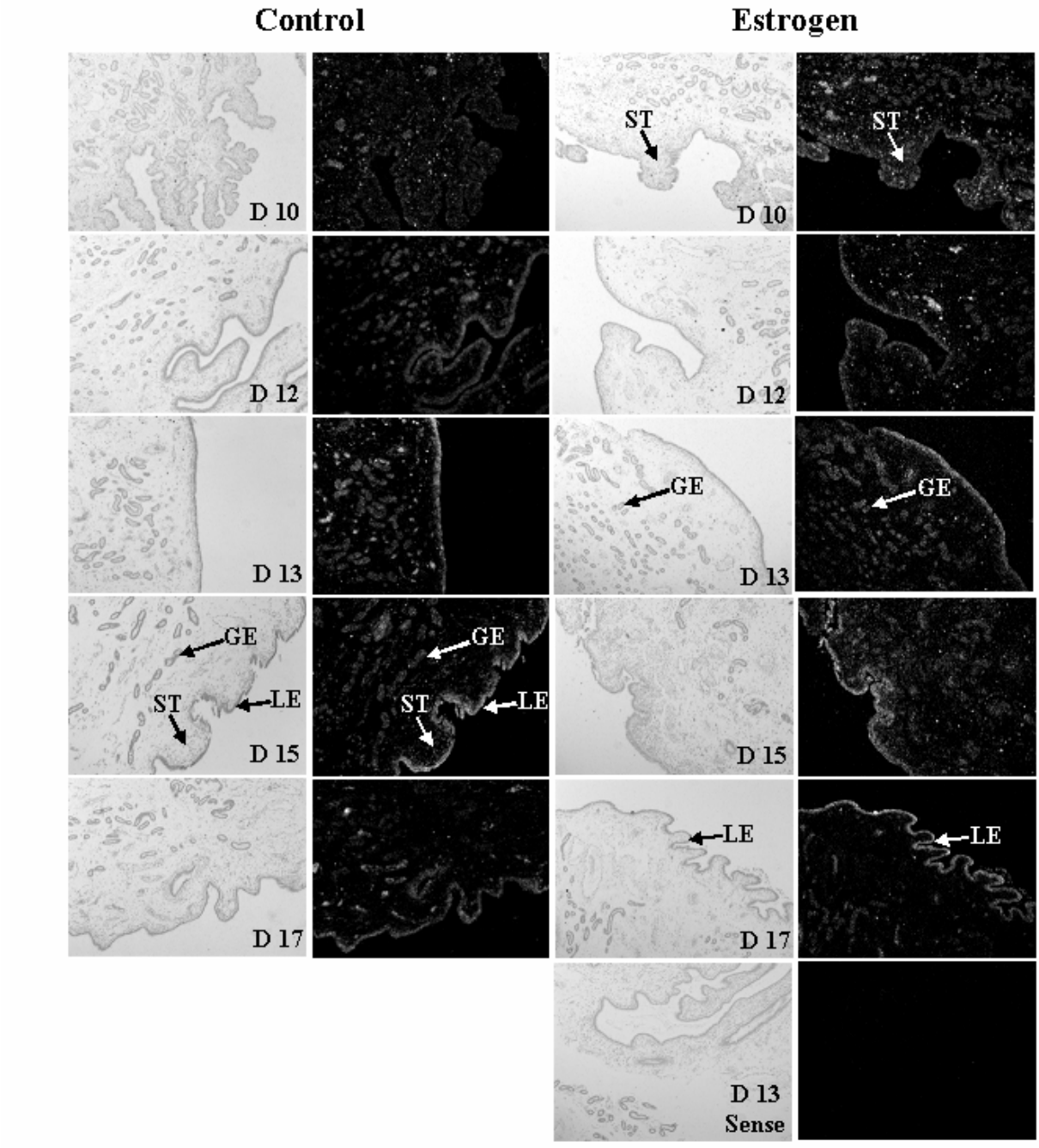
Control
Estrogen
D 10
D 12
D 13
D 15
D 17
D 13
Sense
ST
GE
LE

Figure 4.5. *In Situ* hybridization analysis of CD24 mRNA expression in porcine endometrium on Day 12 of gestation in the presence and absence of a conceptus. Protected transcripts in endometrium was visualized by liquid emulsion autoradiography for 8 wks and imaged under bright-field and dark-field illumination. Note the lack of expression in the LE of endometrium distant from the conceptus (upper half of the panel) and the amplified expression of CD24 in adjacent to the conceptus trophectoderm (lower half of the panel). CD24 expression is expressed abundantly by the trophectoderm conceptus. 4X Objective and 10X eyepiece for original magnification 40X.

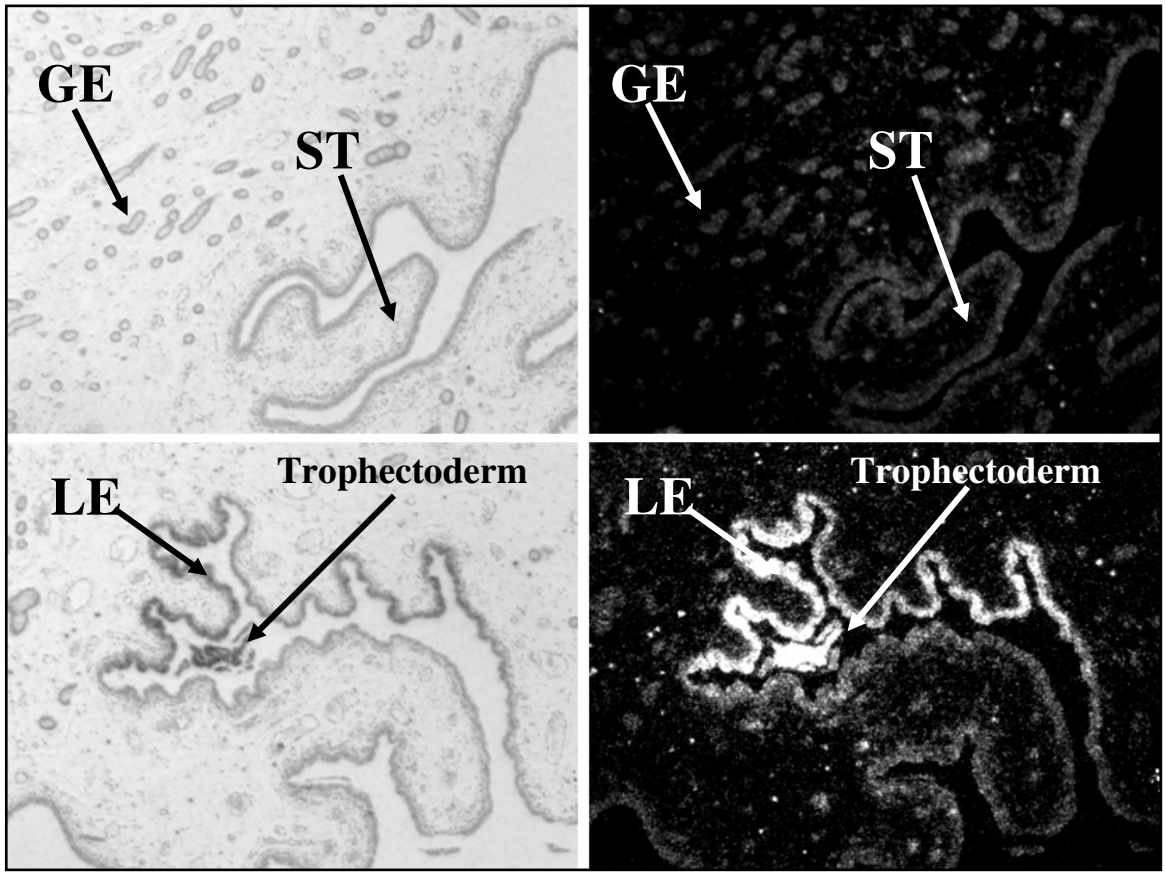
GE
ST
GE
ST
LE
Trophectoderm
LE
Trophectoderm

Figure 4.6. *In situ* hybridization analysis of NMB mRNA expression in porcine endometrium during early gestation in response to estradiol cypionate (EC) or corn oil (CO) given i.m. on Days 9 and 10 of gestation. Protected transcripts in endometrium from Days 10, 12, 13, 15 and 17 of each treatment were visualized by liquid emulsion autoradiography and imaged under bright-field and dark-field illumination. Note the expression is very specifically limited to the LE. Expression is greatest on Days 12 and 13 of CO gilts while expression appeared prematurely elevated on Day 10 and reduced on Day 13 in LE of EC gilts. A representative section on Day 13 CO hybridized with radiolabeled sense cRNA probe (sense) to serve as a negative control. All other images are representative of four biological replications. 4X Objective and 10X eyepiece for original magnification 40X.

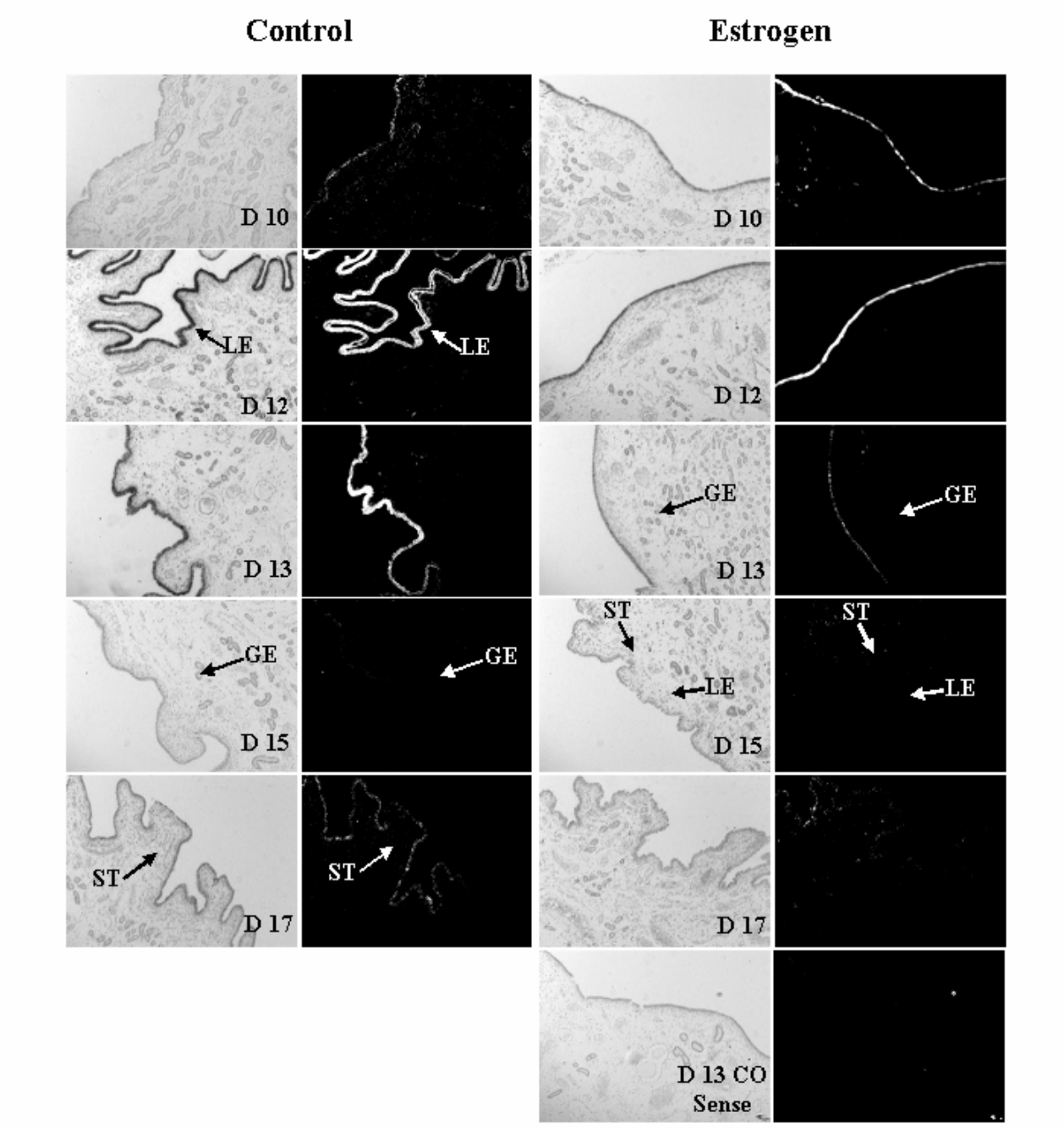
Control
Estrogen
D 10
D 10
LE
LE
D 12
D 12
D 13
GE
GE
D 13
GE
GE
ST
ST
LE
LE
D 15
D 15
ST
ST
D 17
D 17
D 13 CO
Sense

Expression of CD24 is also present in the conceptus during the peri-implantation stage of development and appears to be expressed at much greater levels in the LE adjoining to a conceptus as compared to LE distal form the conceptus within the same cross-section (Figure 4.5).

Neuromedin B mRNA expression was localized to the uterine LE (Figure 4.6). Expression of NMB increased in the LE of EC gilts on Days 10 and 12 of pregnancy while increased expression was not increased until Days 13 and 15 of pregnancy in CO gilts. Intensity of NMB expression on Day 17 was similar between treatments.

Discussion

Conceptus synthesis and release of estrogen is an essential component to the establishment of pregnancy in the pig [Bazer and Thatcher, 1977]. While estrogen is a critical constituent of early pregnancy recognition in swine, endometrial exposure to estrogen prior to the normal conceptus secretion results in total pregnancy loss [Blair et al., 1991]. Exogenous exposure of pregnant pigs to estrogen before Day 10 of gestation causes conceptus degeneration between Days 15 and 18 of gestation [Pope et al., 1986, Blair et al., 1991; Ashworth et al., 2006]. Our laboratory has utilized the treatment of pregnant gilts with estrogen on Days 9 and 10 as an endocrine disruptor model to evaluate factors involve with implantation in the pig. Based on our microarray analysis, the greatest number of genes altered from the EC treatment occurred on Day 13 of gestation, five days following the initial estrogen injection. It may be possible that the disruptive response is a result of the confounding interaction between the EC treatment and the developmental events that occur between the elongating conceptus and uterine

endometrium. Not only does the elongating conceptus produce estrogen that alters uterine secretion during normal pregnancy [Geisert et al., 1982b], but there is elevated conceptus production of interleukin-1β (IL-1β) and a concomitant increase in endometrial expression of IL-1 receptors [Tuo et al., 1996b; Ross et al., 2003b]. Interestingly, the EC injection on Days 9 and 10 of gestation in gilts does not alter the pattern of IL-1β secretion by the conceptus [Ashworth et al., 2006], collectively suggesting that a cohesive function existing between simultaneous conceptus secretion of estrogen and IL-1β may be abrogated by the premature estrogen exposure to the uterine endometrium. This may lead to the alteration or inhibition of the initial attachment of the trophectoderm to the uterine endometrium which occurs on Day 13 of gestation [Perry et al., 1981; Dantzer, 1985].

Based on evaluation through the DAVID, several common biological themes affected by EC treatment were clustered to represent the most likely affected biological processes (Table 4.5). It is not surprising that the alterations in gene expression represent processes such as immune, inflammatory, wound, and defense response (annotation cluster 3, Table 4.5) and apoptosis related events (annotation cluster 6) as the phenotypic outcome is pregnancy loss, resulting from conceptus degeneration (Ashworth et al., 2006) and sloughing of the extracellular matrix (Blair et al., 1991). Disruption of cation (calcium or zinc) ion binding (annotation cluster 9) has previously been shown to be disrupted due to exogenous estrogen administration on Days 9 and 10 of gestation (Geisert et al., 1982). Because of their relevant biological effects in protein modification/metabolism, immune/inflammatory response and Ca2+ transport that are critical to conceptus development and ECM formation on the LE during peri-

implantation, we investigated endometrial expression of AR, NMB, SPP1, and CD24 through quantitative RT-PCR.

Many of the genes affected by the EC treatment are known to be differentially regulated in the porcine endometrium during peri-implantation, such as retinol binding protein 4 (Vallet et al., 1996; Groothius et al., 2002), spermidine/spermine N1-acetyltransferase (Green et al., 1996; 1998) and SPP1 (Garlow et al., 2002; Johnson et al., 2003). However, several genes, such as CD24, NMB, AR and allograft inflammatory factor 1, have little literature regarding their association with the uterine endometrium during implantation in the pig. Numerous sequences represented on the array that lacked a quality annotation that appeared to be estrogen regulated were also identified during the period of endometrial receptivity and conceptus attachment during pregnancy (Tables 4.2-4.4).

Aldose reductase is the rate-limiting enzyme of the polyol pathway responsible for the reduction of glucose to sorbitol while consuming an NADPH, and is also involved in the reduction on toxic aldehydes, created by reactive oxygen species, to inactive alcohols [see review, Brownlee, 2001]. Following the conversion of glucose to sorbitol via AR, sorbitol can be utilized to produce fructose. During normal pregnancy in the pig, the expression of AR mRNA is transient and localized to the endometrial LE (Figures 4.1A and 4.3). Peri-implantation expression of AR in sheep appears to be regulated by the trophectoderm, for which expression is elevated between Days 12 and 17 of gestation [Lee et al., 1998]. In human endometrial ST cells, IL-1β significantly up-regulates the expression of AR [Rossi et al., 2005]. The induction of AR gene expression in the pig may be regulated through conceptus IL-1β as the peak AR expression is concurrent to

previously reported peak IL-1β gene and protein production [Ross et al., 2003b]. The critical nature of AR expression in the LE during implantation may be associated with both glucose and toxic aldheyde reduction. It is likely that AR plays a critical role in production of sorbitol from glucose to be utilized in fructose production. Pregnant gilts have higher levels of glucose and fructose [Zavy et al., 1982] following conceptus estrogen stimulation. While glucose itself is a vital energy substrate, conversion of glucose to fructose may also provide a critical carbon source for DNA and RNA synthesis while conceptuses undergo the dramatic increase in transcriptional activity and cellular mitosis following the initiation of trophoblastic elongation, occurring concomitant with LE AR expression. Indirectly, the alteration in AR expression leading to the potential shift in available fructose in the uterine lumen may affect the fructation, and subsequently, the activity and biological function of specific proteins during periimplantation development in the pig.

Secreted phosphoprotein 1, also referred to as osteopontin, has been previously shown to be expressed in the uterine LE and GE of pigs during early pregnancy and is sustained through at least to Day 85 of gestation [Garlow et al., 2002]. Estrogen, when given on Days 11-15 of the estrous cycle induces the expression of SPP1 in the LE but not in GE on Day 15 [White et al. 2005]. Our data indicates that estrogen stimulates LE expression of SPP1 in a progesterone primed uterus. In the CO pregnant gilts, conceptus estrogen synthesis and release stimulated SPP1 expression on Day 15 while early administration of estrogen in EC gilts prematurely induced LE expression.

SPP1 has a superfluity of potential functions in the uterus during the establishment of pregnancy in species forming an epitheliochorial type of placentation,

such as the pig [Johnson et al., 2003]. These include contributions to extracellular matrix formation, migration of immune cells, alterations in intracellular calcium levels, and activation of phosphotidylinositol 3'-kinase activity; and has also been hypothesized to form as a bridging ligand between the uterine LE and the conceptus trophectoderm [see review; Johnson et al. 2003]. The induction of SPP1 following EC treatment may be related to several of these aspects. Blair et al., [1991] documented the sloughing off of the extracellular matrix of gilts by Day 15 of gestation following injections of estradiol valerate (EV) on Days 9 and 10, also resulting in total conceptus mortality. A single estradiol injection of EV on Day 11 of the estrous cycle results in an approximate 4.5-fold increase in calcium concentrations in uterine flushings 12 and 24 h post injection (Geisert et al. 1982a). However, there is no increase in uterine luminal calcium content 24 h after treatment of gilts with EV on Day 9 which also dramatically (> 12-fold) reduces the surge release of calcium in uterine flushing of pregnant gilts on Day 12 [Gries et al., 1989]. While impossible to directly link EC alteration of SPP1 expression in the LE of gilts during early pregnancy based on these data, the associations regarding disrupted ECM formation and endometrial calcium secretion resemble the pattern of disruption that estrogen causes in SPP1 mRNA expression.

Similar to SPP1, the expression of CD24 was also localized to the uterine LE and prematurely elevated in EC treated gilts. CD24 is a membrane bound molecule whose structure lacks a cytoplasmic fraction and has specific binding ability for P-selectin, phenotypically suggesting CD24 may serve as a mucin-like adhesion molecule [review; Kristiansen et al., 2004]. However, the interaction of P-selectin and CD24 may also induce excessive TH1 lymphocyte trafficking as over-expression of P-selectin is

associated with increased TH1 lymphocytes in human patients suffering from spontaneous miscarriage [Zenclussen et al., 2001]. Interestingly, treatment of abortion prone mice (CBA/J x DBA/2J) with anti-P-selectin monoclonal antibody prior to implantation significantly reduced the occurrence of abortion and the production of IFN-γ and TNF-α production by decidual lymphocytes [Bertoja et al., 2005]. Because of the multiple roles CD24 has with immune response, the contribution CD24 over-expression in EC treated gilts may elicit an elevated immune response disrupting conceptus attachment to the uterine surface. While P-selectin expression is not well characterized in the pig, an mRNA sequence has been isolated from uterine endometrium during early pregnancy, sequenced, and annotated as P-selectin (GenBank accession number: DQ097865); suggesting that CD24 may serve as a bridging ligand during the attachment and adhesion of the conceptus trophectoderm to the uterine endometrium. It is clear that as early as Day 12 of gestation both the conceptus and the endometrium are producing copious amounts of CD24 in a spatiotemporal manner (Figure 4.5). If expression of P-selectin by the endometrium is required for CD24 bridging during attachment, it is possible that increased expression by the uterine endometrium in response to the EC treatment resulted in excessive P-selectin/CD24 binding prior to the conceptus ability to express CD24 and bind P-selectin on the LE resulting in attachment failure.

Neuromedin B is a bombesin-like peptide first discovered in porcine spinal cord [Minamino et al., 1988]. Immunologically, NMB has been shown to be expressed by multiple cancer cell lines and, like other bombesin-like peptides, can negatively influence IL-12 production and the maturation, antigen presentation, and endocytotic capability of dendritic cells [Makarenkova et al., 2003]. Interestingly, the greatest endometrial NMB

gene expression occurred in CO animals on Day 13 of gestation. Treatment of pregnant gilts with estrogen caused a significant increase or advancement in NMB expression on Day 12 on the LE (Figure 4.1D and 4.6). There is a void in the literature regarding the role of endometrial NMB expression in establishment of pregnancy in the pig as well as its role in other species. NMB has been demonstrated to stimulate smooth muscle contractions in a variety of tissues including the uterus [see review; Ohki-Hamazaki et al., 2000]. While the expression of NMB and its receptor, NMB-R, has been shown to affect maternal and emotional behavior [Yamada et al., 2002a; 2002b]; NMB has also been shown to increase the release of arachidonic acid and promote cell growth [Moody et al., 1995] and elevate cellular Ca^{2+} concentrations [Wang et al., 1992] in C6 glioma cancer cells through bombesin receptors. The promoted cell growth is consistent with NMB and its receptor, NMB-R, functioning as mitogens in epithelial cells lining the colon while elevated NMB-R was associated with those epithelial cells that had differentiated into tumor cells [Matusiak et al., 2005]. The expression of bombesin-like peptides does appear to be a significant factor during pregnancy as neuromedin U was also shown to be differentially expressed in response to EC on Day 13 of gestation (Table 4.3). Bombesin-like peptide receptors, specifically, gastrin-releasing peptide receptor and NMB-R are expressed in the developing mouse embryo throughout gestation [Battey et al., 1994]. Because of the ability for bombesin-like peptides to function as mitogens affecting cell growth it is requisite to determine the expression patterns of NMB-R in both the elongating conceptus and uterine endometrium during the establishment of pregnancy in the pig.

Premature estrogen exposure affects multiple factors in the uterine endometrium

that are common in that their abnormal expression, whether increased or decreased, is advanced approximately 48 h compared to normal expression. These alterations in gene expression may cause an asynchrony between the endometrium and conceptus similar to that described by Polge (1982) where embryos transferred greater than 48 h out of synchrony with the uterine endometrium fail to establish pregnancy. Geisert et al. (1991) demonstrated that gestation Day 6 embryos transferred into a more advanced uterine environment (48 h) are degenerate within 36 hours following transfer. Uniquely, conceptus loss as a result of estrogen exposure on Day 9 and 10 does not occur before Day 12, as conceptuses continue to elongate and don't become degenerate until approximately Day 15 of gestation. These data suggest that exogenous estrogen administration causes significant alterations in endometrial gene expression on Days 12 and 13 of gestation and may prevent attachment and promote immunological rejection of the conceptus resulting in its deterioration by Day 15 of gestation.

Chapter V

ACTIVATION OF THE TRANSCRIPTION FACTOR, NUCLEAR FACTOR KAPPA B, DURING THE ESTROUS CYCLE AND EARLY PREGNANCY IN THE PIG

Introduction

The diversion from cyclicity to establishment of pregnancy in any spontaneously ovulating species requires distinct alterations in uterine molecular events that allow for attachment and implantation of a developing conceptus. Given the uterine proinflammatory response during early conceptus development, it is possible that the transcription factor, nuclear factor κB (NFκB), is intricately involved in the regulation of the cascade of events regulating early pregnancy establishment in pigs. NFκB consists of multiple subunits that have a common Rel homology domain [Ghosh et al., 1998]. Inactive NFκB is sequestered in the cytoplasm through binding to inhibitors of NFκB (IκBs) until activation of IκB kinases, which results in the release and ubiquitination of IκB and the subsequent translocation of NFκB dimers into the nucleus regulating transcription of NFκB responsive genes [Ghosh et al., 1998; Ali and Mann, 2004]. NFκB activation can be the result of numerous stimuli such as bacterial endotoxin lipopolysaccharide, reactive oxygen species, and cytokines such as tumor necrosis factor α (TNFα) and interleukin-1β (IL-1β). It is likely that the pregnancy specific increase of IL-1β in the uterine lumen during conceptus elongation and attachment in pigs [Ross et

al., 2003b] may regulate the activation of NFκB and transcription of regulated genes, such as prostaglandin synthase-2 (PTGS2). Interestingly, PTGS2 expression is not pregnancy specific as the gene and enzyme is significantly upregulated in the luminal epithelium (LE) of gilts beginning on Days 10-12 of the estrous cycle and early pregnancy [Ashworth et al., 2006]. Indomethacin, a non-steroidal anti-inflammatory drug that inhibits prostaglandin synthesis through NFκB [Takada et al., 2004], results in the loss of embryos when given on Days 11 to 16 of pregnancy in the pig [Kraeling et al., 1985]. While elevated PTGS2 mediated prostaglandin production by the uterine endometrium of cyclic and pregnant gilts could be mediated by mechanisms independent of NFκB, results suggest a relationship between the NFκB and elevated PTGS2 in the uterine endometrium.

While NFκB transcription regulation in the endometrium is likely, the mechanisms by which it is regulated in the uterus is elusive. We hypothesize NFκB activation of PTGS2 transcription in the uterine endometrium is progesterone driven as conceptus production of IL-1β [Ross et al., 2003a] and estradiol-17β [Geisert et al., 1982b] does not affect PTGS2 expression in the uterine LE. Plasma concentrations of progesterone are high during diestrus inducing a LE specific downregulation of progesterone receptor protein in pigs on Days 10 to 12 of the estrous cycle and pregnancy [Geisert et al., 1994]. Progesterone receptor regulation of transcription is cell specific as protein expression persists in the underlying stroma during the time of attachment in the pig [Geisert et al., 1994]. The downregulation of progesterone receptor in the pig uterine LE prior to and during the opening of the implantation window is associated with endometrial transcriptional changes leading to either uterine receptivity for conceptus

development and attachment to the uterine surface during pregnancy or pathways releasing prostaglandin F2α to regress the corpora lutea and initiate a return to estrus [Geisert et al., 2006]. In fact the association of progesterone receptor downregulation temporal to the opening of the implantation window and conceptus attachment is not limited to the pig. Progesterone receptor downregulation in the uterine LE is generally associated with the opening of the implantation window in the human [Lessey et al., 1988, 1996], baboon [Fazleabas et al., 1999], sheep [Spencer and Bazer, 1995], cattle [Meikle et al., 2001] and horses [Hartt et al., 2005].

Although the specific downregulation of progesterone receptor in the LE has been well established, the pathway for this important biological event is not known. Progesterone receptor is capable of regulating transcription of genes through its interactions with NFκB as RelA and progesterone receptor are mutually repressive of each other [Kalkoven et al., 1996]. Thus we propose that regulation of progesterone receptor expression in the uterine LE involves an interaction with NFκB. The objective of this study was to characterize the contributing factors NFκB p50/RelA activation during the estrous cycle and early pregnancy in pig uterine endometrium.

Materials and Methods

Animals

Research was conducted in accordance with the Guiding Principles for Care and Use of Animals promoted by the Society for the Study of Reproduction and approved by the Oklahoma State Institutional Animal Care and Use Committee. Cyclic, crossbred

gilts of similar age (8-10 mo) and weight (100-130 kg) were checked for estrous behavior twice daily in the presence of an intact boar. Onset of estrus was designated Day 0 of the estrous cycle. Gilts were naturally mated with fertile boars at the onset of their second estrus (Day 0 of estrous cycle) and again 24 h later.

Tissue Collection

During the observation of estrus, gilts were randomly assigned to be either pregnant or cyclic. Gilts destined for pregnancy were mated by natural service from intact boars at the onset of estrus and again 24 h later. Uteri were collected from cyclic gilts on Days 0, 5, 7.5, 10, 12, 13, 15 and 17 of the estrous cycle while uteri were collected from pregnant gilts on Days 10, 12, 13, 15 and 17. Gilts were hysterectomized (n = 4 gilts/status/day) through midventral laporatomy as previously described by Gries et al. [1989]. Following induction of anesthesia with 1.8 mL of i.m. administration of a cocktail consisting of 2.5 mL (Xylazine; 100 mg/mL, Miles Inc., Shawnee Mission, KS) and 2.5 mL Vetamine (Ketamine HCL; 100 mg/mL, Molli Krodt Veterinary, Mundelein, IL) in 500 mg of Telazol (Tiletamine HCl and Zolazepum HCl; Fort Dodge, Syracuse, NE), anesthesia was maintained with a closed circuit system of halothane (5%) and oxygen (1.5 liters/min). Immediately following removal, each uterine horn was flushed with 20 mL of a physiological saline and conceptuses were removed. Uterine flushings were transferred to a 50 mL conical tube and centrifuged at 1000 rpm for 1 min to remove cell debris. Uterine flushings were stored at -80^{o}C until utilized. Following conceptus removal, one uterine horn was cut along its anti-mesometrial border, and endometrium (5-10 g) was removed with sterile scissors and snap-frozen in liquid

nitrogen and stored at -80°C until analyzed. Cross sections of uteri were also fixed in 4 % paraformaldehyde and dehydrated in 70% ethanol to use for *in situ* hybridization.

RNA Isolation

Total RNA was extracted from uterine endometrium tissue using the RNAwiz reagent (Ambion, Inc., Austin, TX) according to manufacturer's recommendations. Approximately 500 mg of endometrium was homogenized in 5 mL RNAwiz reagent using a Virtishear homogenizer (Virtis Company Inc., Gardiner, NY). RNA pellets were rehydrated in nuclease-free H_2O and stored at -80°C. RNA content was estimated spectrophotmetrically and purity determined by the 260:280 ratio. RNA quality and integrity was assessed through gel electrophoresis.

Protein Extraction

Cytoplasmic and nuclear protein fractions were prepared using a previously established method [Deryckere and Gannon, 1994; Nakamura et al., 2004a]. Briefly, 5.0 mg of uterine endometrium from cyclic (Days 5, 10 and 13) and pregnant (Days 10 and 13) gilts (n = 4/day/status) was pulverized in liquid nitrogen. Pulverized tissue was re-suspended in lysis buffer [150 mM NaCl, 10 mM Hepes-KOH (pH 7.9), 1 mM ethylenediaminetetraacetic acid (EDTA), 0.6% NP-40 and 1X Protease inhibitor cocktail (Pierce Biotechnology, Rockford, IL)] and homogenized with a loosely fitted pestle in a Dounce homogenizer (Wheaton, Millville, NJ). Homogenate was centrifuged at 1000 x g for 1 min at 4°C then supernatant was transferred to a new tube, incubated in ice for 5 min followed by additional centrifugation at 3300 x g, for 5 min at 4°C. The supernatant,

containing the cytoplasmic protein fraction was transferred and stored at -80°C while the pelleted nuclei were resuspended in 200 µl of nuclear extraction buffer [25% glycerol, 20 mM Hepes KOH (pH 7.9), 420 mM NaCl, 1.2 mM $MgCl_2$, 0.2 mM EDTA, 0.5 mM DL-Dithiothreitol (DTT) and 1X protease inhibitor cocktail]. Resuspended nuclei were incubated on ice for 30 min, vigorously vortexing intermittently. The nuclear suspension was centrifuged at 12 000 x g for 5 min at 4°C. Following centrifugation, the supernatant containing the nuclear protein extract was transferred to a new tube and stored at -80°C. Total protein concentrations were determined using the method of Bradford [1976] through the Bio-Rad protein assay (Bio-Rad Laboratories, Hercules, CA).

NFκB Activity

Activity of NFκB in cytoplasmic and nuclear protein fractions from uterine endometrium of pregnant and cyclic gilts was determined through an electrophoretic mobility shift assay and a transcription factor ELISA specific for NFκB p65 activity.

Electrophoretic Mobility Shift Assay

The electrophoretic mobility shift assay (EMSA) was conducted using a commercially available kit that specifically interrogates activated NFκB (Panomics, Fremont, CA). A total of 20 µg (representing a pool of 5 µg from 4 biological replications) was utilized in the EMSA. Pools assayed represented cytoplasmic and nuclear protein fractions isolated from uterine endometrium of cyclic gilts on Days 5, 10 and 13 and from endometrium from pregnant gilts on Days 10 and 13. Briefly, following hybridization of the protein sample with labeled probe, the hybridization mixture was

electrophoresed through a 6% polyacrylamide gel, transferred to a positively charged nylon membrane and crosslinked using ultra violet rays. Chemiluminescence detection was conducted according to manufacture's protocol. Membranes were exposed to Biomax MR film and developed. Positive control was the hybridization of control protein, included in the kit, with labeled probe. Negative controls included the hybridization of endometrial sample (Day 13 pregnant, cytoplasmic fraction) with labeled probe, but in the presence of 100-fold excess cold probe. Positive control probe and nuclear extract were included in the kit.

NFκB RelA ELISA

The presence of the NFκB RelA in nuclear and cytoplasmic protein extractions was determined using the TransAM NFκB RelA transcription factor assay kit (Active Motif, Carlsbad, CA). The assay utilizes a 96-well format for which each well contains immobilized oligonucleotide containing the NFκB consensus sequence. NFκB RelA was assayed in both nuclear and cytoplasmic protein fractions collected from endometrium of gilts on Days 5, 10 and 13 of the estrous cycle and Days 10 and 13 of pregnancy (n = 4 gilts per status/day). All samples, positive control nuclear extract and blank (using nuclear extraction buffer) were assayed in duplicate according to the manufacturer's recommendations. Positive control nuclear extract was included in the kit and excess wild-type and mutated NFκB consensus sequence oligo was added in excess to other control wells to determine specificity. Following protein/DNA binding and washing of the wells, anti-RelA primary and HRP-conjugated secondary antibodies, including with the assay kit, were utilized to determined relative amounts of bound RelA. Following

secondary antibody binding, the wells were developed colorimetrically and absorbance at 450 nm was determined. The optical density (OD) for each sample was first corrected by subtraction of the Blank OD and subsequently corrected for total protein in the sample.

In Situ Hybridization

Hybridization

Progesterone receptor (PR), estrogen receptor α (ERα), and receptor activator of NFκB (RANK), mRNA were localized in porcine uterine cross-sections by *in situ* hybridization using methods previously described [Johnson et al., 1999]. Paraffin embedded cross-sections (~5 µm) were deparaffinized, rehydrated, and deproteinated; then hybridized with radiolabeled antisense or sense porcine cRNA probes (5.0×10^6 counts per minute/slide) synthesized through *in vitro* transcription with [α-^{35}S] uridine 5-triphosphate (MP Biomedicals, Irvine, CA) using a linearized plasmid template. Following hybridization washes, and RNase A digestion, hybridized slides were exposed to Biomax maximum resolution film (Eastman Kodak, New Haven, CT) overnight to determine signal strength. Autoradiography was performed using NTB liquid photographic emulsion (Eastman Kodak). Slides were dipped in emulsion and exposed at 4°C for a period of time relative to signal strength, developed in Kodak D-19 developer, counterstained with Harris modified hematoxylin (Fisher Scientific, Fairlawn, NJ), dehydrated, and protected with cover slips.

Photomicrography

Digital photomicrographs of *in situ* hybridization, bright-field and dark-field images of liquid emulsion autoradiography, were collected using a Nikon Eclipse E6000 microscope interfaced with the CoolSNAPcf digital camera equipped with a cooled charge-coupled device (Photometrics, Tucson, AZ) and imaging software (MetaVue, Molecular Devices, Downington, PA).

Quantitative One-Step RT-PCR

Quantitative analysis of NFκB RelA, NFκB p50, RANK, Toll-like receptor-4 (TLR-4), and inhibitors of κB (IκBα and IκBβ) and were assayed using quantitative real-time RT-PCR and a fluorescent reporter as previously described [Ashworth et al., 2006]. The PCR amplification was conducted using the ABI PRISM 7500 Sequence Detection System (PE Applied Biosystems, Foster City, CA). The real-time detection during each amplification cycle was done by using a sequence specific dual-labeled fluorescent probe designed to have a 5' reporter dye (6-FAM) and a 3' quenching dye (TAMRA) nested between the forward and reverse sequence specific primers. All primers and probes utilized for quantitative analysis for each target gene are presented in Table 5.1. One hundred nanograms of synthesized cDNA were assayed for each sample in duplicate. Thermal cycling conditions using the dual labeled probe were 50^{o}C for 30 min, 95^{o}C for 15 min, followed by 40 repetitive cycles of 95^{o}C for 15 sec and a combined annealing/extension stage, 59^{o}C for 1 min. Fluorescent data acquisition was done during the annealing/extension phase. 18S ribosomal RNA was assayed as a normalization control to correct for loading discrepancies. Following RT-PCR, quantitation of gene

Table 5.1 Primer and probe sequences used for quantitative RT-PCR analysis.

Target[a]	Forward/Reverse Primers (5'→3')[b]	Fluorescent Reporter[c]	Length of Amplicon[d]	GenBank Accession #[e]
RANK	GCTGACTCTGGAAGAGAAGGTGTT GCCCTGTCCACATATTCGTCTTCTGT	ATGTGCTGTCCAGACGGTGGTGGTGCCTGT	192 bp	CB475057
TLR-4	ATGGCCTTTCTCTCCTGCCTGA AGGTCCAGTATCTTGACTGATGTGGG	ATCTGAGAGCTGGGACCCTTGCGTGCAGGT	139 bp	AB188301
NFκB p50	CCCATGTAGACAGCACCACCTATGAT ACAGAGGCTCAAAGTTCTCCACCA	ACCAGGCTGGCAGCTCTCCTCAAAGCAGCA	132 bp	NM_001048232
NFκB RelA	ACATGGACTTCTCAGCCCTTCTGA CCGAAGACATCACCCAAAGATGCT	ACACCTGCTCTGCCCAGAGCACTGGGTT	168 bp	CN155798
IκBα	TGTGATCCTGAGCTCCGAGACTTT TTGTAGTTGGTGGCCTGCAGAATG	TCTACACCTTGCCTGTGAGCAGGGCTGCCT	143 bp	NM_001005150
IκBβ	TCATTCTGCAGGTCCAGGTACTCA CACTTGGCGGTGATTCATCAGCAT	TGGATTTCCTCCTGGGCTTTGCTGCTGGCA	89 bp	AK231853

[a]The amplification target: RANK, Receptor activator of NFκB; TLR-4, Toll-like receptor 4; NFκB p50, Nuclear factor κB p50 subunit; NFκB RelA, Nuclear factor κB RelA subunit, IκBα and IκBβ, Inhibitors of κB α and β, respectively.
[b]The forward and reverse DNA oligos used in the amplification of the target. Forward and reverse do not necessarily indicate the *in vivo* direction of transctiption.
[c]The DNA oligo sequence of the dual-labeled probe (possessing the FAM reporting dye on the 5' end and the TAMRA quenching dye on the 3' end) used to measure amount of amplified target during each cycle of quantitative RT-PCR.
[d]The length of the amplicon created during PCR.
[e]The accession number to the porcine sequence that was utilized during primer and probe design.

amplification was made by determining the cycle threshold (C_T) based on the fluorescence detected within the geometric region of the semilog view of the amplification plot. Relative quantitative analysis of target gene expression was evaluated using the comparative C_T method as previously described [Hettinger et al. 2001; Ashworth et al., 2006]. The ΔC_T value was determined by subtracting the target C_T of each sample from its respective ribosomal 18S C_T value. Calculation of $\Delta\Delta C_T$ involves using the single greatest sample ΔC_T value (the sample with the lowest expression) as an arbitrary constant to subtract from all other sample ΔC_T values. Relative mRNA units for each sample were calculated assuming an amplification efficiency of 2 during the geometric region of amplification, and applying the equation, $2^{\Delta\Delta Ct}$. Relative mRNA units in figures 5.6-5.8 are presented as mean ± SEM.

Statistical Analysis

Statistical analysis was conducted to determine differences for both the TransAM NFκB RelA assay and the quantitative RT-PCR results. Analysis was conducted using the corrected OD values through PROC MIXED of the Statistical Analysis System. The effects of day, pregnancy status, and protein fraction; as well as all possible interacting effects. Data are presented as mean OD ± SEM.

Quantitative RT-PCR ΔC_T values; representing the raw, normalized data, were used for analyses, also through PROC MIXED. Analysis of endometrial gene expression tested for the effect of day, status and day x status interaction. Significance between means of specific effects ($P < 0.05$) was determined by probability differences of least

squares means. Figures representing relative mRNA units have superscripts above bars depicting significant differences as determined by the ΔC_T values ($P < 0.05$).

Results

Activation of NFκB

Electrophoretic Mobility Shift Assay

The EMSA effectively identified shifted probe containing the NFκB consensus sequence when hybridized with both nuclear and cytoplasmic protein extract of endometrium from cyclic and pregnant gilts (Figure 5.1). The probe hybridized with the positive control (Figure 5.1, far right lane) while hybridization of the probe with cytoplasmic extract from Day 13 pregnant endometrium fail to bind in the presence of 100-fold excess cold probe (second lane from the right). There were two shifted regions identified for all days evaluated. Interestingly, while both of the shifted regions (Figure 5.1, B and C arrows) were present in the nuclear protein fraction, only one of the regions was present in the cytoplasmic fraction (Figure 5.1, B arrow). Based on visual assessment, no differences in the amount of bound oligo are apparent between any of the days which the cytoplasmic protein fractions were evaluated. Alternatively, the amount of bound oligo in the hybridization containing the nuclear fraction from Day 5, cyclic endometrium was less than that of the nuclear fraction evaluated during mid-luteal phase (Days 10 and 13) of both cyclic and pregnant endometrium (Figure 5.1).

Figure 5.1. Electrophoretic mobility shift assay was conducted using a commercially available EMSA as described in the *Materials and Methods*. Nuclear and cytoplasmic protein fractions extracted from gilts on Days 5, 10, and 13 of the estrous cycle and Days 10 and 13 of pregnancy were exposed to an oligo containing an NFκB consensus sequence followed by electrophoresis through a polyacrylamide gel and transferred to a positively charged membrane. Labeled oligo was detected through chemiluminescence. Unbound, labeled oligo migrates the most rapidly and is indicated with an arrow (A), while bound oligo, migrating slower is shifted towards the upper end of the gel (indicated by the B and C arrows). Note the lack of a shifted labeled oligo for the negative control in which 100 fold excess unlabeled probe was added to the hybridization reaction. The cytoplasmic fraction represented a single shift while two shifts, indicative of multiple NFκB dimers, was indicated by the nuclear fraction. Each lane is equally represented by protein extracted from endometrium of four gilts.

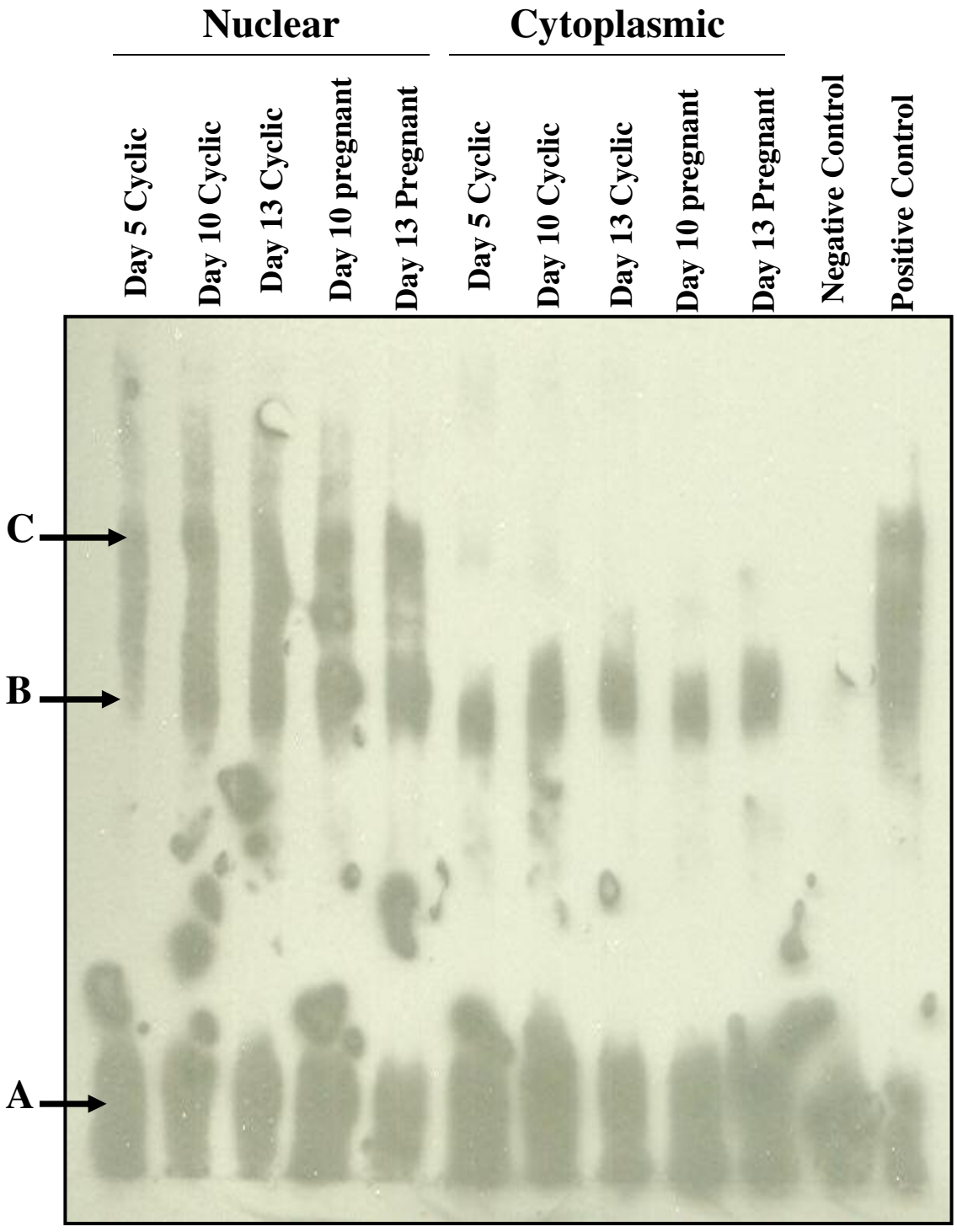
Nuclear
Cytoplasmic
Day 5 Cyclic
Day 10 Cyclic
Day 13 Cyclic
Day 10 pregnant
Day 13 Pregnant
Day 5 Cyclic
Day 10 Cyclic
Day 13 Cyclic
Day 10 pregnant
Day 13 Pregnant
Negative Control
Positive Control
C
B
A

NFκB RelA ELISA

There was a day x status ($P = 0.05$) and status x protein fraction ($P = 0.001$) interaction for the detected amount of NFκB RelA. Differences in the amount of RelA in the nuclear fraction were insignificant between the days of the estrous cycle and pregnancy evaluated (Figure 5.2). In contrast, the amount of RelA in the cytoplasmic compartment was greater during the mid-luteal phase (Day 13) compared to Day 5. Furthermore, the amount of RelA in the cytoplasmic fraction was greater than the amount in the nuclear fraction on Days 10 and 13 in comparison to Day 5, for which there was no detectable difference in RelA between the cytoplasmic and nuclear protein fractions. While this difference in cellular compartment was present in both cyclic and pregnant gilts, the difference appeared to be greater in the pregnant gilts (Figure 5.2).

In Situ Hybridization

Estrogen Receptor α

Endometrial expression of ERα was localized to the uterine luminal epithelium (LE), glandular epithelium (GE) and stromal cells (ST) during estrus (Day 0) when expression was greatest (Figure 5.3). By Day 5, expression was still apparent in all cell types of the endometrium albeit at a reduced abundance. Decline in ERα expression continued in all cell types being nearly devoid by Day 7.5 of the estrous cycle and Day 10 of both the estrous cycle and pregnancy. On Day 12 and 13 of pregnancy, ERα expression was elevated in the LE. Expression during Day 12 of the estrous cycle was modest compared to Day 13 cyclic endometrium exhibiting elevated ERα mRNA in the GE. GE expression of ERα was transient as expression in cyclic gilts steadily increased

Figure 5.2. Transcription factor assay to determine relative amounts of activated NFκB RelA in the nuclear (day effect, $P = 0.005$) and cytoplasmic (day effect, $P = 0.006$; status effect, $P < 0.001$) protein fractions of endometrium collected from gilts on Days 5, 10 and 13 of the estrous cycle and Days 10 and 13 of pregnancy (n = 4/day/status). Relative optical density for each sample was corrected for total protein concentration in the sample. Data is presented as relative O.D. mean ± SEM.

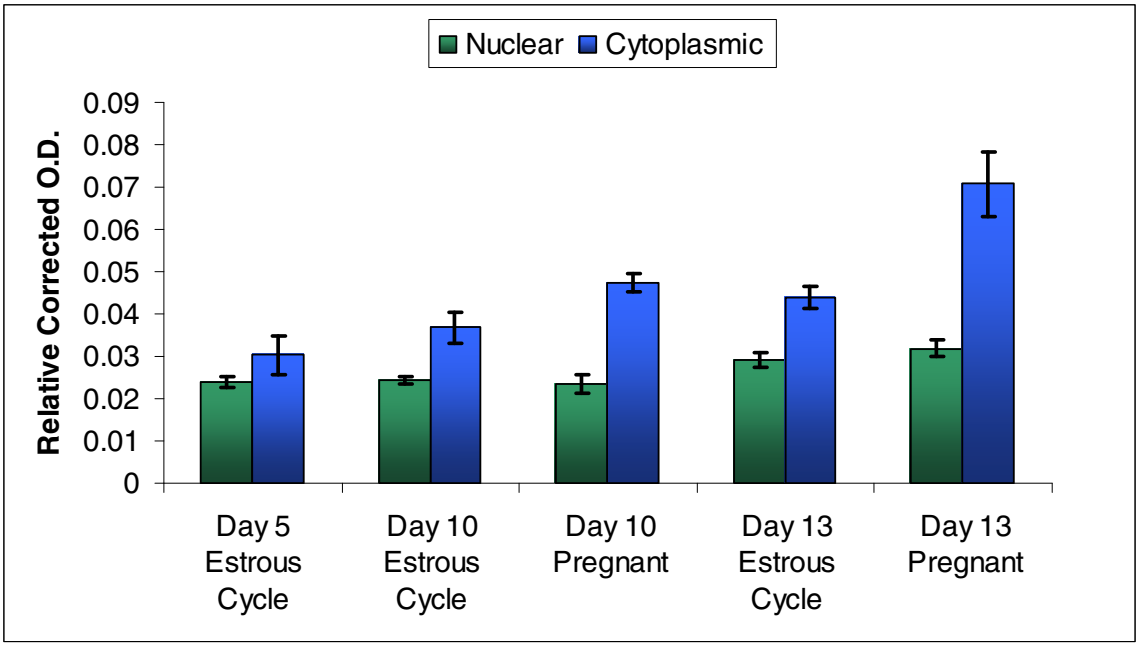
Nuclear
Cytoplasmic
Relative Corrected O.D.
0.09
0.08
0.07
0.06
0.05
0.04
0.03
0.02
0.01
0
Day 5 Estrous Cycle
Day 10 Estrous Cycle
Day 10 Pregnant
Day 13 Estrous Cycle
Day 13 Pregnant

Figure 5.3. *In Situ* hybridization analysis of ERα mRNA expression in porcine endometrium during the estrous cycle and early pregnancy. Protected transcripts in endometrium from Days 0, 5, 7.5, 10, 12, 13, 15 and 17 of the estrous cycle and Days 10, 12, 13, 15 and 17 of pregnancy were visualized by liquid emulsion autoradiography and imaged under bright-field and dark-field illumination. Note the greatest expression is prior to (Day 17), during (Day 0) and after estrus (Day 5). ERα expression is abundant in the luminal epithelium (LE) and glandular epithelium (GE) during Days 0 and 5 while only in the LE on Day 17 of the estrous cycle. A representative Day 5 section was hybridized with radiolabeled sense cRNA probe to serve as a negative control. All other images are representative from four biological replications. 4X Objective and 10X eyepiece for original magnification 40X

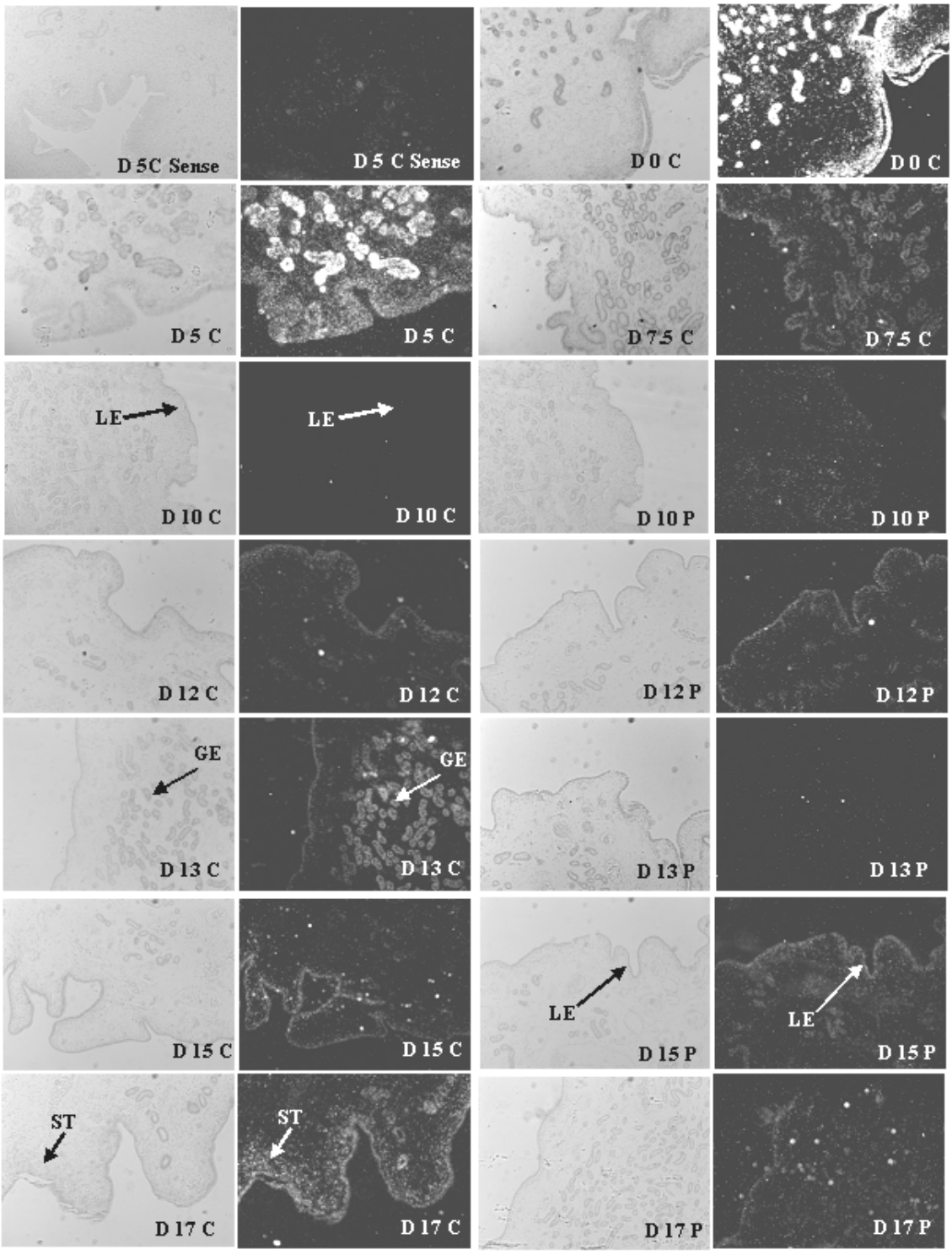
D 5C Sense
D 5 C Sense
D 0 C
D 0 C
D 5 C
D 5 C
D 7.5 C
D 7.5 C
LE
D 10 C
LE
D 10 C
D 10 P
D 10 P
D 12 C
D 12 C
D 12 P
D 12 P
GE
D 13 C
GE
D 13 C
D 13 P
D 13 P
D 15 C
D 15 C
LE
D 15 P
LE
D 15 P
ST
D 17 C
ST
D 17 C
D 17 P
D 17 P

in the LE on Days 15 and 17 of the estrous cycle. While ERα expression on Day 15 of was similar between cyclic and pregnant gilts, by Day 17 LE expression was much less during pregnancy (Figure 5.3).

Progesterone Receptor

Similar to ERα mRNA expression, PR was localized to the LE, GE and ST on estrus (Day 0) and began to dramatically decline as plasma content of circulating follicular estrogen decreased (Figure 5.4). PR gene expression on Day 7.5 and 10 of the estrous cycle was detectable, although greatly reduced, while it was near devoid by Day 12 of the estrous cycle and early pregnancy except for expression persisting in the ST cells. PR expression remained at the lowest level throughout the remainder of the estrous cycle and pregnancy until its expression began to increase in the LE of cyclic gilts following luteolysis while remaining suppressed in the LE at Days 15 and 17 in pregnant gilts (Figure 5.4).

Receptor Activator of NFκB

RANK expression in the uterus was undetectable for many of the days of the estrous cycle and pregnancy although the greatest expression appeared to occur in LE on Day 0 during estrus. The expression was visible, although modestly, in the LE and ST during the mid-luteal phase, Days 10 to 13 of both cyclic and pregnant gilts (Figure 5.5). While LE expression of RANK was low on Days 15 and 17 of the estrous cycle, LE expression in pregnant gilts was devoid on the same Days (Figure 5.5)

Figure 5.4. *In Situ* hybridization analysis of progesterone receptor (PR) mRNA expression in porcine endometrium during the estrous cycle and early pregnancy. Protected transcripts in endometrium from Days 0, 5, 7.5, 10, 12, 13, 15 and 17 of the estrous cycle and Days 10, 12, 13, 15 and 17 of pregnancy were visualized by liquid emulsion autoradiography and imaged under bright-field and dark-field illumination. Note the greatest expression is during (Day 0) and after estrus (Day 5) abundant in the luminal epithelium (LE) and glandular epithelium (GE) and stromal (ST) cell types. PR expression is greatly reduced in the LE and GE by Day 10 and nearly devoid on Day 12 of the estrous cycle and pregnancy, although still present in ST cells. A representative Day 5 section was hybridized with radiolabeled sense cRNA probe (sense) to serve as a negative control. All other images are representative from four biological replications. 4X Objective and 10X eyepiece for original magnification 40X.

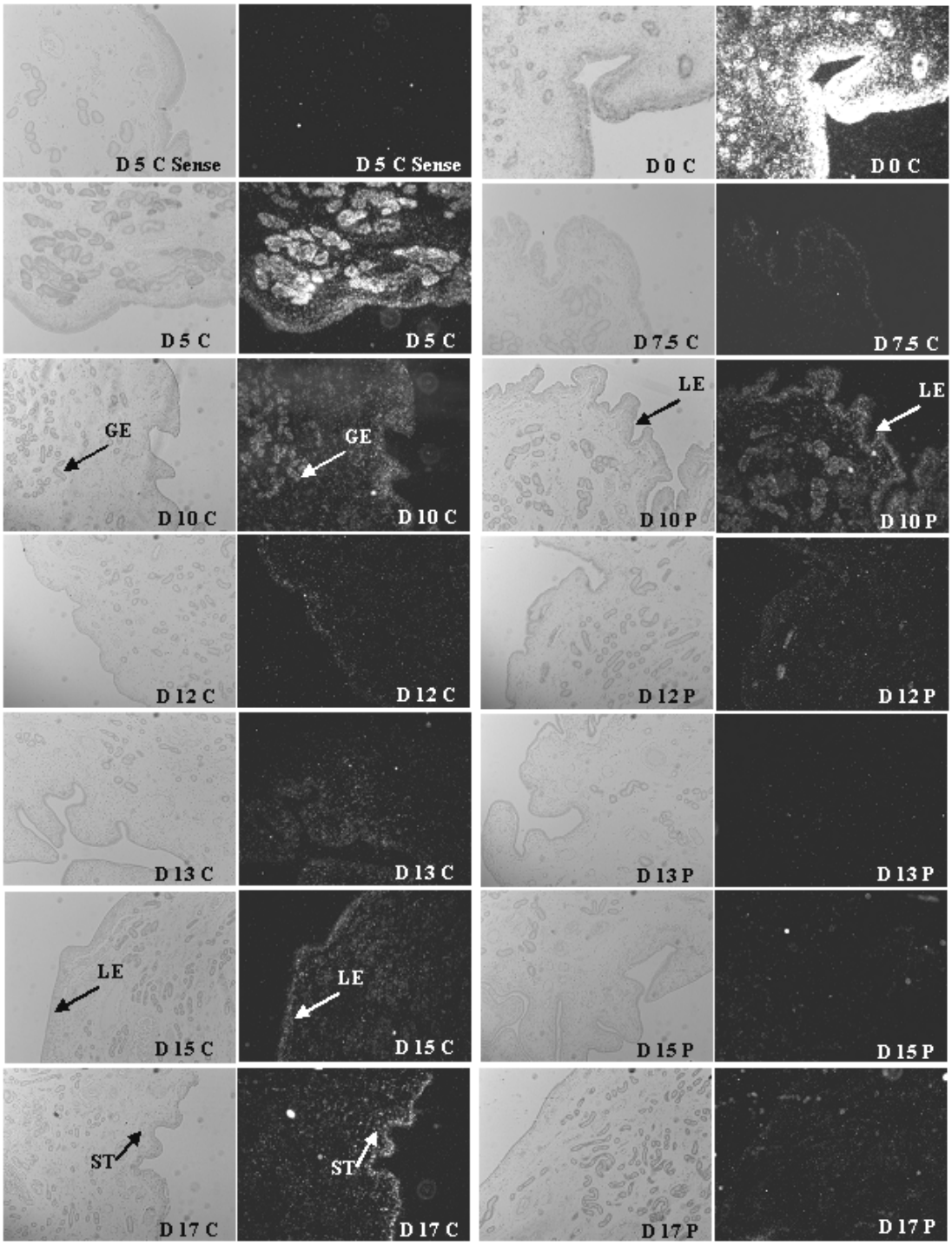
D 5 C Sense
D 5 C Sense
D 0 C
D 0 C
D 5 C
D 5 C
D 7.5 C
D 7.5 C
GE
GE
D 10 C
D 10 C
LE
LE
D 10 P
D 10 P
D 12 C
D 12 C
D 12 P
D 12 P
D 13 C
D 13 C
D 13 P
D 13 P
LE
LE
D 15 C
D 15 C
D 15 P
D 15 P
ST
ST
D 17 C
D 17 C
D 17 P
D 17 P

Figure 5.5. *In Situ* hybridization analysis of receptor activator of NFκB (RANK) mRNA expression in porcine endometrium during the estrous cycle and early pregnancy. Protected transcripts in endometrium from Days 0, 5, 7.5, 10, 12, 13, 15 and 17 of the estrous cycle and Days 10, 12, 13, 15 and 17 of pregnancy were visualized by liquid emulsion autoradiography and imaged under bright-field and dark-field illumination. While expression was low in all tissues evaluated, evidence of RANK expression is detected in the LE on Day 12 of the estrous cycle and pregnancy. A representative Day 12 pregnant section was hybridized with radiolabeled sense cRNA probe (sense) to serve as a negative control. All other images are representative from four biological replications. 4X objective and 10X eyepiece for original magnification 40X.

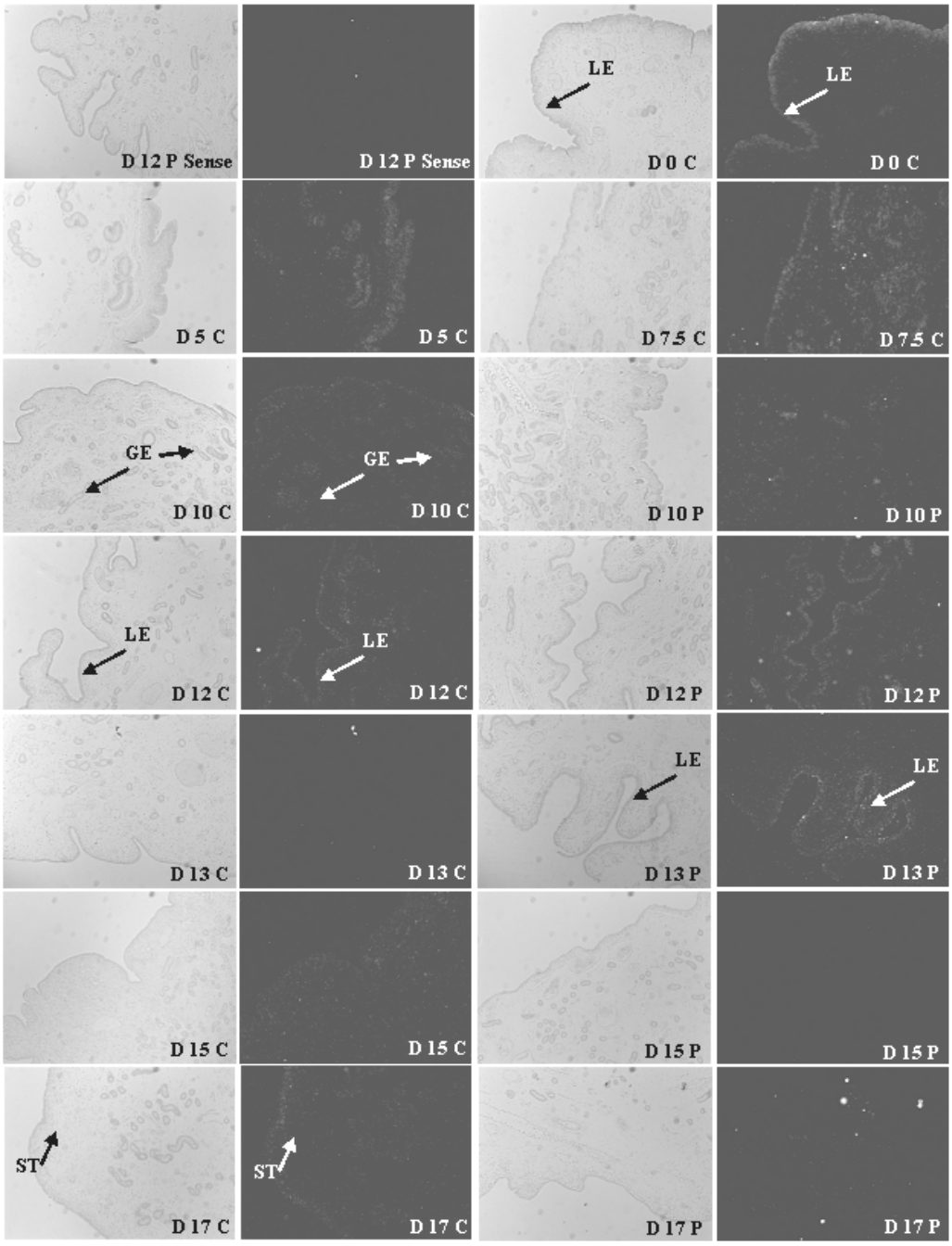
D 12 P Sense
D 12 P Sense
LE
D 0 C
LE
D 0 C
D 5 C
D 5 C
D 7.5 C
D 7.5 C
GE
D 10 C
GE
D 10 C
D 10 P
D 10 P
LE
D 12 C
LE
D 12 C
D 12 P
D 12 P
D 13 C
D 13 C
LE
D 13 P
LE
D 13 P
D 15 C
D 15 C
D 15 P
D 15 P
ST
D 17 C
ST
D 17 C
D 17 P
D 17 P

Quantitative RT-PCR

The mRNA abundance for two receptors which possess the capability of inducing NFκB activity, RANK and TLR-4; in addition to two NFκB regulated genes, NFκB RelA and p50 subunits, were assayed using quantitative RT-PCR.

NFκB Mediating Receptors

There was no significant day ($P = 0.92$) or status ($P = 0.34$) effect detected for the expression of RANK. Messenger RNA levels were not different in uterine endometrium throughout the days of the estrous cycle and early pregnancy in pigs (Figure 5.6).

There was a day x status interaction ($P = 0.017$) on the mRNA abundance for TLR-4 (Figure 5.6). Expression was least on Day 5 of the estrous cycle and greatest on Day 13 of pregnancy. While expression on Days 10 through 17 of the estrous cycle were greater than Days 5 and 7.5 ($P < 0.05$), endometrium of pregnant gilts expressed significantly more TLR-4 mRNA transcript than cyclic gilts on Days 10, 12, 13, 15 and 17 ($P < 0.05$).

NFκB Subunits: p50 and RelA

A significant day x pregnancy status interaction was detected for NFκB p50 gene expression ($P < 0.01$). Messenger RNA abundance for NFκB p50 was greatest during estrus and least on Day 5 (Figure 5.7). NFκB p50 expression increased steadily during diestrus being 2 to 3-fold greater in endometrium collected from Days 12, 13, 15 and 17 compared to Day 5 ($P < 0.05$). On Day 13 of gestation, expression was about 2-fold greater when compared to Day 13 of the estrous cycle ($P < 0.05$) while the inverse was

Figure 5.6. Relative mRNA abundance for receptor mediators of NFκB activation. Expression differences for endometrial RANK (Top panel; effect of day, $P < 0.93$; effect of status, $P = 0.34$) and TLR-4 (Lower panel; day x status effect, $P = 0.017$), in cyclic (orange bar) and pregnant (yellow bar) gilts. Relative abundance of mRNA was calculated from the quantitative RT-PCR analysis as described in *Materials and Methods.* Bars without common lowercase superscripts represent a statistical difference ($P < 0.05$) between day/status combinations. Superscripts are not included in the upper panel as no main or interacting effects were detected. Relative mRNA units are presented as mean ± SEM.

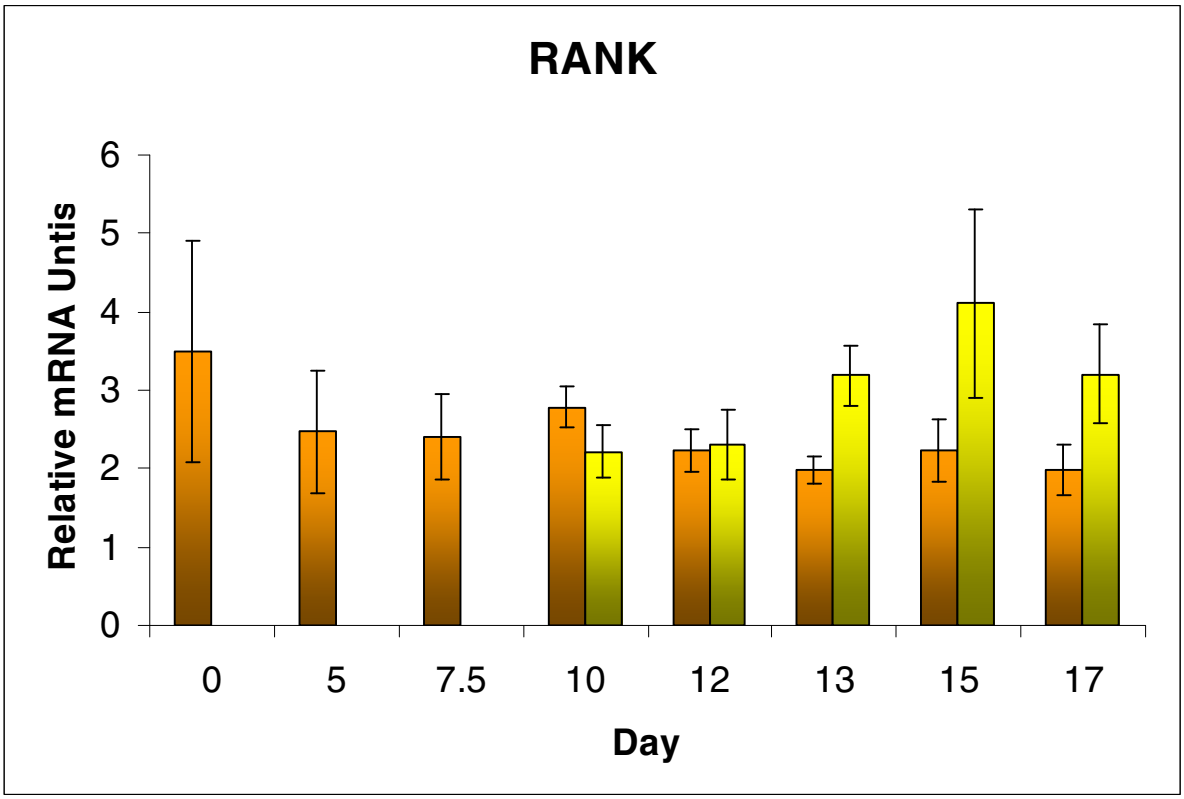
RANK
Relative mRNA Untis
6
5
4
3
2
1
0
0
5
7.5
10
12
13
15
17
Day

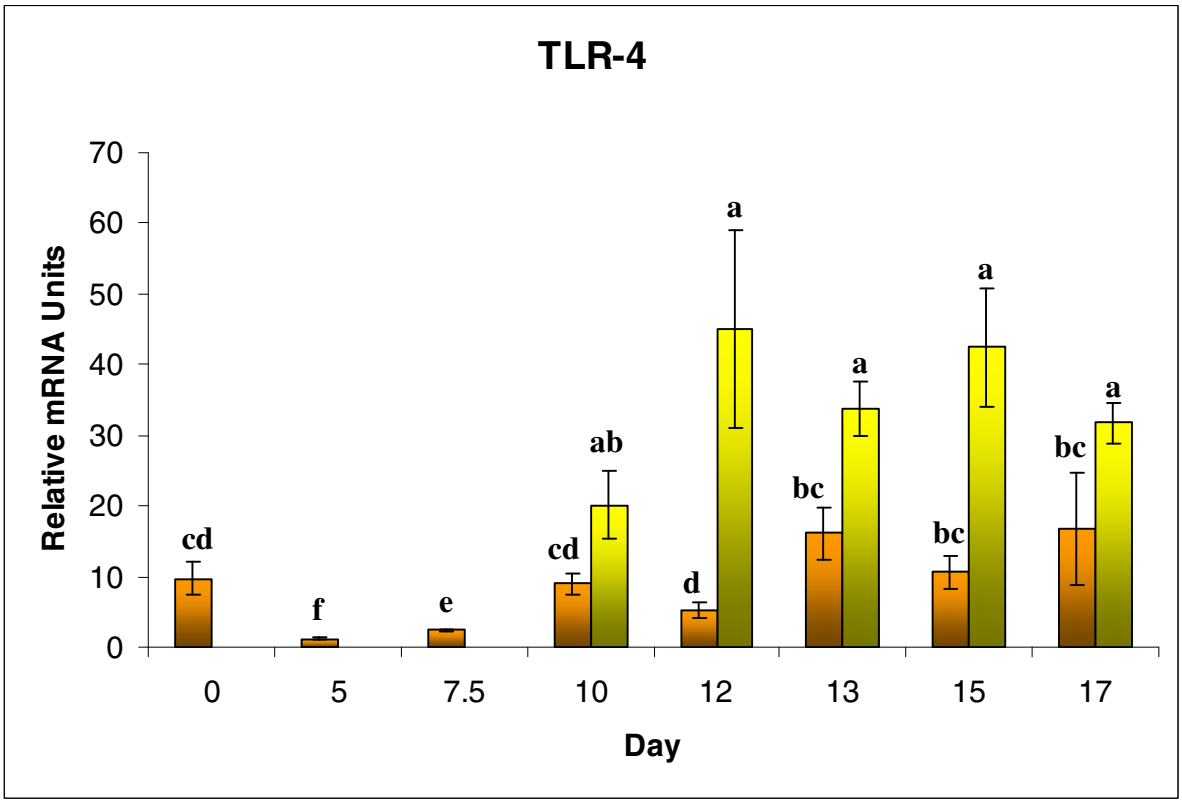
TLR-4
Relative mRNA Units
70
60
50
40
30
20
10
0
cd
f
e
cd
ab
d
a
bc
a
bc
a
bc
a
0
5
7.5
10
12
13
15
17
Day

Figure 5.7. Relative mRNA abundance for NFκB subunits, p50 and RelA. Expression differences for endometrial p50 (Top panel; day x status interaction, $P < 0.01$) and RelA (Lower panel; day x status effect, $P = 0.017$), in cyclic (orange bar) and pregnant (yellow bar) gilts. Relative abundance of mRNA was calculated from the quantitative RT-PCR analysis as described in *Materials and Methods.* Bars without common lowercase superscripts represent a statistical difference ($P < 0.05$) between day/status combinations. Relative mRNA units are presented as mean ± SEM.

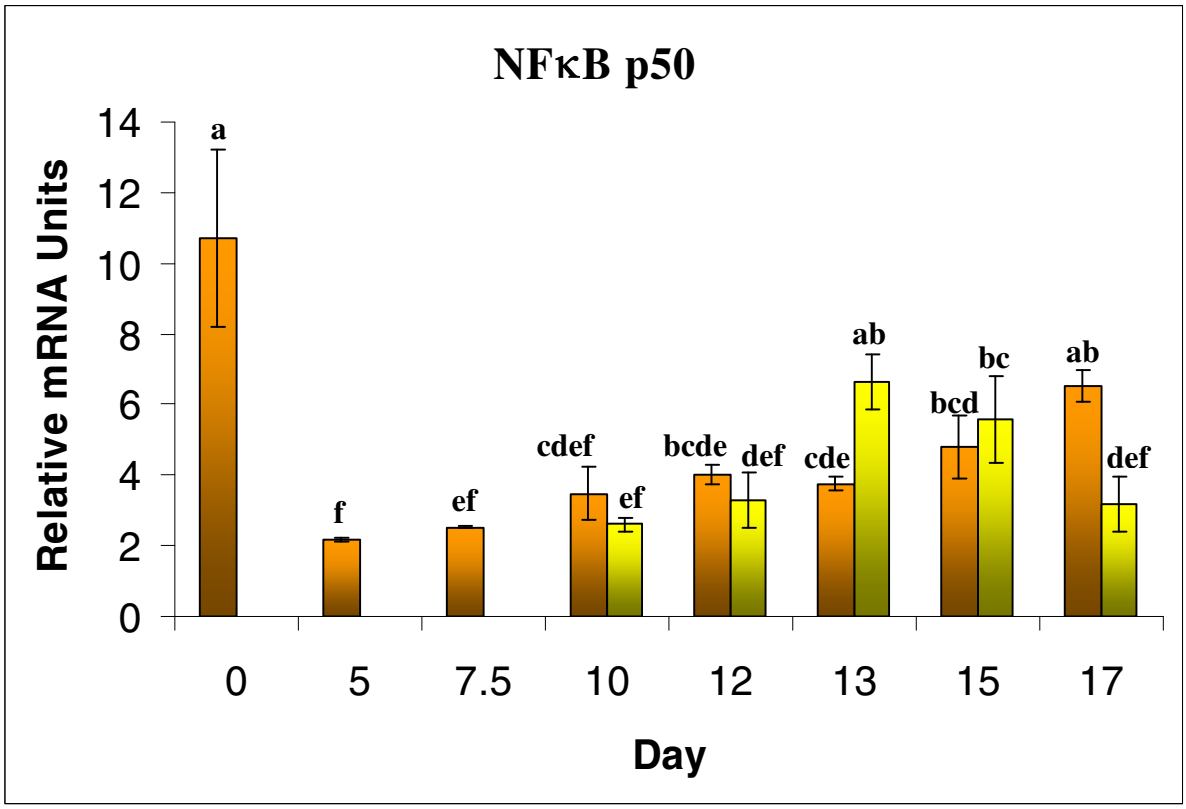
NFκB p50
Relative mRNA Units
14
12
10
8
6
4
2
0
a
f
ef
cdef
ef
bcde
def
cde
ab
bcd
bc
ab
def
0
5
7.5
10
12
13
15
17
Day

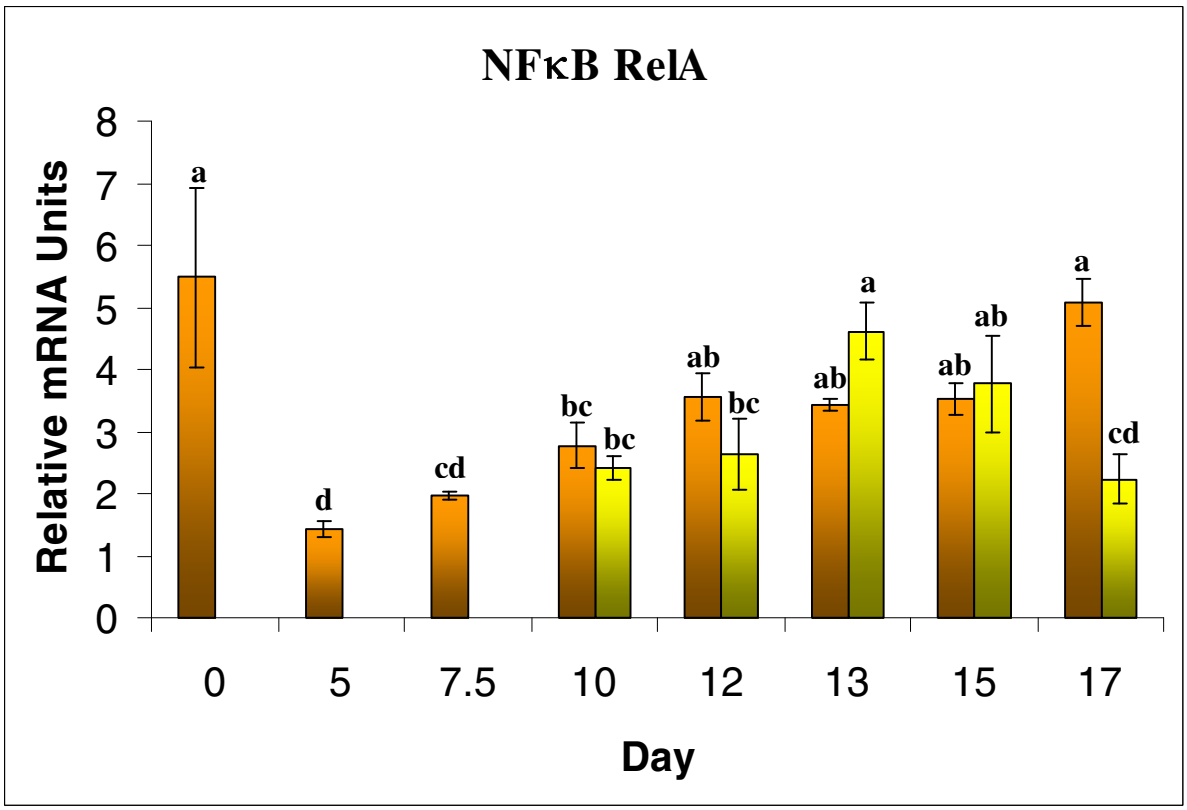
NFκB RelA
Relative mRNA Units
8
7
6
5
4
3
2
1
0
a
d
cd
bc
bc
ab
bc
ab
a
ab
ab
a
cd
0
5
7.5
10
12
13
15
17
Day

true when comparing Day 17 of the estrous cycle and pregnancy. Although endometrium from cyclic gilts expressed more p50 transcript than pregnant gilts, the difference across days was not significant ($P < 0.05$, Figure 5.7).

Similar to NFκB p50, a day x status interaction ($P < 0.013$) affected the mRNA abundance of RelA in the endometrium from cycle and pregnant gilts. Like the p50 subunit, RelA expression was greatest in endometrium collected during estrus, about 4-fold greater that Day 5 of the estrous cycle which was the lowest expression of RelA mRNA. After Day 5 of the estrous cycle, expression increased in both cyclic and pregnant gilts on Days 10, 12, 13, and 15 ($P < 0.05$; Figure 5.7). While expression remained elevated on Day 17 of the estrous cycle, expression returned to basal levels on Day 17 of gestation, representing about a 2.3-fold difference in gene expression ($P < 0.05$).

Inhibitors of NFκB

Gene expression for IκBα was affected by day ($P = 0.001$) but not status ($P = 0.15$). Status did not affect the expression of IκBα ($P = 0.23$). IκBα mRNA abundance was greatest during estrus, being at least 7-fold greater in comparison to all other days assayed ($P < 0.05$). There were no differences in gene expression between all other Days as mRNA abundance remained at a consistent level from Day 5 through Day 17 (Figure 5.8).

There was a tendency for a day x status ($P = 0.08$), day ($P = 0.07$) and status ($P = 0.09$). The greatest expression differences existed during estrus and Day 17 of estrous

Figure 5.8. Relative mRNA abundance for endometrial IκBα (Top panel; effect of day, $P < 0.001$) and IκBβ (Lower panel; day x status effect, $P = 0.079$), in cyclic (orange bar) and pregnant (yellow bar) gilts. Relative abundance of mRNA was calculated from the quantitative RT-PCR analysis as described in *Materials and Methods.* Bars without common lowercase superscripts represent a statistical difference ($P < 0.05$) between day/status combinations whereas differences in uppercase superscripts represent statistical differences between days of gestation. Relative mRNA units are presented as mean ± SEM.

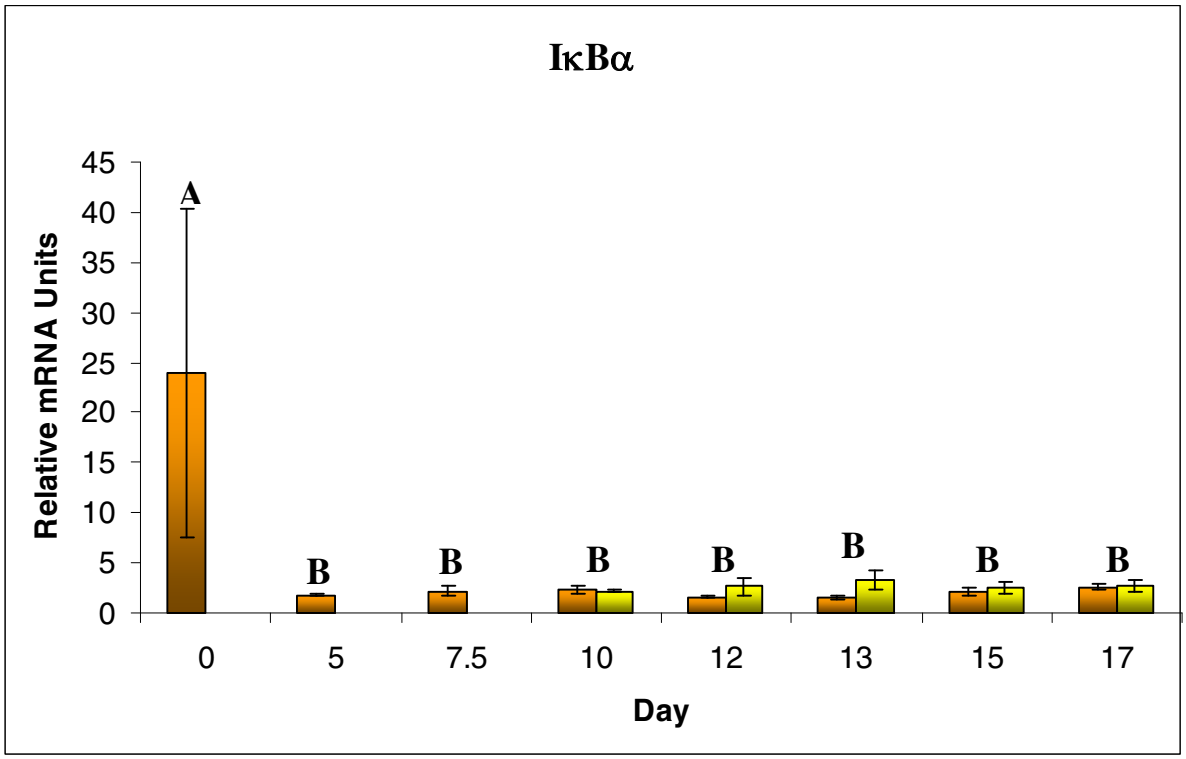
IκBα
Relative mRNA Units
45
40
35
30
25
20
15
10
5
0
A
B
B
B
B
B
B
B
0
5
7.5
10
12
13
15
17
Day

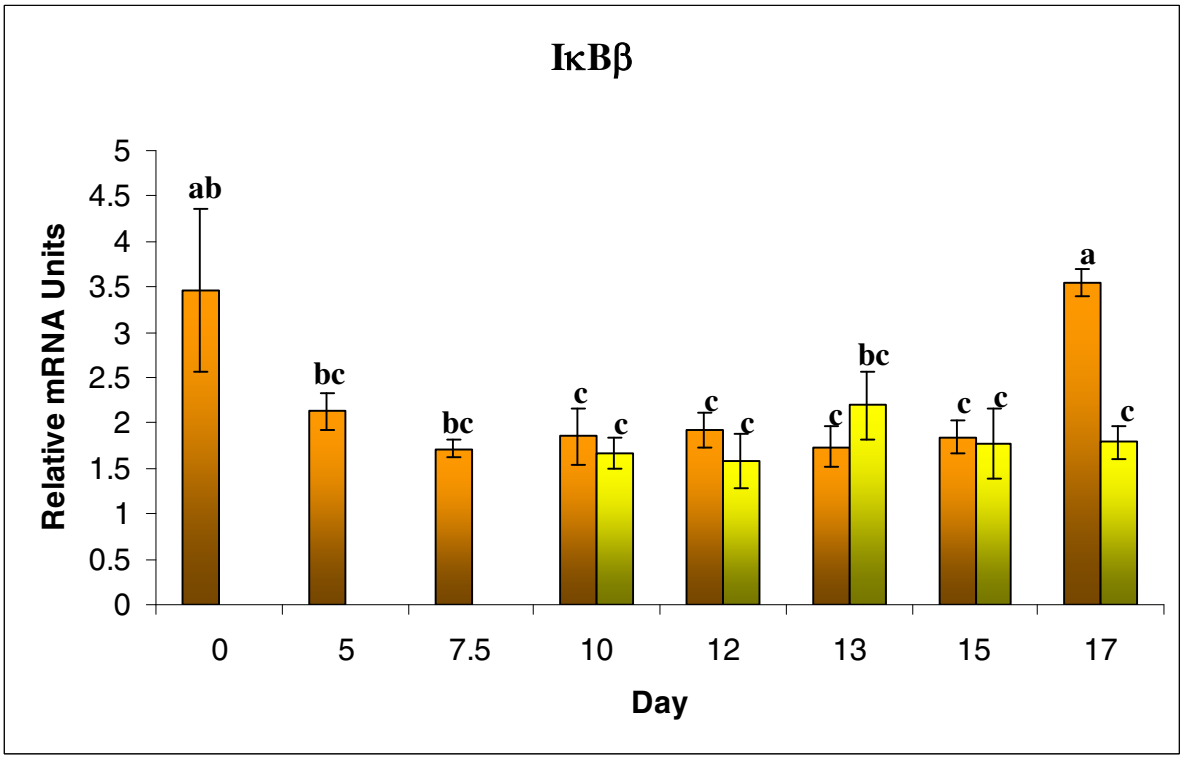
IκBβ
Relative mRNA Units
5
4.5
4
3.5
3
2.5
2
1.5
1
0.5
0
ab
bc
bc
c
c
c
c
c
bc
c
c
a
c
0
5
7.5
10
12
13
15
17
Day

cycle. IκBβ mRNA abundance was greater ($P < 0.05$) in endometrium of Day 17 cyclic gilts with expression levels similar to Day 0 but was about 2-fold greater compared to all other days during diestrus and early pregnancy (Days 5 to 15). No differences were detected between Days 5 to 15 of the estrous cycle or pregnancy (Figure 5.8).

Discussion

The establishment of pregnancy requires diversion from the pathway of cyclicity and return estrus following the opening of the implantation window and uterine receptivity in pigs. Progesterone driven transcriptional regulation of specific endometrial factors during the mid-luteal phase critically contributes to both induction of luteolysis resulting in return to estrus in cyclic animals and conceptus growth and expansion to establish pregnancy in bred females. We have suggested a relationship between PR expression and the activation of NFκB in the endometrial LE regulates the transcription of specific genes, such as PTGS2 [Ashworth et al., 2006; Geisert et al., 2006].

Establishment of pregnancy in mice has been shown to involve the NFκB system. Not only does the activation of NFκB during the implantation window in mice occur [Nakamura et al., 2004a]; it has also been shown to be required for uterine receptivity through its affects on leukaemia inhibitory factor (LIF) expression, as LIF administration restores normal implantation during pregnancy when NFκB function is compromised [Nakmura et al., 2004b]. Interestingly, peak LIF secretion by the pig uterus occurs on Day 12 of the estrous cycle [Anegon et al., 1994], as well as upregulation of uterine PTGS2 [Ashworth et al., 2006], an NF κB regulated gene [Kniss et al., 2001; Takada et al., 2004], and we now demonstrate an increased p50 and RelA gene expression (Figure

5.7), both of which can be induced through NFκB [McNulty et al., 2001]. These NFκB regulated factors are all in congruence with the opening of the implantation window in the pig. Based on the expression patterns of these genes in conjunction with the EMSA (Figure 5.1) and RelA ELISA (Figure 5.2) it appears that transcriptional control of uterine endometrium during the initiation of implantation is regulated by NFκB possessing the RelA subunit.

Steroid hormones, as well as their receptors, have in many studies been shown to affect NFκB activity in a variety of tissues. Kalkoven et al. [1996] demonstrated the ability of both PR and NFκB RelA to be mutually repressive of each other, which suggests that the loss of PR during the opening of the implantation window may be related to elevated expression of NFκB regulated genes in the uterine endometrium during the estrous cycle and early pregnancy. Downregulation of PR expression in the uterine LE is temporally associated with uterine receptivity in the pig and other numerous mammalian species [Lessey et al., 1988, 1996; Fazleabas et al., 1999; Spencer and Bazer, 1995; Meikle et al., 2001; Hartt et al., 2005]. The ability for PR downregulation to affect the timing of uterine receptivity appears to carry over into the timing of the overall length of estrous cycle. Progesterone itself functions as a regulator of PR gene expression; confirmed by the present data where PR gene expression in uterine LE declined after prolonged (7 to 8 days) stimulation by progesterone, increasing following regression of the corpora lutea and return to estrus. In human myometrial cells, ablation of PR allows increased IL-1β induced PTGS2 expression [Hardy et al., 2006]. These authors also demonstrated the ability of progesterone to reduce IL-1β induced PTGS2 expression, likely through progesterone's ability to induce the expression of the inhibitor of NFκB,

IκBα. During the estrous cycle and pregnancy in the pig, IκBα and IκBβ were both expressed at the greatest levels during estrus (Figure 5.8) when PR expression was also greatest (Figure 5.4). However, while PR is elevated at estrus, progesterone production is minimal, suggesting that if IκB regulation in the pig uterus does occur through PR, it is either a ligand independent mechanism or that elevated progesterone concentrations drive down IkB expression contrary to the observation described by Hardy et al. [2006].

The hypothesis, that progesterone driven downregulation of PR regulates uterine receptivity and the estrous cycle, is supported by the demonstration of shortened estrous cycles in sheep and cattle given progesterone supplementation shortly after estrus, prior to normal endogenous progesterone secretion by the corpora lutea [Ottobre et al., 1980; Garrett et al., 1988]. Additionally, administration of the PR antagonist, mifepristone, on Days 3-5 of the ovine estrous cycle results in a delay of luteolysis [Morgan et al., 1993]. Collectively, these studies suggest that PR is involved in the regulation of PG production. Indomethacin, an inhibitor of NFκB induced PTGS2 expression [Takada et al., 2004], when given to pigs during early gestation ablates PG production [Kraeling et al., 1985], suggesting that uterine PG production during diestrus in the pig is NFκB regulated. Demonstrating that altering either PR expression levels or NFκB activation, these studies independently suggest the ability of both PR and NFκB to regulate PG production during the period of luteolysis.

The temporal affiliation between the gene expression patterns of TLR-4 and RANK (Figure 5.1B) and NFκB inducible genes, NFκB p50 (Figure 5.2A), NFκB RelA (Figure 5.2B), PTGS2 (Ashworth et al., 2006) and LIF (Anegon et al., 1994) in the uterine LE is suggestive of the involvement of TLR-4 and/or RANK during the activation

of NFκB during the initiation of uterine receptivity during the estrous cycle and early pregnancy in pigs. Because a mutual repression between RelA and PR exists [Kalkoven et al., 1996], what regulates this activation of NFκB and potentially, the subsequent down-regulation of PR in the uterine endometrium remains unclear. The expression of RANK and its ligand (RANKL), both involved in bone remodeling and mammary gland development [Jones et al., 2002; Cao and Karin, 2003], provide one such potential mechanism. Expression of RANKL can be stimulated by progesterone [Srivastava et al., 2003] suggesting the potential of RANK mediated NFκB activation in the pig endometrium if RANKL is capable of signaling through endometrial stromal cells which still express PR during the implantation window in the pig [Geisert et al., 1994]. This novel hypothesis has been presented [Geisert et al., 2006] and is supported by the expression of RANK in the uterine endometrium (Figure 5.5); however no communications to our knowledge have indicated the presence of RANKL or RANK in the uterus of other mammalian species.

TLR-4 provides a more likely mechanism of NFκB activation in the pig as its expression pattern is temporally associated with that of the NFκB regulated genes, PTGS2 [Ashworth et al., 2006], LIF [Anegon et al., 1994], and the NFκB subunits, p50 and RelA (Figure 5.7) in the pig uterine endometrium. TLR-4 expression has been demonstrated in endometrial LE of a variety of species. In addition to the pig, TLR-4 has also been shown to be expressed in the uterine LE and ST of mice [Soboll et al., 2006], women [Schaefer et al., 2004, Fazeli et al., 2005] and cattle [Herath et al., 2006]. While TLR-4 was originally described for its ability to respond to the gram-negative cell wall component, lipopolysaccharide (LPS; Poltorak et al., 1998) recent data suggests a

variety of endogenous ligands, such as heat shock proteins (HSPs) 60 and 70, fibrinogen, fibronectin, heparan sulfate, certain β-defensins, and high mobility group box 1 protein also possess the ability to stimulate TLR-4 signaling [Tsan and Gao, 2004]. While the suggestion that TLR-4 expression in the uterus allows the ability to respond to foreign bacterial pathogens is valid, its roles in uterine biology in conjunction with endogenous ligand expression should not be overlooked. In women, heat shock proteins increase during the late proliferative and early secretory phase of the menstrual cycle [Tabibzadeh et al., 1996] suggesting steroid hormone involvement in HSP regulation in the uterus. Of the other mentioned endogenous ligands, fibronectin and heparin sulfate have both been suggested to be involved in the attachment of the pig conceptus to the uterine LE [Burghardt et al., 1997], occurring temporal and spatially to TLR-4 increased expression in the uterine endometrium (Figure 5.6).

Based on these data and the literature presented hitherto, it appears that NFκB activation is a critical component to the opening of the implantation window. However, stringent regulation of NFκB activation is necessary to prevent an all-out inflammatory response, which could otherwise potentially compromise pregnancy. It is possible that the conceptus could augment the activation of NFκB through at least two mechanisms. The first possible mechanism is the spatiotemporal peak in conceptus secretion of IL-1β with uterine expression of IL-1 receptors on Day 12 of gestation [Ross et al., 2003a]. The second possible mechanism for augmented NFκB activation is through conceptus expression of TLR-4 endogenous ligands; fibronectin and fibrinogen [Tsan and Gao, 2004], both of which are upregulated during Days 11 to 14 of gestation 8.9 and 12.8 fold, respectively (Table A.3, Cluster 1 and Cluster 13, respectively). Both of these

mechanisms seem plausible as the amount of cytoplasmic RelA sequestered in the cytoplasm was greatest on Day 13 of pregnant gilts compared to cyclic gilts and conceptus absence (Figure 5.2). Bovine endometrial explants respond to LPS, the bacterial TLR-4 ligand, by increasing PG production, with a notable increased PGE to PGF ratio, while *in vitro* stimulation of LE or ST cells with LPS resulting in PTGS2 gene expression could be ablated with an LPS antagonist [Herath et al., 2006]. Prostaglandin production peaks during the mid-luteal phase for both PGE and PGF during both the estrous cycle and pregnancy in the pig; however, a marked increase in the PGE:PGF ratio is detected in pregnant gilts compared to cyclic gilts [Christenson et al., 1994], further suggesting a relationship between pregnancy PG production ratios and TLR-4 conceptus stimulation.

While total endometrial RelA detected was greatest in pregnant gilts supports conceptus augmented NFκB activation, being limited to the cytoplasm is indicative of in place regulatory mechanisms preventing overwhelming inflammatory response. The concomitant estrogen secretion by the conceptus [Geisert el al., 1982b] temporal to conceptus production of both IL-1β and endogenous TLR-4 ligands may be one way NFκB transcriptional activity is regulated. Ghilsetti et al. [2005] demonstrated the *in vitro* ability of estrogen, signaling through ERα and not ERβ, of preventing activated NFκB in the cytoplasm from being translocated into the nucleus of the cell and inducing transcription. Interestingly, the upregulation of ERα on Days 12 and 13 of gestation in the uterine LE (Figure 5.3) is temporally associated with the elevated uterine luminal estradiol-17β [Geisert et al., 1982b] and the pregnancy associated elevation of activated NFκB p65 in the cytoplasmic protein fractions (Figure 5.1 and 5.2). Typically, the

degradation of IκB's result not only in the ability for the activated NFκB dimer to bind DNA, but also exposes the nuclear localization signal necessary for expedited transport to the nucleus of the cell [Ali and Mann, 2004]. These data suggest that while the p50/RelA is capable of binding DNA, the heterodimer remains primarily in the cytoplasm of the cell. The temporal relationship of endometrial ERα expression and conceptus estradiol secretion provides a potential mechanism by which this occurs. If this mechanism does occur during pregnancy in the pig, it is likely that other mechanisms are also in place as cytoplasmic RelA also increases in uterine endometrium from gilts during the estrous cycle.

The opening of the implantation window is the initiating point of the period during gestation at which specific endometrial alterations occur to allow the attachment of the conceptus trophectoderm. It is this period of development that requires the formation of a communication network between the developing conceptus and the maternal endometrium with dysfunction on the part of resulting in the inability to establish pregnancy. Steroid hormones, progesterone and estrogen, no doubt serve a fundamental responsibility in the pattern of endometrial secretions and the induction of uterine receptivity. The steroid hormone receptors ERα and PR, through their ability to affect the transcriptional activity of NFκB, are likely a critical component to inducing and regulating the degree of transcription necessary in the uterine endometrium for the establishment of pregnancy in the pig.

Chapter VI

SUMMARY AND CONCLUSION

The establishment of pregnancy in any mammalian species requires smoothly orchestrated molecular events at the conceptus uterine interface during Days 11 to 14 of gestation. It is during this period that the conceptuses produce both IL-1β and estadiol-17β concomitant with the rapid elongation of the conceptus trophectoderm. Sufficient secretory capacity of the pig conceptus [Polge et al., 1966; Dziuk, 1968] and an adequate extent of trophoblastic elongation [Stroband and Van der Lende, 1990] are requirements for the establishment of pregnancy and conceptus survival in the pig. Acquiring these major conceptus developmental landmarks requires the temporal and spatial expression of the appropriate mRNA transcripts to generate a phenotype suitable for continued growth and development. However, little information has been isolated specifically identifying a large number of conceptus transcripts that are critical for this stage of development.

Not only is appropriate conceptus development critical for the establishment of pregnancy in the pig, uterine endometrial function regulating uterine receptivity and conceptus attachment are necessary components for pregnancy establishment. Two major factors regulating endometrial function during the period of conceptus attachment and implantation are conceptus synthesis and release of estradiol-17β and the endometrial downregulation of the progesterone receptor.

Collectively, the studies presented in this thesis use three separate approaches to better understand the biology of pregnancy establishment in pigs with respect to development during Days 11 to 14 of gestation. This short period of development relative to the overall length of gestation is critical due to the numeruous physiological events occurring in both the conceptus and the endometrium required for pregnancy establishment in the pig. Conceptus trophoblastic elongation is simultaneous with endometrial programming that allows uterine receptivity, and uterine receptivity can be modified in response to conceptus secretory factors, such as estradiol-17β [Geisert et al., 1982b] and IL-1β [Ross et al., 2003b].

The use of the Affymetrix GeneChip® Porcine Genome Array effectively identified hundreds of porcine genes that are differentially expressed during the developmental period consisting of trophoblastic elongation and the initial attachment of the conceptus trophectoderm to the maternal uterine endometrium. Surprisingly, the morphological transition from spherical to tubular represented differential expression of very few genes, suggesting the possibility that spherical conceptuses possess the capacity for rapid trophoblastic elongation but lack the stimulatory mechanism which induces it. In contrast, Day 12 filamentous conceptuses, whose morphological difference from that of tubular conceptuses is a matter of a few hours of development, differentially express over 450 genes in comparison to spherical or tubular morphologies. This rapid modification in the mRNA population is continued in Day 14 conceptuses. The hundreds of genes that are differentially expressed during this period of development represent an array of biological processes occurring during this stage of conceptus development.

Many of the genes that were differentially expressed represented core biological processes such as cell motility, energy catabolism, amino acid transport, apoptosis regulation, cell growth, transcriptional regulation, and ATP utilization. The use of clustering analysis allowed the characterization of genes by their expression patterns in the conceptus during this stage of development and also allowed the association of genes whose expression patterns were similar. We have identified the transient expression of over 150 genes (Table A3, k-means clusters 4, 7, 14, 21 and 24) that could be considered molecular markers of rapid trophoblastic elongation while the genes associated with expression increasing in Day 14 conceptuses mark those factors whose expression is temporal to placental layer differentiation during the attachment to the uterine endometrium [Friess et al., 1980].

The data presented herein were also complementary of previously identified factors which are differentially expressed, such as PTGS2 [Wilson et al., 2002], steroidogenic acute regulatory factor [Blomberg et al., 2005], transforming growth factor β [Gupta et al., 1996], epidermal growth factor receptor [Vaughn et al., 1992], interferon-γ [La Bonnardiere et al., 2002], and retinol binding protein [Yelich et al., 1997a]. We have also identified numerous factors, which up unto this point were not associated with conceptus development in any species such as B-cell linker and angiomotin. Alternatively, the identification of genes whose expression during pig development is novel, which have been documented to be expressed during embryonic development in other species, such as chemokine14 ligand and parathyroid hormone like related hormone, now have a better biological function assessment due to their associations with the developmental processes occurring in pig conceptuses temporal to their expression.

The identification of genes whose spatiotemporal expression patterns, such as angiomotin, being associated with not only cell migration [Troyanovsky et al., 2001], but the localization to the lamellipodia of migrating cells [Levchenko et al., 2003]. The identified factors differentially expressed during pig conceptus development that are also in cells phenotypically resembling trophectodermal cells in the pig conceptus during elongation [Geisert et al., 1982c] provide numerous factors for which future studies can be designed.

Estrogen is a critical component for the establishment of pregnancy in the pig [Bazer and Thatcher, 1977] but can also be detrimental if uterine endometrial exposure to estrogen occurs at an abnormal time during early gestation [Pope et al., 1986, Blair et al., 1991; Ashworth et al., 2006]. The critical relationship between the temporally acceptable point of endometrial exposure to estrogen during pregnancy and its affect on conceptus survivability suggests that spatiotemporal regulation of key factors affecting pregnancy outcome occur through estrogen. Also, while it is widely accepted that estrogen is the maternal recognition of pregnancy signal, the molecular mechanisms behind estrogen stimulation are not well described. Our approach has allowed the identification of endometrial genes affected by estrogen stimulation in the presence of other conceptus secreted factors.

Interestingly, the majority of transcriptional differences were detected on Day 13 of gestation following exogenous estrogen exposure on Days 9 and 10, after conceptus estrogen is also secreted into the uterine lumen. Of the genes identified to be regulated by exogenous estrogen we specifically evaluated the spatiotemporal expression patterns of four through *in situ* hybridization and quantitative RT-PCR.

Aldose reductase and neuromedin B were significantly downregulated in the uterine luminal epithelium on Day 13 in response to exogenous estrogen on Days 9 and 10 while secreted phosphoprotein-1 and CD24 antigen were upregulated in the luminal epithelium by estrogen on Day 13. Aldose reductase is a critical component in the formation of fructose from glucose, both of which markedly increase during peri-implantation development in the pig [Zavy et al., 1982], suggesting potential role providing energy during conceptus growth and trophoblastic elongation. Alternatively, neuromedin B, secreted phosphoprotein 1, and CD24 have all been shown in a variety of tissues to regulate immunity [Makarenkova et al., 2003; Johnson et al., 2003; Zenclussen et al., 2001; Bertoja et al., 2005]. Also as previously mentioned, CD24 [Kristiansen et al., 2004] and secreted phosphoprotein 1 [Johnson et al., 2003] have been associated with ligand bridging between cells suggesting potential roles in conceptus attachment to the luminal epithelium. If indeed the function of these estrogen regulated genes is to regulate conceptus trophectoderm attachment to the uterine luminal epithelium, the premature and overexpression of these factors could alter the uterine extracellular matrix to an extent not favorable for conceptus attachment, resulting in the delayed conceptus mortality that was described.

These alterations in gene expression demonstrated in the uterine endometrium are similar to the asynchrony between the endometrium and conceptus described by Polge (1982) where embryos transferred greater than 48 h out of synchrony with the uterine endometrium fail to establish pregnancy. These data suggest that exogenous estrogen administration causes significant alterations in endometrial gene expression on Days 12 and 13 of gestation and may prevent attachment and promote immunological rejection of

the conceptus resulting in its deterioration by Day 15 of gestation. However, the underlying implication is that during normal gestation, conceptus induced changes through endogenous estradiol-17β secretion occur synchronously to the dramatic expression and phenotypic changes that enable the conceptus to survive in an uterine environment following estrogen stimulation.

The opening of the implantation window is a critical process which occurs during peak progesterone production by the corpora lutea, is characterized by uterine receptivity to conceptus attachment, and occurs in all reproductively capable gilts, regardless if mating, fertilization and early conceptus development have transpired. Endometrial phenotype during uterine receptivity is poised to secrete prostaglandins in an endocrine fashion, resulting in luteolysis and a return to estrus or release prostaglandins in and exocrine fashion, sustaining the corpora lutea; and establish a communication network with the developing conceptus, thereby commencing gestation. The downregulation of progesterone receptor [Lessey et al., 1988, 1996; Fazleabas et al., 1999; Spencer and Bazer, 1995; Meikle et al., 2001; Hartt et al., 2005] and the activation of NFκB [Nakamura et al., 2004a] during pregnancy establishment is not unique to the pig. We were interested in the molecular factors that contribute to this endometrial phenotype.

This study evaluated potential mechanisms by which endometrial modifications can occur through the interplay between RelA and progesterone receptor. The utilization of an EMSA and NFκB RelA ELISA confirmed the presence and likely activation of NFκB in the uterine endometrium around the time of progesterone receptor downregulation in the uterine luminal epithelium. The temporal expression of NFκB

regulated genes, NFκB p50 and RelA; as well as LIF [Anegon et al., 1994] and PTGS2 [Ashworth et al., 2006] also confirm NFκB activation.

Two potential mechanisms of NFκB activation were evaluated, one through receptor activator of NFκB (RANK) and the other being toll-like receptor 4 (TLR-4), which is also capable of inducing the cascade of events resulting in activated NFκB. While both of these receptors were identified in the pig uterine endometrium, RANK appeared to be constitutively expressed while TLR-4 expression was temporally associated with the expression patterns for the NFκB activated genes in the uterus such as PGTS2, p50 and RelA. TLR-4 expression also provides the potential for regulation through the stimulation by the developing conceptuses, which significantly increase mRNA production for fibronectin and fibrinogen, both TLR-4 endogenous ligands, during the implantation window.

The involvement of steroid hormones, as well as their receptors, has in many studies been shown to affect NFκB activity in a variety of tissues. Estrogen, progesterone, and their receptors have been shown in multiple tissue types to regulate NFκB activity [Kalkoven et al., 1996; Ghilsetti et al., 2005, Hardy et al., 2006] and as described, these mechanisms associate well with the steroid hormone regulation of the estrous cycle and early pregnancy in the pig.

While these three individual studies were designed separately, each investigating specific biological areas during diestrus of the estrous cyclic and peri-implantation development during pregnancy; collectively they contribute to a better overall understanding of pregnancy establishment not only in the pig, but in all mammalian species. Collectively, these three studies bring novel insight to the understanding of the

estrogenic affects on uterine receptivity, regulation of the opening of the implantation window, and the identification of factors affecting conceptus ability to reach the developmental landmarks required to hit the “window”.

These data have supplied a wealth of information that could be used for the generation of many hypothesis’ to describe the specific functions of genes that regulate conceptus trophoblastic elongation, estrogen’s molecular role as the maternal recognition of pregnancy signal and NFκB activation and function as it relates to the endocrine/exocrine theory of prostaglandin production during pregnancy establishment in the pig.

Current technologies, such as RNA interference, delivery of antisense morpholinos, and transgenic swine embryo development have reached an efficacy that can be applied for agricultural and biological gain. Through gene knock-down, knock-out and knock-in methods, the specific genes that regulate trophoblastic elongation and subsequent placental function can be identified, providing specific targets through which modifications can be determined to improve pig reproductive efficiency.

LITERATURE CITED

Ait-Azzouzene D, Gendron MC, Houdayer M, Langkopf A, Burki K, Nemazee D, Kanellopoulos-Langevin C. Maternal B lymphocytes specific for paternal histocompatibility antigens are partially deleted during pregnancy. J Immunol 1998; 161:2677-2683.

Ali S and Mann DA. Signal transduction via the NF-κB pathway: targeted treatment modality for infection, inflammation and repair. Cell Biochem Funct 2004; 22:67-79.

Altschul S, Gish W, Miller W, Myers E, Lipman D. Basic local alignment search tool. J Mol Biol 1990; 215:403-410.

Anderson LL. Growth, protein content and distribution of early pig embryos. Anat Rec 1978; 190:143-154.

Anegon I, Cuturi MC, Godard A, Moreau M, Terqui M, Martinat-Botte F, Soulillou JP. Presence of leukaemia inhibitory factor and interleukin 6 in porcine uterine secretions prior to conceptus attachment. Cytokine 1994; 6:493-499.

Ashworth MD, Ross JW, Hu J, White FJ, Stein DR, DeSilva U, Johnson GA, Spencer TE, Geisert RD. Expression of porcine endometrial prostaglandin synthase during the estrous cycle and early pregnancy, and following endocrine disruption of pregnancy. Biol Reprod 2006; 74:1007-1015.

Ashworth MD. Analysis of endometrial gene and protein alterations following endocrine disruption in the pregnant gilt. Oklahoma State Electronic Thesis Database 2005; http://e-archive.library.okstate.edu/dissertations/AAI1431062/.

Basha SM, Bazer FW, Roberts RM. Effect of the conceptus on quantitative and qualitative aspects of uterine secretion in pigs. J Reprod Fertil 1980; 60:41-8.

Battey J, Wada E, Wray S. Bombesin receptor gene expression during mammalian development. Ann N Y Acad Sci. 1994; 739:244-252.

Bazer FW, Geisert RD, Thatcher WW, Roberts RM. The establishment and maintenance of pregnancy. In: Control of Pig Reproduction (Edited by Cole DJA, Foxcroft GR) Butterworth Scientific, London, UK 1982; pp.227-252.

Bazer FW, Thatcher WW. Theory of maternal recognition of pregnancy in swine based on estrogen controlled endocrine versus exocrine secretion of prostaglandin $F_{2\alpha}$ by the uterine endometrium. Prostaglandins 1977; 14:397-401.

Bazer FW, Vallet JL, Roberts RM, Sharp DC, Thatcher WW. Role of conceptus secretory products in establishment of pregnancy. J Reprod Fertil 1986; 76:841-850.

Bertoja AZ, Zenclussen ML, Casalis PA, Sollwedel A, Schumacher A, Woiciechowsky C, Volk H, Zenclussen AC. Anti-P- and E-selectin therapy prevents abortion in the CBA/J x DBA/2J combination by blocking the migration of Th1 lymphocytes into the foetal-maternal interface. Cell Immunol 2005; 238:97-102.

Blair RM, Geisert RD, Zavy MT, Yellin T, Fulton RW, Short EC. Endometrial surface and secretory alterations associated with embryonic mortality in gilts administered estradiol valerate on days 9 and 10 of gestation. Biol Reprod 1991; 44:1063-1079.

Blitek A, Waclawik A, Kaczmarek MM, Stadejek T, Pejsak Z, Ziecik AJ. Expression of cyclooxygenase-1 and -2 in the porcine endometrium during the oestrous cycle and early pregnancy. Reprod Dom Anim 2006; 41:251-257.

Blomberg LA and Zuelke KA. Expression analysis of the steroidogenic acute regulatory protein (STAR) gene in developing porcine conceptuses. Mol Reprod Dev 2005; 72:419-429.

Blomberg LA, Long EL, Sonstegard TS, Van Tassell CP, Dobrinsky JR, Zuelke KA. Serial analysis of gene expression during elongation of the peri-implantation porcine trophectoderm (conceptus). Phsyiol Genomics 2005; 20:188-194.

Bost F, Diarra-Mehrpour M, Martin JP. Inter-α-trypsin inhibitor proteoglycan family: A group of proteins binding and stabilizing the extracellular matrix. Eur J Biochem 1998; 252:339-346.

Bowen JA and Hunt JS. The role of integrins in reproduction. Proc Soc Exp Biol Med 2000; 223:331-343.

Bowen JA, Bazer FW, Burghardt RC. Spatial and temporal analyses of integrin and Muc-1 expression in porcine uterine epithelium and trophectoderm in vivo. Biol Reprod 1996; 55:1098-1106.

Bowen JA, Bazer FW, Burghardt RC. Spatial and temporal analyses of integrin and Muc-1 expression in porcine uterine epithelium and trophectoderm in vitro. Biol Reprod 1997; 56:409-415.

Bradford MM. A rapid and sensitive method for the quantitation of microgram quantities of protein utilizing the principle of protein-dye binding. Anal Biochem 1976; 72:248-254.

Braga VMM, Gendler SJ. Modulation of Muc-1 mucin expression in the mouse uterus during the estrous cycle, early pregnancy and placentation. J Cell Sci 1993; 105:397-405.

Brownlee M. Biochemistry and molecular cell biology of diabetic complications. Nature 2001; 414:813-820.

Burgess AW. Epidermal growth factor and transforming growth factor alpha. BR Med Bull 1989; 45:401-424.

Burghardt RC, Bowen JA, Newton GR, Bazer FW. Extracellular matrix and the implantation cascade in pigs. In: Control of Pig Reproduction V (Edited by Foxcroft GR, Geisert RD, Doberska C). Cambridge, UK, J Reprod Fertil Suppl 1997; 52:151-164.

Cao Y and Karin M. NF-κB in mammary gland development and breast cancer. J Mammary Gland Biol Neoplasia 2003; 8:215-223.

Carraway KL, Idris M. Regulation of sialomucin complex/Muc4 in the female rat reproductive tract. Biochem Soc Trans 2001; 29:162-166.

Chastant S, Monget P, Terqui M. Localization and quantification of insulin-like growth factor-I (IGF-I) and IGF-II/mannose-6-phosphate (IGF-II/M6P) receptors in pig embryos during early pregnancy. Biol Reprod 1994; 51:588-596.

Chen EI, Yates JR. Maspin and tumor metastasis. IUBMB Life. 2006; 58:25-29.

Choi I, Simmen RC Simmen FA. Molecular cloning of cytochrome P450 aromatase complementary deoxyribonucleic acid from periimplantation porcine and equine blastocysts identifies multiple novel 5'-untranslated exons expressed in embryos, endometrium, and placenta. Endocrinology 1996; 137:1457-1467.

Christenson LK, Farley DB, Anderson LH, Ford SP. Luteal maintenance during early pregnancy in the pig: role for prostaglandin E2. Prostaglandins 1994; 47:61-75.

Christenson RK, Leymaster KA, Young LD. Justification of unilateral hysterectomy-ovariectomy as a model to evaluate uterine capacity in swine. J Anim Sci 1987; 65:738-744.

Corbin CJ, Khalil MW, Conley AJ. Functional ovarian and placental isoforms of porcine aromatase. Mol Cell Endocrinol 1995; 113:29-37.

Corner GW. The problem of embryonic pathology in mammals, with observations upon intrauterine mortality in the pig. Am J Anat 1923; 31:523-545.

Couse JF and Korach KS. Estrogen receptor null mice: What have we learned and where will they lead us? Endocrine Reviews 1999; 20:358-417.

Czech MP. Structures and functions of the receptors for insulin and the insulin-like growth factors. J Anim Sci 1986; 63:27-38.

Dantzer V. Electron microscopy of the initial stages of placentation in the pig. Anat Embryol 1985; 172:281-293.

Dardik A, Schultz RM. Blastocoel expansion in the preimplantation mouse embryo: stimulatory effect of TGF-alpha and EGF. Development 1991; 113:919-930.

Darnell JE Jr. Studies of IFN-induced transcriptional activation uncover the Jak-Stat pathway. J Interferon Cytokine Res. 1998; 18:549-554.

Davis AJ, Fleet IR, Harrison FA, Maule Walker FM. Pulmonary metabolism of prostaglandin $F_{2\alpha}$ in the conscious nonpregnant ewe and sow. J Physiol, London 1979; 301:86.

Davis DL, Blair RM. Studies of uterine secretions and products of primary cultures of endometrial cells in pigs. In: Control of Pig Reproduction IV (Edited by Foxcroft GR, Hunter MG and Doberska C). Cambridge, UK, J Reprod Fertil Suppl 1993; 48:143-155.

Davis DL, Pakrasi PL, Dey SK. Prostaglandins in swine blastocysts. Biol Reprod 1983; 28:1114-1118.

Dekaney CM, Ing NH, Bustamante L, Madrigal MM, Jaeger LA. Estrogen and progesterone peri-implantation porcine conceptuses. Biol Reprod 1998; 58 (Suppl. 1):92 (Abstract).

Deryckere F, Gannon F. A one-hour minipreparation technique for extraction of DNA-binding proteins from animal tissues. Biotechniques 1994; 16:405.

Dhindsa DS, Dzuik PF. Effects of pregnancy in the pig after killing embryos or fetuses in one uterine horn in early pregnancy. J Anim Sci 1968; 27:122-126.

Diaz FJ, Anderson LE, Wu YL, Rabot A, Tsai SJ, Wiltbank MC. Regulation of progesterone and prostaglandin $F_{2\alpha}$ production in the CL. Mol Cell Endocrinol 2002; 191:65-80.

Dunne FP, Ratcliffe WA, Mansour P, Heath DA. Parathyroid hormone related protein (PTHrP) gene expression in fetal and extra-embryonic tissues of early pregnancy. Hum Reprod 1994; 9:149-156.

Dziuk PJ. Effect of number of embryos and uterine space on embryo survival in the pig. J Anim Sci 1968; 27:673-676.

Eisen MB, Spellman PT, Brown PO, Botstein D. Cluster analysis and display of genome-wide expression patterns. Proc Nat Acad Sci 1998; 95:14863-14868.

El-Hashash AH, Kimber SJ. PTHrP induces changes in cell cytoskeleton and E-cadherin and regulates Eph/Ephrin kinases and RhoGTPases in murine secondary trophoblast cells. Dev Biol 2006; 290:13-31.

Enders AC. Implantation in the nine-banded armadillo: How does a single blastocyst form four embryos? Placenta 2002; 23:71-85.

Engelhart H, Croy BA, King GJ. Conceptus influences the distribution of uterine leukocytes during early porcine pregnancy. Biol Reprod 2002; 66:1875-1880.

Ernkvist M, Aase K, Ukomadu C, Wohlschlegel J, Blackman R, Veitonmaki N, Bratt A, Dutta A, Holmgren L. p130-Angiomotin associates to actin and controls endothelial cell shape. FEBS Journal 2006; 273:200-2011.

Fazeli A, Bruce C, Anumba DO. Characterization of Toll-like receptors in the female reproductive tract in humans. Hum Reprod 2005; 20:1372-1378.

Fazleabas AT, Kim JJ, Srinivasan S, Donnelly KM, Brudney A, Jaffe RC. Implantation in the baboon: endometrial responses. Semin Reprod Endocrinol 1999; 17:257-265.

Ferrell AD, Malayer JR, Carraway KL, Geisert RD. Sialomucin complex (Muc4) expression in porcine endometrium during the oestrous cycle and early pregnancy. Reprod Dom Anim 2003; 38:1-3.

Ford SP Christenson RK. Blood flow to uteri of sows during the estrous cycle and early pregnancy: local effect of the conceptus on the uterine blood supply. Biol Reprod 1979; 21:617-624.

Ford SP, Christenson RK, Ford JJ. Uterine blood flow and uterine arterial, venous and lumenal concentrations of oestrogens on days 11, 13 and 15 after oestrus in pregnant and nonpregnant sows. J Reprod Fertil 1982b; 64:185-190.

Ford SP, Christenson RK. Direct effects of oestradiol-17β and prostaglandin E-2 in protecting pig corpora lutea from a luteolytic dose of prostaglandin F-2α. J Reprod Fert 1991; 93:203-209.

Ford SP, Magness RR, Farley DB, Van Orden DE. Local and systemic effects of intrauterine estradiol-17β on luteal function of nonpregnant sows. J Anim Sci 1982a; 55:657-664.

Ford SP. Embryonic and fetal development in different genotypes in pigs. In: Control of Pig Reproduction V (Edited by Foxcroft GR, Geisert RD, Doberska C.) Cambridge, UK, J Reprod Fertil Suppl 1997; 52:165-176.

Frank M, Bazer FW, Thatcher WW, Wilcox CJ. A study of prostaglandin F2alpha as the luteolysin in swine: III effects of estradiol valerate on prostaglandin F, progestins, estrone and estradiol concentrations in the utero-ovarian vein of nonpregnant gilts. Prostaglandins 1977; 14:1183-96.

Friess AE, Sinowatz F, Skolek-Winnisch R, Trautner W. The placenta of the pig I. Finestructural changes of the placenta barrier during pregnancy. Anat Embryol 1980; 158:179-191.

Gadsby J, Rose L, Sriperumbudur R, Ge Z. The role of intra-luteal factors in the control of the porcine corpus luteum. In: Control of Pig Reproduction VII (Edited by Ashworth CJ and Kraeling RR) Cambridge, UK, J Reprod Fertil Suppl 2006; 62:69-83.

Gadsby JE, Balapure AK, Britt JH, Fitz TA. Prostaglandin F2 alpha receptors on enzyme-dissociated pig luteal cells throughout the estrous cycle. Endocrinology 1990; 126:787-795.

Gardner ML, First NL, Casida LE. Effect of exogenous estrogens on corpus luteum maintenance in gilts. J Anim Sci 1963; 22:132-134.

Garlow JE, Ka H, Johnson GA, Burghardt RC, Jaeger LA, Bazer FW. Analysis of osteopontin at the maternal-placental interface in pigs. Biol Reprod 2002; 66:718-725.

Garrett JE, Geisert RD, Zavy MT, Gries LK, Wettemann RP, Buchanan DS. Effect of exogenous progesterone on prostaglandin F2 alpha release and the interestrous interval in the bovine. Prostaglandins 1988; 36:85-96.

Geisert RD, Brenner RM, Moffatt RJ, Harney JP, Yellin T, Bazer FW. Changes in oestrogen receptor protein, mRNA expression and localization in endometrium of cyclic and pregnant gilts. Reprod Fertil Dev 1993; 5:247-260.

Geisert RD, Brookbank JW, Roberts RM, Bazer FW. Establishment of pregnancy in the pig: II. Cellular remodeling of the porcine blastocyst during elongation on day 12 of pregnancy. Biol Reprod 1982c; 27:941-955.

Geisert RD, Brookbank JW, Roberts RM, Bazer FW. Establishment of pregnancy in the pig: I. Interrelationships between preimplantation development of the pig blastocyst and uterine endometrial secretions. Biol Reprod 1982b; 27:925-939.

Geisert RD, Chamberlain CS, Vonnahme KA, Malayer JR, Spicer LJ. Possible role of kallikrein in proteolysis of insulin-like growth factor binding proteins during the oestrous cycle and early pregnancy in pigs. Reproduction 2001; 121:719-28.

Geisert RD, Morgan GL, Zavy MT, Blair RM, Gries LK, Cox A, Yellin T. Effect of asynchronous transfer and oestrogen administration on survival and development of porcine embryos. J Reprod Fertil 1991; 93:475-481.

Geisert RD, Pratt TN, Bazer FW, Mayes JS, Watson GH. Immunocytochemical localization and changes in endometrial progestin receptor protein during the porcine oestrous cycle and early pregnancy. Reprod Fertil Dev 1994; 6:749-760.

Geisert RD, Ross JW, Ashworth MD, White FJ, Johnson GA, DeSilva U. Maternal recognition of pregnancy signal or endocrine disruptor: the two faces of oestrogen during establishment of pregnancy in the pig. In: Control of Pig Reproduction VII (Edited by Ashworth CJ and Kraeling RR) Cambridge, UK, J Reprod Fertil Suppl 2006; 62:131-145.

Geisert RD, Schmitt RAM. Early embryonic survival in the pig: Can it be improved? J Anim Sci 2000; 80(E. Suppl. 1):1-12.

Geisert RD, Thatcher WM, Roberts RM, Bazer FW. Establishment of Pregnancy in the Pig: III. Endometrial secretory response to estradiol valerate administered on day 11 of the estrous cycle. Biol Reprod 1982a; 27:957-965.

Geisert RD, Yelich JV, Pratt T, Pomp D. Expression of an inter-α-trypsin inhibitor heavy chain-like protein in the pig endometrium during the oestrus cycle and early pregnancy in the pig. J Reprod Fertil 1998; 114:35-43.

Geisert RD, Yelich JV. Regulation of conceptus development and attachment in pigs. In: Control of Pig Reproduction V (Edited by Foxcroft GR, Geisert RD, Doberska C.) Cambridge, UK, J Reprod Fertil Suppl 1997; 52:133-149.

Geisert RD, Zavy MT Wettemann RP, Biggers BG. Length of psuedopregnancy and pattern of uterine protein release as influenced by time and duration of oestrogen administration in the pig. J Reprod Fertil 1987; 79:163-172.

Geisert RD, Zavy MT, Moffatt RJ, Blair RM, Yellin T. Embryonic steroids and establishment of pregnancy in pigs. In: Control of Pig Reproduction III (Edited by Cole DJA, Foxcroft GR, Weir BJ) Cambridge, UK, J Reprod Fertil Suppl 1990; 40:293-305.

Ghisletti S, Meda C, Maggi A, Vegeto E. 17β-Estradiol inhibits inflammatory gene expression by controlling NF-kB intracellular localization. Mol Cell Biol 2005; 25:2957-2968.

Ghosh S, May MJ, Kopp EB. NF-kappa B and Rel proteins: evolutionarily conserved mediators of immune responses. Annu Rev Immunol 1998; 16:225-260.

Glynn D Jr., Sherman BT, Hosack DA, Yang J, Baseler MW, Lane HC, Lempicki RA. DAVID: Database for Annotation, Visualization, and Integrated Discovery. Genome Biology 2003; 4: P3.

Graddy LG, Kowalski AA, Simmen FA, Davis SL, Baumgartner WW, Simmen RC. Multiple isoforms of porcine aromatase are encoded by three distinct genes. J Steroid Biochem Mol Biol 2000; 73:49-57.

Green ML, Blaeser LL, Simmen FA, Simmen RC. Molecular cloning of spermidine/spermine N1-acetyltransferase from the periimplantation porcine uterus by messenger ribonucleic acid differential display: temporal and conceptus-modulated gene expression. Endocrinology 1996; 137:5447-5455.

Green ML, Chung TE, Reed KL, Modric T, Badinga L, Yang J, Simmen FA, Simmen RC. Paracrine inducers of uterine endometrial spermidine/spermine N1-acetyltransferase gene expression during early pregnancy in the pig. Biol Reprod 1998; 59:1251-1258.

Green ML, Simmen RC, Simmen FA. Developmental regulation of steroidogenic enzyme gene expression in the periimplantation porcine conceptus: a paracrine role for insulin-like growth factor-I. Endocrinology 1995; 136:3961-70.

Gries LK, Geisert RD, Zavy MT, Garret JE, Morgan GL. Uterine secretory alterations coincident to embryonic mortality in the gilt after exogenous estrogen administration. J Anim Sci 1989; 67:276-284.

Groothuis PG, McGuire WJ, Vallet JL, Grieger DM, Davis DL. Retinol and estradiol regulation of retinol binding protein and prostaglandin production by porcine uterine epithelial cells in vitro. J Anim Sci 2002; 80:2688-2694.

Gupta A, Bazer FW, Jaeger LA. Differential expression of beta transforming growth factors (TGF beta 1, TGF beta 2, and TGF beta 3) and their receptors (type I and type II) in peri-implantation porcine conceptuses. Biol Reprod 1996; 55:796-802.

Gupta A, Ing NH, Bazer FW, Bustamante LS, Jaeger LA. Beta transforming growth factors (TGFβ) at the porcine conceptus-maternal interface. Part I: Expression of TGFβ1, TGFβ2, and TGFβ3 messenger ribonucleic acids. Biol Reprod 1998; 59:905-910.

Guthrie HD and Lewis GS. Production of prostaglandin $F_{2\alpha}$ and estrogen by embryonal membranes and endometrium and metabolism of prostaglandin $F_{2\alpha}$ by embryonal membranes, endometrium and lung from gilts. Dom Anim Endocrinol 1986; 3:185-198.

Guthrie HD, Grimes RW, Cooper BS, Hammond JM. Follicular atresia in pigs: measurement and physiology. J Anim Sci 1995; 73:2834-2844.

Hannan NJ, Jones RL, White CA, Salamonsen LA. The chemokines, CX3CL1, CCL14, and CCL4, promote human trophoblast migration at the feto-maternal interface. Biol Reprod 2006; 74:896-904.

Hardy DB, Janowski BA, Corey DR, Mendelson CR. Progesterone receptor (PR) plays a major anti-inflammatory role in human myometrial cells by antagonism of NF-κB activation of cyclooxygenase 2 (COX-2) expression. Mol Endocrinol 2006; Epub ahead of print.

Harney JP, Ali M, Vedeckis WV, Bazer FW. Porcine conceptus and endometrial retinoid-binding proteins. Reprod Fertil Dev 1994; 6:211-219.

Harney JP, Mirando MA, Smith LC, Bazer FW. Retinol-binding protein: A major secretory product of the pig conceptus. Biol Reprod 1990; 42:523-532.

Hartt LS, Carling SJ, Joyce MM, Johnson GA, Vanderwall DK, Ott TL. Temporal and spatial associations of oestrogen receptor alpha and progesterone receptor in the endometrium of cyclic and early pregnant mares. Reproduction 2005; 130:241-250.

Herath S, Fischer DP, Werling D, Williams Ej, Lilly ST, Dobson H, Bryant CE, Sheldon IM. Expression and function of the Toll-like receptor 4 in the endometrial cells of the uterus. Endocrinology 2006; 147:562-570.

Herrmann BG, Labiet S, Poustka A, King TR, Lehrach H. Cloning of the T gene required in mesoderm formation in the mouse. Nature 1990; 343:617-622.

Hettinger AM, Allen MR, Zhang BR, Goad DW, Malayer JR, Geisert RD. Presence of the acute phase protein, bikunin, in the endometrium of gilts during estrous cycle and early pregnancy. Biol Reprod 2001; 65:507-513.

Heuser CH, Streeter GL. Early stages in the development of pig embryos, from the period of initial cleavage to the time of appearance of limb-buds. Contrib Embryol Carnegie Inst 1929; 20:3-29.

Hewitt SC, Goulding EH, Eddy EM, Korach KS. Studies using the estrogen receptor α knockout uterus demonstrates that implantation but not decidualization-associated signaling is estrogen dependent. Biol Reprod 2002; 67:1268-1277.

Hofig A, Simmen FA, Bazer FW, Simmen RC. Effects of insulin-like growth factor-I on aromatase cytochrome P450 activity and oestradiol biosynthesis in preimplantation porcine conceptuses in vitro. J Endocrinol 1991; 130:245-250.

Huang JC, Liu DY, Yadollah S, Wu KV and Dawood MY. Interleukin-1β induces cyclooxygenase-2 gene expression in cultured endometrial stromal cells. J Clin Endo Metab 1998; 83:538-541.

Hynes RO. Integrins: versatility, modulation, and signaling in cell adhesion. Cell 1992; 69:11-25.

Jaeger LA, Johnson GA, Ka H, Garlow JG, Burghardt RC, Spencer TE, Bazer FW. Functional analysis of autocrine and paracrine signaling at the uterine-conceptus interface in pigs. In: Control of Pig Reproduction VI (Edited by Geisert RD, Niemann H, Doberska C) Caimbridge, UK, J Reprod Fertil Suppl 2001; 58:191-207.

Johnson GA, Burghardt RC, Bazer FW, Spencer TE. Osteopontin: Roles in implantation and placentation. Biol Reprod 2003; 69:1458-1471.

Johnson GA, Spencer TE, Hansen TR, Austin KJ, Burghardt RC, Bazer FW. Expression of the interferon tau inducible ubiquitin cross-reactive protein in the ovine uterus. Biol Reprod 1999; 61:312-318.

Jones DH, Kong YY, Penninger JM. Role of RANKL and RANK in bone loss and arthritis. Anna Rheum Dis 2002; 61:ii32-ii39.

Kalkoven E, Wissink S, van der Saag PT, van der Burg B. Negative interaction between the RelA (p65) subunit of NF-κB and the progesterone receptor. J Biol Chem 1996; 271:6217-6224.

Keys JL, King GL. Microscopic examination of porcine conceptus-maternal interface between days 10 and 19 of pregnancy. Am J Anat 1990; 188:221-238.

Kidder HE, Casida LE, Grummer RH. Some effects of estrogen injections on estrual cycle of gilts. J Anim Sci 1955; 14:470-474.

King GJ, Atkinson BA, Robertson HA. Implantation and early placentation in domestic ungulates. J Reprod Fertil 1982; 31:17-30.

King GJ, Rjamahendran R. Comparison of plasma progesterone profiles in cyclic, pregnant, psuedopregnant and hysterectomized pigs between 8 and 27 days after oestrus. J Endocrinol 1988; 119:111-116.

Kniss Da, Rovin B, Fertel RH and Zimmermann PD. Blockade of NF-κB activation prohibits TNF-α-induced cyclooxygenase-2 gene expression in ED27 trophoblast-like cells. Placenta 2001; 22:80-89.

Ko Y, Choi I, Green ML, Simmen FA, Simmen RCM. Transient expression of the cytochrome P450 aromatase gene in elongation porcine blastocysts is correlated with uterine insulin-like growth factor levels during peri-implantation development. Mol Reprod Dev 1994; 37:1-11.

Kol S, Kehat I, Adashi EY. Ovarian interleukin-1-induced gene expression: privileged genes threshold theory. Med Hypotheses 2002; 58:6-8.

Kowalski AA, Graddy LG, Choi I, Katzenellenbogen BS, Simmen FA, Simmen RCM. Expression of estrogen receptor (ER)-α and -β and progesterone receptor (PR) by porcine embryos suggests potential autocrine functions in development. Biol Reprod 2000; 62 (Suppl. 1):106 (Abstract).

Kowalski AA, Graddy LG, Vale-Cruz DS, Choi I, Katzenellenbogen BS, Simmen FA, Simmen RC. Molecular cloning of porcine estrogen receptor-β complementary DNAs and developmental expression in periimplantation embryos. Biol Reprod 2002; 66:760-769.

Kraeling RR, Rampacek GB, Fiorello NA. Inhibition of pregnancy with indomethacin in mature gilts and prepubertal gilts induced to ovulate. Biol Reprod 1985; 32:105-110.

Kristiansen G, Sammar M, Altevogt P. Tumour biological aspects of CD24, a mucin-like adhesion molecule. J Mol Histol 2004; 35:255-262.

Kruessel JS, Huang HY, Wen Y, Kloodt AR, Bielfeld P, Polan ML. Different pattern of interleukin-1β-(IL-1β), interleukin-1 receptor antagonist-(IL-1ra) and interleukin-1 receptor type I-(IL-1R tI) mRNA-expression in single preimplantation mouse embryos at various developmental stages. J Reprod Immunol 1997; 33:103-120.

La Bonnardiere C, Flechon JE, Battegay S, Flechon B, Degrouard J, Lefevre F. Polarized porcine trophoblastic cell lines spontaneously secrete interferon-gamma. Placenta 2002; 23:716-726.

Lee CY, Green ML, Simmen RC, Simmen FA. Proteolysis of insulin-like growth factor-binding proteins (IGFBPs) within the pig uterine lumen associated with peri-implantation conceptus development. J Reprod Fertil 1998; 112:369-377.

Lee RS, Wheeler TT, Peterson AJ. Large-format, two-dimensional polyacrylamide gel electrophoresis of ovine periimplantation uterine luminal fluid proteins: identification of aldose reductase, cytoplasmic actin, and transferring as conceptus-synthesized proteins. Biol Reprod 1998; 59:743-752.

Lee SH, Zhao SH, Recknor JC, Nettleton D, Orley S, Kang SK, Lee BC, Hwang WS, Tuggle CK. Transcriptional profiling using a novel cDNA array identifies differential gene expression during porcine embryo elongation. Mol Reprod Dev 2005; 71:129-139.

Lee TH, Wisniewski HG, Vilcek J. A novel secretory tumor necrosis factor-inducible protein (TSG-6) is a member of the family of hyaluronate binding proteins, closely related to the adhesion receptor CD44. J Cell Biol 1992; 116:545-557.

Lefevre F, Martinat-Botte F, Guillomot M, Zouari K, Charley B, La Bonnardiere C. Interferon-gamma gene and protein are spontaneously expressed by the porcine trophectoderm early in gestation. Eur J Immunol 1990; 20:2485-2490.

Lessey BA, Killam AP, Metzger DA, Haney AF, Greene GL, McCary Jr KS. Immunohistochemical analysis of human uterine estrogen and progesterone receptors throughout the menstrual cycle. J Clin Endocrinol Metab 1988; 67:334-340.

Lessey BA, Yeh I, Castelbaum AJ, Fritz MA, Ilesanmi AO, Korzeniowski P, Sun J, Chwalisz K. Endometrial progesterone receptors and markers of uterine receptivity in the window of implantation. Fertil Steril 1996; 65:477-483.

Lessey BA. Integrins and reproduction revisited. Eur J Obstet Gynecol Reprod Biol 1995; 62:264-265.

Letcher R, Simmen RCM, Bazer FW, Simmen FA. Insulin-like growth factor-I expression during early conceptus development in the pig. Biol Reprod 1989; 41:1143-1151.

Levchenko T, Aase K, Troyanovsky B, Bratt A, Holmgren L. Loss of responsiveness to chemotactic factors by deletion of the C-terminal protein interaction site of angiomotin. J Cell Sci 2003; 116:3803-3810.

Lindhard A, Bentin-Ley U, Ravn V, Islin H, Hviid T, Rex S, Bangsboll S, Sorensen S. Biochemical evaluation of endometrial function at the time of implantation. Fertil and Steril 2002; 78:221-233.

Long GG, Diekman MA. Effect of purified zearalenone on early gestation in gilts. J Anim Sci 1984; 59:1662-1670.

Longenecker DE, Day BN. Fertility level of sows superovulated at post-weaning estrus. J Anim Sci. 1968; 27:709-711.

Loughran G, Healy, NC, Kiely PA, Huigsloot M, Kedersha NL, O'Connor R. Mystique is a new insulin-like growth factor-I-regulated PDZ-LIM domain protein that promotes cell attachment and migration and suppresses anchorage-independent growth. Mol Biol Cell 2005; 16:1811-1822.

Ma WG, Song H, Das SK, Paria BC, Dey SK. Estrogen is a critical determinant that specifies the duration of the window of uterine receptivity for implantation. Proc Natl Acad Sci U. S. A. 2003; 100:2963-2968.

Maddox-Hyttel P, Dinnyes A, Laurincik J, Rath D, Niemann H, Rosenkranz C, Wilmut I. Gene expression during pre- and peri-implantation embryonic development in pigs. In: Control of Pig Reproduction VI (Edited by Geisert RD, Niemann H, Doberska C) Caimbridge, UK, J Reprod Fertil Suppl 2001; 58:175-189.

Makarenkova VP, Shurin GV, Tourkova IL, Balkir L, Pirtskhalaishvili G, Perez L, Gerein V, Siegfried JM, Shurin MR. Lung cancer-derived bombesin-like peptides down-regulate the generation and function of human dendritic cells. J Neuroimmunol 2003; 145:55-67.

Mantovani A, Muzio M, Ghessi P, Colotta C, Introna M. Regulation of inhibitory pathways of the interleukin-1 system. Ann N Y Acad Sci 1998; 840:338-351.

Mathialagan N, Bixby JA, Roberts RM. Expression of interleukin-6 in porcine, ovine, and bovine preimplantation conceptuses. Mol Reprod Dev 1992; 32:324-330.

Mattson BA, Overstrom EW, Albertini DF. Endodermal cytoskeletal rearrangements during preimplantation pig morphogenesis. Biol Reprod 1990; 42:195-205.

Matusiak D, Glover S, Nathaniel R, Matkowskyj K, Yang J, Benya RV. Neuromedin B and its receptor are mitogens in both normal and malignant epithelial cells lining the colon. Am J Physiol Gastrointest Liver Physiol 2005; 288:G718-G728.

McCracken JA, Custer EE, Lamsa JC. Luteolysis: a neuroendocrine-mediated event. Physiol Rev 1999; 79:263-323.

McNeer RR, Carraway CAC, Fregien NL, Carraway KL. Characterization of the expression and steroid hormone control of sialomucin complex in the rat uterus: Implications for uterine receptivity. J Cell Physiol 1998; 176:110-119.

McNulty SE, Tohidian NB, Meyskens FL Jr. RelA, p50 and inhibitor of kappa B alpha are elevated in human metastatic melanoma cells and respond aberrantly to ultraviolet light B. Pigment Cell Res 2001; 14:456-465.

Meikle A, Sahlin L, Ferraris A, Masironi B, Blanc JE, Rodriguez-Irazoqui M, Reodriguez Pinon M, Kindahl H, Forsberg M. Endometrial mRNA expression of oestrogen receptor α, progesterone receptor and insulin-like growth factor-I (IGF-1) throughout the bovine oestrous cycle. Anim Reprod Sci 2001; 68:45-56.

Mellor AL, Munn DH. Immunology at the maternal-fetal interface: lessons for T cell tolerance and suppression. Annu Rev Immunol 2000; 18:367-391.

Mesa H, Safranski TJ, Johnson RK, Lamberson WR. Correlated response in placental efficiency in swine selected for an index of components of litter size. J Anim Sci 2003; 81:74-79.

Miller H, Poon S, Hibbert B, Rayner K, Chen YX, O'Brien ER. Modulation of estrogen signaling by the novel interaction of heat shock protein 27, a biomarker for atherosclerosis, and estrogen receptor beta: mechanistic insight into the vascular effects of estrogens. Arterioscler Thromb Vasc Biol 2005; 25:10-14.

Minamino N, Kanqawa K, Matsuo H. Neuromedin B and neuromedin Ca. Two mammalian bombesin-like peptides identified in porcine spinal cord and brain. Ann N Y Acad Sci 1988; 547:373-390.

Modric T, Kowalski AA, Green ML, Simmen RCM and Simmen FA. Pregnancy-dependent expression of leukaemia inhibitory factor (LIF), LIF receptor-β and interleukin 6 (IL-6) messenger ribonucleic acids in the porcine female reproductive tract. Placenta 2000; 21:345-353.

Moeljono MPE, Bazer FW, Thatcher WW. A study of prostaglandin $F_{2\alpha}$ as the luteolysin in swine: I. Effect of in prostaglandin $F_{2\alpha}$ hysterectomized gilts. Prostaglandins 1976; 11:737-743.

Moody TW, Fagarasan M, Zia F. Neuromedin B stimulates arachidonic acid release, c-fos gene expression, and the growth of C6 glioma cells. Peptides 1995; 16:1133-1140.

Morgan GL, Geisert RD, McCann JP, Bazer FW, Ott TL, Mirando MA, Stewart M. Failure of luteolysis and extension of the interoestrous interval in sheep treated with the progesterone antagonist mifepristone (RU 486). J Reprod Fertil 1993; 98:451-457.

Morgan GL, Geisert RD, Zavy MT, Fazleabas AT. Development and survival of pig blastocysts after oestrogen administration on day 9 or days 9 and 10 of pregnancy. J Reprod Fertil 1987b; 80:133-141.

Morgan GL, Geisert RD, Zavy MT, Shawley RV, Fazleabas AT. Development of pig blastocysts in a uterine environment advanced by exogenous oestrogen. J Reprod Fertil 1987a; 80:125-131.

Nakamura H, Kimura T, Ogita K, Koyama S, Tsujie T, Tsutsui T, Shimoya K, Koyama M, Kaneda Y, Murata Y. Alteration of the timing of implantation by in vivo gene transfer: delay of implantation by suppression of nuclear factor kappaB activity and partial rescue by leukemia inhibitory factor. Biochem Biophys Res Commun 2004b; 321:886-892.

Nakamura H, Kimura T, Ogita K, Nakamura T, Takemura M, Shimoya K, Koyama S, Tsujie T, Koyama M, Murata Y. NF-kappaB activation at implantation window of the mouse uterus. Am J Reprod Immunol 2004a; 51:16-21.

Nara BS, Darmadja D, First NL. Effect of removal of follicles, corpora lutea or ovaries on maintenance of pregnancy in swine. J Anim Sci 1981; 52:794-801.

Ni H, Ding N, Harper MJK, Yang Z. Expression of leukemia inhibitory factor receptor and gp130 in mouse uterus during early pregnancy. Mol Reprod Devel 2002; 63:143-150.

Niemann H and Wrenzycki C. Alterations of expression of developmentally important genes in preimplantation bovine embryos by in vitro culture conditions: implications for subsequent development. Theriogenology 2000; 53:21-34.

Niitsu N, Higashihara M, Honma Y. Human B-cell lymphoma cell lines are highly sensitive to apoptosis induced by all-trans retinoic acid and interferon-gamma. Leuk Res 2002; 26:745-755.

Ohki-Hamazaki H. Neuromedin B. Prog Neurobiol 2000; 62:297-312.

Ottobre JS, Lewis GS, Thayne WV, Inskeep EK. Mechanism by which progesterone shortens the estrous cycle of the ewe. Biol Reprod 1980; 23:1046-1053.

Pappu R, Cheng AM, Li B, Gong Q, Chiu C, Griffin N, White M, Sleckman BP, Chan AC. Requirement for B cell linker protein (BLNK) in B cell development. Science 1999; 286:1949-1954.

Perry JS, Heap RB, Amoroso EC. Steroid hormone production by pig blastocysts. Nature, Lond. 1973; 245:45-47.

Perry JS, Heap RB, Burton RD, Gadsby JE. Endocrinology of the blastocyst and its role in the establishment of pregnancy. J Reprod Fertil Suppl 1976; 25:85-104.

Perry JS. The mammalian fetal membranes. Reprod Fertil 1981; 62:321-335.

Pickard AR, Miller SJ, Ashworth CJ. Synchronous onset of oestradiol-17β secretion by Meishan conceptuses. Reprod Biol Endocrinol 2003; 1:16 http://www.rbej.com/content/1/1/16.

Pierson Cr, McGowen R, Grignon D, Sakr W, Dey J, Sheng S. Maspin is up-regulated in premalignant prostate epithelia. Prostate 2002; 53:255-262.

Polge C, Rowson LEA, Chang MC. The effect of reducing the number of embryos during early stages of gestation on the maintenance of pregnancy in the pig. J Reprod Fertil 1966; 12:395-397.

Polge C. Fertilization in the pig and horse. J Reprod Fertil 1978; 54:461-470.

Polge C. Embryo transplantation and preservation. In: Control of Pig Reproduction (Edited byDJA Cole and GR Foxcroft) Cambridge, UK, J Reprod Fertil Suppl (1982) pp. 277-292.

Pollard JW, Hunt JS, Wiktor-Jedrzejczak W, Stanley ER. A pregnancy defect in the osteopetrotic (op/op) mouse demonstrates the requirement for CSF-1 in female fertility. Dev Biol 1991; 148:273-83.

Poltorak A, He X, Smirnova I, Liu MY, van Huffel C, Du X, Birdwell D, Alejos E, Silva M, Galanos C, Freudenberg M, Ricciardi-Castagnoli P, Layton B, Beutler B. Defective LPS signaling in C3H/HeJ and C57BL/10ScCr mice: mutations in Tlr4 gene. Science 1998; 282:2085-2088.

Pope WF, Lawyer MS, Butler WR, Foote RH, First NL. Response shift in the ability of gilts to remain pregnant following exogenous estradiol-17 beta exposure. J Anim Sci. 1986; 63:1208-10.

Pope WF, Lawyer MS, First NL. The effect of exogenous estradiol on litter size in a typical swine herd. Theriogenology 1987; 28:9-14.

Pope WF, Wilde MH, Xie S. Effect of electrocautery of nonovulated Day-1 follicles on subsequent morphological variation among Day-11 porcine embryos. Biol Reprod 1988a; 39:882-887.

Pope WF, Xie S, Broermann DM, Nephew KP. Causes and consequences of early embryonic diversity in pigs. In: Control of Pig Reproduction III (Edited by Cole DJA, Foxcroft GR, Weir BJ) Cambridge, UK, J Reprod Fertil Suppl 1990; 40:251-260.

Pope WF. Embryonic Mortality in Swine. In: Embryonic Mortality in Domestic Species (Edited by Zavy MT, Geisert RD), CRC Press, Boca Raton 1994; pp. 53-78.

Pope, WF. Uterine asynchrony: A cause of embryonic loss. Biol Reprod 1988b; 39:999-1003.

Potts JT. Parathyroid hormone: past and present. J Endocrinol 2005; 187:311-325.

Pusateri AE, Rothschild MF, Warner CM, Ford SP. Changes in morphology, cell number, cell size and cellular estrogen content or individual littermate pig conceptuses on days 9 to 13 of gestation. J Anim Sci 1990; 68:3727-3735.

Raghupathy R. TH1-type immunity is incompatible with successful pregnancy. Immunol Today 1997; 18:478-482.

Rechler MM. Insulin-like growth factor binding proteins. Vitam Horm 1993; 47:1-114.

Richards JS, Russel DL, Ochsner S, Espey LL. Ovulation: New dimensions and new regulators of the inflammatory-like response. Annu Rev Physiol 2002; 64:69-92.

Roberts RM. Xie S, Trout WE. Embryo-uterine interactions in pigs during week 2 of pregnancy. In: Control of Pig Reproduction IV (Edited by Foxcroft GR, Hunter MG, Doberska C) Caimbridge, UK, J Reprod Fertil Suppl 1993; 48:171-186.

Ross JW, Ashworth MD, Hurst AG, Malayer JR, Geisert RD. Analysis and Characterization of Differential Gene Expression During Rapid Trophoblastic Elongation in the Pig Using Suppression Subtractive Hybridization. Reprod Biol Endocrin 2003b; 1:23 http://www.RBEj.com/content/1/1/23.

Ross JW, Malayer JR, Ritchey JW, Geisert RD. Characterization of the interleukin-1β system during porcine trophoblastic elongation and early placental attachment. Biol Reprod 2003a; 69:1251-1259.

Rossi M, Sharkey AM, Vigano P, Fiore G, Furlong R, Florio P, Ambrosini G, Smith SK, Petraglia F. Identification of genes regulated by interleukin-1beta in human endometrial stromal cells. Reproduction 2005; 130:721-729.

Samuel CA, Perry JS. The ultrastructure of pig trophoblast transplanted to an ectopic site in the uterine wall. J Anat 1972; 113:139-149.

Sato Y, Higuchi T, Yoshioka S, Tatsumi K, Fujiwara H, Fujii S. Trophoblasts acquire a chemokine receptor, CCR1, as they differentiate towards invasive phenotype. Development 2003; 130:5519-5532.

Schaefer TM, Desouza K, Fahey JV, Beagley KW, Wira CR. Toll-like receptor (TLR) expression and TLR-mediated cytokine/chemokine production by human uterine epithelial cells. Immunology 2004; 112:428-436.

Short RV. An introduction to some of the problems of intersexuality. J Reprod Fertil Suppl. 1969; 7:Suppl 7:1-8.

Simmen FA, Simmen RC, Geisert RD, Martinat-Botte F, Bazer FW, Terqui M. Differential expression, during the estrous cycle and pre- and postimplantation

conceptus development, of messenger ribonucleic acids encoding components of the pig uterine insulin-like growth factor system. Endocrinology 1992; 130:1547-56.

Smith TPL, Fahrenkrug SC, Rohrer GA, Simmen FA, Rexroad CE, Keele JW. Mapping of expressed sequence tags from a porcine early embryonic cDNA library. Anim Genet 2001; 32:66-72.

Smith WL, Dewitt DL. Prostaglandin endoperoxide H synthases-1 and -2. Adv Immunol 1996; 62:167-215.

Soboll G, Shen L, Wira CR. Expression of Toll-like receptors (TLR) and responsiveness to TLR agonists by polarized mouse uterine epithelial cells in culture. Biol Reprod 2006; 75:131-139.

Soede NM, Kemp B. Expression of oestrus and timing of ovulation in pigs. In: Control of Pig Reproduction V (Edited by Foxcroft GR, Geisert RD, Doberska C.) Cambridge, UK, J Reprod Fertil Suppl 1997; 52:91-103.

Soede NM, Noorhuizen JPTM, Kemp B. The duration of ovulation in pigs, studied by transrectal ultrasonography, is not related to early embryonic diversity. Theriogenology 1992; 38:653-666.

Spencer TE, Bazer FW. Temporal and spatial alterations in uterine estrogen receptor and progesterone receptor gene expression during the estrous cycle and early pregnancy in the ewe. Biol Reprod 1995; 53:1527-1543.

Srivastava S, Matsuda M, Hou Z, Baily JP, Kitazawa R, Herbst MP, Horseman ND. Receptor activator of NF-kappaB ligand induction via Jak2 and Stat5a in mammary epithelial cells. J Biol Chem 2003; 278:46171-46178.

Stroband HW, Van der Lende T. Embryonic and uterine development during pregnancy. In: Control of Pig Reproduction III (Edited by Cole DJA, Foxcroft GR, Weir BJ) Cambridge, UK, J Reprod Fertil Suppl 1990; 40:261-277.

Surveyor GA, Gendler SJ, Pemberton L, Das SK, Chakraborty I, Julian J, Pimental RA, Wegner CC, Dey SK, Carson DD. Expression and steroid hormonal control of Muc-1 in the mouse uterus. Endocrinology 1995; 136:3639-3647.

Tabibzadeh S, Kong QF, Satyaswaroop PG, Babaknia A. Heat shock proteins in human endometrium throughout the menstrual cycle. Hum Reprod 1996; 11:633-640.

Takacs R and Kauma S. The expression of interleukin-1α, interleukin-1β, and interleukin-1 receptor type I mRNA during preimplantation mouse development. J Reprod Immunol 1996; 32:27-35.

Takada Y, Bhardwaj A, Potdar P and Aggarwal BB. Nonsteroidal anti-inflammatory agents differ in their ability to suppress NF-kappaB activation, inhibition of expression of cyclooxygenase-2 and cyclin D1, and abrogation of tumor cell proliferation. Oncogene 2004; 23:9247-9258.

Thompson JN, Howell J, Pitt GAJ. Vitamin A and reproduction in rats. Proceedings of the Royal Society of London Series 1964; B159:510-535.

Tomanek M, Kopecny V, Kanka J. Genome reactivation in developing early pig embryos: an ultrastructural and autoradiographic analysis. Anat Embryol 1989; 180:309-316.

Tripp HRH. Reproduction in elephant-shrews (macroscelididae) with special reference to ovulation and implantation. J Reprod Fertil 1971; 26:149-159.

Trout WE, Hall JA, Stallings-Mann ML, Galvin JA, Anthony RV, Roberts RM. Steroid regulation of the synthesis and secretion of retinol-binding protein by the uterus of the pig. Endocrinology 1992; 130:2557-2564.

Troyanovsky B, Levchenko T, Mansson G, Matvijenko O, Holmgren L. Angiomotin: an angiostatin binding protein that regulates endothelial cell migration and tube formation. J Cell Biol 2001; 152:1247-1254.

Tsan M, Gao B. Endogenous ligands of toll-like receptors. J Leukoc Biol 2004; 76:514-519.

Tucci J, Beck F. Expression of parathyroid hormone-related protein (PTHrP) and the PTH/PTHrP receptor in the rat uterus during early pregnancy and following artificial deciduoma induction. J Reprod Fertil 1998; 112:1-10.

Tuo W, Bazer FW. Expression of oncofetal fibronectin in porcine conceptuses and uterus throughout gestation. Reprod Fertil Dev 1996a; 8:1207-13.

Tuo W, Harney JP, Bazer FW. Colony-stimulating factor-1 in conceptus and uterine tissues in pigs. Biol Reprod 1995; 53:133-142.

Tuo W, Harney JP, Bazer FW. Developmentally regulated expression of interleukin-1β by peri-implantation conceptuses in swine. J Reprod Immunol 1996b; 31:185-198.

Vallet JL and Christenson RK. Uterine space affects placental protein secretion in swine. Biol Reprod 1993; 48:575-584.

Vallet JL, Christenson RK, McGuire WJ. Association between uteroferrin, retinol-binding protein, and transferrin within the uterine and conceptus compartments during pregnancy in swine. Biol Reprod 1996; 55:1172-1178.

Vallet JL, Christenson RK, Trout WE, Klemcke HG. Conceptus, progesterone and breed effects on uterine protein secretion in swine. J Anim Sci 1998; 76:2657-2670.

Vallet JL. Fetal erythropoiesis and other factors which influence uterine capacity in swine. J Appl Anim Res 2000; 17:1-26.

Van Why SK, Mann AS< Ardito T, Thulin G, Ferris S, Macleod MA, Kashqarian M, Siegel NJ. Hsp27 associates with actin and limits injury in energy depleted renal epithelia. J Am Soc Nephrol 2003; 14:98-106.

Vaughan TJ, James PS, Pascall JC, Brown KD. Expression of the genes for TGFα, EGF and the EGF receptor during early pig development. Development 1992; 116:663-669.

Vonnahme KA, Wilson ME, Foxcroft GR, Ford SP. Impacts on conceptus survival in a commercial swine herd. J Anim Sci 2002; 80:553-559.

Wang LH, Battey JF, Wada E, Lin JT, Mantey S, Coy DH, Jensen RT. Activation of neuromedin B-preferring bombesin receptors on rat glioblastoma C-6 cells increases cellular Ca2+ and phosphoinositides. Biochem J 1992; 286:641-648.

Wegmann TG, Lin H, Guilbert L, Mosmann TR. Bidirectional cytokine interactions in the maternal-fetal relationship: is successful pregnancy a T_H2 phenomenon? Immunol Today 1993; 14:353-356.

Weng H, Ayoubi P. GPAP (GenePix Pro Auto-Processor) for online preprocessing, normalization and statistical analysis of primary microarray data. (In Preparation).

White FJ, Ross JW, Joyce MM, Geisert RD, Burghardt RC, Johnson GA. Steroid regulation of cell specific secreted phosphoprotein 1 (osteopontin) expression in the pregnant porcine uterus. Biol Reprod 2005; 73:1294-1301.

Whitworth KM, Agca C, Kim JG, Patel RV, Springer GK, Bivens NJ, Forrester LJ, Mathialagan N, Green JA, Prather RS. Transcriptional profiling of pig embryogenesis by using a 15-K member unigene set specific for pig reproductive tissues and embryos. Biol Reprod 2005; 72:1437-1451.

Wiktor-Jedrzejczak W, Bartocci A, Ferrante AW Jr, Ahmed-Ansari A, Sell KW, Pollard JW, Stanley ER. Total absence of colony-stimulating factor 1 in the macrophage-deficient osteopetrotic (*op/op*) mouse. Proc Natl Acad Sci USA 1990; 87:4828-4832.

Wilde MH and Pope WF. Stage dependent synthesis of estradiol by porcine blastocysts. 20th Ann Meet Midwest Sect Amer Soc Anim Sci 1987; 87: (Abstract).

Wilson ME, Biensen NJ, Ford SP. Novel insight into the control of litter size in pigs, using placental efficiency as a selection tool. J Anim Sci 1999; 77:1654-1658.

Wilson ME, Fahrenkrug SC, Smith T, Rohrer GA, Ford SP. Differential expression of cyclooxygenase-2 around the time of elongation in the pig conceptus. Animal Reprod Sci 2002; 71:229-237.

Wilson ME, Sonstegard TS, Smith TP, Fahrenkrug SC, Ford SP. Differential gene expression during elongation in the preimplantation pig embryo. Genesis 2000; 26: 9-14.

Wislocky GB, Dempsey EW. Histochemical reactions of the placenta of the pig. Am J Anat 1946; 78:181-225.

Wood GW, Hausmann E, Choudhuri R. Relative role of CSF-1, MCP-1/JE, and RANTES in macrophage recruitment during successful pregnancy. Mol Reprod Devel 1997; 46:62-70.

Wu MC, Chen ZY, Jarrell VL, Dziuk PJ. Effect of initial length of uterus per embryo on fetal survival and development in the pig. J Anim Sci 1989; 67:1767-1772.

Yamada K, Santo-Yamada Y, Wada E, Wada K. Role of bombesin (BN)-like peptides/receptors in emotional behavior by comparison of three strains of BN-like peptide receptor knockout mice. Mol Psychiatry 2002; 7:113-117.

Yamada K, Santo-Yamada Y, Wada K. Restraint stress impaired maternal behavior in female mice lacking the neuromedin B receptor (NMB-R) gene. Neursci Lett 2002; 330:163-166.

Yelich JV, Pomp D, Geisert RD. Detection of transcripts for retinoic acid receptors, retinol binding protein, and transforming growth factors during rapid trophoblastic elongation in the porcine blastocyst. Biol Reprod 1997b; 57:286-294.

Yelich JV, Pomp D, Geisert RD. Ontogeny of elongation and gene expression in the early developing porcine conceptus. Biol Reprod 1997a; 57:1256-1265.

Ying CW, Hsu WL, Hong WF, Cheng WTK, Yang YC. Progesterone receptor gene expression in preimplantation pig embryos. Eur J Endocrinol 2000; 143:697-703.

Zavy MT, Clark WR, Sharp DC, Roberts RM, Bazer FW. Comparison of glucose, fructose, ascorbic acid and glucosephosphate isomerase enzymatic activity in uterine flushings from nonpregnant and pregnant gilts and pony mares. Biol Reprod 1982; 27:1147-1158.

Zenclussen AC, Fest S, Sehmsdorf U, Hagen E, Klapp BF, Arck PC. Upregulation of decidual P-selectin expression is associated with an increased number of Th1 cell populations in patients suffering from spontaneous abortions. Cell Immunol 2001; 213:94-103.

Appendix I

Additional Tables Characterizing Conceptus Gene Expression Data During Trophoblastic Elongation and the Establishment of Pregnancy in the Pig

Table A.1. Differentially expressed genes during the transition from Spherical to Day 12 filamentous conceptuses.

Probe Set ID[a]	GenBank Accesion Number[b]	P Value[c]	Fold Change[d]	Putative Identity Following Annotation Based on Homology to Known GenBank Identities[e]	Gene Title Assigned By Affymetrix Annotation[f]	Gene Symbol[g]
Ssc.4142.1.S1_at	NM_181644	0.00046	59.22	hypothetical protein DKFZp761N1114	Transcribed locus, strongly similar to NP_857595.2 hypothetical protein DKFZp761N1114 [Homo sapiens]	
Ssc.4193.1.S1_at	#N/A	0.00000	52.43	#N/A	Transcribed locus	
Ssc.22563.1.S1_at	NM_006581	0.00005	27.76	fucosyltransferase 9	Transcribed locus, strongly similar to NP_001005380.1 alpha-1,3-fucosyltransferase 9 [Canis familiaris]	
Ssc.7106.1.S1_at	NM_001801	0.00009	25.39	cysteine dioxygenase; type I	Clone Clu_1053.scr.msk.p1.Contig1, mRNA sequence	
Ssc.942.1.S1_at	NM_000165	0.00094	24.64	gap junction protein; alpha 1; 43kDa	Transcribed locus, strongly similar to NP_000156.1 connexin 43; oculodentodigital dysplasia (syndactyly type III) [Homo sapiens]	
Ssc.9288.1.A1_at	NM_020799	0.00000	20.8	associated molecule with the SH3 domain of STAM	Transcribed locus, strongly similar to NP_065850.1 associated molecule with the SH3 domain of STAM (AMSH) like protein; associated molecule with the SH3 domain of STAM (AMSH) - Family Protein [Homo sapiens]	
Ssc.4425.1.S1_at	#N/A	0.00022	19.28	#N/A	Transcribed locus	
Ssc.29867.1.A1_at	NM_001001557	0.00000	19.09	growth differentiation factor 6	Transcribed locus	
Ssc.27300.2.A1_a_at	NM_001001557	0.00000	19.03	growth differentiation factor 6	Transcribed locus	
Ssc.9991.1.S1_at	NM_198966	0.00085	16.87	parathyroid hormone-like hormone	parathyroid hormone-like hormone	PTHLH
Ssc.7588.1.A1_at	#N/A	0.00003	15.91	#N/A	Transcribed locus	
Ssc.23994.1.A1_at	#N/A	0.00099	15.56	#N/A	Transcribed locus	
Ssc.7314.1.A1_at	NM_000963	0.00045	14.81	prostaglandin-endoperoxide synthase 2	prostaglandin G/H synthase-2	PGHS-2

Ssc.4004.1.A1_at	NM_015180	0.00000	11.34	spectrin repeat containing; nuclear envelope 2	Transcribed locus, moderately similar to NP_055995.3 synaptic nuclei expressed gene 2 isoform a; nesprin 2; synaptic nuclei expressed gene 2; nucleus and actin connecting element [Homo sapiens]	
Ssc.455.1.S1_at	NM_001623	0.00023	10.87	allograft inflammatory factor 1	allograft inflammatory factor-1	AIF1
Ssc.12561.1.A1_at	NM_005504	0.00003	10.29	branched chain aminotransferase 1; cytosolic	Transcribed locus	
Ssc.23271.1.S1_at	#N/A	0.00013	8.77	#N/A	Transcribed locus	
Ssc.6969.1.A1_at	NM_017440	0.00001	7.88	Mdm4; transformed 3T3 cell double minute 1; p53 binding pr	Transcribed locus, strongly similar to XP_509206.1 PREDICTED: similar to nuclear protein double minute 1 [Pan troglodytes]	
Ssc.24509.1.A1_at	NM_014211	0.00028	7.81	gamma-aminobutyric acid	Transcribed locus	
Ssc.18004.1.A1_at	#N/A	0.00003	7.75	#N/A	Transcribed locus	
Ssc.27388.1.S1_at	NM_020128	0.00008	7.71	Mdm4; transformed 3T3 cell double minute 1; p53 binding pro	Transcribed locus, moderately similar to NP_059136.1 nuclear protein double minute 1 [Homo sapiens]	
Ssc.16475.1.S1_at	NM_003489	0.00002	7.55	nuclear receptor interacting protein 1	Transcribed locus	
Ssc.27508.1.A1_at	NM_015265	0.00071	7.46	SATB family member 2	Transcribed locus	
Ssc.9586.2.S1_at	NM_004657	0.00007	7.28	serum deprivation response	Transcribed locus	
Ssc.30064.1.A1_at	#N/A	0.00000	7.21	#N/A	Transcribed locus	
Ssc.19413.1.A1_at	NM_003107	0.00078	6.89	SRY	Transcribed locus	
Ssc.12565.1.A1_at	NM_005504	0.00026	6.42	branched chain aminotransferase 1; cytosolic	Transcribed locus, strongly similar to NP_005495.2 branched chain aminotransferase 1, cytosolic [Homo sapiens]	
Ssc.15335.1.S1_at	#N/A	0.00010	6.14	#N/A	Transcribed locus	
Ssc.22876.1.S1_at	NM_015864	0.00030	6.1	chromosome 6 open reading frame 32	Transcribed locus, strongly similar to XP_518275.1 PREDICTED: similar to chromosome 6 open reading frame 32 [Pan troglodytes]	

Ssc.13665.1.A1_at	NM_006089	0.00018	5.97	sex comb on midleg-like 2	Transcribed locus, strongly similar to XP_528899.1 PREDICTED: sex comb on midleg-like 2 [Pan troglodytes]	
Ssc.19360.1.S1_at	NM_020379	0.00001	5.94	mannosidase; alpha; class 1C; member 1	Transcribed locus, strongly similar to NP_065112.1 mannosidase, alpha, class 1C, member 1; 1,2-alpha-mannosidase IC; Mannosyl-oligosaccharide 1,2-alpha-mannosidase IC; Processing alpha-1,2-mannosidase IC	
Ssc.27738.1.S1_at	NM_015265	0.00011	5.92	SATB family member 2	Transcribed locus	
Ssc.21647.1.A1_at	NM_018131	0.00000	5.9	chromosome 10 open reading frame 3	Transcribed locus	
Ssc.7399.1.A1_at	#N/A	0.00009	5.83	#N/A	Transcribed locus	
Ssc.27407.1.A1_at	NM_003489	0.00006	5.81	nuclear receptor interacting protein 1	Transcribed locus	
Ssc.11757.1.S1_at	NM_001003688	0.00005	5.34	SMAD; mothers against DPP homolog 1	mothers against decapentaplegic homolog 1	MADH1
Ssc.29811.1.A1_at	NM_147150	0.00058	5.32	PALM2-AKAP2 protein	Transcribed locus	
Ssc.23944.1.A1_at	#N/A	0.00012	4.88	#N/A	Transcribed locus	
Ssc.14340.3.S1_at	NM_004862	0.00033	4.81	lipopolysaccharide-induced TNF factor	Transcribed locus, strongly similar to XP_547124.1 PREDICTED: similar to TBX1 protein [Canis familiaris]	
Ssc.14126.1.A1_at	#N/A	0.00025	4.8	#N/A	Transcribed locus	
Ssc.5165.1.S1_at	#N/A	0.00010	4.72	#N/A	Transcribed locus	
Ssc.21328.1.S1_at	NM_018050	0.00006	4.7	MANSC domain containing 1	Transcribed locus, weakly similar to NP_060520.2 MANSC domain containing 1 [Homo sapiens]	
Ssc.13284.1.A1_at	NM_001010927	0.00094	4.67	T-cell lymphoma invasion and metastasis 2	Transcribed locus, strongly similar to XP_541162.1 PREDICTED: hypothetical protein XP_541162 [Canis familiaris]	
Ssc.17206.1.A1_at	NM_133367	0.00073	4.67	progestin and adipoQ receptor family member VIII	Transcribed locus	
Ssc.9063.1.A1_at	#N/A	0.00004	4.57	#N/A	Transcribed locus	

Ssc.25773.1.S1_at	NM_133265	0.00014	4.41	angiomotin	Transcribed locus	
Ssc.26944.1.S1_at	#N/A	0.00007	4.41	#N/A	Transcribed locus	
Ssc.4093.1.A1_at	NM_000619	0.00033	4.26	interferon; gamma	interferon gamma	IFNG
Ssc.10328.1.A1_at	NM_001010000	0.00020	4.21	Rho GTPase activating protein 28	Transcribed locus	
Ssc.5016.1.A1_at	#N/A	0.00001	4.2	#N/A	Transcribed locus	
Ssc.29855.1.A1_at	NM_031942	0.00026	4.15	cell division cycle associated 7	Transcribed locus	
Ssc.11197.1.S1_at	NM_001540	0.00002	4.14	heat shock 27kDa protein 1	Heat shock 27kDa protein 1	Hsp27
Ssc.14400.1.A1_at	NM_147156	0.00023	3.99	transmembrane protein 23	Transcribed locus	
Ssc.10319.1.A1_at	NM_023016	0.00021	3.95	chromosome 2 open reading frame 26	Transcribed locus	
Ssc.20258.1.S1_at	#N/A	0.00084	3.92	#N/A	Transcribed locus	
Ssc.6357.1.S1_at	NM_002245	0.00048	3.86	potassium channel; subfamily K; member 1	Transcribed locus, strongly similar to NP_067720.1 potassium channel, subfamily K, member 1 [Rattus norvegicus]	
Ssc.15740.1.S2_at	NM_003376	0.00053	3.85	vascular endothelial growth factor	vascular endothelial growth factor	VEGFA
Ssc.383.1.S1_at	NM_139212	0.00016	3.85	homeodomain-only protein	odd homeobox 1 protein	OB1
Ssc.14419.1.S1_at	XM_376652	0.00019	3.78	distal-less homeo box 6	Transcribed locus	
Ssc.15740.2.S1_a_at	NM_003376	0.00015	3.68	vascular endothelial growth factor	vascular endothelial growth factor	VEGFA
Ssc.3853.1.S1_at	NM_004816	0.00009	3.64	chromosome 9 open reading frame 61	Transcribed locus, strongly similar to XP_520063.1 PREDICTED: similar to chromosome 9 open reading frame 61; Friedreich ataxia region gene X123 [Pan troglodytes]	
Ssc.13805.1.S1_at	NM_133265	0.00032	3.56	angiomotin	Transcribed locus	
Ssc.4900.2.S1_at	NM_016441	0.00001	3.53	cysteine-rich motor neuron 1	Transcribed locus	
Ssc.847.1.S1_at	NM_006286	0.00003	3.49	transcription factor Dp-2	Transcribed locus, strongly similar to XP_516790.1 PREDICTED: similar to Transcription factor Dp-2 (E2F dimerization partner 2) [Pan troglodytes]	

Ssc.27454.3.S1_a_at	NM_004044	0.00003	3.39	5-aminoimidazole-4-carboxamide ribonucleotide formyltransf	Transcribed locus, strongly similar to XP_545634.1 PREDICTED: similar to 5-aminoimidazole-4-carboxamide ribonucleotide formyltransferase/IMP cyclohydrolase [Canis familiaris]	
Ssc.27454.2.S1_at	NM_004044	0.00007	3.36	5-aminoimidazole-4-carboxamide ribonucleotide formyltransf	Transcribed locus, strongly similar to XP_545634.1 PREDICTED: similar to 5-aminoimidazole-4-carboxamide ribonucleotide formyltransferase/IMP cyclohydrolase [Canis familiaris]	
Ssc.26446.2.S1_a_at	NM_015143	0.00051	3.26	methionyl aminopeptidase 1	Transcribed locus, strongly similar to NP_780433.1 methionyl aminopeptidase 1 [Mus musculus]	
Ssc.5605.1.A1_at	NM_002222	0.00039	3.21	inositol 1;4;5-triphosphate receptor; type 1	Transcribed locus	
Ssc.18546.1.S1_at	NM_016441	0.00008	3.1	cysteine-rich motor neuron 1	Transcribed locus, strongly similar to XP_532931.1 PREDICTED: hypothetical protein XP_532931 [Canis familiaris]	
Ssc.1696.1.A1_at	NM_001004417	0.00013	3.07	formin-like 2	Transcribed locus, moderately similar to NP_035841.1 formin-like 3 protein; WW domain binding protein 3 [Mus musculus]	
Ssc.9321.1.S1_at	NM_025078	0.00051	3.04	PQ loop repeat containing 1	Transcribed locus	
Ssc.28645.1.A1_at	NM_003045	0.00004	3.03	solute carrier family 7	cationic amino acid transporter-1	SLC7A1
Ssc.3088.1.S1_at	#N/A	0.00052	3.03	#N/A	Transcribed locus	
Ssc.30743.1.S1_at	NM_145753	0.00040	3	pleckstrin homology-like domain; family B; member 2	Transcribed locus, strongly similar to NP_700461.1 pleckstrin homology-like domain, family B, member 2 [Mus musculus]	
Ssc.23921.1.S1_at	#N/A	0.00011	2.99	#N/A	Transcribed locus	
Ssc.23922.1.A1_at	NM_018169	0.00085	2.97	hypothetical protein FLJ10652	Transcribed locus, weakly similar to XP_534845.1 PREDICTED: similar to Bicaudal D homolog 1 isoform 1 [Canis familiaris]	
Ssc.5039.2.S1_at	NM_178568	0.00025	2.94	reticulon 4 receptor-like 1	Transcribed locus	

Ssc.4676.1.A1_at	NM_018211	0.00049	2.86	hypothetical protein FLJ10770	Transcribed locus	
Ssc.29842.1.A1_at	#N/A	0.00075	2.85	#N/A	Glycerol-3-phosphate dehydrogenase	MGPD
Ssc.4214.1.A1_at	#N/A	0.00027	2.85	#N/A	Transcribed locus	
Ssc.8027.1.A1_at	NM_001018057	0.00009	2.82	dickkopf homolog 3	Transcribed locus, moderately similar to XP_534060.1 PREDICTED: similar to Dickkopf related protein-3 precursor (Dkk-3) (Dickkopf-3) (hDkk-3) (UNQ258/PRO295) [Canis familiaris]	
Ssc.13553.1.A1_at	#N/A	0.00015	2.81	#N/A	Transcribed locus, moderately similar to NP_112298.1 guanine nucleotide binding protein, alpha q polypeptide [Rattus norvegicus]	
Ssc.2864.1.S1_at	NM_006094	0.00014	2.76	deleted in liver cancer 1	Transcribed locus	
Ssc.29596.1.A1_at	#N/A	0.00000	2.75	#N/A	Transcribed locus, strongly similar to NP_659491.2 hypothetical protein LOC146845 [Homo sapiens]	
Ssc.1850.1.A1_at	NM_022343	0.00092	2.73	chromosome 9 open reading frame 19	Clone Clu_25395.scr.msk.p1.Contig1, mRNA sequence	
Ssc.27520.1.A1_at	XM_086186	0.00001	2.72	hypothetical protein FLJ13815	Transcribed locus, moderately similar to XP_547305.1 PREDICTED: similar to hypothetical protein FLJ13511 [Canis familiaris]	
Ssc.25948.1.S1_at	#N/A	0.00090	2.69	#N/A	Transcribed locus	
Ssc.22297.1.S1_at	#N/A	0.00059	2.68	#N/A	Transcribed locus	
Ssc.6418.1.S1_at	#N/A	0.00055	2.68	#N/A	Transcribed locus, strongly similar to XP_534557.1 PREDICTED: similar to FDFT1 protein [Canis familiaris]	
Ssc.27995.1.A1_at	NM_013282	0.00005	2.67	ubiquitin-like; containing PHD and RING finger domains; 1	Transcribed locus	
Ssc.5039.1.A1_at	NM_178568	0.00001	2.64	reticulon 4 receptor-like 1	Transcribed locus	
Ssc.30400.1.A1_at	#N/A	0.00087	2.63	#N/A	Transcribed locus	
Ssc.8528.1.A1_at	#N/A	0.00001	2.63	#N/A	Transcribed locus	
Ssc.1849.1.A1_at	#N/A	0.00004	2.61	#N/A	Clone Clu_29461.scr.msk.p1.Contig2, mRNA sequence	

Ssc.24421.1.S1_at	NM_018169	0.00043	2.6	hypothetical protein FLJ10652	Transcribed locus, weakly similar to XP_132966.3 RIKEN cDNA 2810474O19 [Mus musculus]	
Ssc.6034.1.S1_at	NM_033102	0.00000	2.58	prostate cancer associated protein 6	Transcribed locus, strongly similar to NP_149093.1 prostein protein [Homo sapiens]	
Ssc.19005.1.A1_at	NM_015009	0.00043	2.57	PDZ domain containing RING finger 3	Transcribed locus, strongly similar to XP_041363.10 PREDICTED: PDZ domain containing RING finger 3 [Homo sapiens]	
Ssc.7554.1.S1_at	NM_013242	0.00001	2.56	gene trap locus 3	Clone Clu_6033.scr.msk.p1.Contig1, mRNA sequence	
Ssc.8774.2.A1_at	NM_006745	0.00021	2.54	sterol-C4-methyl oxidase-like	Sterol-C4-methyl oxidase-like protein	SC4MOL
Ssc.21617.1.A1_at	#N/A	0.00006	2.53	#N/A	Transcribed locus	
Ssc.17512.1.S1_at	#N/A	0.00052	2.52	#N/A	Transcribed locus	
Ssc.14376.1.A1_at	#N/A	0.00060	2.5	#N/A	Transcribed locus	
Ssc.7839.1.A1_at	NM_012307	0.00004	2.49	erythrocyte membrane protein band 4.1-like 3	Transcribed locus	
Ssc.24556.1.S1_at	NM_025181	0.00000	2.49	solute carrier family 35; member F5	Transcribed locus, strongly similar to NP_079457.2 solute carrier family 35, member F5 [Homo sapiens]	
Ssc.1116.1.S1_at	NM_001304	0.00001	2.48	carboxypeptidase D	Transcribed locus	
Ssc.8084.1.S1_at	NM_006094	0.00050	2.48	deleted in liver cancer 1	Transcribed locus, strongly similar to XP_532822.1 PREDICTED: hypothetical protein XP_532822 [Canis familiaris]	
Ssc.7881.1.A1_at	NM_145753	0.00064	2.48	pleckstrin homology-like domain; family B; member 2	Transcribed locus	
Ssc.24556.2.S1_a_at	NM_025181	0.00070	2.47	solute carrier family 35; member F5	Transcribed locus, strongly similar to NP_079457.2 solute carrier family 35, member F5 [Homo sapiens]	
Ssc.19008.1.A1_at	#N/A	0.00037	2.47	#N/A	Transcribed locus	
Ssc.5287.1.S1_at	#N/A	0.00029	2.47	#N/A	Transcribed locus	

Ssc.6670.2.S1_at	NM_012319	0.00081	2.46	solute carrier family 39	Transcribed locus, strongly similar to NP_631882.1 solute carrier family 39 (metal ion transporter), member 6; endoplasmic reticulum membrane protein [Mus musculus]	
Ssc.21060.1.A1_at	NM_014498	0.00015	2.46	golgi phosphoprotein 4	Transcribed locus, strongly similar to XP_516862.1 PREDICTED: similar to golgi phosphoprotein 4; type II Golgi membrane protein; 130 kDa golgi-localized phosphoprotein; cis Golgi-localized calcium-binding protein [Pan troglodytes]	
Ssc.25282.1.S1_at	NM_001018009	0.00058	2.45	SH3-domain binding protein 5	Transcribed locus	
Ssc.25195.1.A1_at	#N/A	0.00022	2.45	#N/A	Transcribed locus	
Ssc.23488.1.S1_at	NM_000637	0.00003	2.44	glutathione reductase	glutathione reductase	GSR
Ssc.7517.1.A1_at	NM_024680	0.00008	2.43	likely ortholog of mouse E2F transcription factor 8	Transcribed locus, moderately similar to XP_508325.1 PREDICTED: similar to FLJ23311 protein [Pan troglodytes]	
Ssc.16621.1.S1_at	NM_004170	0.00042	2.42	solute carrier family 1	high-affinity glutamate transporter EAAC1	SLC1A1
Ssc.4900.1.A1_at	NM_016441	0.00006	2.42	cysteine-rich motor neuron 1	Transcribed locus	
Ssc.24444.1.A1_at	NM_004816	0.00082	2.41	chromosome 9 open reading frame 61	Transcribed locus, strongly similar to XP_355152.2 similar to chromosome 9 open reading frame 61; Friedreich ataxia region gene X123 [Mus musculus]	
Ssc.16259.1.S1_at	NM_002069	0.00034	2.4	guanine nucleotide binding protein	Gi-alpha-1 protein	GNAI1
Ssc.21179.1.S1_at	#N/A	0.00036	2.4	#N/A	Transcribed locus	
Ssc.25289.1.S1_at	NM_001259	0.00085	2.39	cyclin-dependent kinase 6	Transcribed locus	
Ssc.23207.1.S1_at	NM_007212	0.00079	2.38	ring finger protein 2	Clone Clu_5595.scr.msk.p1.Contig1, mRNA sequence	
Ssc.11796.1.S1_at	NM_031934	0.00075	2.37	RAB34; member RAS oncogene family	Clone Clu_91425.scr.msk.p1.Contig1, mRNA sequence	
Ssc.1205.1.S1_at	#N/A	0.00002	2.37	#N/A	Transcribed locus	
Ssc.16693.1.S1_at	NM_012106	0.00077	2.36	ADP-ribosylation factor-like 2	Clone Clu_6027.scr.msk.p1.Contig1,	

				binding protein	mRNA sequence	
Ssc.1084.1.S1_at	NM_016472	0.00009	2.36	chromosome 14 open reading frame 129	Transcribed locus	
Ssc.24344.1.S1_at	NM_001379	0.00006	2.35	DNA		
Ssc.26386.2.S1_a_at	NM_016101	0.00049	2.35	comparative gene identification transcript 37	PUA protein	LOC595107
Ssc.11797.1.A1_at	NM_145804	0.00012	2.34	ankyrin repeat and BTB	Transcribed locus	
Ssc.7771.1.A1_at	XM_034274	0.00021	2.34	v-myb myeloblastosis viral oncogene homolog	Transcribed locus	
Ssc.12845.1.S1_at	NM_001259	0.00056	2.33	cyclin-dependent kinase 6	Transcribed locus	
Ssc.7066.1.S1_at	NM_020774	0.00023	2.33	mindbomb homolog 1	Transcribed locus	
Ssc.25963.1.A1_at	#N/A	0.00045	2.33	#N/A	Transcribed locus	
Ssc.25198.1.A1_at	NM_000274	0.00029	2.32	ornithine aminotransferase	Transcribed locus, strongly similar to XP_508094.1 PREDICTED: ornithine aminotransferase [Pan troglodytes]	
Ssc.24679.1.S1_at	NM_020774	0.00027	2.32	mindbomb homolog 1	Transcribed locus	
Ssc.2099.1.S1_at	NM_138555	0.00033	2.32	kinesin family member 23	Transcribed locus, strongly similar to XP_535528.1 PREDICTED: similar to kinesin family member 23 isoform 1 [Canis familiaris]	
Ssc.27249.1.S1_at	NM_005221	0.00011	2.31	distal-less homeo box 5	Transcribed locus, strongly similar to XP_539430.1 PREDICTED: similar to Homeobox protein DLX-5 [Canis familiaris]	
Ssc.19326.1.A1_at	NM_016343	0.00042	2.29	centromere protein F; 350400ka	Transcribed locus, moderately similar to NP_057427.2 centromere protein F (350/400kD); centromere protein F (350/400kD, mitosin); mitosin; CENP-F kinetochore protein; AH antigen; cell-cycle-dependent 350K nuclear protein [Homo sapiens]	

Ssc.20740.1.S1_at	#N/A	0.00090	2.28	#N/A	Transcribed locus, weakly similar to XP_548196.1 PREDICTED: similar to Neurabin-II (Neural tissue-specific F-actin binding protein II) (Protein phosphatase 1 regulatory subunit 9B) (Spinophilin) (p130) (PP1bp134) [Canis familiaris]	
Ssc.2056.1.S1_at	NM_022343	0.00001	2.27	chromosome 9 open reading frame 19	Clone Clu_25395.scr.msk.p1.Contig1, mRNA sequence	
Ssc.25441.2.S1_at	NM_018169	0.00052	2.25	hypothetical protein FLJ10652	Transcribed locus, moderately similar to NP_060639.1 hypothetical protein FLJ10652 [Homo sapiens]	
Ssc.10906.1.A1_at	#N/A	0.00011	2.23	#N/A	Transcribed locus	
Ssc.21326.1.S1_at	#N/A	0.00017	2.23	#N/A	Transcribed locus	
Ssc.27454.1.S1_at	NM_004044	0.00061	2.22	5-aminoimidazole-4-carboxamide ribonucleotide formyltransf	Transcribed locus, strongly similar to XP_545634.1 PREDICTED: similar to 5-aminoimidazole-4-carboxamide ribonucleotide formyltransferase/IMP cyclohydrolase [Canis familiaris]	
Ssc.7554.2.S1_at	NM_013242	0.00004	2.22	gene trap locus 3	Clone Clu_6033.scr.msk.p1.Contig1, mRNA sequence	
Ssc.5082.1.A1_at	#N/A	0.00093	2.22	#N/A	Transcribed locus, weakly similar to XP_537924.1 PREDICTED: hypothetical protein XP_537924 [Canis familiaris]	
Ssc.27311.1.S1_at	#N/A	0.00032	2.21	#N/A	Transcribed locus	
Ssc.30686.1.S1_at	#N/A	0.00020	2.21	#N/A	Transcribed locus	
Ssc.18038.1.A1_at	NM_005204	0.00012	2.19	mitogen-activated protein kinase kinase kinase 8	Transcribed locus, strongly similar to NP_005195.2 mitogen-activated protein kinase kinase kinase 8; Cancer Osaka thyroid oncogene; cot (cancer Osaka thyroid) oncogene; Ewing sarcoma transformant; proto-oncogene serine/threoine protein kinase; tumor progression locus-2 [Homo sapiens]	
Ssc.15592.1.S1_at	NM_020190	0.00071	2.19	olfactomedin-like 3	Clone Clu_2389.scr.msk.p1.Contig3,	

					mRNA sequence	
Ssc.19350.1.S1_at	NM_016545	0.00032	2.18	immediate early response 5	Transcribed locus, strongly similar to NP_057629.1 immediate early response 5 [Homo sapiens]	
Ssc.19150.1.S1_at	NM_197966	0.00095	2.18	BH3 interacting domain death agonist	BH3 interacting domain death agonist	BID
Ssc.27533.1.A1_at	NM_022473	0.00067	2.16	zinc finger protein 106 homolog	Transcribed locus, strongly similar to NP_071918.1 zinc finger protein 106 homolog; zinc finger protein 106 homolog (mouse) [Homo sapiens]	
Ssc.25405.1.S1_at	NM_145119	0.00007	2.16	praja 1	Transcribed locus	
Ssc.15912.1.A1_at	NM_000165	0.00043	2.15	gap junction protein; alpha 1; 43kDa	connexin 43	CX43
Ssc.26446.1.S1_at	NM_015143	0.00048	2.14	methionyl aminopeptidase 1	Transcribed locus, strongly similar to NP_780433.1 methionyl aminopeptidase 1 [Mus musculus]	
Ssc.5073.1.A1_at	NM_004456	0.00004	2.12	enhancer of zeste homolog 2	Transcribed locus, strongly similar to NP_031996.1 enhancer of zeste homolog 1 [Mus musculus]	
Ssc.19290.2.A1_at	#N/A	0.00017	2.1	#N/A	Transcribed locus	
Ssc.11694.1.S1_at	NM_002166	0.00077	2.07	inhibitor of DNA binding 2; dominant negative helix-loop-h	Clone rcad07b_d12.y1.abd, mRNA sequence	
Ssc.19011.1.S1_at	NM_003983	0.00009	2.07	solute carrier family 7	Transcribed locus	
Ssc.6238.3.S1_at	NM_016282	0.00017	2.07	adenylate kinase 3	Clone Clu_26689.scr.msk.p1.Contig1, mRNA sequence	
Ssc.27842.1.S1_at	NM_017746	0.00003	2.07	testis expressed sequence 10	Transcribed locus, strongly similar to XP_532012.1 PREDICTED: similar to nbla10363 [Canis familiaris]	
Ssc.31097.1.A1_at	NM_020774	0.00000	2.07	mindbomb homolog 1	Transcribed locus	
Ssc.8582.1.S1_at	NM_031307	0.00000	2.06	pseudouridylate synthase 3	Transcribed locus, moderately similar to XP_536533.1 PREDICTED: similar to pseudouridylate synthase 3 [Canis familiaris]	
Ssc.7570.2.S1_at	NM_004170	0.00006	2.05	solute carrier family 1	Transcribed locus	
Ssc.21965.1.S1_at	NM_138285	0.00001	2.05	nucleoporin 35kDa	Clone Clu_5208.scr.msk.p1.Contig1,	

					mRNA sequence	
SscAffx.8.1.S1_s_at	NM_002467	0.00064	2.03	v-myc myelocytomatosis viral oncogene homolog	c-myc proto-oncogene	MYC
Ssc.13743.1.S1_at	NM_016472	0.00068	2.03	chromosome 14 open reading frame 129	Transcribed locus	
Ssc.20404.1.S1_at	NM_001618	0.00027	2.02	poly	Transcribed locus, strongly similar to XP_547506.1 PREDICTED: similar to Poly [ADP-ribose] polymerase-1 (PARP-1) (ADPRT) (NAD(+) ADP-ribosyltransferase-1) (Poly[ADP-ribose] synthetase-1) [Canis familiaris]	
Ssc.26271.2.S1_at	NM_006824	0.00022	2.02	EBNA1 binding protein 2	Transcribed locus, strongly similar to NP_006815.1 EBNA1 binding protein 2; nucleolar protein p40; homolog of yeast EBNA1-binding protein; nuclear FGF3 binding protein; EBNA1-binding protein 2 [Homo sapiens]	
Ssc.18850.1.S1_at	NM_016548	0.00013	2.02	golgi phosphoprotein 2	Transcribed locus, strongly similar to XP_533506.1 PREDICTED: similar to golgi phosphoprotein 2 [Canis familiaris]	
Ssc.19249.2.S1_a_at	NM_017832	0.00047	2.01	hypothetical protein FLJ20457	Transcribed locus, moderately similar to XP_532026.1 PREDICTED: similar to hypothetical protein FLJ20457 [Canis familiaris]	
Ssc.26771.1.S1_at	#N/A	0.00006	2.01	#N/A	Transcribed locus	
Ssc.8475.1.A1_at	#N/A	0.00004	2.01	#N/A	Transcribed locus	
Ssc.21987.2.S1_at	NM_001550	0.00098	2	interferon-related developmental regulator 1	interferon-related developmental regulator 1	IFRD1
Ssc.19318.1.S1_at	#N/A	0.00038	2	#N/A	Transcribed locus	
Ssc.12430.3.S1_at	NM_002744	0.00079	-2	protein kinase C; zeta	Transcribed locus, strongly similar to NP_002735.2 protein kinase C, zeta [Homo sapiens]	

Ssc.28182.1.A1_at	NM_006301	0.00075	-2	mitogen-activated protein kinase kinase kinase 12	Transcribed locus, weakly similar to NP_006292.2 mitogen-activated protein kinase kinase kinase 12; leucine zipper protein kinase; zipper protein kinase; protein kinase MUK; dual leucine zipper kinase DLK [Homo sapiens]	
Ssc.1624.1.S1_at	NM_006369	0.00007	-2	leucine rich repeat containing 41	Transcribed locus, strongly similar to NP_006360.3 MUF1 protein; likely ortholog of mouse MUF1; elongin BC-interacting leucine-rich repeat protein [Homo sapiens]	
Ssc.20226.1.S1_at	NM_015528	0.00003	-2	ring finger protein 167	Transcribed locus, strongly similar to NP_056343.1 ring finger protein 167 [Homo sapiens]	
Ssc.12114.1.S1_a_at	NM_005186	0.00080	-2.01	calpain 1;	micromolar calcium-activated neutral protease 1 isoform B	CAPN1
Ssc.12402.1.A1_at	#N/A	0.00003	-2.01	#N/A	Transcribed locus	
Ssc.21963.1.S1_at	NM_004295	0.00011	-2.02	TNF receptor-associated factor 4	Transcribed locus, strongly similar to NP_004286.2 TNF receptor-associated factor 4 isoform 1; tumor necrosis receptor-associated factor 4A; malignant 62; cysteine-rich domain associated with ring and TRAF domain [Homo sapiens]	
Ssc.1323.1.A1_at	NM_005578	0.00089	-2.02	LIM domain containing preferred translocation partner in l	Transcribed locus	
Ssc.8501.2.A1_at	NM_006407	0.00006	-2.02	ADP-ribosylation-like factor 6 interacting protein 5	PRA1 family protein-like protein	
Ssc.29845.1.A1_at	NM_022087	0.00048	-2.02	UDP-N-acetyl-alpha-D-galactosamine:polypeptide N-acetylgal	Transcribed locus, strongly similar to XP_539924.1 PREDICTED: similar to N-acetylgalactosaminyltransferase; similar to Q10473 (PID:g1709559) [Canis familiaris]	
Ssc.8213.2.A1_at	NM_024613	0.00097	-2.02	pleckstrin homology domain containing; family F	Transcribed locus	

Ssc.25450.1.S1_at	#N/A	0.00099	-2.02	#N/A	Transcribed locus	
Ssc.25748.1.S1_at	NM_004504	0.00001	-2.03	HIV-1 Rev binding protein	Transcribed locus	
Ssc.27214.2.S1_at	NM_004924	0.00018	-2.03	actinin; alpha 4	Transcribed locus, strongly similar to NP_004915.2 actinin, alpha 4 [Homo sapiens]	
Ssc.21456.1.S1_at	NM_014584	0.00016	-2.03	ERO1-like	Transcribed locus, strongly similar to NP_055399.1 ERO1-like; ERO1 (S. cerevisiae)-like [Homo sapiens]	
Ssc.11338.1.S1_a_at	NM_016417	0.00004	-2.03	chromosome 14 open reading frame 87	Clone Clu_43784.scr.msk.p1.Contig1, mRNA sequence	
Ssc.10155.1.S1_at	NM_017634	0.00012	-2.03	potassium channel tetramerisation domain containing 9	Transcribed locus, strongly similar to NP_060104.2 potassium channel tetramerisation domain containing 9 [Homo sapiens]	
Ssc.15594.2.S1_at	#N/A	0.00007	-2.03	#N/A	Clone rcut39_i19.y1.abd, mRNA sequence	
Ssc.13508.1.A1_at	NM_016048	0.00034	-2.04	isochorismatase domain containing 1	Clone Clu_9851.scr.msk.p1.Contig2, mRNA sequence	
Ssc.18476.2.S1_a_at	NM_033389	0.00087	-2.04	slingshot homolog 2	Transcribed locus	
Ssc.7608.2.S1_at	NM_018184	0.00013	-2.05	ADP-ribosylation factor-like 10C	Clone Clu_1719.scr.msk.p1.Contig3, mRNA sequence	
Ssc.3574.1.A1_at	NM_145687	0.00003	-2.05	mitogen-activated protein kinase kinase kinase kinase 4	Transcribed locus	
Ssc.27168.1.S1_at	#N/A	0.00012	-2.05	#N/A	Transcribed locus	
Ssc.17250.1.S1_at	NM_000320	0.00075	-2.07	quinoid dihydropteridine reductase	quinoid dihydropteridine reductase	QDPR
Ssc.5353.2.S1_at	NM_016598	0.00003	-2.07	zinc finger; DHHC-type containing 3	Transcribed locus, strongly similar to XP_533859.1 PREDICTED: similar to ZDHHC3 protein [Canis familiaris]	
Ssc.23539.1.S1_at	NM_152911	0.00021	-2.07	polyamine oxidase	Transcribed locus, weakly similar to XP_542910.1 PREDICTED: similar to polyamine oxidase isoform 1 [Canis familiaris]	
Ssc.8444.1.S1_at	XM_371706	0.00010	-2.07	hypothetical protein KIAA1109	Transcribed locus, strongly similar to XP_371706.3 [Homo sapiens]	

Ssc.11910.1.S1_at	NM_001981	0.00013	-2.08	epidermal growth factor receptor pathway substrate 15	Transcribed locus, strongly similar to NP_001972.1 epidermal growth factor receptor pathway substrate 15 [Homo sapiens]	
Ssc.1657.1.S1_at	NM_005688	0.00033	-2.08	ATP-binding cassette; sub-family C	Transcribed locus	
Ssc.2466.1.S1_at	NM_014045	0.00044	-2.08	low density lipoprotein receptor-related protein 10	Transcribed locus, strongly similar to XP_537364.1 PREDICTED: similar to low density lipoprotein receptor-related protein 10 [Canis familiaris]	
Ssc.26275.1.S1_at	NM_015600	0.00001	-2.08	chromosome 20 open reading frame 22	Transcribed locus, strongly similar to NP_056415.1 chromosome 20 open reading frame 22 [Homo sapiens]	
Ssc.5793.2.S1_at	NM_014698	0.00005	-2.09	KIAA0792	Transcribed locus, strongly similar to XP_375848.2 PREDICTED: KIAA0792 gene product [Homo sapiens]	
Ssc.9284.1.S1_at	NM_020728	0.00047	-2.09	family with sequence similarity 62	Transcribed locus, strongly similar to XP_519490.1 PREDICTED: similar to KIAA1228 protein [Pan troglodytes]	
Ssc.10990.1.A1_at	#N/A	0.00027	-2.09	#N/A	Transcribed locus	
Ssc.15594.3.S1_at	#N/A	0.00001	-2.09	#N/A	Clone rcut39_i19.y1.abd, mRNA sequence	
Ssc.4957.1.S1_at	#N/A	0.00007	-2.09	#N/A	Transcribed locus	
Ssc.18096.1.A1_at	NM_198353	0.00031	-2.1	potassium channel tetramerisation domain containing 8	Transcribed locus	
Ssc.6618.1.A1_at	XM_290546	0.00014	-2.1	KIAA0830 protein	Transcribed locus	
Ssc.12099.1.A1_at	#N/A	0.00002	-2.11	#N/A	Clone Clu_607.scr.msk.p1.Contig1, mRNA sequence	
Ssc.5580.1.S1_at	#N/A	0.00069	-2.11	#N/A	Transcribed locus	
Ssc.8355.1.A1_at	NM_018330	0.00013	-2.12	KIAA1598	Transcribed locus	
Ssc.6193.1.A1_at	NM_130781	0.00013	-2.12	RAB24; member RAS oncogene family	Clone Clu_22104.scr.msk.p1.Contig2, mRNA sequence	
Ssc.19024.1.A1_at	NM_139182	0.00024	-2.12	centaurin; delta 1	Transcribed locus	
Ssc.17293.1.A1_at	NM_020940	0.00050	-2.13	KIAA1600	Transcribed locus	

Ssc.12826.2.A1_a_at	NM_138463	0.00098	-2.13	hypothetical protein BC014072	Transcribed locus, moderately similar to XP_511362.1 PREDICTED: similar to hypothetical protein BC014072 [Pan troglodytes]	
Ssc.5257.1.S1_at	NM_006577	0.00087	-2.16	UDP-GlcNAc:betaGal beta-1;3-N-acetylglucosaminyltransferas	Transcribed locus	
Ssc.16537.1.S1_at	NM_007229	0.00018	-2.17	protein kinase C and casein kinase substrate in neurons 2	Transcribed locus, strongly similar to XP_525616.1 PREDICTED: protein kinase C and casein kinase substrate in neurons 2 [Pan troglodytes]	
Ssc.2760.1.A1_at	NM_018841	0.00085	-2.17	guanine nucleotide binding protein	Transcribed locus	
Ssc.9420.1.A1_at	NM_201281	0.00000	-2.17	myotubularin related protein 2	Transcribed locus, strongly similar to NP_057240.3 myotubularin-related protein 2 isoform 1 [Homo sapiens]	
Ssc.22732.1.S1_at	#N/A	0.00079	-2.17	#N/A	Transcribed locus	
Ssc.2413.1.S1_at	NM_000336	0.00006	-2.18	sodium channel; nonvoltage-gated 1; beta	Transcribed locus, strongly similar to NP_000327.1 sodium channel, nonvoltage-gated 1, beta [Homo sapiens]	
Ssc.21999.1.S1_a_at	NM_000694	0.00000	-2.18	aldehyde dehydrogenase 3 family; member B1	Transcribed locus, moderately similar to XP_129134.2 RIKEN cDNA C130048D07 [Mus musculus]	
Ssc.17453.1.S1_at	NM_001684	0.00032	-2.19	ATPase; Ca++ transporting; plasma membrane 4	Transcribed locus	
Ssc.8213.1.A1_at	NM_024613	0.00044	-2.19	pleckstrin homology domain containing; family F	Transcribed locus	
Ssc.6615.1.S1_at	#N/A	0.00056	-2.19	#N/A	Transcribed locus	
Ssc.55.1.S1_at	NM_005228	0.00023	-2.2	epidermal growth factor receptor	epidermal growth factor receptor	EGFR
Ssc.26898.1.A1_at	#N/A	0.00005	-2.2	#N/A	Transcribed locus	
Ssc.27147.1.A1_at	NM_177532	0.00074	-2.21	Ras association	Transcribed locus, moderately similar to NP_958834.1 Ras association (RalGDS/AF-6) domain family 6 isoform b; putative RAS binding protein [Homo sapiens]	
Ssc.5001.2.A1_at	#N/A	0.00078	-2.21	#N/A	Transcribed locus	

Ssc.27521.1.S1_at	NM_020324	0.00047	-2.23	ATP-binding cassette; sub-family D	Transcribed locus, strongly similar to NP_005041.1 ATP-binding cassette, sub-family D, member 4 isoform 1; peroxisomal membrane protein 1-like [Homo sapiens]	
Ssc.28434.1.A1_at	NM_025219	0.00024	-2.23	DnaJ	Transcribed locus, strongly similar to NP_079495.1 DnaJ (Hsp40) homolog, subfamily C, member 5; cysteine string protein [Homo sapiens]	
Ssc.25022.1.A1_at	#N/A	0.00003	-2.23	#N/A	Transcribed locus	
Ssc.8002.1.A1_at	#N/A	0.00084	-2.23	#N/A	Transcribed locus	
Ssc.21905.1.S1_at	#N/A	0.00060	-2.25	#N/A	Transcribed locus	
Ssc.12634.1.S1_at	NM_014320	0.00017	-2.26	heme binding protein 2	Clone Clu_24795.scr.msk.p1.Contig2, mRNA sequence	
Ssc.10917.1.A1_at	NM_181354	0.00065	-2.26	oxidation resistance 1	Transcribed locus	
Ssc.17918.1.A1_at	#N/A	0.00002	-2.26	#N/A	Transcribed locus	
Ssc.18606.2.A1_at	#N/A	0.00034	-2.26	#N/A	Transcribed locus	
Ssc.779.1.S1_at	NM_004433	0.00019	-2.27	E74-like factor 3	Transcribed locus, strongly similar to XP_547356.1 PREDICTED: similar to E74-like factor 3 (ets domain transcription factor, epithelial-specific) [Canis familiaris]	
Ssc.24739.1.A1_at	#N/A	0.00024	-2.27	#N/A	Transcribed locus	
Ssc.14180.1.A1_at	NM_015458	0.00009	-2.28	myotubularin related protein 9	Transcribed locus	
Ssc.6738.1.S1_at	NM_032622	0.00013	-2.28	ligand of numb-protein X	Transcribed locus, strongly similar to XP_532373.1 PREDICTED: similar to ligand of numb-protein X 1 [Canis familiaris]	
Ssc.19359.2.S1_at	#N/A	0.00001	-2.28	#N/A	Transcribed locus	
Ssc.8061.1.A1_at	#N/A	0.00011	-2.28	#N/A	Transcribed locus	
Ssc.27912.1.S1_at	NM_020747	0.00001	-2.29	zinc finger protein 608	Transcribed locus, strongly similar to XP_114432.3 PREDICTED: zinc finger protein 608 [Homo sapiens]	
Ssc.13318.1.A1_at	#N/A	0.00055	-2.29	#N/A	Transcribed locus	
Ssc.28427.1.A1_at	#N/A	0.00020	-2.29	#N/A	Transcribed locus	

Ssc.22078.1.A1_at	NM_003561	0.00034	-2.3	phospholipase A2; group X	Transcribed locus, moderately similar to NP_003552.1 phospholipase A2, group X [Homo sapiens]	
Ssc.19622.1.A1_at	NM_007183	0.00000	-2.3	plakophilin 3	Transcribed locus, moderately similar to XP_420926.1 PREDICTED: similar to plakophilin-3 [Gallus gallus]	
Ssc.23305.1.S1_at	NM_018342	0.00084	-2.3	hypothetical protein FLJ11155	Transcribed locus	
Ssc.3578.1.S1_at	NM_020533	0.00002	-2.3	mucolipin 1	Transcribed locus, strongly similar to NP_065394.1 mucolipin 1; mucolipidin [Homo sapiens]	
Ssc.9792.1.S1_at	NM_020940	0.00005	-2.3	KIAA1600	Voltage-dependent anion channel 2	VDAC2
Ssc.1957.1.A1_at	NM_000259	0.00023	-2.31	myosin VA	Transcribed locus, strongly similar to XP_510412.1 PREDICTED: similar to myosin I heavy chain isoform [Pan troglodytes]	
Ssc.9918.1.A1_at	NM_004504	0.00007	-2.32	HIV-1 Rev binding protein	Transcribed locus, strongly similar to NP_034602.1 HIV-1 Rev binding protein [Mus musculus]	
Ssc.28933.1.S1_at	#N/A	0.00035	-2.32	#N/A	Transcribed locus	
Ssc.5432.1.A1_at	#N/A	0.00032	-2.32	#N/A	Transcribed locus	
Ssc.5458.1.S1_at	NM_015913	0.00039	-2.33	thioredoxin domain containing 12	Transcribed locus, strongly similar to NP_056997.1 endoplasmic reticulum thioredoxin superfamily member, 18 kDa; thioredoxin-like protein p19 [Homo sapiens]	
Ssc.30212.1.A1_at	#N/A	0.00035	-2.33	#N/A	Transcribed locus	
Ssc.3980.1.A1_at	NM_014936	0.00014	-2.34	ectonucleotide pyrophosphatasephosphodiesterase 4	Transcribed locus	
Ssc.14164.1.A1_at	#N/A	0.00002	-2.34	#N/A	Transcribed locus	
Ssc.21915.3.A1_at	#N/A	0.00044	-2.34	#N/A	Transcribed locus	
Ssc.5158.1.S1_at	NM_024819	0.00033	-2.35	hypothetical protein FLJ22955	Transcribed locus	
Ssc.9953.1.A1_at	#N/A	0.00081	-2.36	#N/A	Transcribed locus	

Ssc.15316.1.S1_at	NM_001311	0.00004	-2.37	cysteine-rich protein 1	Transcribed locus, moderately similar to XP_422218.1 PREDICTED: similar to LIM only protein HLP [Gallus gallus]	
Ssc.6528.1.S1_at	NM_006412	0.00041	-2.38	1-acylglycerol-3-phosphate O-acyltransferase 2	Transcribed locus, moderately similar to NP_006403.2 1-acylglycerol-3-phosphate O-acyltransferase 2 (lysophosphatidic acid acyltransferase, beta); lysophosphatidic acid acyltransferase beta; Berardinelli-Seip congenital lipodsytrophy [Homo sapiens]	
Ssc.1808.1.S1_at	#N/A	0.00017	-2.38	#N/A	Transcribed locus	
Ssc.18404.1.A1_at	#N/A	0.00004	-2.38	#N/A	Transcribed locus	
Ssc.9908.1.A1_at	#N/A	0.00025	-2.38	#N/A	Transcribed locus	
Ssc.30785.1.S1_at	NM_007063	0.00004	-2.39	TBC1 domain family; member 8	Transcribed locus, strongly similar to NP_008994.1 TBC1 domain family, member 8 (with GRAM domain); vascular Rab-GAP/TBC-containing; BUB2-like protein 1 [Homo sapiens]	
Ssc.16485.1.S1_at	NM_004252	0.00006	-2.4	solute carrier family 9	Transcribed locus, strongly similar to XP_540418.1 PREDICTED: similar to ERM-binding phosphoprotein [Canis familiaris]	
Ssc.29905.1.A1_at	#N/A	0.00013	-2.4	#N/A	Transcribed locus	
Ssc.4233.1.S1_at	NM_022776	0.00036	-2.42	oxysterol binding protein-like 11	Transcribed locus, strongly similar to oxysterol-binding protein-like protein 11 [Canis familiaris]	
Ssc.18085.1.A1_at	#N/A	0.00002	-2.42	#N/A	Transcribed locus	
Ssc.19359.1.A1_at	#N/A	0.00007	-2.42	#N/A	Transcribed locus	
Ssc.29821.1.A1_at	#N/A	0.00041	-2.42	#N/A	Transcribed locus	
Ssc.1588.1.S1_at	NM_017567	0.00034	-2.43	N-acetylglucosamine kinase	Clone Clu_7114.scr.msk.p1.Contig2, mRNA sequence	
Ssc.5622.1.A1_at	#N/A	0.00056	-2.44	#N/A	Transcribed locus	

Ssc.2672.1.S1_at	NM_012156	0.00008	-2.47	erythrocyte membrane protein band 4.1-like 1	Transcribed locus, strongly similar to NP_067713.1 erythrocyte protein band 4.1-like 1 isoform L [Rattus norvegicus]	
Ssc.12650.1.A1_at	NM_014616	0.00000	-2.47	ATPase; Class VI; type 11B	Transcribed locus	
Ssc.1600.3.S1_at	NM_020734	0.00007	-2.47	KIAA1238 protein	Transcribed locus, strongly similar to XP_132812.2 RIKEN cDNA 4931417E21 [Mus musculus]	
Ssc.24831.1.A1_at	NM_133373	0.00002	-2.47	phospholipase C; delta 3	Transcribed locus, strongly similar to XP_548052.1 PREDICTED: similar to mKIAA1964 protein [Canis familiaris]	
Ssc.25088.1.A1_at	#N/A	0.00026	-2.47	#N/A	Transcribed locus	
Ssc.5314.1.S1_at	NM_006149	0.00007	-2.48	lectin; galactoside-binding; soluble; 4	L-36 lactose binding protein	LGALS4
Ssc.4671.1.A1_at	#N/A	0.00093	-2.48	#N/A	Transcribed locus	
Ssc.6441.1.A1_at	NM_016029	0.00016	-2.49	dehydrogenasereductase	Clone Clu_25564.scr.msk.p1.Contig2, mRNA sequence	
Ssc.21192.3.S1_at	NM_145687	0.00048	-2.49	mitogen-activated protein kinase kinase kinase kinase 4	Transcribed locus, strongly similar to XP_538452.1 PREDICTED: similar to mitogen-activated protein kinase kinase kinase kinase 4 isoform 2 [Canis familiaris]	
Ssc.1600.1.A1_a_at	NM_020734	0.00027	-2.5	KIAA1238 protein	Transcribed locus, strongly similar to XP_132812.2 RIKEN cDNA 4931417E21 [Mus musculus]	
Ssc.8895.1.S1_at	NM_004568	0.00010	-2.51	serine	Transcribed locus, moderately similar to NP_035584.1 serine (or cysteine) proteinase inhibitor, clade B, member 6b; serine protease inhibitor 12 [Mus musculus]	
Ssc.15250.1.S1_at	#N/A	0.00009	-2.51	#N/A	Transcribed locus, moderately similar to XP_533195.1 PREDICTED: similar to CD82 antigen (Inducible membrane protein R2) (C33 antigen) (IA4) [Canis familiaris]	

Ssc.10025.3.S1_at	NM_005195	0.00046	-2.52	CCAATenhancer binding protein	Transcribed locus, strongly similar to XP_519748.1 PREDICTED: hypothetical protein XP_519748 [Pan troglodytes]	
Ssc.16392.2.A1_at	NM_199054	0.00089	-2.53	MAP kinase interacting serinethreonine kinase 2	Transcribed locus	
Ssc.1868.1.S1_at	NM_000901	0.00017	-2.56	nuclear receptor subfamily 3; group C; member 2	mineralocorticoid receptor	NR3C2
Ssc.5179.1.A1_at	NM_006549	0.00000	-2.56	calciumcalmodulin-dependent protein kinase kinase 2; beta	Transcribed locus	
Ssc.10327.1.A1_at	#N/A	0.00014	-2.56	#N/A	Transcribed locus	
Ssc.6783.1.S1_at	NM_012338	0.00033	-2.59	tetraspanin 12	Transcribed locus	
Ssc.23310.1.S1_at	NM_000434	0.00033	-2.6	sialidase 1	Transcribed locus, strongly similar to XP_538838.1 PREDICTED: similar to Sialidase 1 precursor (Lysosomal sialidase) (N-acetyl-alpha-neuraminidase 1) (Acetylneuraminyl hydrolase) (G9 sialidase) [Canis familiaris]	
Ssc.12938.1.A1_at	NM_004841	0.00002	-2.6	RAS protein activator like 2	Transcribed locus	
Ssc.1746.1.A1_at	NM_138782	0.00017	-2.6	FCH domain only 2	Transcribed locus, strongly similar to NP_766179.1 hypothetical protein 5832424M12 [Mus musculus]	
Ssc.8699.1.A1_at	#N/A	0.00031	-2.6	#N/A	Transcribed locus	
Ssc.14533.1.S1_at	NM_002910	0.00055	-2.61	renin binding protein	N-acyl-D-glucosamine 2-epimerase	RENBP
Ssc.15578.1.A1_at	NM_018205	0.00001	-2.61	leucine rich repeat containing 20	Transcribed locus	
Ssc.27746.1.S1_at	NM_198925	0.00054	-2.61	sema domain; immunoglobulin domain	Transcribed locus, strongly similar to XP_545859.1 PREDICTED: similar to Semaphorin 4B precursor [Canis familiaris]	
Ssc.11670.3.A1_at	XM_496093	0.00021	-2.61	similar to PERP; TP53 apoptosis effector; p53-i	Clone Clu_21503.scr.msk.p1.Contig1, mRNA sequence	
Ssc.24540.1.S1_at	#N/A	0.00024	-2.62	#N/A	Transcribed locus	

Ssc.18246.1.S1_at	NM_004529	0.00015	-2.63	myeloidlymphoid or mixed-lineage leukemia	Transcribed locus, strongly similar to XP_538677.1 PREDICTED: similar to Myeloid/lymphoid or mixed lineage-leukemia translocation to 3 homolog [Canis familiaris]	
Ssc.1600.1.A1_at	NM_020734	0.00043	-2.63	KIAA1238 protein	Transcribed locus, strongly similar to XP_132812.2 RIKEN cDNA 4931417E21 [Mus musculus]	
Ssc.18893.1.A1_at	#N/A	0.00085	-2.64	#N/A	Transcribed locus, moderately similar to NP_057479.1 butyrate-induced transcript 1 [Homo sapiens]	
Ssc.422.1.S1_at	NM_000876	0.00008	-2.65	insulin-like growth factor 2 receptor	Mannose-6-phosphate/insulin-like growth factor II receptor (m6p/igf2r) mRNA, 3'UTR	
Ssc.24390.1.A1_at	XM_370777	0.00015	-2.66	Similar to Lysophospholipase	Transcribed locus, moderately similar to XP_370777.3 PREDICTED: similar to lysophospholipase [Homo sapiens]	
Ssc.21187.1.S1_at	#N/A	0.00013	-2.66	#N/A	Transcribed locus	
Ssc.29965.1.A1_at	#N/A	0.00019	-2.67	#N/A	Transcribed locus	
Ssc.13637.1.A1_at	NM_002737	0.00001	-2.7	protein kinase C; alpha	Transcribed locus	
Ssc.1285.1.S1_at	#N/A	0.00004	-2.7	#N/A	Transcribed locus	
Ssc.25172.1.S1_at	NM_000820	0.00016	-2.71	growth arrest-specific 6	Transcribed locus, strongly similar to XP_542676.1 PREDICTED: similar to Growth-arrest-specific protein 6 precursor (GAS-6) [Canis familiaris]	
Ssc.1817.1.S1_at	NM_020728	0.00069	-2.71	family with sequence similarity 62	Transcribed locus	
Ssc.4529.1.S1_at	NM_181776	0.00016	-2.71	solute carrier family 36	Transcribed locus, moderately similar to XP_518043.1 PREDICTED: similar to solute carrier family 36 (proton/amino acid symporter), member 2; proton/amino acid transporter 2; tramdorin [Pan troglodytes]	
Ssc.18860.1.S1_at	#N/A	0.00034	-2.71	#N/A	Transcribed locus	
Ssc.6833.1.S1_at	NM_001731	0.00001	-2.72	B-cell translocation gene 1	Transcribed locus	

Ssc.4739.1.S1_at	NM_024959	0.00007	-2.73	solute carrier family 24	Transcribed locus, strongly similar to NP_079235.2 solute carrier family 24 member 6; sodium/potassium/calcium exchanger [Homo sapiens]	
Ssc.29953.1.A1_at	#N/A	0.00004	-2.74	#N/A	Transcribed locus	
Ssc.27835.1.S1_at	NM_020132	0.00043	-2.75	1-acylglycerol-3-phosphate O-acyltransferase 3	Transcribed locus, strongly similar to XP_514932.1 PREDICTED: 1-acylglycerol-3-phosphate O-acyltransferase 3 [Pan troglodytes]	
Ssc.12430.1.S1_at	NM_002744	0.00013	-2.76	protein kinase C; zeta	Transcribed locus, strongly similar to NP_002735.2 protein kinase C, zeta [Homo sapiens]	
Ssc.8309.1.A1_at	NM_016245	0.00002	-2.78	dehydrogenasereductase	Transcribed locus	
Ssc.3255.1.S1_at	NM_024071	0.00008	-2.79	zinc finger; FYVE domain containing 21	Transcribed locus, moderately similar to NP_076976.1 zinc finger, FYVE domain containing 21; hypothetical protein MGC2550 [Homo sapiens]	
Ssc.26084.1.S1_at	NM_001001323	0.00096	-2.82	ATPase; Ca++ transporting; plasma membrane 1	Plasma membrane calcium ATPase isoform 1, (ATP2B1 gene)	
Ssc.13485.1.A1_at	#N/A	0.00041	-2.83	#N/A	Transcribed locus	
Ssc.26169.1.S1_at	#N/A	0.00022	-2.83	#N/A	Transcribed locus	
Ssc.17458.1.S1_at	#N/A	0.00004	-2.84	#N/A	Transcribed locus, strongly similar to XP_535481.1 PREDICTED: similar to rabconnectin-3 [Canis familiaris]	
Ssc.3770.1.A1_at	#N/A	0.00022	-2.84	#N/A	Transcribed locus	
Ssc.1641.1.S1_at	NM_004356	0.00010	-2.85	CD81 antigen	Transcribed locus, strongly similar to NP_004347.1 CD81 antigen; target of antiproliferative antibody 1; 26 kDa cell surface protein TAPA-1 [Homo sapiens]	
Ssc.6276.1.S1_at	NM_020676	0.00072	-2.85	abhydrolase domain containing 6	Transcribed locus, strongly similar to NP_065727.3 abhydrolase domain containing 6; lipase protein [Homo sapiens]	

Ssc.23758.2.A1_at	NM_181785	0.00003	-2.85	hypothetical protein LOC283537	Transcribed locus, moderately similar to XP_534517.1 PREDICTED: hypothetical protein XP_534517 [Canis familiaris]	
Ssc.17760.1.S1_at	NM_002886	0.00003	-2.86	RAP2B; member of RAS oncogene family	Transcribed locus, strongly similar to NP_082988.1 RAP2B, member of RAS oncogene family [Mus musculus]	
Ssc.94.1.A1_at	NM_004999	0.00003	-2.88	myosin VI	unconventional myosin	MYO6
Ssc.4641.1.A1_at	NM_017771	0.00003	-2.88	PX domain containing serinethreonine kinase	Transcribed locus, strongly similar to NP_060241.2 PX domain containing serine/threonine kinase; PX serine/threonine kinase [Homo sapiens]	
Ssc.5085.1.A1_at	NM_006290	0.00013	-2.89	tumor necrosis factor; alpha-induced protein 3	Transcribed locus	
Ssc.25222.1.S1_at	NM_005817	0.00023	-2.9	mannose-6-phosphate receptor binding protein 1	TIP47	
Ssc.6699.1.A1_at	NM_000252	0.00001	-2.91	myotubularin 1	Transcribed locus	
Ssc.16392.2.A1_a_at	NM_199054	0.00002	-2.91	MAP kinase interacting serinethreonine kinase 2	Transcribed locus	
Ssc.23139.1.S1_at	NM_002886	0.00003	-2.94	RAP2B; member of RAS oncogene family	Transcribed locus, strongly similar to NP_082988.1 RAP2B, member of RAS oncogene family [Mus musculus]	
Ssc.24375.1.S1_at	NM_024109	0.00024	-2.94	hypothetical protein MGC2654	Transcribed locus	
Ssc.17674.1.A1_at	#N/A	0.00042	-2.95	#N/A	Transcribed locus	
Ssc.26354.1.S1_at	#N/A	0.00001	-2.95	#N/A	Transcribed locus	
Ssc.1623.1.S1_at	NM_004415	0.00028	-2.97	desmoplakin	Transcribed locus, weakly similar to NP_004406.1 desmoplakin; desmoplakin (DPI, DPII) [Homo sapiens]	
Ssc.7985.1.S1_at	NM_001682	0.00094	-3	ATPase; Ca++ transporting; plasma membrane 1	plasma membrane Ca2+ pump (PMCA1b)	ATP2B1
Ssc.5879.4.S1_a_at	NM_172171	0.00096	-3	calciumcalmodulin-dependent protein kinase	calcium/calmodulin-dependent protein kinase II gamma	CAMK2G
Ssc.14047.2.A1_at	#N/A	0.00063	-3.03	#N/A	Transcribed locus	

Ssc.24460.1.A1_at	#N/A	0.00020	-3.03	#N/A	Transcribed locus	
Ssc.11362.2.S1_at	NM_004879	0.00072	-3.05	etoposide induced 2.4 mRNA	Transcribed locus, strongly similar to XP_522242.1 PREDICTED: similar to EI24 protein [Pan troglodytes]	
Ssc.7292.1.S1_at	#N/A	0.00054	-3.05	#N/A	Transcribed locus	
Ssc.8373.1.A1_at	#N/A	0.00025	-3.08	#N/A	Transcribed locus	
Ssc.26824.1.A1_at	NM_004686	0.00016	-3.09	myotubularin related protein 7	Transcribed locus, strongly similar to NP_062306.1 myotubularin related protein 7 [Mus musculus]	
Ssc.2795.2.S1_at	NM_004059	0.00030	-3.13	cysteine conjugate-beta lyase; cytoplasmic	Transcribed locus, moderately similar to NP_765992.2 cysteine conjugate-beta lyase; cytoplasmic (glutamine transaminase K, kyneurenine aminotransferase) [Mus musculus]	
Ssc.16937.1.A1_at	NM_021202	0.00003	-3.14	tumor protein p53 inducible nuclear protein 2	Transcribed locus	
Ssc.19455.2.S1_at	NM_001003794	0.00015	-3.15	monoglyceride lipase	Transcribed locus, strongly similar to NP_009214.1 monoglyceride lipase isoform 1; lysophospholipase-like [Homo sapiens]	
Ssc.24039.1.S1_at	#N/A	0.00021	-3.15	#N/A	Transcribed locus	
Ssc.2142.1.S1_at	NM_080881	0.00001	-3.2	drebrin 1	Transcribed locus, strongly similar to XP_546204.1 PREDICTED: similar to drebrin E [Canis familiaris]	
Ssc.16334.1.S2_at	NM_138578	0.00029	-3.2	BCL2-like 1	anti-apoptotic Bcl-xL	BCL2L1
Ssc.2925.1.S1_at	NM_017797	0.00003	-3.21	BTB	Transcribed locus, strongly similar to NP_060267.2 BTB (POZ) domain containing 2 [Homo sapiens]	
Ssc.30264.1.A1_at	#N/A	0.00010	-3.22	#N/A	Transcribed locus	
Ssc.26450.1.A1_at	NM_173570	0.00050	-3.24	zinc finger; DHHC-type containing 23	Transcribed locus	
Ssc.6163.1.A1_at	NM_005239	0.00044	-3.25	v-ets erythroblastosis virus E26 oncogene homolog 2	Transcribed locus	

Ssc.10534.3.A1_a_at	NM_006506	0.00003	-3.27	RAS p21 protein activator 2	Transcribed locus, strongly similar to NP_006497.2 RAS p21 protein activator 2; GTPase-activating protein of RAS [Homo sapiens]	
Ssc.2142.2.S1_at	NM_080881	0.00005	-3.27	drebrin 1	Transcribed locus, strongly similar to XP_546204.1 PREDICTED: similar to drebrin E [Canis familiaris]	
Ssc.10002.1.A1_at	#N/A	0.00055	-3.27	#N/A	Transcribed locus	
Ssc.15252.1.S1_at	NM_201533	0.00014	-3.28	diacylglycerol kinase; zeta 104kDa	Transcribed locus, strongly similar to NP_963290.1 diacylglycerol kinase, zeta 104kDa isoform 1; diacylglycerol kinase, zeta (104kD) [Homo sapiens]	
Ssc.2795.1.S1_at	NM_004059	0.00075	-3.35	cysteine conjugate-beta lyase; cytoplasmic	Transcribed locus, moderately similar to NP_765992.2 cysteine conjugate-beta lyase; cytoplasmic (glutamine transaminase K, kyneurenine aminotransferase) [Mus musculus]	
Ssc.1028.1.S1_at	NM_032312	0.00043	-3.36	hypothetical protein MGC11061	Clone Clu_12742.scr.msk.p1.Contig1, mRNA sequence	
Ssc.18773.1.A1_at	#N/A	0.00011	-3.36	#N/A	Clone rski0137_l13.y1.abd, mRNA sequence	
Ssc.943.1.S1_at	NM_198538	0.00017	-3.38	suprabasin	Transcribed locus, moderately similar to NP_940940.1 HLAR698 [Homo sapiens]	
Ssc.19164.1.A1_at	#N/A	0.00002	-3.38	#N/A	Transcribed locus	
Ssc.21290.1.S1_at	NM_014779	0.00041	-3.4	TSC22 domain family; member 2	Transcribed locus	
Ssc.2070.1.S1_at	NM_012156	0.00000	-3.41	erythrocyte membrane protein band 4.1-like 1	Transcribed locus	
Ssc.24938.1.S1_at	NM_001004431	0.00006	-3.42	meteorin; glial cell differentiation regulator-like	Transcribed locus, moderately similar to XP_209073.2 PREDICTED: hypothetical protein XP_209073 [Homo sapiens]	
Ssc.29966.1.A1_s_at	#N/A	0.00000	-3.42	#N/A	Transcribed locus, strongly similar to XP_539924.1 PREDICTED: similar to N-acetylgalactosaminyltransferase; similar to Q10473 (PID:g1709559)	

					[Canis familiaris]	
Ssc.16120.1.S1_at	NM_005536	0.00018	-3.43	inositol	myo-inositol monophosphatase	IMPA1
Ssc.22221.1.S1_a_at	NM_000167	0.00040	-3.46	glycerol kinase	Transcribed locus, moderately similar to XP_225769.2 PREDICTED: glucokinase activity, related sequence 1 [Rattus norvegicus]	
Ssc.9286.1.A1_at	#N/A	0.00047	-3.46	#N/A	Transcribed locus	
Ssc.3442.1.S1_at	#N/A	0.00007	-3.49	#N/A	Transcribed locus	
Ssc.21227.1.S1_at	NM_080881	0.00000	-3.55	drebrin 1	Transcribed locus, strongly similar to XP_546204.1 PREDICTED: similar to drebrin E [Canis familiaris]	
Ssc.25396.1.A1_at	#N/A	0.00006	-3.59	#N/A	Transcribed locus	
Ssc.7469.1.S1_at	NM_022087	0.00003	-3.62	UDP-N-acetyl-alpha-D-galactosamine:polypeptide N-acetylgal	Transcribed locus, strongly similar to XP_539924.1 PREDICTED: similar to N-acetylgalactosaminyltransferase; similar to Q10473 (PID:g1709559) [Canis familiaris]	
Ssc.6323.1.S1_at	NM_001122	0.00030	-3.63	adipose differentiation-related protein	adipose differentiation-related protein	ADRP
Ssc.1126.1.A1_at	NM_006714	0.00000	-3.64	sphingomyelin phosphodiesterase; acid-like 3A	Transcribed locus, moderately similar to NP_006705.1 acid sphingomyelinase-like phosphodiesterase 3A; acid sphingomyelinase-like phosphodiesterase; 0610010C24Rik [Homo sapiens]	
Ssc.23746.1.S1_at	NM_015385	0.00019	-3.66	sorbin and SH3 domain containing 1	Transcribed locus, strongly similar to XP_484807.1 sorbin and SH3 domain containing 1 [Mus musculus]	

Ssc.27550.1.S1_at	NM_003358	0.00000	-3.69	UDP-glucose ceramide glucosyltransferase	Transcribed locus, strongly similar to XP_538788.1 PREDICTED: similar to Ceramide glucosyltransferase (Glucosylceramide synthase) (GCS) (UDP-glucose:N-acylsphingosine D-glucosyltransferase) (UDP-glucose ceramide glucosyltransferase) (GLCT-1) [Canis familiaris]	
Ssc.24718.1.S1_at	NM_005536	0.00003	-3.69	inositol	Transcribed locus	
Ssc.12176.1.S1_at	NM_022036	0.00011	-3.74	G protein-coupled receptor; family C; group 5; member C	Transcribed locus, strongly similar to NP_071319.2 G protein-coupled receptor family C, group 5, member C isoform a; retinoic acid responsive gene protein; orphan G-protein coupled receptor [Homo sapiens]	
Ssc.6425.1.A1_at	#N/A	0.00012	-3.74	#N/A	Transcribed locus, moderately similar to NP_005679.1 ATP-binding cassette, sub-family C, member 5; canalicular multispecific organic anion transporter C [Homo sapiens]	
Ssc.26303.1.A1_at	#N/A	0.00050	-3.78	#N/A	Transcribed locus	
Ssc.5000.1.A1_at	#N/A	0.00000	-3.83	#N/A	Transcribed locus, moderately similar to NP_004439.1 v-erb-b2 erythroblastic leukemia viral oncogene homolog 2, neuro/glioblastoma derived oncogene homolog; Avian erythroblastic leukemia viral (v-erb-b2) oncogene homolog 2; v-erb-b2 avian erythroblastic leukemia viral oncogene homolog 2 (neuro/glioblastoma derived oncogene homolog) [Homo sapiens]	
Ssc.13891.1.A1_at	NM_152869	0.00031	-3.84	regucalcin	Transcribed locus, strongly similar to XP_538011.1 PREDICTED: similar to regucalcin [Canis familiaris]	
Ssc.31172.3.S1_at	NM_001006946	0.00005	-3.86	syndecan 1	Transcribed locus	
Ssc.24128.1.A1_at	#N/A	0.00005	-3.86	#N/A	Transcribed locus	

Ssc.2179.1.S1_at	NM_024980	0.00000	-3.87	G protein-coupled receptor 157	Transcribed locus, moderately similar to NP_796340.1 RIKEN cDNA F730108M23 gene [Mus musculus]	
Ssc.10307.1.A1_at	#N/A	0.00006	-3.88	#N/A	Transcribed locus	
Ssc.14211.1.A1_at	#N/A	0.00011	-3.93	#N/A	Transcribed locus	
Ssc.19175.2.S1_at	#N/A	0.00008	-3.95	#N/A	Transcribed locus	
Ssc.28415.1.S1_at	NM_031308	0.00010	-4.06	epiplakin 1	Transcribed locus, strongly similar to XP_372063.2 PREDICTED: similar to epiplakin [Homo sapiens]	
Ssc.25149.1.S1_at	#N/A	0.00002	-4.06	#N/A	Transcribed locus, moderately similar to XP_540332.1 PREDICTED: similar to membrane-associated guanylate kinase-related 3 [Canis familiaris]	
Ssc.27241.1.S1_at	NM_170692	0.00007	-4.1	RAS protein activator like 2	Transcribed locus, strongly similar to XP_537177.1 PREDICTED: similar to Ras GTPase-activating protein nGAP (RAS protein activator like 1) [Canis familiaris]	
Ssc.23264.1.A1_at	#N/A	0.00009	-4.13	#N/A	Transcribed locus, moderately similar to XP_537446.1 PREDICTED: similar to KIAA1344 protein [Canis familiaris]	
Ssc.25412.1.A1_at	#N/A	0.00043	-4.14	#N/A	Transcribed locus	
Ssc.25189.1.S1_a_at	NM_020784	0.00038	-4.15	KIAA1344	Transcribed locus, strongly similar to XP_051699.4 PREDICTED: KIAA1344 [Homo sapiens]	
Ssc.28921.1.S1_at	#N/A	0.00003	-4.23	#N/A	Transcribed locus	
Ssc.21382.1.A1_at	NM_004419	0.00004	-4.28	dual specificity phosphatase 5	Transcribed locus	
Ssc.30194.1.A1_at	NM_207015	0.00051	-4.38	N-acetylated alpha-linked acidic dipeptidase 2	Transcribed locus, moderately similar to NP_996898.1 N-acetylated alpha-linked acidic dipeptidase 2 [Homo sapiens]	
Ssc.13473.1.A1_at	#N/A	0.00071	-4.4	#N/A	Transcribed locus	

Ssc.2176.1.A1_at	NM_203372	0.00004	-4.42	acyl-CoA synthetase long-chain family member 3	Transcribed locus, strongly similar to NP_004448.2 acyl-CoA synthetase long-chain family member 3; lignoceroyl-CoA synthase; fatty-acid-Coenzyme A ligase, long-chain 3 [Homo sapiens]	
Ssc.29231.1.A1_at	#N/A	0.00011	-4.44	#N/A	Transcribed locus	
Ssc.31172.1.S1_at	NM_001006946	0.00000	-4.46	syndecan 1	Transcribed locus	
Ssc.22476.1.A1_at	XM_373594	0.00008	-4.49	hypothetical LOC387992	Transcribed locus	
Ssc.2492.2.S1_at	NM_001001669	0.00000	-4.5	FLJ41603 protein	Transcribed locus	
Ssc.24593.1.A1_at	#N/A	0.00074	-4.57	#N/A	Transcribed locus	
Ssc.5887.1.A1_at	#N/A	0.00096	-4.57	#N/A	Transcribed locus, strongly similar to NP_938018.1 solute carrier family 37 (glycerol-3-phosphate transporter), member 2 [Homo sapiens]	
Ssc.428.23.A1_at	#N/A	0.00026	-4.58	#N/A	T-cell receptor alpha chain mRNA C-region, 3' end of cds	
Ssc.25134.1.A1_at	NM_020784	0.00018	-4.62	KIAA1344	Transcribed locus, moderately similar to XP_051699.4 PREDICTED: KIAA1344 [Homo sapiens]	
Ssc.12176.3.S1_at	NM_018653	0.00003	-4.72	G protein-coupled receptor; family C; group 5; member C	Transcribed locus, strongly similar to NP_071319.2 G protein-coupled receptor family C, group 5, member C isoform a; retinoic acid responsive gene protein; orphan G-protein coupled receptor [Homo sapiens]	
Ssc.4204.1.S1_at	NM_004130	0.00046	-4.76	glycogenin	Transcribed locus, strongly similar to NP_004121.2 glycogenin [Homo sapiens]	
Ssc.2746.1.A1_at	#N/A	0.00025	-4.78	#N/A	Transcribed locus	
Ssc.28059.1.A1_at	XM_498662	0.00017	-4.84	hypothetical gene supported by AK092922; AL8319	Transcribed locus	
Ssc.1093.3.S1_at	NM_012193	0.00026	-4.88	frizzled homolog 4	Transcribed locus	
Ssc.25230.1.S1_at	NM_012193	0.00011	-4.88	frizzled homolog 4	Transcribed locus	

Ssc.25155.1.S1_at	NM_018390	0.00033	-4.89	phosphatidylinositol-specific phospholipase C; X domain con	Transcribed locus, moderately similar to NP_060860.1 hypothetical protein FLJ11323 [Homo sapiens]	
Ssc.2197.1.S1_at	NM_018004	0.00053	-5.17	transmembrane protein 45A	Transcribed locus, moderately similar to XP_535720.1 PREDICTED: hypothetical protein XP_535720 [Canis familiaris]	
Ssc.26693.1.S1_at	NM_002639	0.00003	-5.2	serine	Transcribed locus, strongly similar to XP_533382.1 PREDICTED: hypothetical protein XP_533382 [Canis familiaris]	
Ssc.26816.1.S1_at	NM_145176	0.00000	-5.37	solute carrier family 2	Transcribed locus, moderately similar to NP_660159.1 solute carrier family 2 (facilitated glucose transporter), member 12 [Homo sapiens]	
Ssc.4105.1.S1_at	#N/A	0.00000	-5.42	#N/A	Transcribed locus	
Ssc.19539.2.S1_at	NM_018941	0.00076	-5.46	ceroid-lipofuscinosis; neuronal 8	Transcribed locus, moderately similar to NP_036130.1 ceroid-lipofuscinosis, neuronal 8; motor neuron degeneration [Mus musculus]	
Ssc.16963.1.S1_at	NM_004776	0.00000	-5.52	UDP-Gal:betaGlcNAc beta 1;4-galactosyltransferase; polype	Transcribed locus, strongly similar to XP_512417.1 PREDICTED: glutaryl-Coenzyme A dehydrogenase [Pan troglodytes]	
Ssc.27052.1.A1_at	#N/A	0.00000	-5.71	#N/A	Transcribed locus	
Ssc.27177.1.S1_at	NM_006095	0.00003	-5.88	ATPase; aminophospholipid transporter	Transcribed locus, strongly similar to NP_006086.1 ATPase, aminophospholipid transporter (APLT), class I, type 8A, member 1; ATPase II; aminophospholipid translocase [Homo sapiens]	
Ssc.2963.1.S1_at	#N/A	0.00008	-5.89	#N/A	Transcribed locus	
Ssc.16333.1.S1_at	NM_000927	0.00002	-6.05	ATP-binding cassette; sub-family B	ATP-binding cassette, sub-family B (MDR/TAP), member 1	ABCB1
Ssc.3832.1.S1_at	NM_004925	0.00001	-6.14	aquaporin 3	Transcribed locus, similar to Aqp3 [Canis familiaris]	

Ssc.24978.2.S1_at	#N/A	0.00058	-6.16	#N/A	Transcribed locus	
Ssc.30871.1.A1_at	NM_033285	0.00052	-6.27	tumor protein p53 inducible nuclear protein 1	Transcribed locus	
Ssc.4272.1.A1_at	#N/A	0.00085	-6.4	#N/A	Transcribed locus	
Ssc.4076.1.S1_at	NM_015225	0.00036	-6.41	KIAA0367	Transcribed locus	
Ssc.3785.1.S1_a_at	XM_379250	0.00031	-6.53	hypothetical LOC401115	Transcribed locus	
Ssc.19482.1.A1_at	#N/A	0.00011	-6.61	#N/A	Transcribed locus	
Ssc.5848.1.S1_at	NM_004776	0.00002	-6.69	UDP-Gal:betaGlcNAc beta 1;4-galactosyltransferase; polype	Transcribed locus, strongly similar to NP_004767.1 UDP-Gal:betaGlcNAc beta 1,4- galactosyltransferase 5; beta-1,4-GalT IV; beta4-GalT IV [Homo sapiens]	
Ssc.19442.1.A1_at	#N/A	0.00006	-6.77	#N/A	Transcribed locus	
Ssc.12727.1.A1_at	#N/A	0.00000	-6.8	#N/A	Transcribed locus	
Ssc.5848.2.S1_a_at	NM_004776	0.00003	-6.94	UDP-Gal:betaGlcNAc beta 1;4-galactosyltransferase; polype	Transcribed locus, strongly similar to NP_004767.1 UDP-Gal:betaGlcNAc beta 1,4- galactosyltransferase 5; beta-1,4-GalT IV; beta4-GalT IV [Homo sapiens]	
Ssc.21383.1.A1_at	NM_178500	0.00024	-6.94	phosphatase; orphan 1	Transcribed locus, strongly similar to XP_511946.1 PREDICTED: hypothetical protein XP_511946 [Pan troglodytes]	
Ssc.27177.2.S1_at	#N/A	0.00006	-7.32	#N/A	Transcribed locus, strongly similar to NP_006086.1 ATPase, aminophospholipid transporter (APLT), class I, type 8A, member 1; ATPase II; aminophospholipid translocase [Homo sapiens]	
Ssc.16236.1.S1_at	NM_001935	0.00001	-7.58	dipeptidylpeptidase 4	dipeptidyl peptidase IV	DPPIV
Ssc.27292.1.S1_at	#N/A	0.00099	-7.72	#N/A	Transcribed locus	
Ssc.29750.1.A1_at	NM_033285	0.00018	-7.79	tumor protein p53 inducible nuclear protein 1	Transcribed locus	
Ssc.5434.1.A1_at	NM_033274	0.00037	-7.98	a disintegrin and metalloproteinase domain 19	Transcribed locus	

Ssc.3012.1.S1_at	NM_181597	0.00013	-8.64	uridine phosphorylase 1	Transcribed locus	
Ssc.6055.1.A1_at	NM_181785	0.00001	-8.86	hypothetical protein LOC283537	Transcribed locus, moderately similar to XP_534517.1 PREDICTED: hypothetical protein XP_534517 [Canis familiaris]	
Ssc.27433.1.S1_at	NM_000359	0.00019	-9.01	transglutaminase 1	Transcribed locus, strongly similar to NP_001003079.1 transglutaminase 1 [Canis familiaris]	
Ssc.12727.2.A1_at	#N/A	0.00002	-9.01	#N/A	Transcribed locus	
Ssc.2492.1.A1_at	#N/A	0.00010	-9.2	#N/A	Transcribed locus	
Ssc.27182.1.S1_at	NM_017682	0.00000	-9.61	vitelliform macular dystrophy 2-like 1	Transcribed locus, moderately similar to XP_512414.1 PREDICTED: similar to Bestrophin 2 (Vitelliform macular dystrophy 2-like protein 1) [Pan troglodytes]	
Ssc.64.1.S1_at	NM_004827	0.00000	-10.26	ATP-binding cassette; sub-family G	brain multidrug resistance protein	BMDP
Ssc.12802.1.A1_at	#N/A	0.00000	-10.52	#N/A	Transcribed locus	
Ssc.29246.1.A1_at	NM_199461	0.00049	-10.66	nanos homolog 1	Transcribed locus	
Ssc.17364.1.S1_at	NM_015444	0.00063	-11.8	Ras-induced senescence 1	Transcribed locus	
Ssc.29840.1.A1_at	#N/A	0.00044	-11.81	#N/A	Transcribed locus	
Ssc.27372.1.S1_at	#N/A	0.00000	-12.59	#N/A	Transcribed locus	
Ssc.1534.1.A1_at	NM_015385	0.00001	-12.71	sorbin and SH3 domain containing 1	Transcribed locus	
Ssc.24311.1.S1_at	#N/A	0.00083	-16.29	#N/A	Transcribed locus, weakly similar to NP_112603.1 placental-like alkaline phosphatase preproprotein; testicular and thymus alkaline phosphatase; Nagao isozyme; germ cell alkaline phosphatase [Homo sapiens]	
Ssc.26185.1.S1_at	#N/A	0.00047	-17.27	#N/A	Transcribed locus	
Ssc.24503.1.S1_at	XM_496688	0.00006	-18.39	hypothetical protein BC012029	Transcribed locus	
Ssc.10403.1.S1_at	NM_012101	0.00004	-19.37	tripartite motif-containing 29	Transcribed locus, similar to tripartite motif protein TRIM29 isoform beta [Canis familiaris]	

Ssc.6056.1.S1_at	NM_181797	0.00049	-19.65	potassium voltage-gated channel; KQT-like subfamily; membe	Transcribed locus	
Ssc.27264.1.S1_at	NM_024861	0.00001	-21.19	hypothetical protein FLJ22671	Transcribed locus, moderately similar to hypothetical protein FLJ22671 [Homo sapiens]	
Ssc.29858.1.A1_at	NM_000927	0.00000	-25.81	ATP-binding cassette; sub-family B	Transcribed locus	
Ssc.8594.1.A1_at	NM_013314	0.00002	-28.75	B-cell linker	Transcribed locus, strongly similar to NP_037446.1 B-cell linker; B cell linker protein [Homo sapiens]	
Ssc.7243.1.A1_at	NM_199168	0.00023	-44.53	chemokine	Transcribed locus	
Ssc.19431.1.S1_at	NM_005021	0.00002	-63	ectonucleotide pyrophosphatasephosphodiesterase 3	Transcribed locus, moderately similar to NP_005012.1 ectonucleotide pyrophosphatase/phosphodiesterase 3; phosphodiesterase-I beta; gp130RB13-6; phosphodiesterase I/nucleotide pyrophosphatase 3 [Homo sapiens]	

[a]The Affymetrix ID is specific to a porcine sequence for which a specific probe set was designed to interrogate.
[b]GenBank Accession number assigned for those genes, as associated with the Affymetrix ID, having homology to annotated human genes.
[c]The probability for statistical differences was determined using unpaired t-tests via dChip described in Chapter 3.
[d]Only those genes significantly different and with a fold change equal or greater than 2.0 were included.
[e]This annotation refers to the targets whose interrogated sequence had significant homology to an annotated human sequence.
[f]This annotation was assigned by Affymetrix.
[g]Acronyms for genes have been assigned by Affymetrix.

Table A.2. Differentially expressed genes during the transition from Day 12 to Day 14 filamentous conceptuses.

Probe Set ID[a]	GenBank Accesion Number[b]	P Value[c]	Fold Change[d]	Putative Identity Following Annotation Based on Homology to Known GenBank Identities[e]	Gene Title Assigned By Affymetrix Annotation[f]	Gene Symbol[g]
Ssc.19394.1.A1_at	#N/A	0.00023	38.75	#N/A	Transcribed locus, strongly similar to NP_653308.1 prominin 2; prominin-related protein [Homo sapiens]	
Ssc.4815.1.A1_at	#N/A	0.00008	37.15	#N/A	Transcribed locus	
Ssc.15316.2.S1_at	NM_001311	0.00020	36.87	cysteine-rich protein 1	Transcribed locus, moderately similar to XP_422218.1 PREDICTED: similar to LIM only protein HLP [Gallus gallus]	
Ssc.20438.1.S1_at	NM_000959	0.00074	19.36	prostaglandin F receptor	Transcribed locus	
Ssc.4984.1.S1_at	NM_004887	0.00075	19.07	chemokine	chemokine	CXCL14
Ssc.2197.1.S1_at	NM_018004	0.00044	13.72	transmembrane protein 45A	Transcribed locus, moderately similar to XP_535720.1 PREDICTED: hypothetical protein XP_535720 [Canis familiaris]	
Ssc.18707.1.A1_at	#N/A	0.00045	13.47	#N/A	Transcribed locus, strongly similar to NP_003610.1 neurotrypsin precursor; brain-specific serine protease 3; leydin [Homo sapiens]	
Ssc.20578.1.S1_at	#N/A	0.00074	11.99	#N/A	Transcribed locus	
Ssc.10942.1.S1_at	NM_053013	0.00009	11.18	enolase 3	Transcribed locus, strongly similar to XP_484728.1 similar to Eno1 protein [Mus musculus]	
Ssc.5165.1.S1_at	#N/A	0.00010	9.03	#N/A	Transcribed locus	
Ssc.11131.1.S1_at	NM_003380	0.00086	8.48	vimentin	Transcribed locus, strongly similar to XP_535175.1 PREDICTED: similar to vimentin [Canis familiaris]	
Ssc.29483.1.A1_at	#N/A	0.00059	7.69	#N/A	Transcribed locus	
Ssc.6057.1.A1_at	NM_015550	0.00021	7.52	oxysterol binding protein-like 3	Transcribed locus	
Ssc.29437.1.S1_at	#N/A	0.00034	6.9	#N/A	Transcribed locus	

Ssc.19579.2.S1_at	#N/A	0.00096	6.52	#N/A	Transcribed locus, strongly similar to nuclear receptor subfamily 2, group F, member 2 [Pan troglodytes]	
Ssc.1544.1.S1_at	NM_000257	0.00082	5.96	myosin; heavy polypeptide 7; cardiac muscle; beta	beta-myosin heavy chain	MYH7
Ssc.22082.1.A1_at	#N/A	0.00038	5.63	#N/A	Transcribed locus, strongly similar to NP_066566.3 disabled homolog 1; disabled (Drosophila) homolog 1 [Homo sapiens]	
Ssc.24345.1.S1_at	NM_015556	0.00020	5.52	signal-induced proliferation-associated 1 like 1	Transcribed locus, strongly similar to NP_056371.1 signal-induced proliferation-associated 1 like 1; signal-induced proliferation-associated 1-like 1 [Homo sapiens]	
Ssc.8479.1.A1_at	NM_005410	0.00016	5.28	selenoprotein P; plasma; 1	Transcribed locus, weakly similar to NP_005401.2 selenoprotein P precursor [Homo sapiens]	
Ssc.16989.1.A1_at	NM_001753	0.00011	5.09	caveolin 1; caveolae protein; 22kDa	Transcribed locus	
Ssc.15695.1.S1_at	NM_006744	0.00030	5.04	retinol binding protein 4; plasma	retinol-binding protein	RBP4
Ssc.2824.1.S1_at	NM_198234	0.00096	4.43	ribonuclease; RNase A family; 1	Clone Clu_87699.scr.msk.p1.Contig1, mRNA sequence	
Ssc.5737.1.S1_at	NM_078467	0.00027	4.36	cyclin-dependent kinase inhibitor 1A	Transcribed locus, moderately similar to XP_532125.1 PREDICTED: similar to p21/WAF1 [Canis familiaris]	
Ssc.8373.1.A1_at	#N/A	0.00007	4.31	#N/A	Transcribed locus	
Ssc.7588.1.A1_at	#N/A	0.00022	4.25	#N/A	Transcribed locus	
Ssc.18578.1.S1_at	NM_175842	0.00083	3.95	spermine oxidase	Transcribed locus, strongly similar to XP_514493.1 PREDICTED: similar to polyamine oxidase isoform 1; polyamine oxidase; chromosome 20 open reading frame 16; flavin-containing spermine oxidase; putative cyclin G1 interacting protein; flavin containing amine oxidase [Pan troglodytes]	

Ssc.18014.1.A1_at	NM_052954	0.00077	3.92	cysteine and tyrosine-rich 1	Transcribed locus	
Ssc.18030.1.A1_at	#N/A	0.00072	3.89	#N/A	Transcribed locus	
Ssc.9286.1.A1_at	#N/A	0.00053	3.88	#N/A	Transcribed locus	
Ssc.20258.1.S1_at	#N/A	0.00068	3.77	#N/A	Transcribed locus	
Ssc.26224.1.S1_at	NM_199171	0.00056	3.69	transmembrane; prostate androgen induced RNA	Transcribed locus, strongly similar to transmembrane prostate androgen-induced protein isoform a [Homo sapiens]	
Ssc.17518.1.S1_at	NM_000674	0.00008	3.61	adenosine A1 receptor	Transcribed locus, strongly similar to NP_000665.1 adenosine A1 receptor [Homo sapiens]	
Ssc.5683.1.S1_a_at	NM_022371	0.00077	3.55	torsin family 3; member A	Transcribed locus, strongly similar to XP_547446.1 PREDICTED: similar to ADIR1 [Canis familiaris]	
Ssc.4914.1.A1_at	NM_032181	0.00064	3.47	hypothetical protein FLJ13391	Transcribed locus, strongly similar to XP_525794.1 PREDICTED: similar to hypothetical protein FLJ13391 [Pan troglodytes]	
Ssc.4266.1.S1_at	#N/A	0.00079	3.45	#N/A	Transcribed locus	
Ssc.23077.1.A1_at	#N/A	0.00016	3.43	#N/A	Transcribed locus	
Ssc.18996.2.A1_a_at	NM_003963	0.00052	3.38	transmembrane 4 L six family member 5	Transcribed locus, moderately similar to NP_003954.2 transmembrane 4 superfamily member 5; tetraspan transmembrane protein L6H [Homo sapiens]	
Ssc.21848.1.S1_at	NM_014292	0.00000	3.35	chromobox homolog 6	Transcribed locus	
Ssc.26253.1.S1_at	#N/A	0.00091	3.33	#N/A	Transcribed locus	
Ssc.1308.1.S1_at	NM_002081	0.00048	3.29	glypican 1	Transcribed locus, moderately similar to NP_002072.1 glypican 1 precursor [Homo sapiens]	
Ssc.8609.1.A1_at	NM_014456	0.00006	3.29	programmed cell death 4	Transcribed locus, strongly similar to XP_535012.1 PREDICTED: similar to programmed cell death 4 isoform 1 [Canis familiaris]	

Ssc.19323.1.S1_at	NM_138389	0.00001	3.29	hypothetical protein BC001096	Transcribed locus, strongly similar to NP_612398.1 hypothetical protein BC001096 [Homo sapiens]	
Ssc.18540.1.S1_at	#N/A	0.00005	3.23	#N/A	Transcribed locus, strongly similar to NP_005838.3 solute carrier family 23 (nucleobase transporters), member 1 isoform a; sodium-dependent vitamin C transporter-1; yolk sac permease-like molecule 3; solute carrier family 23 (nucleobase transporters), member 2; Na(+)/L-ascorbic acid transporter 1 [Homo sapiens]	
Ssc.25410.1.S1_at	#N/A	0.00028	3.16	#N/A	Transcribed locus	
Ssc.3016.1.S1_at	#N/A	0.00018	3.15	#N/A	Transcribed locus	
Ssc.21617.1.A1_at	#N/A	0.00003	3.14	#N/A	Transcribed locus	
Ssc.9504.1.A1_at	#N/A	0.00035	3.14	#N/A	Transcribed locus	
Ssc.6988.1.A1_at	NM_138766	0.00048	3.03	peptidylglycine alpha-amidating monooxygenase	Transcribed locus, strongly similar to NP_037132.2 peptidylglycine alpha-amidating monooxygenase [Rattus norvegicus]	
Ssc.4676.1.A1_at	NM_018211	0.00030	3.02	hypothetical protein FLJ10770	Transcribed locus	
Ssc.19579.3.S1_at	NM_021005	0.00097	3.01	nuclear receptor subfamily 2; group F; member 2	Transcribed locus, strongly similar to nuclear receptor subfamily 2, group F, member 2 [Pan troglodytes]	
Ssc.25051.1.S1_at	NM_016950	0.00091	2.96	sparcosteonectin; cwcv and kazal-like domains proteoglycan	Transcribed locus, moderately similar to NP_058646.1 testican 3 [Homo sapiens]	
Ssc.27354.1.S1_at	NM_139244	0.00009	2.96	syntaxin binding protein 5	Transcribed locus, strongly similar to XP_533442.1 PREDICTED: hypothetical protein XP_533442 [Canis familiaris]	
Ssc.28006.1.A1_at	NM_152526	0.00007	2.95	amyotrophic lateral sclerosis 2	Transcribed locus, moderately similar to NP_995585.1 amyotrophic lateral sclerosis 2 (juvenile), partitioning-defective 3-like [Homo sapiens]	

Ssc.5580.1.S1_at	#N/A	0.00024	2.93	#N/A	Transcribed locus	
Ssc.12842.1.S1_at	NM_001753	0.00049	2.92	caveolin 1; caveolae protein; 22kDa	Caveolin 1	CAV1
Ssc.16346.1.S1_at	NM_022972	0.00062	2.92	fibroblast growth factor receptor 2	fibroblast growth factor receptor	FGFR2
Ssc.23169.1.S1_at	NM_002856	0.00097	2.91	poliovirus receptor-related 2	Transcribed locus, moderately similar to NP_002847.1 poliovirus receptor-related 2 (herpesvirus entry mediator B); nectin 2; poliovirus receptor-like 2; herpesvirus entry mediator B (poliovirus receptor-related 2); herpesvirus entry protein B; poliovirus receptor related 2 [Homo sapiens]	
Ssc.25002.1.S1_at	NM_031283	0.00099	2.91	transcription factor 7-like 1	Transcribed locus, strongly similar to NP_112573.1 HMG-box transcription factor TCF-3 [Homo sapiens]	
Ssc.19873.1.S1_at	NM_194071	0.00006	2.91	cAMP responsive element binding protein 3-like 2	Transcribed locus	
Ssc.18900.1.A1_at	#N/A	0.00048	2.91	#N/A	Transcribed locus	
Ssc.6382.1.A1_at	NM_024607	0.00007	2.86	protein phosphatase 1; regulatory	Transcribed locus	
Ssc.20353.1.S1_at	#N/A	0.00009	2.84	#N/A	Transcribed locus	
Ssc.3021.1.A1_at	#N/A	0.00001	2.82	#N/A	Transcribed locus	
Ssc.12412.1.A1_at	NM_022044	0.00029	2.81	stromal cell-derived factor 2-like 1	Transcribed locus, strongly similar to NP_071327.1 stromal cell-derived factor 2-like 1; AP000553.C22.4; OTTHUMT00000075032 [Homo sapiens]	
Ssc.26363.1.S1_at	NM_012262	0.00000	2.78	heparan sulfate 2-O-sulfotransferase 1	Transcribed locus, strongly similar to NP_036394.1 heparan sulfate 2-O-sulfotransferase 1 [Homo sapiens]	
Ssc.17312.1.A1_at	XM_373497	0.00080	2.78	hypothetical LOC387763	Transcribed locus, strongly similar to NP_001003058.1 CMP-sialic acid transporter [Canis familiaris]	

Ssc.29043.2.A1_at	NM_205860	0.00097	2.77	nuclear receptor subfamily 5; group A; member 2	Transcribed locus, strongly similar to NP_995582.1 nuclear receptor subfamily 5, group A, member 2 isoform 1; CYP7A promoter-binding factor; fetoprotein-alpha 1 (AFP) transcription factor; b1-binding factor, hepatocyte transcription factor which activates enhancer II of hepatitis B virus; liver receptor homolog 1 [Homo sapiens]	
Ssc.13380.1.A1_at	#N/A	0.00032	2.76	#N/A	Transcribed locus	
Ssc.23905.1.A1_at	#N/A	0.00097	2.75	#N/A	Transcribed locus	
Ssc.9588.1.A1_at	#N/A	0.00048	2.75	#N/A	Transcribed locus	
Ssc.19212.1.S1_at	NM_000387	0.00042	2.73	solute carrier family 25	Clone Clu_23714.scr.msk.p1.Contig3, mRNA sequence	
Ssc.30989.1.A1_at	XM_035299	0.00081	2.73	zinc finger; SWIM domain containing 6	Transcribed locus	
Ssc.19873.1.S1_a_at	NM_194071	0.00004	2.69	cAMP responsive element binding protein 3-like 2	Transcribed locus	
Ssc.2642.1.S1_at	NM_003312	0.00096	2.67	thiosulfate sulfurtransferase	Transcribed locus, strongly similar to XP_515109.1 PREDICTED: similar to TST [Pan troglodytes]	
Ssc.29435.1.A1_at	NM_003483	0.00086	2.67	high mobility group AT-hook 2	Transcribed locus	
Ssc.9391.1.A1_at	NM_014734	0.00037	2.67	KIAA0247	Transcribed locus	
Ssc.18375.1.A1_at	NM_006378	0.00056	2.65	sema domain; immunoglobulin domain	Transcribed locus	
Ssc.19579.1.A1_at	NM_021005	0.00028	2.65	nuclear receptor subfamily 2; group F; member 2	Transcribed locus, strongly similar to XP_523164.1 PREDICTED: similar to nuclear receptor subfamily 2, group F, member 2 [Pan troglodytes]	
Ssc.31053.1.A1_at	NM_004487	0.00012	2.63	golgi autoantigen; golgin subfamily b; macrogolgin	Transcribed locus, moderately similar to XP_516685.1 PREDICTED: golgi autoantigen, golgin subfamily b, macrogolgin (with transmembrane signal), 1 [Pan troglodytes]	
Ssc.14376.1.A1_at	#N/A	0.00047	2.63	#N/A	Transcribed locus	

Ssc.22563.1.S1_at	NM_006581	0.00013	2.62	fucosyltransferase 9	Transcribed locus, strongly similar to NP_001005380.1 alpha-1,3-fucosyltransferase 9 [Canis familiaris]	
Ssc.21188.1.S1_at	NM_021195	0.00048	2.62	claudin 6	Transcribed locus, strongly similar to NP_067018.1 claudin 6 [Homo sapiens]	
Ssc.16982.1.S1_at	NM_014061	0.00033	2.61	melanoma antigen family H; 1	Transcribed locus, strongly similar to NP_076277.1 melanoma antigen, family H, 1 [Mus musculus]	
Ssc.24304.2.A1_at	NM_182801	0.00091	2.6	hypothetical protein FLJ39155	Transcribed locus	
Ssc.27592.2.S1_at	NM_003956	0.00045	2.58	cholesterol 25-hydroxylase	Transcribed locus, moderately similar to XP_220063.2 PREDICTED: similar to Cholesterol 25-hydroxylase [Rattus norvegicus]	
Ssc.31000.1.A1_at	XM_294353	0.00038	2.58	similar to RIKEN cDNA 6332401O19 gene	Transcribed locus, strongly similar to RIKEN cDNA 6332401O19 gene [Homo sapiens]	
Ssc.24540.1.S1_at	#N/A	0.00020	2.58	#N/A	Transcribed locus	
Ssc.7145.1.A1_at	#N/A	0.00014	2.58	#N/A	Transcribed locus, moderately similar to XP_509017.1 PREDICTED: similar to splicing factor, arginine/serine-rich 2, interacting protein; SC35-interacting protein 1 [Pan troglodytes]	
Ssc.772.1.S1_at	NM_014316	0.00071	2.56	calcium regulated heat stable protein 1; 24kDa	Clone Clu_112017.scr.msk.p1.Contig2, mRNA sequence	
Ssc.12628.1.A1_at	NM_207015	0.00018	2.54	N-acetylated alpha-linked acidic dipeptidase 2	Transcribed locus, weakly similar to XP_355456.2 similar to N-acetylated alpha-linked acidic dipeptidase 2 [Mus musculus]	
Ssc.1896.2.A1_a_at	NM_000156	0.00081	2.5	guanidinoacetate N-methyltransferase	Transcribed locus, strongly similar to NP_000147.1 guanidinoacetate N-methyltransferase isoform a [Homo sapiens]	
Ssc.8950.1.A1_at	#N/A	0.00001	2.49	#N/A	Transcribed locus	
Ssc.55.1.S1_at	NM_005228	0.00002	2.47	epidermal growth factor receptor	epidermal growth factor receptor	EGFR

Ssc.19075.1.A1_at	NM_022739	0.00050	2.47	SMAD specific E3 ubiquitin protein ligase 2	Transcribed locus, strongly similar to NP_073576.1 SMAD specific E3 ubiquitin protein ligase 2; E3 ubiquitin ligase SMURF2 [Homo sapiens]	
Ssc.19620.1.S1_at	NM_199262	0.00046	2.47	Sp6 transcription factor	Transcribed locus	
Ssc.26215.1.S1_at	NM_019896	0.00005	2.43	polymerase	Transcribed locus, strongly similar to XP_540212.1 PREDICTED: hypothetical protein XP_540212 [Canis familiaris]	
Ssc.16312.1.S1_at	NM_006825	0.00003	2.42	cytoskeleton-associated protein 4	Unidentified hepatic protein mRNA	
Ssc.11659.1.A1_at	#N/A	0.00065	2.38	#N/A	Transcribed locus	
Ssc.19459.1.A1_at	#N/A	0.00005	2.38	#N/A	Transcribed locus	
Ssc.3832.1.S1_at	NM_004925	0.00082	2.34	aquaporin 3	Transcribed locus, strongly similar to XP_531973.1 PREDICTED: similar to Aqp3 protein [Canis familiaris]	
Ssc.24330.1.S1_at	NM_004820	0.00019	2.31	cytochrome P450; family 7; subfamily B; polypeptide 1	Transcribed locus, moderately similar to XP_544102.1 PREDICTED: similar to oxysterol 7alpha-hydroxylase [Canis familiaris]	
Ssc.21408.1.S1_at	NM_006260	0.00051	2.31	DnaJ	Transcribed locus, weakly similar to XP_359458.1 hypothetical protein MG05319.4 [Magnaporthe grisea 70-15]	
Ssc.3409.1.A1_at	NM_213662	0.00020	2.31	signal transducer and activator of transcription 3	Transcribed locus, strongly similar to NP_003141.2 signal transducer and activator of transcription 3 isoform 2; acute-phase response factor; DNA-binding protein APRF [Homo sapiens]	
Ssc.10777.1.A1_at	#N/A	0.00029	2.31	#N/A	Transcribed locus	
Ssc.11502.1.A1_at	#N/A	0.00002	2.31	#N/A	Transcribed locus	
Ssc.8427.1.A1_at	NM_018999	0.00096	2.29	KIAA1128	Transcribed locus	
Ssc.12430.1.S1_at	NM_002744	0.00047	2.28	protein kinase C; zeta	Transcribed locus, strongly similar to NP_002735.2 protein kinase C, zeta [Homo sapiens]	
Ssc.9936.1.A1_at	NM_001002860	0.00001	2.26	BTB	Transcribed locus	

Ssc.7304.2.A1_at	NM_005544	0.00003	2.26	insulin receptor substrate 1	Transcribed locus, strongly similar to NP_005535.1 insulin receptor substrate 1 [Homo sapiens]	
Ssc.1986.1.S1_at	NM_080591	0.00024	2.26	prostaglandin-endoperoxide synthase 1	Transcribed locus, moderately similar to NP_000953.2 prostaglandin-endoperoxide synthase 1 isoform 1 precursor; prostaglandin G/H synthase and cyclooxygenase [Homo sapiens]	
Ssc.16540.1.S1_at	NM_002827	0.00051	2.25	protein tyrosine phosphatase; non-receptor type 1	Transcribed locus	
Ssc.27912.1.S1_at	NM_020747	0.00097	2.25	zinc finger protein 608	Transcribed locus, strongly similar to XP_114432.3 PREDICTED: zinc finger protein 608 [Homo sapiens]	
Ssc.24138.1.A1_at	#N/A	0.00035	2.25	#N/A	Transcribed locus	
Ssc.29710.1.A1_at	#N/A	0.00037	2.25	#N/A	Transcribed locus	
Ssc.24233.1.S1_at	NM_015170	0.00028	2.24	sulfatase 1	Transcribed locus, strongly similar to NP_055985.1 sulfatase 1; sulfatase FP [Homo sapiens]	
Ssc.13553.1.A1_at	#N/A	0.00043	2.24	#N/A	Transcribed locus, moderately similar to NP_112298.1 guanine nucleotide binding protein, alpha q polypeptide [Rattus norvegicus]	
Ssc.5226.1.S1_at	NM_015252	0.00061	2.23	EH domain binding protein 1	Transcribed locus, strongly similar to XP_515506.1 PREDICTED: hypothetical protein XP_515506 [Pan troglodytes]	
Ssc.11401.1.A1_a_at	NM_007110	0.00037	2.22	telomerase-associated protein 1	Transcribed locus, moderately similar to NP_009041.2 telomerase-associated protein 1; telomerase protein component 1 [Homo sapiens]	
Ssc.22444.2.A1_at	#N/A	0.00013	2.22	#N/A	Transcribed locus	
Ssc.5966.1.A1_at	NM_024324	0.00046	2.2	hypothetical protein MGC11256	Transcribed locus, moderately similar to hypothetical protein MGC11256; cystein-rich with EGF-like domains 2 [Homo sapiens]	
Ssc.17280.2.A1_at	#N/A	0.00059	2.19	#N/A	Transcribed locus	

Ssc.2688.1.S1_at	NM_182924	0.00027	2.17	MICAL-like 2	Transcribed locus, moderately similar to NP_078999.1 MICAL-like 2 isoform 2 [Homo sapiens]	
Ssc.18306.1.A1_at	#N/A	0.00089	2.17	#N/A	Transcribed locus	
Ssc.4740.2.A1_at	#N/A	0.00050	2.17	#N/A	Transcribed locus	
Ssc.14521.1.S1_at	NM_153326	0.00095	2.16	aldo-keto reductase family 1; member A1	aldehyde reductase	ALR1
Ssc.14277.1.A1_at	#N/A	0.00030	2.16	#N/A	Transcribed locus	
Ssc.3670.1.S1_a_at	NM_022356	0.00024	2.15	leucine proline-enriched proteoglycan	Transcribed locus, strongly similar to NP_446119.1 leprecan 1 [Rattus norvegicus]	
Ssc.19892.1.A1_at	NM_024408	0.00042	2.15	Notch homolog 2	Transcribed locus	
Ssc.6352.1.S1_at	NM_000581	0.00098	2.14	glutathione peroxidase 1	cytosolic glutathione peroxidase	GPX1
Ssc.4228.1.S1_at	NM_015537	0.00076	2.13	nasal embryonic LHRH factor	Transcribed locus, strongly similar to NP_056352.3 nasal embryonic LHRH factor; nasal embryonic luteinizing hormone-releasing hormone factor [Homo sapiens]	
Ssc.19416.1.A1_at	#N/A	0.00040	2.13	#N/A	Transcribed locus	
Ssc.21595.1.S1_at	#N/A	0.00059	2.11	#N/A	Alpha-stimulatory subunit of GTP-binding protein	PORGSA1
Ssc.24596.1.S1_at	#N/A	0.00023	2.1	#N/A	Transcribed locus	
Ssc.24608.1.S1_at	#N/A	0.00013	2.09	#N/A	Transcribed locus	
Ssc.27249.1.S1_at	NM_005221	0.00022	2.08	distal-less homeo box 5	Transcribed locus, strongly similar to XP_539430.1 PREDICTED: similar to Homeobox protein DLX-5 [Canis familiaris]	
Ssc.25182.1.A1_at	#N/A	0.00030	2.08	#N/A	Transcribed locus	
Ssc.16689.1.S1_at	NM_003980	0.00003	2.07	microtubule-associated protein 7	Transcribed locus, moderately similar to XP_533419.1 PREDICTED: hypothetical protein XP_533419 [Canis familiaris]	
Ssc.10775.1.A1_at	#N/A	0.00009	2.07	#N/A	Transcribed locus	

Ssc.26025.1.S1_at	NM_017641	0.00069	2.06	kinesin family member 21A	Transcribed locus, strongly similar to XP_534839.1 PREDICTED: similar to Kinesin family member 21A (Kinesin-like protein KIF2) (NY-REN-62 antigen) [Canis familiaris]	
Ssc.14336.1.A1_at	#N/A	0.00092	2.06	#N/A	Transcribed locus	
Ssc.30240.1.A1_at	#N/A	0.00031	2.06	#N/A	Transcribed locus	
Ssc.31070.1.S1_at	NM_012201	0.00058	2.05	golgi apparatus protein 1	Transcribed locus, strongly similar to NP_033175.1 golgi apparatus protein 1; selectin, endothelial cell, ligand [Mus musculus]	
Ssc.2187.1.S1_at	NM_015267	0.00051	2.05	cut-like 2	Transcribed locus	
Ssc.6511.1.A1_at	#N/A	0.00082	2.05	#N/A	Transcribed locus	
Ssc.19873.2.S1_at	NM_194071	0.00081	2.04	cAMP responsive element binding protein 3-like 2	Transcribed locus	
Ssc.27182.1.S1_at	NM_017682	0.00068	2.03	vitelliform macular dystrophy 2-like 1	Transcribed locus, moderately similar to XP_512414.1 PREDICTED: similar to Bestrophin 2 (Vitelliform macular dystrophy 2-like protein 1) [Pan troglodytes]	
Ssc.4084.1.S1_at	XM_371474	0.00098	2.03	plexin B2	Transcribed locus	
Ssc.31006.2.A1_at	#N/A	0.00055	2.03	#N/A	Transcribed locus, strongly similar to XP_508612.1 PREDICTED: similar to PTPRF interacting protein alpha 1 isoform a; LAR-interacting protein 1 [Pan troglodytes]	
Ssc.26941.1.S1_at	#N/A	0.00058	2.02	#N/A	Transcribed locus	
Ssc.17572.1.S1_at	NM_032840	0.00044	2.01	hypothetical protein FLJ14800	Transcribed locus	
Ssc.30295.1.A1_at	#N/A	0.00058	2.01	#N/A	Transcribed locus	
Ssc.3043.1.S1_at	NM_152999	0.00065	2	six transmembrane epithelial antigen of the prostate 2	Transcribed locus	
Ssc.5362.1.S1_at	NM_014397	0.00094	-2.02	NIMA	Transcribed locus	

Ssc.20740.1.S1_at	#N/A	0.00032	-2.02	#N/A	Transcribed locus, weakly similar to XP_548196.1 PREDICTED: similar to Neurabin-II (Neural tissue-specific F-actin binding protein II) (Protein phosphatase 1 regulatory subunit 9B) (Spinophilin) (p130) (PP1bp134) [Canis familiaris]	
Ssc.2768.2.S1_at	NM_000437	0.00082	-2.03	platelet-activating factor acetylhydrolase 2; 40kDa	Transcribed locus, moderately similar to XP_535348.1 PREDICTED: similar to platelet-activating factor acetylhydrolase 2 [Canis familiaris]	
Ssc.27871.2.S1_at	NM_139274	0.00011	-2.03	acetyl-Coenzyme A synthetase 2	Clone Clu_5971.scr.msk.p1.Contig1, mRNA sequence	
Ssc.18495.2.S1_at	#N/A	0.00084	-2.03	#N/A	Transcribed locus	
Ssc.19213.1.S1_at	NM_173553	0.00082	-2.04	hypothetical protein FLJ25801	Transcribed locus, moderately similar to XP_540017.1 PREDICTED: similar to hypothetical protein FLJ25801 [Canis familiaris]	
Ssc.19150.1.S1_s_at	NM_197966	0.00078	-2.06	BH3 interacting domain death agonist	BH3 interacting domain death agonist	BID
Ssc.8305.1.A1_at	#N/A	0.00075	-2.08	#N/A	Transcribed locus	
Ssc.24630.1.A1_at	NM_016045	0.00060	-2.09	chromosome 20 open reading frame 45	Clone Clu_13954.scr.msk.p1.Contig1, mRNA sequence	
Ssc.3802.1.S1_at	NM_139207	0.00098	-2.1	nucleosome assembly protein 1-like 1	Transcribed locus, weakly similar to NP_004528.1 nucleosome assembly protein 1-like 1; HSP22-like protein interacting protein; NAP-1 related protein [Homo sapiens]	
Ssc.4863.1.S1_at	NM_003798	0.00066	-2.12	catenin	Transcribed locus, strongly similar to NP_003789.1 catenin (cadherin-associated protein), alpha-like 1; alpha-catulin [Homo sapiens]	
Ssc.22083.1.S1_at	NM_005746	0.00070	-2.12	pre-B-cell colony enhancing factor 1	Pre-B-cell colony enhancing factor 1 transcript variant 1 (PBEF1)	
Ssc.24556.2.S1_a_at	NM_025181	0.00076	-2.13	solute carrier family 35; member F5	Transcribed locus, strongly similar to NP_079457.2 solute carrier family 35,	

					member F5 [Homo sapiens]	
Ssc.3666.1.A1_at	#N/A	0.00035	-2.13	#N/A	Transcribed locus	
Ssc.13793.2.S1_at	NM_006479	0.00037	-2.15	RAD51 associated protein 1	Transcribed locus, moderately similar to NP_006470.1 RAD51-interacting protein [Homo sapiens]	
Ssc.6618.1.A1_at	XM_290546	0.00023	-2.15	KIAA0830 protein	Transcribed locus	
Ssc.24870.1.S1_at	NM_005100	0.00058	-2.17	A kinase	Transcribed locus, moderately similar to XP_533451.1 PREDICTED: hypothetical protein XP_533451 [Canis familiaris]	
Ssc.7106.1.S1_at	NM_001801	0.00006	-2.18	cysteine dioxygenase; type I	Clone Clu_1053.scr.msk.p1.Contig1, mRNA sequence	
Ssc.26446.1.S1_at	NM_015143	0.00075	-2.18	methionyl aminopeptidase 1	Transcribed locus, strongly similar to NP_780433.1 methionyl aminopeptidase 1 [Mus musculus]	
Ssc.1429.1.A1_at	NM_004537	0.00041	-2.21	nucleosome assembly protein 1-like 1	Clone Clu_594.scr.msk.p1.Contig8, mRNA sequence	
Ssc.11450.1.S1_at	NM_001288	0.00014	-2.22	chloride intracellular channel 1	chloride intracellular channel 1	CLIC1
Ssc.24403.1.S1_at	NM_002040	0.00096	-2.22	GA binding protein transcription factor; alpha subunit 60k	Transcribed locus, strongly similar to NP_002031.2 GA binding protein transcription factor, alpha subunit (60kD); GA-binding protein transcription factor, alpha subunit (60kD); human nuclear respiratory factor-2 subunit alpha [Homo sapiens]	
Ssc.2963.1.S1_at	#N/A	0.00073	-2.22	#N/A	Transcribed locus	
Ssc.23953.1.S1_at	NM_022484	0.00098	-2.23	hypothetical protein FLJ13576	Transcribed locus	
Ssc.6940.1.A1_at	NM_022337	0.00096	-2.25	RAB38; member RAS oncogene family	Transcribed locus, strongly similar to XP_542265.1 PREDICTED: similar to RAB38 [Canis familiaris]	
Ssc.8577.1.A1_at	NM_152265	0.00031	-2.26	basic transcription factor 3-like 4	Transcribed locus	
Ssc.11714.2.A1_at	#N/A	0.00064	-2.3	#N/A	Transcribed locus, strongly similar to hypothetical protein dJ122O8.2 [Homo sapiens]	

Ssc.16722.2.S1_at	NM_152391	0.00061	-2.31	chromosome 2 open reading frame 22	Transcribed locus, moderately similar to NP_689604.1 hypothetical protein MGC33602 [Homo sapiens]	
Ssc.17965.1.S1_at	NM_153347	0.00025	-2.31	hypothetical protein FLJ90119	Transcribed locus, strongly similar to XP_521860.1 PREDICTED: similar to hypothetical protein FLJ90119 [Pan troglodytes]	
Ssc.8027.1.A1_at	NM_001018057	0.00094	-2.33	dickkopf homolog 3	Transcribed locus, moderately similar to Dickkopf related protein-3 precursor (Dkk-3) (Dickkopf-3) (hDkk-3) (UNQ258/PRO295) [Canis familiaris]	
Ssc.3452.1.A1_at	NM_182540	0.00002	-2.34	DEADH	Transcribed locus	
Ssc.15740.2.S1_a_at	NM_003376	0.00052	-2.38	vascular endothelial growth factor	vascular endothelial growth factor	VEGFA
Ssc.21922.1.S1_at	NM_021630	0.00019	-2.43	PDZ and LIM domain 2	Transcribed locus, strongly similar to NP_067643.2 PDZ and LIM domain 2 isoform 2; mystique [Homo sapiens]	
Ssc.21101.1.S1_at	NM_000688	0.00029	-2.47	aminolevulinate; delta-; synthase 1	Transcribed locus, strongly similar to NP_000679.1 aminolevulinate, delta, synthase 1 [Homo sapiens]	
Ssc.24795.1.A1_at	#N/A	0.00010	-2.47	#N/A	Transcribed locus, strongly similar to NP_079184.1 hypothetical protein FLJ12973 [Homo sapiens]	
Ssc.29247.1.A1_at	#N/A	0.00010	-2.51	#N/A	Transcribed locus	
Ssc.19150.1.S1_at	NM_197966	0.00035	-2.55	BH3 interacting domain death agonist	BH3 interacting domain death agonist	BID
Ssc.26621.1.S1_at	NM_153694	0.00040	-2.56	synaptonemal complex protein 3	Transcribed locus, moderately similar to NP_710161.1 synaptonemal complex protein 3 [Homo sapiens]	
Ssc.10263.1.A1_at	NM_152903	0.00034	-2.59	kelch repeat and BTB	Transcribed locus	
Ssc.10226.1.A2_at	NM_004040	0.00079	-2.63	ras homolog gene family; member B	Transcribed locus, strongly similar to NP_786886.1 ras homolog gene family, member C; Aplysia RAS-related homolog 9 (oncogene RHO H9); RAS homolog gene family, member C (oncogene RHO H9)	

Ssc.22261.1.S1_at	NM_017686	0.00027	-2.64	ganglioside induced differentiation associated protein 2	Transcribed locus, strongly similar to ganglioside induced differentiation associated protein 2 [Homo sapiens]	
Ssc.1058.1.S1_at	NM_007285	0.00087	-2.65	GABA	Clone Clu_4417.scr.msk.p1.Contig2, mRNA sequence	
Ssc.1432.1.A1_at	NM_000413	0.00008	-2.66	hydroxysteroid	Transcribed locus, moderately similar to NP_000404.1 hydroxysteroid (17-beta) dehydrogenase 1; Estradiol 17-beta-dehydrogenase-1 [Homo sapiens]	
Ssc.23809.2.S1_at	#N/A	0.00063	-2.67	#N/A	Transcribed locus	
Ssc.2165.2.S1_a_at	NM_006142	0.00038	-2.7	stratifin	Transcribed locus, strongly similar to XP_544477.1 PREDICTED: similar to stratifin [Canis familiaris]	
Ssc.24968.2.S1_at	NM_014062	0.00019	-2.7	nin one binding protein	Transcribed locus, strongly similar to XP_546853.1 PREDICTED: similar to nin one binding protein [Canis familiaris]	
Ssc.5389.2.S1_at	NM_005530	0.00055	-2.71	isocitrate dehydrogenase 3	Clone Clu_241.scr.msk.p1.Contig4, mRNA sequence	
Ssc.24970.2.S1_at	NM_032839	0.00066	-2.73	disrupted in renal carcinoma 2	Transcribed locus, strongly similar to NP_116228.1 disrupted in renal carcinoma 2; Renal cell carcinoma 4 [Homo sapiens]	
Ssc.24430.1.S1_at	NM_033274	0.00057	-2.75	a disintegrin and metalloproteinase domain 19	Transcribed locus	
Ssc.383.1.S1_at	NM_139212	0.00068	-2.81	homeodomain-only protein	odd homeobox 1 protein	OB1
Ssc.3088.1.S1_at	#N/A	0.00067	-2.83	#N/A	Transcribed locus	
Ssc.8213.2.A1_at	NM_024613	0.00068	-2.9	pleckstrin homology domain containing; family F	Transcribed locus	
Ssc.21248.1.S1_at	NM_022047	0.00007	-3.03	differentially expressed in FDCP 6 homolog	Transcribed locus, strongly similar to XP_518424.1 PREDICTED: similar to differentially expressed in FDCP 6 homolog; IRF4-binding protein [Pan troglodytes]	
Ssc.4891.1.A1_at	NM_032717	0.00020	-3.04	hypothetical protein MGC11324	Transcribed locus, moderately similar to NP_061213.2 putative	

					lysophosphatidic acid acyltransferase [Mus musculus]	
Ssc.25577.1.S1_at	#N/A	0.00012	-3.39	#N/A	Transcribed locus	
Ssc.24921.3.S1_a_at	NM_199166	0.00080	-3.67	aminolevulinate; delta-; synthase 1	Transcribed locus, moderately similar to NP_000679.1 aminolevulinate, delta, synthase 1 [Homo sapiens]	
Ssc.3442.1.S1_at	#N/A	0.00029	-3.73	#N/A	Transcribed locus	
Ssc.7602.1.A1_at	#N/A	0.00001	-3.77	#N/A	Transcribed locus	
Ssc.9392.2.S1_at	#N/A	0.00054	-3.95	#N/A	Transcribed locus	
Ssc.5404.1.S1_at	NM_019556	0.00015	-4.05	motile sperm domain containing 1	Transcribed locus	
Ssc.9392.3.A1_at	#N/A	0.00069	-4.26	#N/A	Transcribed locus	
Ssc.25037.2.S1_at	NM_016300	0.00058	-4.33	cyclic AMP-regulated phosphoprotein; 21 kD	Transcribed locus, strongly similar to XP_526169.1 PREDICTED: similar to cyclic AMP-regulated phosphoprotein, 21 kD isoform 1 [Pan troglodytes]	
Ssc.7568.1.A1_at	XM_378780	0.00009	-4.35	hypothetical protein LOC126536	Transcribed locus	
Ssc.20489.1.S1_at	NM_002391	0.00046	-4.52	midkine	Clone rese36c_i5.y1.abd, mRNA sequence	
Ssc.27614.1.S1_at	NM_013402	0.00014	-4.73	fatty acid desaturase 1	delta-5 fatty acid desaturase	FADS1
Ssc.1595.1.S1_a_at	#N/A	0.00047	-5.04	#N/A	Transcribed locus	
Ssc.23963.1.S1_at	NM_014059	0.00030	-5.16	response gene to complement 32	Clone rmed06c_i24.y1.abd, mRNA sequence	
Ssc.26868.1.S1_at	NM_002863	0.00016	-5.19	phosphorylase; glycogen; liver	Transcribed locus, moderately similar to XP_537443.1 PREDICTED: similar to liver glycogen phosphorylase [Canis familiaris]	
Ssc.1303.1.S1_at	NM_030666	0.00048	-5.58	serine	Transcribed locus, weakly similar to XP_541071.1 PREDICTED: hypothetical protein XP_541071 [Canis familiaris]	
Ssc.1013.1.A1_at	NM_145792	0.00084	-5.75	microsomal glutathione S-transferase 1	glutathione S-transferase	MGST1
Ssc.18343.1.A1_at	NM_001006625	0.00009	-5.98	lung type-I cell membrane-associated glycoprotein	Transcribed locus	

Ssc.6940.1.A1_s_at	NM_022337	0.00007	-6.75	RAB38; member RAS oncogene family	Transcribed locus, strongly similar to XP_542265.1 PREDICTED: similar to RAB38 [Canis familiaris]	
Ssc.115.1.S1_s_at	NM_002133	0.00040	-6.9	heme oxygenase	heme oxygenase	HMOX1
Ssc.881.1.S1_at	NM_145202	0.00026	-8.02	proline-rich acidic protein 1	Transcribed locus, weakly similar to proline-rich acidic protein 1; uterine-specific proline-rich acidic protein [Homo sapiens]	
Ssc.14484.1.A1_at	NM_031226	0.00077	-10.64	cytochrome P450; family 19; subfamily A; polypeptide 1	cytochrome P450 19A1	CYP19A1
Ssc.27256.1.S1_at	NM_000405	0.00010	-12.76	GM2 ganglioside activator	Transcribed locus, moderately similar to NP_000396.2 GM2 ganglioside activator precursor; cerebroside sulfate activator protein; sphingolipid activator protein 3; GM2 ganglioside activator protein [Homo sapiens]	
Ssc.2825.1.S1_at	#N/A	0.00051	-12.92	#N/A	Transcribed locus, moderately similar to XP_538963.1 PREDICTED: similar to Glutathione S-transferase 8 (GST 8-8) (Chain 8) (GST class-alpha) [Canis familiaris]	
Ssc.279.1.S2_at	NM_000349	0.00021	-63.67	steroidogenic acute regulator	steroidogenic acute regulatory protein	STAR
Ssc.26876.1.A1_at	#N/A	0.00031	-66.94	#N/A	Transcribed locus	

[a]The Affymetrix ID is specific to a porcine sequence for which a specific probe set was designed to interrogate.
[b]GenBank Accession number assigned for those genes, as associated with the Affymetrix ID, having homology to annotated human genes.
[c]The probability for statistical differences was determined using unpaired t-tests via dChip described in Chapter 3.
[d]Only those genes significantly different and with a fold change equal or greater than 2.0 were included.
[e]This annotation refers to the targets whose interrogated sequence had significant homology to an annotated human sequence.
[f]This annotation was assigned by Affymetrix.
[g]Acronyms for genes have been assigned by Affymetrix.

Table A.3 Genes grouped within a k-means cluster in association with their putative identity.

K-Means Cluster[a]	Affymetrix ID[b]	Expression Comparison[c] S vs. T	S vs. D12F	S vs. D14F	NM Accession Number[d]	NM Annotation[e]
Cluster 1	Ssc.28006.1.A1_at	1.4	2.5	7.4	NM_152526	amyotrophic lateral sclerosis 2
	Ssc.26224.1.S1_at	1.6	2.1	7.7	NM_199171	transmembrane; prostate androgen induced RNA
	Ssc.27041.1.A1_at	1.2	2.2	7.7	NM_153013	hypothetical protein FLJ30596
	Ssc.8965.1.A1_at	1.7	3.0	7.8	NM_001430	endothelial PAS domain protein 1
	Ssc.14465.1.A1_at	1.5	2.4	7.8	NM_018976	solute carrier family 38; member 2
	Ssc.2047.1.S1_at	-1.1	2.5	8.0	NM_014923	fibronectin type III domain containing 3A
	Ssc.21617.1.A1_at	1.3	2.5	8.0	#N/A	#N/A
	Ssc.16989.1.A1_at	1.2	1.6	8.0	NM_001753	caveolin 1; caveolae protein; 22kDa
	Ssc.8676.1.S1_at	-1.3	3.2	8.1	NM_021005	nuclear receptor subfamily 2; group F; member 2
	Ssc.4511.1.S1_at	1.6	3.1	8.1	NM_004753	dehydrogenasereductase
	Ssc.17283.1.A1_at	1.1	3.2	8.3	#N/A	#N/A
	Ssc.2143.1.S1_at	-1.2	1.7	8.4	#N/A	#N/A
	Ssc.29483.1.A1_at	-1.1	1.1	8.5	#N/A	#N/A
	Ssc.4266.1.S1_at	1.8	2.5	8.6	#N/A	#N/A
	Ssc.18996.1.S1_at	-1.0	2.4	8.6	NM_003963	transmembrane 4 L six family member 5
	Ssc.4676.1.A1_at	-1.0	2.9	8.6	NM_018211	hypothetical protein FLJ10770
	Ssc.7242.1.A1_at	1.1	1.9	8.7	NM_014393	staufen; RNA binding protein; homolog 2
	Ssc.13439.1.A1_at	-1.0	1.2	8.7	#N/A	#N/A
	Ssc.6906.1.A1_at	1.2	3.6	8.9	NM_014923	fibronectin type III domain containing 3A
	Ssc.3373.1.A1_at	-1.2	1.9	9.0	#N/A	#N/A
	Ssc.21113.2.S1_at	1.2	1.6	9.1	#N/A	#N/A
	Ssc.9517.1.A1_at	-1.6	2.8	9.1	NM_000441	solute carrier family 26; member 4
	Ssc.3920.1.S1_at	1.8	2.6	9.1	NM_020182	transmembrane; prostate androgen induced RNA
	Ssc.9154.1.A1_at	-1.8	1.4	9.5	NM_004466	glypican 5
	Ssc.1544.1.S1_at	1.1	1.6	9.6	NM_000257	myosin; heavy polypeptide 7; cardiac muscle; beta
	Ssc.10942.1.S1_at	-1.3	-1.1	9.8	NM_053013	enolase 3
	Ssc.24345.1.S1_at	1.2	1.8	10.0	NM_015556	signal-induced proliferation-associated 1 like 1
	Ssc.29437.1.S1_at	1.2	1.5	10.0	#N/A	#N/A
	n = 28	**1.2**	**2.2**	**8.6**		

Cluster 2	Ssc.28336.1.A1_at	-1.2	2.0	5.1	NM_001018009	SH3-domain binding protein 5
	Ssc.6869.1.A1_at	-1.2	-1.2	5.1	#N/A	#N/A
	Ssc.16027.1.S1_at	1.3	1.9	5.2	NM_003256	tissue inhibitor of metalloproteinase 4
	Ssc.17283.2.S1_at	1.1	2.1	5.2	#N/A	#N/A
	Ssc.30657.1.S1_at	1.4	2.5	5.2	NM_173854	solute carrier family 41; member 1
	Ssc.4914.1.A1_at	1.0	1.5	5.3	NM_032181	hypothetical protein FLJ13391
	Ssc.21848.1.S1_at	1.1	1.6	5.3	NM_014292	chromobox homolog 6
	Ssc.3967.1.A1_at	1.1	1.6	5.4	NM_001497	UDP-Gal:betaGlcNAc beta 1;4- galactosyltransferase;
	Ssc.10801.1.A1_at	-1.1	1.8	5.4	NM_173552	hypothetical protein MGC33365
	Ssc.29473.1.A1_at	-1.0	2.3	5.4	#N/A	#N/A
	Ssc.15886.1.S1_at	1.2	2.8	5.4	NM_032991	caspase 3; apoptosis-related cysteine protease
	Ssc.18224.1.S1_at	1.1	2.8	5.4	#N/A	#N/A
	Ssc.30550.1.A1_at	1.1	-1.0	5.5	#N/A	#N/A
	Ssc.11555.1.S1_at	1.2	2.5	5.5	NM_015544	DKFZP564K1964 protein
	Ssc.2697.1.S1_at	-1.1	1.5	5.5	#N/A	#N/A
	Ssc.22248.1.A1_at	1.0	1.7	5.6	#N/A	#N/A
	Ssc.10731.1.A1_at	-1.0	1.0	5.6	NM_002581	pregnancy-associated plasma protein A; pappalysin 1
	Ssc.19579.3.S1_at	-1.1	1.9	5.7	NM_021005	nuclear receptor subfamily 2; group F; member 2
	Ssc.22082.1.A1_at	-1.2	1.1	5.9	#N/A	#N/A
	Ssc.1702.1.S1_at	-1.7	2.3	5.9	NM_145290	G protein-coupled receptor 125
	Ssc.8516.1.A1_at	1.2	1.9	6.0	NM_145740	glutathione S-transferase A1
	Ssc.889.1.A1_a_at	1.3	1.5	6.0	NM_002614	PDZ domain containing 1
	Ssc.1276.1.S1_at	1.1	2.7	6.0	NM_002165	inhibitor of DNA binding 1; dominant negative helix-loop-h
	Ssc.18996.2.A1_a_at	-1.0	1.8	6.0	NM_003963	transmembrane 4 L six family member 5
	Ssc.8479.1.A1_at	1.2	1.2	6.2	NM_005410	selenoprotein P; plasma; 1
	Ssc.13553.1.A1_at	-1.2	2.8	6.3	#N/A	#N/A
	Ssc.3549.1.S1_at	1.7	3.2	6.4	NM_001430	endothelial PAS domain protein 1
	Ssc.15648.1.S1_at	1.4	3.1	6.4	XM_043653	brain expressed X-linked-like 1
	Ssc.12102.1.A1_at	1.2	2.5	6.5	NM_014668	GREB1 protein
	Ssc.11187.1.S1_at	1.1	3.0	6.5	NM_000201	intercellular adhesion molecule 1
	Ssc.1882.1.S1_at	-1.5	1.7	6.5	NM_000141	fibroblast growth factor receptor 2
	Ssc.14376.1.A1_at	-1.2	2.5	6.6	#N/A	#N/A
	Ssc.11374.1.S1_at	-1.1	2.8	6.6	NM_015696	glutathione peroxidase 7

Cluster 2 cont.	Ssc.1866.1.S1_at	1.1	2.0	6.7	NM_032876	jub; ajuba homolog
	Ssc.30465.1.A1_at	1.1	2.5	6.9	#N/A	#N/A
	Ssc.5260.1.A1_at	1.3	2.1	7.0	#N/A	#N/A
	n = 36	**1.1**	**2.0**	**5.9**		
Cluster 3	Ssc.15335.1.S1_at	2.0	6.1	6.3	#N/A	#N/A
	Ssc.14419.1.S1_at	-1.0	3.8	6.6	XM_376652	distal-less homeo box 6
	Ssc.8562.3.A1_at	2.6	3.9	6.6	NM_001901	connective tissue growth factor
	Ssc.1407.1.A1_at	1.6	5.8	6.7	NM_007203	PALM2-AKAP2 protein
	Ssc.3853.1.S1_at	1.3	3.6	6.7	NM_004816	chromosome 9 open reading frame 61
	Ssc.13665.1.A1_at	-1.3	6.0	6.7	NM_006089	sex comb on midleg-like 2
	Ssc.26944.1.S1_at	1.5	4.4	7.0	#N/A	#N/A
	Ssc.21647.1.A1_at	1.1	5.9	7.4	NM_018131	chromosome 10 open reading frame 3
	Ssc.1407.2.S1_at	1.5	5.7	7.4	NM_007203	PALM2-AKAP2 protein
	Ssc.30789.1.A1_at	1.5	3.8	7.4	#N/A	#N/A
	Ssc.9537.1.S1_at	-1.1	4.7	7.6	NM_012342	BMP and activin membrane-bound inhibitor homolog
	Ssc.7944.1.A1_at	-1.2	4.2	8.0	#N/A	#N/A
	Ssc.24190.1.S1_at	1.5	4.8	8.5	NM_003865	homeo box
	Ssc.14126.1.A1_at	2.0	4.8	8.6	#N/A	#N/A
	Ssc.2976.1.S1_at	1.2	5.1	8.6	NM_004821	heart and neural crest derivatives expressed 1
	Ssc.23944.1.A1_at	1.0	4.9	8.8	#N/A	#N/A
	Ssc.29811.1.A1_at	1.5	5.3	9.0	NM_147150	PALM2-AKAP2 protein
	Ssc.27404.1.S1_at	1.7	4.5	9.1	NM_004405	distal-less homeo box 2
	Ssc.11757.1.S1_at	1.1	5.3	9.6	NM_001003688	SMAD; mothers against DPP homolog 1
	n = 19	**1.4**	**4.9**	**7.7**		
Cluster 4	Ssc.21175.1.S1_at	2.6	2.6	-6.9	NM_001017372	solute carrier family 27
	Ssc.1013.1.A1_at	2.1	2.3	-2.5	NM_145792	microsomal glutathione S-transferase 1
	Ssc.115.1.S1_s_at	1.2	3.2	-2.2	NM_002133	heme oxygenase
	Ssc.27614.1.S1_at	1.8	3.2	-1.5	NM_013402	fatty acid desaturase 1
	Ssc.1595.1.S1_a_at	1.8	3.6	-1.4	#N/A	#N/A
	Ssc.26446.2.S1_a_at	1.1	3.3	-1.0	NM_015143	methionyl aminopeptidase 1
	Ssc.3088.1.S1_at	1.1	3.0	1.1	#N/A	#N/A
	Ssc.27454.3.S1_a_at	-1.3	3.4	1.1	NM_004044	5-aminoimidazole-4-carboxamide ribonucleotide formyltransf
	Ssc.27454.2.S1_at	-1.2	3.4	1.1	NM_004044	5-aminoimidazole-4-carboxamide ribonucleotide formyltransf

Cluster 4 cont.	Ssc.8027.1.A1_at	1.3	2.8	1.2	NM_001018057	dickkopf homolog 3
	Ssc.21922.1.S1_at	2.9	3.2	1.3	NM_021630	PDZ and LIM domain 2
	Ssc.383.1.S1_at	1.2	3.9	1.4	NM_139212	homeodomain-only protein
	Ssc.17206.1.A1_at	1.7	4.7	1.4	NM_133367	progestin and adipoQ receptor family member VIII
	Ssc.15740.2.S1_a_at	1.0	3.7	1.6	NM_003376	vascular endothelial growth factor
	Ssc.15740.1.S2_at	-1.1	3.9	1.8	NM_003376	vascular endothelial growth factor
	Ssc.10319.1.A1_at	1.3	4.0	2.2	NM_023016	chromosome 2 open reading frame 26
	Ssc.22043.1.S1_at	-1.4	4.3	2.4	NM_001546	inhibitor of DNA binding 4; dominant negative helix-loop-h
	n = 17	**1.4**	**3.4**	**1.2**		
Cluster 5	Ssc.279.1.S2_at	1.7	1.2	-54.0	NM_000349	steroidogenic acute regulator
	Ssc.27593.1.S1_at	2.3	-6.9	-46.0	NM_003239	transforming growth factor; beta 3
	Ssc.279.1.S1_at	2.0	1.4	-37.1	NM_000349	steroidogenic acute regulator
	Ssc.6138.1.S1_at	2.5	-6.3	-10.8	#N/A	#N/A
	Ssc.22559.1.S1_at	2.3	-2.2	-10.5	#N/A	#N/A
	Ssc.4415.1.S1_at	2.2	-3.7	-5.7	NM_000697	arachidonate 12-lipoxygenase
	Ssc.3102.1.S1_at	2.0	1.2	-5.6	NM_012152	endothelial differentiation; lysophosphatidic acid G-protei
	Ssc.5396.1.S1_at	2.9	1.7	-4.6	NM_198392	transcription factor 21
	Ssc.15588.1.S2_at	3.1	-3.2	-4.4	NM_000598	insulin-like growth factor binding protein 3
	Ssc.20017.2.S1_at	1.8	-1.4	-4.3	NM_005964	myosin; heavy polypeptide 10; non-muscle
	Ssc.14085.1.A1_at	1.9	-1.6	-4.0	#N/A	#N/A
	Ssc.5471.1.A1_at	1.9	-4.0	-3.9	#N/A	#N/A
	Ssc.7157.1.A1_at	2.1	-1.1	-3.4	NM_000519	hemoglobin; delta
	Ssc.26781.1.A1_at	1.9	-2.5	-3.4	#N/A	#N/A
	Ssc.4580.1.A1_at	1.9	-1.3	-2.9	NM_152277	dendritic cell-derived ubiquitin-like protein
	Ssc.12356.1.A1_at	2.1	-1.0	-2.2	NM_024315	chromosome 7 open reading frame 23
	Ssc.7403.1.A1_at	2.1	-1.2	-1.8	#N/A	#N/A
	Ssc.27288.1.S1_at	2.3	1.1	-1.8	NM_033505	selenoprotein I
	Ssc.28471.2.S1_at	2.2	1.1	-1.7	NM_001894	casein kinase 1; epsilon
	Ssc.14204.3.S1_at	2.9	-1.2	-1.7	#N/A	#N/A
	Ssc.14204.1.A1_at	2.7	-1.3	-1.4	#N/A	#N/A
	Ssc.4127.2.A1_at	2.1	-1.1	-1.3	NM_005168	Rho family GTPase 3
	Ssc.4127.1.A1_at	2.4	1.3	-1.3	NM_005168	Rho family GTPase 3
	Ssc.16202.1.S1_at	2.7	-1.6	-1.3	#N/A	#N/A

Cluster 5 cont.	Ssc.9607.1.A1_at	2.9	-2.3	-1.2	NM_203417	Down syndrome critical region gene 1
	Ssc.3189.1.A1_at	2.1	-2.5	1.1	NM_004414	Down syndrome critical region gene 1
	n = 26	**2.3**	**-1.3**	**-2.5**		
Cluster 6	Ssc.3673.1.S1_at	1.4	-5.3	-125.9	NM_003049	solute carrier family 10
	Ssc.26876.1.A1_at	1.1	-1.8	-120.0	#N/A	#N/A
	Ssc.14095.1.A1_at	1.6	-6.2	-28.6	#N/A	#N/A
	Ssc.14484.3.A1_a_at	1.5	-1.4	-27.7	NM_031226	cytochrome P450; family 19; subfamily A; polypeptide 1
	Ssc.14541.1.S1_s_at	1.4	-1.5	-25.5	NM_031226	cytochrome P450; family 19; subfamily A; polypeptide 1
	Ssc.27433.1.S1_at	1.5	-9.0	-20.0	NM_000359	transglutaminase 1
	Ssc.14484.1.A1_at	1.2	-1.6	-16.8	NM_031226	cytochrome P450; family 19; subfamily A; polypeptide 1
	Ssc.7751.1.A1_at	1.5	-7.2	-16.7	#N/A	#N/A
	Ssc.2282.1.A1_at	1.4	-4.3	-14.3	NM_016357	epithelial protein lost in neoplasm beta
	Ssc.6940.1.A1_s_at	1.2	-2.0	-13.2	NM_022337	RAB38; member RAS oncogene family
	Ssc.6055.1.A1_at	1.4	-8.9	-10.5	NM_181785	hypothetical protein LOC283537
	Ssc.5404.1.S1_at	1.1	-2.4	-9.6	NM_019556	motile sperm domain containing 1
	Ssc.27480.1.S1_at	1.4	-1.7	-9.3	NM_003212	teratocarcinoma-derived growth factor 1
	Ssc.14484.3.S1_at	1.5	-1.3	-9.2	NM_031226	cytochrome P450; family 19; subfamily A; polypeptide 1
	Ssc.6219.1.A1_at	1.4	-2.5	-8.5	#N/A	#N/A
	Ssc.7565.2.S1_at	1.6	-3.0	-8.2	#N/A	#N/A
	Ssc.14422.2.S1_at	1.6	-4.0	-8.2	NM_016206	vestigial-like 3
	Ssc.4272.1.A1_at	1.4	-6.4	-8.1	#N/A	#N/A
	Ssc.14422.1.A1_at	1.5	-3.9	-7.8	#N/A	#N/A
	Ssc.1310.1.S1_at	1.2	-1.9	-7.2	NM_004878	prostaglandin E synthase
	Ssc.18343.1.A1_at	1.1	-1.2	-6.9	NM_001006625	lung type-I cell membrane-associated glycoprotein
	Ssc.26868.1.S1_at	-1.0	-1.3	-6.9	NM_002863	phosphorylase; glycogen; liver
	Ssc.2237.1.A1_at	1.3	-3.1	-6.9	NM_016206	vestigial-like 3
	Ssc.24136.1.A1_at	1.8	-4.8	-6.4	#N/A	#N/A
	Ssc.7470.1.S1_at	1.2	-1.7	-6.4	NM_003212	teratocarcinoma-derived growth factor 1
	Ssc.14533.1.S1_at	1.2	-2.6	-6.4	NM_002910	renin binding protein
	Ssc.7565.1.A1_at	1.3	-3.6	-6.2	NM_016206	vestigial-like 3
	Ssc.20489.1.S1_at	1.2	-1.4	-6.2	NM_002391	midkine
	Ssc.7116.1.A1_at	1.5	-4.6	-6.2	NM_016489	5-nucleotidase; cytosolic III
	Ssc.8213.2.A1_at	1.2	-2.0	-5.9	NM_024613	pleckstrin homology domain containing; family F

Cluster 6 cont.	Ssc.6276.2.S1_at	1.5	-2.8	-5.7	NM_020676	abhydrolase domain containing 6
	Ssc.6276.1.S1_at	1.3	-2.9	-5.5	NM_020676	abhydrolase domain containing 6
	Ssc.9740.1.A1_at	1.7	-2.6	-5.4	#N/A	#N/A
	Ssc.14114.1.A1_at	1.5	-2.6	-5.4	NM_002858	ATP-binding cassette; sub-family D
	Ssc.24018.1.S1_at	1.3	-1.4	-5.3	#N/A	#N/A
	Ssc.2165.2.S1_a_at	1.3	-1.9	-5.2	NM_006142	stratifin
	Ssc.1477.1.A1_at	1.2	-2.8	-5.2	#N/A	#N/A
	Ssc.6654.1.A1_at	1.5	-4.9	-5.0	#N/A	#N/A
	Ssc.4891.1.A1_at	1.5	-1.6	-5.0	NM_032717	hypothetical protein MGC11324
	Ssc.14470.1.S1_at	1.6	-1.4	-4.9	NM_002444	moesin
	Ssc.26809.1.A1_at	1.7	-3.2	-4.8	NM_021020	leucine zipper; putative tumor suppressor 1
	Ssc.231.1.S2_at	1.3	-1.4	-4.7	NM_004109	ferredoxin 1
	Ssc.21917.3.S1_at	1.3	-1.8	-4.7	NM_017882	ceroid-lipofuscinosis; neuronal 6; late infantile; variant
	Ssc.529.1.S1_at	1.0	-1.4	-4.7	NM_006432	Niemann-Pick disease; type C2
	Ssc.28162.1.A1_at	1.2	-2.2	-4.7	NM_018841	guanine nucleotide binding protein
	Ssc.7602.1.A1_at	1.5	-1.2	-4.6	#N/A	#N/A
	Ssc.11816.1.A1_at	1.4	-2.2	-4.6	NM_002858	ATP-binding cassette; sub-family D
	Ssc.18377.3.S1_a_at	1.3	-1.7	-4.5	NM_002560	purinergic receptor P2X; ligand-gated ion channel; 4
	Ssc.9739.1.A1_at	1.5	-2.7	-4.5	#N/A	#N/A
	Ssc.13587.1.A1_at	1.4	-2.0	-4.5	NM_001149	ankyrin 3; node of Ranvier
	Ssc.13587.2.S1_at	1.4	-2.6	-4.4	NM_001149	ankyrin 3; node of Ranvier
	Ssc.21016.1.S1_at	1.2	-2.1	-4.4	NM_002906	radixin
	Ssc.12832.1.A1_at	1.4	-2.5	-4.4	NM_052873	MGC16028 similar to RIKEN cDNA 1700019E19 gene
	Ssc.1028.1.S1_at	1.3	-3.4	-4.4	NM_032312	hypothetical protein MGC11061
	Ssc.19659.2.S1_at	1.5	1.2	-4.3	NM_005768	putative protein similar to nessy
	Ssc.18377.3.S1_at	1.3	-1.5	-4.3	NM_002560	purinergic receptor P2X; ligand-gated ion channel; 4
	Ssc.9392.3.A1_at	1.6	-1.0	-4.3	#N/A	#N/A
	Ssc.22399.1.A1_at	1.3	-4.0	-4.2	#N/A	#N/A
	Ssc.1817.1.S1_at	1.3	-2.7	-4.2	NM_020728	family with sequence similarity 62
	Ssc.31120.1.A1_at	1.4	-1.9	-4.1	NM_003743	nuclear receptor coactivator 1
	Ssc.1434.1.A1_at	1.1	-1.8	-4.1	NM_013974	dimethylarginine dimethylaminohydrolase 2
	Ssc.29106.1.S1_at	1.3	-1.7	-4.1	#N/A	#N/A
	Ssc.6940.1.A1_at	1.1	-1.8	-4.1	NM_022337	RAB38; member RAS oncogene family

Cluster 6 cont.	Ssc.17427.1.S1_at	1.3	-1.7	-4.0	NM_006317	brain abundant; membrane attached signal protein 1
	Ssc.6812.1.A1_at	1.1	-1.9	-4.0	#N/A	#N/A
	Ssc.5941.2.S1_at	1.3	-1.4	-4.0	NM_001102	actinin; alpha 1
	Ssc.6163.1.A1_at	1.6	-3.3	-4.0	NM_005239	v-ets erythroblastosis virus E26 oncogene homolog 2
	Ssc.20489.1.S1_s_at	1.1	-1.3	-4.0	NM_002391	midkine
	Ssc.9392.2.S1_at	1.6	-1.0	-4.0	#N/A	#N/A
	Ssc.6163.2.S1_at	1.7	-2.8	-3.9	NM_005239	v-ets erythroblastosis virus E26 oncogene homolog 2
	Ssc.11528.1.A1_at	1.5	-2.9	-3.9	NM_014622	loss of heterozygosity; 11; chromosomal region 2; gene A
	Ssc.1414.1.A1_at	1.5	-2.3	-3.9	NM_147223	nuclear receptor coactivator 1
	Ssc.18377.1.S1_at	1.3	-1.7	-3.9	NM_175567	purinergic receptor P2X; ligand-gated ion channel; 4
	Ssc.21917.1.S1_a_at	1.3	-1.8	-3.9	#N/A	#N/A
	Ssc.3079.1.S1_at	1.4	-3.0	-3.9	NM_012396	pleckstrin homology-like domain; family A; member 3
	Ssc.26816.1.S1_at	1.5	-5.4	-3.9	NM_145176	solute carrier family 2
	Ssc.19688.1.S1_at	1.3	-2.8	-3.8	NM_000079	cholinergic receptor; nicotinic; alpha polypeptide 1
	Ssc.24970.2.S1_at	1.2	-1.4	-3.8	NM_032839	disrupted in renal carcinoma 2
	Ssc.22120.1.S1_a_at	1.2	-2.2	-3.8	NM_001017927	hypothetical protein LOC130355
	Ssc.21382.1.A1_at	1.2	-4.3	-3.7	NM_004419	dual specificity phosphatase 5
	Ssc.29852.1.A1_at	1.2	-1.9	-3.7	#N/A	#N/A
	Ssc.11450.1.S1_at	1.0	-1.7	-3.7	NM_001288	chloride intracellular channel 1
	Ssc.6365.1.A1_at	1.8	-2.1	-3.6	NM_033071	spectrin repeat containing; nuclear envelope 1
	Ssc.25037.2.S1_at	-1.2	1.2	-3.6	NM_016300	cyclic AMP-regulated phosphoprotein; 21 kD
	Ssc.27588.1.S1_at	1.2	-2.9	-3.6	NM_014861	KIAA0703 gene product
	Ssc.18612.1.S1_at	1.1	-1.4	-3.6	#N/A	#N/A
	Ssc.25059.1.A1_at	1.2	-1.8	-3.6	NM_019850	neuronal guanine nucleotide exchange factor
	Ssc.4739.1.S1_at	1.2	-2.7	-3.6	NM_024959	solute carrier family 24
	Ssc.5620.1.A1_at	1.3	-2.9	-3.6	NM_005749	transducer of ERBB2; 1
	Ssc.14257.1.A1_at	1.2	-2.3	-3.6	NM_005749	transducer of ERBB2; 1
	Ssc.8700.1.A1_at	1.2	-1.7	-3.5	NM_005968	heterogeneous nuclear ribonucleoprotein M
	Ssc.1414.2.S1_at	1.4	-1.7	-3.5	NM_003743	nuclear receptor coactivator 1
	Ssc.11816.2.A1_a_at	1.3	-2.3	-3.5	NM_002858	ATP-binding cassette; sub-family D
	Ssc.1432.1.A1_at	1.1	-1.3	-3.4	NM_000413	hydroxysteroid
	Ssc.9918.1.A1_at	1.2	-2.3	-3.4	NM_004504	HIV-1 Rev binding protein
	Ssc.30951.1.A1_at	1.1	-1.7	-3.4	NM_006350	follistatin

Cluster 6 cont.	Ssc.24817.1.A1_at	1.4	-2.3	-3.4	#N/A	#N/A
	Ssc.13729.1.A1_at	1.1	-1.8	-3.4	#N/A	#N/A
	Ssc.5554.1.S1_at	1.3	-1.1	-3.4	NM_030579	outer mitochondrial membrane cytochrome b5
	Ssc.17250.1.S1_at	1.1	-2.1	-3.3	NM_000320	quinoid dihydropteridine reductase
	Ssc.11577.1.A1_at	1.3	-1.4	-3.3	#N/A	#N/A
	Ssc.22641.3.S1_at	1.1	-1.5	-3.3	NM_003708	retinol dehydrogenase 16
	Ssc.9538.1.S1_at	1.1	-1.7	-3.2	NM_173475	hypothetical protein MGC48972
	Ssc.19602.2.S1_at	1.0	-1.7	-3.2	NM_000086	ceroid-lipofuscinosis; neuronal 3; juvenile
	Ssc.31120.2.S1_at	1.4	-1.7	-3.2	NM_147223	nuclear receptor coactivator 1
	Ssc.21770.1.A1_at	1.4	-1.8	-3.2	NM_013304	zinc finger; DHHC-type containing 1
	Ssc.1199.1.A1_at	1.1	-2.2	-3.2	NM_000414	hydroxysteroid
	Ssc.10226.1.A3_at	1.3	-1.2	-3.2	NM_004040	ras homolog gene family; member B
	Ssc.6916.1.S1_at	1.4	-1.9	-3.2	NM_031206	LAS1-like
	Ssc.14162.1.A1_at	1.4	-3.1	-3.2	#N/A	#N/A
	Ssc.10274.1.A1_at	1.1	-1.9	-3.2	#N/A	#N/A
	Ssc.1414.1.A1_a_at	1.3	-1.9	-3.1	NM_147223	nuclear receptor coactivator 1
	Ssc.18511.1.S1_at	1.3	-1.8	-3.1	NM_152359	carnitine palmitoyltransferase 1C
	Ssc.10226.1.A2_at	1.2	-1.2	-3.1	NM_004040	ras homolog gene family; member B
	Ssc.17400.1.S1_at	1.4	-2.1	-3.1	NM_033071	spectrin repeat containing; nuclear envelope 1
	Ssc.12400.1.S1_at	1.4	-1.9	-3.1	NM_014580	solute carrier family 2;
	Ssc.26621.1.S1_at	1.1	-1.2	-3.1	NM_153694	synaptonemal complex protein 3
	Ssc.14480.1.S1_at	1.3	1.1	-3.1	NM_001221	calciumcalmodulin-dependent protein kinase
	Ssc.18456.2.S1_at	1.6	-2.5	-3.0	NM_005239	v-ets erythroblastosis virus E26 oncogene homolog 2
	Ssc.9284.1.S1_at	1.2	-2.1	-3.0	NM_020728	family with sequence similarity 62
	Ssc.25577.1.S1_at	-1.2	1.1	-3.0	#N/A	#N/A
	Ssc.3666.1.A1_at	1.0	-1.4	-3.0	#N/A	#N/A
	Ssc.235.1.S1_a_at	1.5	-1.9	-3.0	NM_001750	calpastatin
	Ssc.13644.1.A1_at	1.1	-1.5	-3.0	#N/A	#N/A
	Ssc.5362.2.S1_at	1.6	-1.2	-3.0	NM_014397	NIMA
	Ssc.18377.2.S1_at	1.2	-1.9	-2.9	NM_002560	purinergic receptor P2X; ligand-gated ion channel; 4
	Ssc.6078.1.A1_at	1.1	-1.8	-2.9	#N/A	#N/A
	Ssc.3452.1.A1_at	1.0	-1.2	-2.9	NM_182540	DEADH
	Ssc.5362.1.S1_at	1.5	-1.4	-2.9	NM_014397	NIMA

Cluster 6 cont.	Ssc.23809.2.S1_at	1.3	-1.1	-2.9	#N/A	#N/A
	Ssc.19175.2.S1_at	1.4	-4.0	-2.9	#N/A	#N/A
	Ssc.16726.1.A1_at	1.2	-2.5	-2.9	#N/A	#N/A
	Ssc.11790.1.S1_at	1.4	-1.6	-2.9	NM_006224	phosphatidylinositol transfer protein; alpha
	Ssc.14470.1.S2_at	1.3	-1.5	-2.9	NM_002444	moesin
	Ssc.24222.1.A1_at	1.1	-1.6	-2.9	NM_198240	restin
	Ssc.12826.2.A1_a_at	1.2	-2.1	-2.8	NM_138463	hypothetical protein BC014072
	Ssc.10263.1.A1_at	-1.2	-1.1	-2.8	NM_152903	kelch repeat and BTB
	Ssc.2768.1.S1_at	1.3	-1.7	-2.8	#N/A	#N/A
	Ssc.3584.2.S1_at	1.1	-1.4	-2.8	NM_001943	desmoglein 2
	Ssc.16934.1.S1_at	1.1	-2.0	-2.8	NM_024417	ferredoxin reductase
	Ssc.12448.1.S1_at	1.2	-2.0	-2.8	#N/A	#N/A
	Ssc.1367.1.A1_at	1.3	-1.5	-2.8	NM_003114	sperm associated antigen 1
	Ssc.18475.3.A1_at	1.4	-1.2	-2.8	NM_152331	peroxisomal acyl-CoA thioesterase 2B
	Ssc.6425.2.S1_at	1.4	-1.5	-2.8	NM_001023587	ATP-binding cassette; sub-family C
	Ssc.11911.1.A1_at	1.4	-1.5	-2.8	NM_145284	similar to hypothetical protein MGC17347
	Ssc.16722.2.S1_at	1.5	-1.2	-2.8	NM_152391	chromosome 2 open reading frame 22
	Ssc.18718.1.A1_at	1.2	-1.9	-2.8	#N/A	#N/A
	Ssc.24968.2.S1_at	1.4	-1.0	-2.7	NM_014062	nin one binding protein
	Ssc.27241.1.S1_at	1.2	-4.1	-2.7	NM_170692	RAS protein activator like 2
	Ssc.4858.1.S1_at	1.6	-2.4	-2.7	NM_001012515	ferrochelatase
	Ssc.19297.1.S1_at	1.3	-1.6	-2.7	NM_000391	tripeptidyl peptidase I
	Ssc.30898.1.S1_at	1.1	-1.6	-2.7	NM_198240	restin
	Ssc.23758.2.A1_at	1.4	-2.9	-2.7	NM_181785	hypothetical protein LOC283537
	Ssc.3584.3.S1_at	1.0	-1.5	-2.7	NM_001943	desmoglein 2
	Ssc.2491.1.S1_at	1.2	-2.4	-2.7	NM_172169	calciumcalmodulin-dependent protein kinase
	Ssc.16934.2.S1_at	1.3	-1.4	-2.7	NM_024417	ferredoxin reductase
	Ssc.235.2.S1_at	1.5	-2.4	-2.7	NM_001750	calpastatin
	Ssc.4747.1.S1_at	-1.0	-1.7	-2.7	NM_013409	follistatin
	Ssc.231.1.S1_at	1.1	-1.1	-2.7	NM_004109	ferredoxin 1
	Ssc.11096.1.S1_at	1.1	-1.4	-2.7	NM_000436	3-oxoacid CoA transferase 1
	Ssc.27871.2.S1_at	1.2	-1.3	-2.7	NM_139274	acetyl-Coenzyme A synthetase 2
	Ssc.1657.1.S1_at	1.2	-2.1	-2.7	NM_005688	ATP-binding cassette; sub-family C

Cluster 6 cont.	Ssc.29845.1.A1_at	1.1	-2.0	-2.7	NM_022087	UDP-N-acetyl-alpha-D-galactosamine:polypeptide N-acetylgal
	Ssc.17250.1.S1_a_at	1.1	-1.7	-2.7	NM_000320	quinoid dihydropteridine reductase
	Ssc.12474.1.A1_at	1.1	-2.0	-2.7	#N/A	#N/A
	Ssc.20355.1.S1_at	1.3	-2.2	-2.6	NM_015178	Rho-related BTB domain containing 2
	Ssc.11404.1.A1_at	1.1	-2.1	-2.6	NM_000332	ataxin 1
	Ssc.460.1.S1_at	1.3	-1.4	-2.6	NM_012094	peroxiredoxin 5
	Ssc.11770.1.S1_at	1.1	-1.7	-2.6	NM_203352	PDZ and LIM domain 7
	Ssc.8845.1.S1_at	1.2	-1.1	-2.6	NM_001423	epithelial membrane protein 1
	Ssc.23919.1.S1_at	1.2	-1.6	-2.6	#N/A	#N/A
	Ssc.2627.2.S1_at	1.1	-1.5	-2.6	NM_002353	tumor-associated calcium signal transducer 2
	Ssc.13485.1.A1_at	1.3	-2.8	-2.6	#N/A	#N/A
	Ssc.6345.1.S1_at	1.0	-1.5	-2.6	NM_024657	zinc finger; CW type with coiled-coil domain 2
	Ssc.8776.1.S1_at	1.5	1.0	-2.6	NM_000781	cytochrome P450; family 11; subfamily A; polypeptide 1
	Ssc.2768.3.S1_at	1.3	-1.3	-2.5	NM_000437	platelet-activating factor acetylhydrolase 2; 40kDa
	Ssc.773.2.S1_a_at	1.0	-1.7	-2.5	NM_080593	histone 1; H2bk
	Ssc.4046.2.S1_at	1.1	-1.4	-2.5	NM_004341	carbamoyl-phosphate synthetase 2; aspartate transcarbamyla
	Ssc.7435.1.A1_at	1.2	-1.5	-2.5	NM_020474	UDP-N-acetyl-alpha-D-galactosamine:polypeptide N-acetylgal
	Ssc.22526.1.A1_at	1.3	-2.9	-2.5	#N/A	#N/A
	Ssc.7024.1.A1_at	1.1	-2.0	-2.5	#N/A	#N/A
	Ssc.16831.1.S1_at	1.1	-1.9	-2.5	NM_032285	hypothetical protein MGC3207
	Ssc.27871.1.S1_at	1.1	-1.7	-2.5	NM_018677	acetyl-Coenzyme A synthetase 2
	Ssc.17461.1.A1_a_at	-1.0	-1.1	-2.5	NM_004411	dynein; cytoplasmic; intermediate polypeptide 1
	Ssc.1527.2.A1_at	1.4	-1.1	-2.5	NM_005415	solute carrier family 20
	Ssc.6425.3.A1_at	1.3	-1.9	-2.5	NM_001023587	ATP-binding cassette; sub-family C
	Ssc.1876.1.S1_at	1.4	1.0	-2.5	NM_005964	myosin; heavy polypeptide 10; non-muscle
	Ssc.7289.1.A1_at	1.2	-1.6	-2.5	NM_001008392	CTD
	Ssc.828.1.S1_at	1.3	-1.4	-2.5	NM_022911	solute carrier family 26; member 6
	Ssc.3897.1.S1_at	1.4	-1.4	-2.5	NM_138501	glycoprotein; synaptic 2
	Ssc.11790.3.A1_a_at	1.2	-1.8	-2.5	NM_006224	phosphatidylinositol transfer protein; alpha
	Ssc.1018.1.S1_at	1.1	-1.5	-2.5	NM_001752	catalase
	Ssc.2768.2.S1_at	1.3	-1.2	-2.5	NM_000437	platelet-activating factor acetylhydrolase 2; 40kDa
	Ssc.26612.1.S1_a_at	1.4	-1.2	-2.5	NM_153344	chromosome 6 open reading frame 141
	Ssc.16722.1.S1_at	1.1	-1.6	-2.4	NM_152391	chromosome 2 open reading frame 22

Cluster 6 cont.	Ssc.19807.1.S1_at	1.3	-1.5	-2.4	NM_014646	lipin 2
	Ssc.7329.1.A1_at	1.1	-2.0	-2.4	#N/A	#N/A
	Ssc.12013.1.A1_at	1.7	-1.7	-2.4	#N/A	#N/A
	Ssc.30436.1.A1_at	-1.0	-1.0	-2.4	NM_199136	hypothetical protein MGC72075
	Ssc.6236.1.S1_at	1.0	-1.9	-2.4	#N/A	#N/A
	Ssc.24886.1.S1_at	1.4	-1.7	-2.4	NM_001676	ATPase; H+K+ transporting; nongastric; alpha polypeptide
	Ssc.9834.2.S1_at	1.0	-1.5	-2.4	#N/A	#N/A
	Ssc.12209.1.A1_at	1.2	-1.3	-2.4	NM_002610	pyruvate dehydrogenase kinase; isoenzyme 1
	Ssc.27365.1.S1_at	1.1	-1.0	-2.4	NM_014961	rap2 interacting protein x
	Ssc.30592.1.S1_at	1.2	-1.5	-2.4	NM_005605	protein phosphatase 3
	Ssc.15469.1.A1_at	1.2	-2.1	-2.4	NM_016395	butyrate-induced transcript 1
	Ssc.13934.1.A1_at	1.1	-1.6	-2.4	NM_002670	plastin 1
	Ssc.25032.1.S1_at	-1.0	-1.6	-2.4	NM_182728	solute carrier family 7
	Ssc.22923.1.S1_at	1.0	-1.4	-2.4	NM_015687	filamin A interacting protein 1
	Ssc.9918.2.A1_at	1.2	-1.4	-2.4	NM_004504	HIV-1 Rev binding protein
	Ssc.21778.1.S1_at	1.2	-2.6	-2.4	NM_144580	chromosome 1 open reading frame 85
	Ssc.3848.1.S1_at	1.1	-1.7	-2.4	NM_015944	CGI-14 protein
	Ssc.28680.1.S1_at	1.2	-1.6	-2.4	NM_002821	PTK7 protein tyrosine kinase 7
	Ssc.2807.2.A1_at	1.1	-1.4	-2.4	NM_001343	disabled homolog 2; mitogen-responsive phosphoprotein
	Ssc.11338.1.S1_a_at	1.1	-2.0	-2.4	NM_016417	chromosome 14 open reading frame 87
	Ssc.11969.1.A1_at	1.3	-1.3	-2.4	NM_005766	FERM; RhoGEF
	Ssc.26786.1.S1_at	1.7	-1.2	-2.4	#N/A	#N/A
	Ssc.16377.2.A1_at	1.3	1.2	-2.4	NM_145740	glutathione S-transferase A1
	Ssc.834.1.S1_at	1.1	-2.1	-2.3	NM_002668	proteolipid protein 2
	Ssc.2966.3.S1_a_at	1.3	1.0	-2.3	NM_138452	dehydrogenasereductase
	Ssc.11715.1.A1_at	1.1	-1.8	-2.3	NM_013349	SCIRP10-related protein
	Ssc.16873.1.S1_at	1.0	-1.7	-2.3	NM_019045	WD repeat domain 44
	Ssc.8161.2.A1_at	1.0	-1.5	-2.3	NM_001981	epidermal growth factor receptor pathway substrate 15
	Ssc.8245.1.A1_at	1.1	-1.3	-2.3	#N/A	#N/A
	Ssc.3802.1.S1_at	1.2	-1.1	-2.3	NM_139207	nucleosome assembly protein 1-like 1
	Ssc.824.1.S1_at	1.4	-3.3	-2.3	NM_006147	interferon regulatory factor 6
	Ssc.1686.1.S1_at	-1.0	-1.2	-2.3	NM_001760	cyclin D3
	Ssc.4469.1.A1_at	1.3	-2.6	-2.3	NM_005197	checkpoint suppressor 1

Cluster 6 cont.	Ssc.5607.2.S1_at	1.0	-1.8	-2.3	NM_003748	aldehyde dehydrogenase 4 family; member A1
	Ssc.30822.1.A1_at	1.5	-1.2	-2.3	NM_004096	eukaryotic translation initiation factor 4E binding protei
	Ssc.17281.1.A1_at	-1.0	-1.3	-2.3	NM_033535	F-box and leucine-rich repeat protein 5
	Ssc.31184.1.S1_at	1.3	-1.1	-2.3	NM_015982	germ cell specific Y-box binding protein
	Ssc.21456.1.S1_at	1.1	-2.0	-2.3	NM_014584	ERO1-like
	Ssc.1844.1.S1_at	1.3	-2.0	-2.3	NM_003995	natriuretic peptide receptor Bguanylate cyclase B
	Ssc.20653.1.S1_at	1.1	-2.0	-2.3	NM_002447	macrophage stimulating 1 receptor
	Ssc.10716.1.A1_at	1.2	-1.7	-2.3	NM_017988	SCY1-like 2
	Ssc.8858.1.S1_at	1.2	-1.7	-2.3	NM_145284	similar to hypothetical protein MGC17347
	Ssc.12596.2.S1_at	1.1	-1.4	-2.3	#N/A	#N/A
	Ssc.23179.1.A1_at	1.3	-2.2	-2.3	NM_005539	inositol polyphosphate-5-phosphatase; 40kDa
	Ssc.17815.1.S1_at	1.2	-1.8	-2.3	NM_002306	lectin; galactoside-binding; soluble; 3
	Ssc.10771.1.A1_at	1.7	-1.6	-2.3	#N/A	#N/A
	Ssc.1588.1.S1_at	1.1	-2.4	-2.3	NM_017567	N-acetylglucosamine kinase
	Ssc.2949.1.S1_at	1.2	-1.8	-2.3	NM_024667	hypothetical protein FLJ12750
	Ssc.4254.1.S1_at	1.1	-1.7	-2.3	#N/A	#N/A
	Ssc.16953.1.S1_at	1.2	-1.6	-2.3	NM_175744	ras homolog gene family; member C
	Ssc.27529.1.A1_at	1.3	-1.4	-2.3	NM_001017972	hect domain and RLD 4
	Ssc.26155.1.A1_at	1.4	-2.0	-2.3	NM_032283	zinc finger; DHHC-type containing 18
	Ssc.7257.1.S1_at	1.1	-2.0	-2.2	#N/A	#N/A
	Ssc.30922.1.A1_at	1.3	-2.0	-2.2	NM_020468	sorting nexin 14
	Ssc.21889.2.A1_at	1.3	-1.5	-2.2	NM_018238	multiple substrate lipid kinase
	Ssc.28567.1.A1_at	1.2	-1.5	-2.2	#N/A	#N/A
	Ssc.2297.1.A1_at	1.1	-1.7	-2.2	#N/A	#N/A
	Ssc.15720.1.A1_at	1.1	-1.5	-2.2	NM_018235	CNDP dipeptidase 2
	Ssc.22622.1.S1_at	1.2	-1.8	-2.2	NM_003971	sperm associated antigen 9
	Ssc.1372.1.A1_at	-1.1	-1.4	-2.2	NM_014900	COBL-like 1
	Ssc.12198.1.A1_at	1.1	-1.3	-2.2	NM_148923	cytochrome b-5
	Ssc.30663.1.A1_at	1.1	1.1	-2.2	NM_015275	KIAA1033
	Ssc.22454.1.S1_at	1.5	-1.9	-2.2	#N/A	#N/A
	Ssc.11822.1.A1_at	1.2	-1.2	-2.2	NM_014220	transmembrane 4 L six family member 1
	Ssc.977.1.A1_at	1.2	-1.2	-2.2	NM_134264	WD repeat and SOCS box-containing 1
	Ssc.24788.1.S1_at	1.3	-1.8	-2.2	#N/A	#N/A

Cluster 6 cont.	Ssc.5968.2.S1_at	1.3	-1.7	-2.2	#N/A	#N/A
	Ssc.1228.1.S1_at	1.0	-1.6	-2.2	NM_002356	myristoylated alanine-rich protein kinase C substrate
	Ssc.13508.2.S1_at	-1.1	-1.3	-2.2	NM_016048	isochorismatase domain containing 1
	Ssc.25835.1.S1_at	-1.0	-1.6	-2.2	#N/A	#N/A
	Ssc.24928.1.S1_at	1.0	-1.6	-2.2	#N/A	#N/A
	Ssc.5968.3.A1_at	1.5	-1.4	-2.2	NM_003901	sphingosine-1-phosphate lyase 1
	Ssc.24226.1.A1_at	1.3	-1.3	-2.2	#N/A	#N/A
	Ssc.20238.2.S1_a_at	1.1	-1.8	-2.2	NM_005471	glucosamine-6-phosphate deaminase 1
	Ssc.4046.1.S1_at	1.1	-1.7	-2.2	NM_004341	carbamoyl-phosphate synthetase 2; aspartate transcarbamyla
	Ssc.22674.1.S1_at	1.1	-1.5	-2.2	NM_139246	chromosome 9 open reading frame 97
	Ssc.1015.1.S1_at	1.1	-1.4	-2.2	NM_001154	annexin A5
	Ssc.4175.1.A1_at	1.7	-1.3	-2.1	NM_033505	selenoprotein I
	Ssc.3749.2.S1_at	-1.1	-1.3	-2.1	XM_051264	thioredoxin reductase 3
	Ssc.30665.1.S1_at	1.0	-1.2	-2.1	NM_152400	hypothetical protein FLJ39370
	Ssc.24182.1.S1_at	1.2	-2.0	-2.1	NM_022918	hypothetical protein FLJ22104
	Ssc.26726.1.S1_a_at	1.2	-1.6	-2.1	NM_012320	lysophospholipase 3
	Ssc.21889.1.S1_at	1.2	-1.5	-2.1	NM_018238	multiple substrate lipid kinase
	Ssc.28330.1.S1_at	-1.1	-1.3	-2.1	NM_006148	LIM and SH3 protein 1
	Ssc.10721.1.A1_at	1.4	-1.1	-2.1	#N/A	#N/A
	Ssc.11071.2.S1_a_at	1.4	-1.3	-2.1	NM_014000	vinculin
	Ssc.20017.3.A1_at	1.5	-1.1	-2.1	NM_005964	myosin; heavy polypeptide 10; non-muscle
	Ssc.13874.2.A1_s_at	1.3	1.0	-2.1	NM_001100	actin; alpha 1; skeletal muscle
	Ssc.4129.2.S1_a_at	-1.0	-1.6	-2.1	NM_198799	breast carcinoma amplified sequence 4
	Ssc.21890.1.S1_at	1.3	-1.1	-2.1	NM_198240	restin
	Ssc.2066.1.S1_at	1.1	1.0	-2.1	NM_016066	glutaredoxin 2
	Ssc.26661.1.S1_at	1.3	-2.0	-2.1	#N/A	#N/A
	Ssc.16363.1.S1_at	1.1	-1.8	-2.1	NM_014547	tropomodulin 3
	Ssc.16363.1.S2_at	1.1	-1.5	-2.1	NM_014547	tropomodulin 3
	Ssc.19224.1.S1_at	1.4	-1.4	-2.1	#N/A	#N/A
	Ssc.1735.1.S1_at	1.0	-1.1	-2.1	NM_001995	acyl-CoA synthetase long-chain family member 1
	Ssc.900.1.A1_at	1.1	-1.7	-2.1	NM_016462	transmembrane protein 14C
	Ssc.24086.1.A1_at	1.1	-1.3	-2.1	NM_001008493	enabled homolog
	Ssc.30827.2.S1_at	1.3	-1.2	-2.1	NM_015173	TBC1

Cluster 6 cont.	Ssc.30540.1.A1_at	1.1	-1.2	-2.1	NM_005188	Cas-Br-M
	Ssc.25026.1.A1_at	1.0	-1.7	-2.1	#N/A	#N/A
	Ssc.19602.1.A1_at	1.0	-1.7	-2.1	NM_000086	ceroid-lipofuscinosis; neuronal 3; juvenile
	Ssc.11499.1.A1_at	1.3	-1.3	-2.1	#N/A	#N/A
	Ssc.24976.1.S1_at	1.2	-2.5	-2.0	NM_005197	checkpoint suppressor 1
	Ssc.14134.1.S1_at	1.1	-1.6	-2.0	NM_020474	UDP-N-acetyl-alpha-D-galactosamine:polypeptide N-acetylgal
	Ssc.3218.1.S1_at	1.0	-1.4	-2.0	NM_003684	MAP kinase interacting serinethreonine kinase 1
	Ssc.24039.1.S1_at	1.2	-3.2	-2.0	#N/A	#N/A
	Ssc.6742.1.A1_at	1.0	-1.3	-2.0	NM_001007100	sterol carrier protein 2
	Ssc.19213.1.S1_at	-1.2	1.0	-2.0	NM_173553	hypothetical protein FLJ25801
	Ssc.6193.1.A1_at	1.2	-2.1	-2.0	NM_130781	RAB24; member RAS oncogene family
	Ssc.23345.1.S1_at	1.2	-1.8	-2.0	NM_001004720	NCK adaptor protein 2
	Ssc.12885.1.A1_at	1.2	-1.4	-2.0	NM_004096	eukaryotic translation initiation factor 4E binding protei
	Ssc.4989.1.A1_at	1.1	-2.0	-2.0	NM_001902	cystathionase
	Ssc.6451.1.S1_at	1.1	-1.9	-2.0	#N/A	#N/A
	Ssc.5870.3.S1_at	1.1	-1.2	-2.0	#N/A	#N/A
	Ssc.6383.1.A1_at	1.1	-1.1	-2.0	#N/A	#N/A
	Ssc.27429.1.A1_at	1.2	-2.4	-2.0	NM_182485	cytoplasmic polyadenylation element binding protein 2
	Ssc.11006.1.S1_at	1.4	-2.3	-2.0	NM_013322	sorting nexin 10
	Ssc.17453.1.S1_at	1.2	-2.2	-2.0	NM_001684	ATPase; Ca++ transporting; plasma membrane 4
	Ssc.26309.1.A1_at	1.2	-2.5	-1.9	NM_005197	checkpoint suppressor 1
	Ssc.11746.1.A1_at	1.4	-2.7	-1.9	NM_032947	putative small membrane protein NID67
	Ssc.25205.1.S1_at	1.4	-2.0	-1.9	#N/A	#N/A
	Ssc.14139.1.A1_at	1.6	-2.4	-1.8	NM_006117	peroxisomal D3;D2-enoyl-CoA isomerase
	Ssc.4274.1.S1_at	1.2	-2.0	-1.8	#N/A	#N/A
	Ssc.7292.1.S1_at	1.4	-3.1	-1.8	#N/A	#N/A
	Ssc.29905.1.A1_at	1.2	-2.4	-1.8	#N/A	#N/A
	Ssc.10232.1.A1_at	1.5	-11.6	-1.8	NM_013262	myosin regulatory light chain interacting protein
	Ssc.8038.1.A1_at	1.4	-2.0	-1.7	NM_030627	cytoplasmic polyadenylation element binding protein 4
	Ssc.10608.1.S1_at	1.5	-2.2	-1.4	NM_030627	cytoplasmic polyadenylation element binding protein 4
	n = 324	**1.2**	**-1.7**	**-2.8**		
Cluster 7	Ssc.3770.1.A1_at	1.1	-2.8	-2.0	#N/A	#N/A
	Ssc.18860.1.S1_at	1.1	-2.7	-1.9	#N/A	#N/A

Cluster 7 cont.	Ssc.5001.2.A1_at	1.0	-2.2	-1.9	#N/A	#N/A
	Ssc.28434.1.A1_at	1.1	-2.2	-1.9	NM_025219	DnaJ
	Ssc.3649.1.A1_at	1.1	-2.5	-1.9	#N/A	#N/A
	Ssc.28182.1.A1_at	-1.1	-2.0	-1.8	NM_006301	mitogen-activated protein kinase kinase kinase 12
	Ssc.5622.1.A1_at	-1.1	-2.4	-1.8	#N/A	#N/A
	Ssc.7608.2.S1_at	-1.1	-2.1	-1.8	NM_018184	ADP-ribosylation factor-like 10C
	Ssc.13318.1.A1_at	-1.1	-2.3	-1.8	#N/A	#N/A
	Ssc.14047.2.A1_at	-1.1	-3.0	-1.8	#N/A	#N/A
	Ssc.18606.1.A1_at	-1.1	-2.1	-1.8	#N/A	#N/A
	Ssc.28044.1.A1_at	-1.1	-3.0	-1.7	#N/A	#N/A
	Ssc.8444.1.S1_at	-1.0	-2.1	-1.7	XM_371706	hypothetical protein KIAA1109
	Ssc.16537.1.S1_at	1.2	-2.2	-1.7	NM_007229	protein kinase C and casein kinase substrate in neurons 2
	Ssc.25172.1.S1_at	-1.1	-2.7	-1.7	NM_000820	growth arrest-specific 6
	Ssc.11815.1.A1_s_at	-1.1	-2.3	-1.7	NM_000426	laminin; alpha 2
	Ssc.8002.1.A1_at	-1.4	-2.2	-1.7	#N/A	#N/A
	Ssc.19359.2.S1_at	-1.1	-2.3	-1.6	#N/A	#N/A
	Ssc.21290.1.S1_at	-1.3	-3.4	-1.6	NM_014779	TSC22 domain family; member 2
	Ssc.3574.1.A1_at	1.1	-2.1	-1.6	NM_145687	mitogen-activated protein kinase kinase kinase kinase 4
	Ssc.28933.1.S1_at	1.1	-2.3	-1.6	#N/A	#N/A
	Ssc.23305.1.S1_at	-1.3	-2.3	-1.6	NM_018342	hypothetical protein FLJ11155
	Ssc.19621.1.A1_at	1.1	-2.1	-1.6	NM_006844	ilvB
	Ssc.3980.1.A1_at	-1.4	-2.3	-1.6	NM_014936	ectonucleotide pyrophosphatasephosphodiesterase 4
	Ssc.5458.1.S1_at	-1.2	-2.3	-1.6	NM_015913	thioredoxin domain containing 12
	Ssc.21963.1.S1_at	-1.1	-2.0	-1.6	NM_004295	TNF receptor-associated factor 4
	Ssc.18528.2.A1_at	1.1	-2.1	-1.6	NM_022736	major facilitator superfamily domain containing 1
	Ssc.19359.1.A1_at	-1.1	-2.4	-1.6	#N/A	#N/A
	Ssc.21905.1.S1_at	-1.4	-2.3	-1.6	#N/A	#N/A
	Ssc.24739.1.A1_at	-1.6	-2.3	-1.6	#N/A	#N/A
	Ssc.27521.1.S1_at	-1.1	-2.2	-1.6	NM_020324	ATP-binding cassette; sub-family D
	Ssc.10990.1.A1_at	-1.0	-2.1	-1.6	#N/A	#N/A
	Ssc.27168.1.S1_at	-1.1	-2.1	-1.6	#N/A	#N/A
	Ssc.9792.1.S1_at	-1.0	-2.3	-1.5	NM_020940	KIAA1600
	Ssc.24634.1.A1_at	-1.0	-2.2	-1.5	#N/A	#N/A

Cluster 7 cont.	Ssc.10155.1.S1_at	-1.1	-2.0	-1.5	NM_017634	potassium channel tetramerisation domain containing 9
	Ssc.1323.1.A1_at	1.1	-2.0	-1.5	NM_005578	LIM domain containing preferred translocation partner in l
	Ssc.30212.1.A1_at	1.0	-2.3	-1.5	#N/A	#N/A
	Ssc.18476.2.S1_a_at	-1.2	-2.0	-1.5	NM_033389	slingshot homolog 2
	Ssc.22078.1.A1_at	-1.0	-2.3	-1.4	NM_003561	phospholipase A2; group X
	Ssc.8699.1.A1_at	-1.2	-2.6	-1.4	#N/A	#N/A
	Ssc.20226.1.S1_at	-1.2	-2.0	-1.4	NM_015528	ring finger protein 167
	Ssc.1624.1.S1_at	-1.0	-2.0	-1.4	NM_006369	leucine rich repeat containing 41
	Ssc.6738.1.S1_at	1.3	-2.3	-1.4	NM_032622	ligand of numb-protein X
	Ssc.15594.3.S1_at	1.2	-2.1	-1.4	#N/A	#N/A
	Ssc.10327.1.A1_at	1.0	-2.6	-1.4	#N/A	#N/A
	Ssc.28427.1.A1_at	-1.1	-2.3	-1.4	#N/A	#N/A
	Ssc.2413.1.S1_at	-1.0	-2.2	-1.4	NM_000336	sodium channel; nonvoltage-gated 1; beta
	Ssc.15594.2.S1_at	-1.1	-2.0	-1.4	#N/A	#N/A
	Ssc.12114.1.S1_a_at	1.1	-2.0	-1.4	NM_005186	calpain 1;
	Ssc.14211.1.A1_at	-1.0	-3.9	-1.4	#N/A	#N/A
	Ssc.5563.1.S1_at	-1.1	-2.7	-1.4	NM_002899	retinol binding protein 1; cellular
	Ssc.12430.3.S1_at	-1.0	-2.0	-1.3	NM_002744	protein kinase C; zeta
	Ssc.19311.1.A1_at	1.2	-2.0	-1.3	NM_015995	Kruppel-like factor 13
	Ssc.5432.1.A1_at	-1.1	-2.3	-1.3	#N/A	#N/A
	Ssc.26898.1.A1_at	-1.4	-2.2	-1.3	#N/A	#N/A
	Ssc.25222.1.S1_at	1.3	-2.9	-1.3	NM_005817	mannose-6-phosphate receptor binding protein 1
	Ssc.2140.1.S1_at	1.1	-2.5	-1.3	NM_173176	PTK2B protein tyrosine kinase 2 beta
	Ssc.27214.2.S1_at	-1.2	-2.0	-1.3	NM_004924	actinin; alpha 4
	Ssc.10608.2.A1_at	1.5	-2.1	-1.3	NM_030627	cytoplasmic polyadenylation element binding protein 4
	Ssc.24460.1.A1_at	-1.1	-3.0	-1.3	#N/A	#N/A
	Ssc.1808.1.S1_at	-1.2	-2.4	-1.3	#N/A	#N/A
	Ssc.27746.1.S1_at	-1.0	-2.6	-1.3	NM_198925	sema domain; immunoglobulin domain
	Ssc.3196.1.S1_at	1.1	-2.1	-1.3	NM_000521	hexosaminidase B
	Ssc.12430.1.S1_at	1.1	-2.8	-1.2	NM_002744	protein kinase C; zeta
	Ssc.4529.1.S1_at	1.1	-2.7	-1.2	NM_181776	solute carrier family 36
	Ssc.25022.1.A1_at	-1.3	-2.2	-1.2	#N/A	#N/A
	Ssc.2466.1.S1_at	1.2	-2.1	-1.2	NM_014045	low density lipoprotein receptor-related protein 10

Cluster 7 cont.	Ssc.6951.1.A1_at	1.3	-4.2	-1.2	#N/A	#N/A
	Ssc.27147.1.A1_at	1.1	-2.2	-1.2	NM_177532	Ras association
	Ssc.1339.1.A1_at	-1.1	-2.2	-1.1	NM_139045	SWISNF related; matrix associated; actin dependent regulator
	Ssc.30194.1.A1_at	-1.1	-4.4	-1.1	NM_207015	N-acetylated alpha-linked acidic dipeptidase 2
	Ssc.10025.3.S1_at	1.1	-2.5	-1.1	NM_005195	CCAATenhancer binding protein
	Ssc.779.1.S1_at	-1.4	-2.3	-1.1	NM_004433	E74-like factor 3
	Ssc.21178.1.S1_at	-1.8	-2.1	-1.1	#N/A	#N/A
	Ssc.24540.1.S1_at	1.0	-2.6	-1.0	#N/A	#N/A
	Ssc.27912.1.S1_at	1.1	-2.3	-1.0	NM_020747	zinc finger protein 608
	Ssc.772.1.S1_at	-1.1	-2.5	1.0	NM_014316	calcium regulated heat stable protein 1; 24kDa
	Ssc.2824.1.S1_at	1.2	-4.1	1.1	NM_198234	ribonuclease; RNase A family; 1
	Ssc.9286.1.A1_at	-1.1	-3.5	1.1	#N/A	#N/A
	Ssc.55.1.S1_at	1.1	-2.2	1.1	NM_005228	epidermal growth factor receptor
	Ssc.10917.1.A1_at	-1.2	-2.3	1.2	NM_181354	oxidation resistance 1
	Ssc.25088.1.A1_at	1.2	-2.5	1.2	#N/A	#N/A
	Ssc.18085.1.A1_at	-1.1	-2.4	1.3	#N/A	#N/A
	Ssc.5580.1.S1_at	1.0	-2.1	1.4	#N/A	#N/A
	Ssc.8373.1.A1_at	1.3	-3.1	1.4	#N/A	#N/A
	Ssc.5118.1.S1_at	1.7	-2.0	1.5	NM_005603	ATPase; Class I; type 8B; member 1
	Ssc.1977.1.S1_at	1.2	-2.6	1.7	NM_006096	N-myc downstream regulated gene 1
	n = 88	**-1.0**	**-2.4**	**-1.3**		
Cluster 8	Ssc.4142.1.S1_at	1.1	59.2	118.2	NM_181644	hypothetical protein DKFZp761N1114
	Ssc.22459.1.A1_at	1.1	15.5	160.3	#N/A	#N/A
	Ssc.7484.1.S1_at	-1.4	45.0	254.7	#N/A	#N/A
	n = 3	**-1.0**	**39.9**	**177.7**		
Cluster 9	Ssc.1583.1.A1_at	1.1	4.4	3.1	NM_001624	absent in melanoma 1
	Ssc.14340.3.S1_at	1.5	4.8	3.1	NM_004862	lipopolysaccharide-induced TNF factor
	Ssc.14400.1.A1_at	1.5	4.0	3.2	NM_147156	transmembrane protein 23
	Ssc.29855.1.A1_at	1.5	4.2	3.3	NM_031942	cell division cycle associated 7
	Ssc.5016.1.A1_at	1.2	4.2	3.5	#N/A	#N/A
	Ssc.9063.1.A1_at	1.2	4.6	3.9	#N/A	#N/A
	Ssc.27431.1.A1_at	1.1	5.1	4.0	NM_005504	branched chain aminotransferase 1; cytosolic
	Ssc.246.1.S1_at	1.1	5.1	4.4	NM_001677	ATPase; Na+K+ transporting; beta 1 polypeptide

Cluster 9 cont.	Ssc.13805.1.S1_at	1.1	3.6	4.5	NM_133265	angiomotin
	Ssc.25773.1.S1_at	1.1	4.4	4.7	NM_133265	angiomotin
	Ssc.6357.1.S1_at	1.2	3.9	4.8	NM_002245	potassium channel; subfamily K; member 1
	Ssc.4093.1.A1_at	-1.0	4.3	4.8	NM_000619	interferon; gamma
	Ssc.11197.1.S1_at	1.2	4.1	4.8	NM_001540	heat shock 27kDa protein 1
	Ssc.310.1.S1_at	-1.1	3.9	4.9	NM_004963	guanylate cyclase 2C
	Ssc.847.1.S1_at	1.0	3.5	5.3	NM_006286	transcription factor Dp-2
	Ssc.12491.1.A1_at	-1.3	3.7	5.3	NM_024015	homeo box B4
	Ssc.196.1.S1_at	1.7	3.7	5.5	NM_000930	plasminogen activator; tissue
	Ssc.1407.3.S1_at	1.4	5.4	5.6	NM_007203	PALM2-AKAP2 protein
	Ssc.21328.1.S1_at	-1.2	4.7	6.0	NM_018050	MANSC domain containing 1
	n = 19	**1.2**	**4.3**	**4.5**		
Cluster 10	Ssc.11255.1.A1_at	-1.0	-9.9	-167.1	NM_001009185	acyl-CoA synthetase long-chain family member 6
	Ssc.19431.1.S1_at	-1.4	-63.0	-110.5	NM_005021	ectonucleotide pyrophosphatasephosphodiesterase 3
	Ssc.24311.1.S1_at	-1.5	-16.3	-40.5	#N/A	#N/A
	Ssc.881.1.S1_at	-1.1	-4.6	-37.0	NM_145202	proline-rich acidic protein 1
	Ssc.24984.1.S1_at	-1.0	-8.1	-34.1	#N/A	#N/A
	Ssc.27256.1.S1_at	1.1	-2.6	-33.6	NM_000405	GM2 ganglioside activator
	Ssc.2825.1.S1_at	-1.0	-2.6	-33.4	#N/A	#N/A
	Ssc.15060.1.S1_at	1.2	-3.4	-28.3	NM_000102	cytochrome P450; family 17; subfamily A; polypeptide 1
	Ssc.1534.1.A1_at	-1.6	-12.7	-28.2	NM_015385	sorbin and SH3 domain containing 1
	Ssc.27264.1.S1_at	-1.1	-21.2	-27.8	NM_024861	hypothetical protein FLJ22671
	Ssc.26185.1.S1_at	-1.7	-17.3	-26.7	#N/A	#N/A
	Ssc.7243.1.A1_at	1.2	-44.5	-26.5	NM_199168	chemokine
	Ssc.10403.1.S1_at	-1.3	-19.4	-25.3	NM_012101	tripartite motif-containing 29
	Ssc.1733.1.A1_at	1.2	-5.6	-22.8	NM_002220	inositol 1;4;5-trisphosphate 3-kinase A
	Ssc.19166.1.S1_s_at	-1.7	-9.3	-22.7	NM_005170	achaete-scute complex-like 2
	Ssc.24430.1.S1_at	1.0	-7.8	-21.5	NM_033274	a disintegrin and metalloproteinase domain 19
	Ssc.24372.1.S1_at	-2.2	-4.9	-19.9	NM_147161	thioesterase; adipose associated
	Ssc.6056.1.S1_at	-2.0	-19.7	-18.2	NM_181797	potassium voltage-gated channel; KQT-like subfamily
	Ssc.8594.1.A1_at	-2.0	-28.8	-17.3	NM_013314	B-cell linker
	Ssc.29840.1.A1_at	-2.0	-11.8	-17.3	#N/A	#N/A
	Ssc.1303.1.S1_at	1.1	-3.0	-16.7	NM_030666	serine

Cluster 10 cont.	Ssc.24503.1.S1_at	-1.3	-18.4	-16.5	XM_496688	hypothetical protein BC012029
	Ssc.3785.1.S1_a_at	-1.3	-6.5	-14.8	XM_379250	hypothetical LOC401115
	Ssc.2963.1.S1_at	-1.7	-5.9	-13.1	#N/A	#N/A
	Ssc.3442.1.S1_at	-1.1	-3.5	-13.0	#N/A	#N/A
	Ssc.4076.1.S1_at	-1.9	-6.4	-12.3	NM_015225	KIAA0367
	Ssc.2492.1.A1_at	1.0	-9.2	-12.0	#N/A	#N/A
	Ssc.17364.1.S1_at	-1.2	-11.8	-12.0	NM_015444	Ras-induced senescence 1
	Ssc.3012.1.S1_at	-2.7	-8.6	-11.9	NM_181597	uridine phosphorylase 1
	Ssc.23963.1.S1_at	-1.5	-2.3	-11.9	NM_014059	response gene to complement 32
	Ssc.2158.1.A1_at	-1.3	-3.7	-11.7	NM_004529	myeloidlymphoid or mixed-lineage leukemia
	Ssc.2746.1.A1_at	-1.0	-4.8	-11.4	#N/A	#N/A
	Ssc.5607.1.S1_at	1.1	-3.2	-11.2	NM_003748	aldehyde dehydrogenase 4 family; member A1
	Ssc.5434.1.A1_at	1.1	-8.0	-10.9	NM_033274	a disintegrin and metalloproteinase domain 19
	Ssc.26690.1.A1_at	-1.1	-2.7	-10.8	XM_090294	hypothetical protein FLJ38508
	Ssc.2887.1.S1_at	1.1	-5.5	-10.7	NM_000941	P450
	Ssc.17965.1.S1_at	-2.0	-4.6	-10.6	NM_153347	hypothetical protein FLJ90119
	Ssc.19539.2.S1_at	-2.3	-5.5	-10.3	NM_018941	ceroid-lipofuscinosis; neuronal 8
	Ssc.28059.1.A1_at	1.2	-4.8	-9.9	XM_498662	hypothetical gene supported by AK092922; AL8319
	Ssc.9114.1.S1_at	1.1	-5.2	-9.8	NM_024636	tumor necrosis factor; alpha-induced protein 9
	Ssc.27372.1.S1_at	-1.1	-12.6	-8.7	#N/A	#N/A
	Ssc.21826.1.S1_at	-1.1	-1.9	-8.5	NM_001632	alkaline phosphatase; placental
	Ssc.4105.1.S1_at	1.1	-5.4	-8.2	#N/A	#N/A
	Ssc.64.1.S1_at	-1.3	-10.3	-7.8	NM_004827	ATP-binding cassette; sub-family G
	Ssc.943.1.S1_at	1.0	-3.4	-7.8	NM_198538	suprabasin
	Ssc.19539.1.A1_at	-2.4	-5.4	-7.7	#N/A	#N/A
	Ssc.27183.1.S1_at	-1.1	-3.7	-7.5	NM_002068	guanine nucleotide binding protein
	Ssc.12727.2.A1_at	1.2	-9.0	-7.1	#N/A	#N/A
	Ssc.3699.1.S1_at	-1.0	-2.0	-7.0	NM_178140	PDZ domain containing 3
	Ssc.12727.1.A1_at	1.1	-6.8	-6.7	#N/A	#N/A
	Ssc.12802.1.A1_at	-1.0	-10.5	-6.7	#N/A	#N/A
	Ssc.24768.1.S1_at	-2.0	-3.4	-6.3	NM_152729	5-nucleotidase; cytosolic II-like 1
	Ssc.4204.1.S1_at	-1.4	-4.8	-6.1	NM_004130	glycogenin
	Ssc.24593.1.A1_at	-1.1	-4.6	-6.1	#N/A	#N/A

Cluster 10 cont.	Ssc.9553.1.A1_s_at	-1.3	-2.1	-6.1	NM_014059	response gene to complement 32
	Ssc.16120.1.S1_at	-1.2	-3.4	-6.1	NM_005536	inositol
	Ssc.25189.1.S1_a_at	1.1	-4.2	-6.0	NM_020784	KIAA1344
	Ssc.16236.1.S1_at	-1.9	-7.6	-6.0	NM_001935	dipeptidylpeptidase 4
	Ssc.16250.1.S2_at	1.0	-4.4	-6.0	NM_173841	interleukin 1 receptor antagonist
	Ssc.26693.1.S1_at	-1.1	-5.2	-5.9	NM_002639	serine
	Ssc.25134.1.A1_at	-1.0	-4.6	-5.9	NM_020784	KIAA1344
	Ssc.21383.1.A1_at	-1.9	-6.9	-5.9	NM_178500	phosphatase; orphan 1
	Ssc.5848.2.S1_a_at	-1.3	-6.9	-5.8	NM_004776	UDP-Gal:betaGlcNAc beta 1;4- galactosyltransferase; polype
	Ssc.25155.1.S1_at	-1.2	-4.9	-5.7	NM_018390	phosphatidylinositol-specific phospholipase C; X domain con
	Ssc.28921.1.S1_at	-1.2	-4.2	-5.6	#N/A	#N/A
	Ssc.13611.1.A1_at	-2.3	-3.4	-5.6	NM_152729	5-nucleotidase; cytosolic II-like 1
	Ssc.27947.1.S1_at	-1.3	-2.9	-5.6	NM_013401	RAB3A interacting protein
	Ssc.16725.1.S1_at	-1.1	-2.5	-5.6	NM_033375	myosin IC
	Ssc.7469.1.S1_at	-1.0	-3.6	-5.6	NM_022087	UDP-N-acetyl-alpha-D-galactosamine:polypeptide N-acetylgal
	Ssc.19455.1.S1_at	1.1	-2.9	-5.6	#N/A	#N/A
	Ssc.16334.1.S2_at	-1.0	-3.2	-5.5	NM_138578	BCL2-like 1
	Ssc.984.1.S1_at	-1.0	-1.8	-5.4	NM_002778	prosaposin
	Ssc.15252.1.S1_at	1.0	-3.3	-5.4	NM_201533	diacylglycerol kinase; zeta 104kDa
	Ssc.1950.1.A1_at	-1.3	-3.8	-5.3	#N/A	#N/A
	Ssc.2285.1.S1_at	1.1	-2.9	-5.3	NM_020424	hypothetical protein A-211C6.1
	Ssc.12680.1.A1_at	-1.1	-2.1	-5.3	NM_015541	leucine-rich repeats and immunoglobulin-like domains 1
	Ssc.12176.1.S1_at	1.1	-3.7	-5.3	NM_022036	G protein-coupled receptor; family C; group 5; member C
	Ssc.1093.3.S1_at	1.1	-4.9	-5.2	NM_012193	frizzled homolog 4
	Ssc.29966.1.A1_s_at	-1.0	-3.4	-5.2	#N/A	#N/A
	Ssc.2674.1.S1_at	1.2	-4.0	-5.2	#N/A	#N/A
	Ssc.18111.1.A1_at	-1.8	-3.8	-5.1	#N/A	#N/A
	Ssc.19063.1.S1_at	-1.3	-2.5	-5.0	#N/A	#N/A
	Ssc.12176.3.S1_at	1.1	-4.7	-5.0	NM_018653	G protein-coupled receptor; family C; group 5; member C
	Ssc.15926.1.S1_at	-1.0	-2.8	-5.0	NM_001285	chloride channel; calcium activated; family member 1
	Ssc.19164.1.A1_at	-1.4	-3.4	-5.0	#N/A	#N/A
	Ssc.2142.2.S1_at	-1.3	-3.3	-5.0	NM_080881	drebrin 1
	Ssc.26303.1.A1_at	-1.3	-3.8	-4.9	#N/A	#N/A

Cluster 10 cont.	Ssc.28415.1.S1_at	-1.2	-4.1	-4.9	NM_031308	epiplakin 1
	Ssc.2492.2.S1_at	1.1	-4.5	-4.9	NM_001001669	FLJ41603 protein
	Ssc.29858.1.A1_at	-1.7	-25.8	-4.9	NM_000927	ATP-binding cassette; sub-family B
	Ssc.1093.2.A1_at	1.1	-5.9	-4.8	NM_012193	frizzled homolog 4
	Ssc.19455.2.S1_at	1.1	-3.2	-4.8	NM_001003794	monoglyceride lipase
	Ssc.773.1.S1_at	1.0	-2.4	-4.8	NM_080593	histone 1; H2bk
	Ssc.7593.1.S1_at	-1.2	-2.0	-4.8	#N/A	#N/A
	Ssc.25230.1.S1_at	1.2	-4.9	-4.8	NM_012193	frizzled homolog 4
	Ssc.24718.1.S1_at	-1.2	-3.7	-4.7	NM_005536	inositol
	Ssc.27182.1.S1_at	-1.4	-9.6	-4.7	NM_017682	vitelliform macular dystrophy 2-like 1
	Ssc.21227.1.S1_at	-1.3	-3.6	-4.7	NM_080881	drebrin 1
	Ssc.13637.1.A1_at	1.1	-2.7	-4.7	NM_002737	protein kinase C; alpha
	Ssc.29246.1.A1_at	-1.9	-10.7	-4.6	NM_199461	nanos homolog 1
	Ssc.13473.1.A1_at	1.1	-4.4	-4.6	#N/A	#N/A
	Ssc.23264.1.A1_at	-1.0	-4.1	-4.5	#N/A	#N/A
	Ssc.6618.1.A1_at	-1.1	-2.1	-4.5	XM_290546	KIAA0830 protein
	Ssc.18773.1.A1_at	1.0	-3.4	-4.4	#N/A	#N/A
	Ssc.2142.1.S1_at	-1.3	-3.2	-4.4	NM_080881	drebrin 1
	Ssc.27550.1.S1_at	1.0	-3.7	-4.4	NM_003358	UDP-glucose ceramide glucosyltransferase
	Ssc.28458.1.A1_at	-1.1	-1.5	-4.4	#N/A	#N/A
	Ssc.5848.1.S1_at	-1.3	-6.7	-4.3	NM_004776	UDP-Gal:betaGlcNAc beta 1;4- galactosyltransferase; polype
	Ssc.3610.1.A1_at	-1.1	-3.3	-4.3	#N/A	#N/A
	Ssc.26450.1.A1_at	-1.4	-3.2	-4.3	NM_173570	zinc finger; DHHC-type containing 23
	Ssc.24414.1.S1_at	-1.1	-2.8	-4.3	NM_004879	etoposide induced 2.4 mRNA
	Ssc.7568.1.A1_at	-1.6	1.0	-4.3	XM_378780	hypothetical protein LOC126536
	Ssc.6323.1.S1_at	-1.3	-3.6	-4.3	NM_001122	adipose differentiation-related protein
	Ssc.422.1.S1_at	-1.2	-2.7	-4.3	NM_000876	insulin-like growth factor 2 receptor
	Ssc.17674.1.A1_at	1.1	-3.0	-4.3	#N/A	#N/A
	Ssc.19482.1.A1_at	-1.1	-6.6	-4.2	#N/A	#N/A
	Ssc.16963.1.S1_at	-1.2	-5.5	-4.2	NM_004776	UDP-Gal:betaGlcNAc beta 1;4- galactosyltransferase; polype
	Ssc.23746.1.S1_at	-1.2	-3.7	-4.2	NM_015385	sorbin and SH3 domain containing 1
	Ssc.11362.2.S1_at	-1.2	-3.1	-4.2	NM_004879	etoposide induced 2.4 mRNA
	Ssc.26354.1.S1_at	-1.2	-3.0	-4.2	#N/A	#N/A

Cluster 10 cont.	Ssc.27369.1.A1_at	1.1	-2.5	-4.2	NM_024422	desmocollin 2
	Ssc.25149.1.S1_at	-1.3	-4.1	-4.1	#N/A	#N/A
	Ssc.12402.1.A1_at	-1.2	-2.0	-4.1	#N/A	#N/A
	Ssc.29231.1.A1_at	1.2	-4.4	-4.1	#N/A	#N/A
	Ssc.9594.1.A1_at	-1.4	-1.7	-4.1	NM_015440	methylenetetrahydrofolate dehydrogenase
	Ssc.29081.1.S1_at	1.2	-3.7	-4.1	#N/A	#N/A
	Ssc.1376.1.S1_at	-1.0	-3.6	-4.1	NM_020432	putative homeodomain transcription factor 2
	Ssc.22476.1.A1_at	-1.1	-4.5	-4.1	XM_373594	hypothetical LOC387992
	Ssc.1641.1.S1_at	-1.1	-2.9	-4.1	NM_004356	CD81 antigen
	Ssc.19602.3.S1_at	-1.0	-1.7	-4.1	NM_000086	ceroid-lipofuscinosis; neuronal 3; juvenile
	Ssc.30264.1.A1_at	-1.1	-3.2	-4.0	#N/A	#N/A
	Ssc.26824.1.A1_at	-1.1	-3.1	-4.0	NM_004686	myotubularin related protein 7
	Ssc.25158.2.A1_at	-1.1	-2.2	-4.0	NM_022725	Fanconi anemia; complementation group F
	Ssc.15818.1.S1_at	-1.3	-2.7	-4.0	NM_000876	insulin-like growth factor 2 receptor
	Ssc.4155.1.S1_at	-1.3	-2.1	-3.9	NM_003566	early endosome antigen 1; 162kD
	Ssc.24938.1.S1_at	-1.2	-3.4	-3.9	NM_001004431	meteorin; glial cell differentiation regulator-like
	Ssc.8213.1.A1_at	1.0	-2.2	-3.9	NM_024613	pleckstrin homology domain containing; family F
	Ssc.1533.1.S1_at	-1.3	-2.0	-3.9	NM_000271	Niemann-Pick disease; type C1
	Ssc.19442.1.A1_at	1.1	-6.8	-3.8	#N/A	#N/A
	Ssc.18132.1.A1_at	-1.2	-1.9	-3.8	NM_138571	histidine triad nucleotide binding protein 3
	Ssc.27177.2.S1_at	-1.3	-7.3	-3.8	#N/A	#N/A
	Ssc.27177.1.S1_at	-1.0	-5.9	-3.8	NM_006095	ATPase; aminophospholipid transporter
	Ssc.23758.1.S1_at	1.1	-2.5	-3.8	#N/A	#N/A
	Ssc.18246.1.S1_at	-1.2	-2.6	-3.8	NM_004529	myeloidlymphoid or mixed-lineage leukemia
	Ssc.16727.1.A1_at	-1.0	-2.1	-3.7	NM_000398	diaphorase
	Ssc.2176.1.A1_at	1.2	-4.4	-3.7	NM_203372	acyl-CoA synthetase long-chain family member 3
	Ssc.8451.1.A1_at	-1.5	-2.0	-3.7	NM_182765	HECT domain containing 2
	Ssc.10002.1.A1_at	-1.2	-3.3	-3.7	#N/A	#N/A
	Ssc.23139.1.S1_at	-1.1	-2.9	-3.7	NM_002886	RAP2B; member of RAS oncogene family
	Ssc.16068.1.S1_at	-1.1	-4.9	-3.6	NM_001004452	olfactory receptor; family 1; subfamily J; member 4
	Ssc.24102.1.S1_at	1.0	-1.9	-3.6	NM_004504	HIV-1 Rev binding protein
	Ssc.25748.1.S1_at	-1.0	-2.0	-3.6	NM_004504	HIV-1 Rev binding protein
	Ssc.8566.1.A1_at	1.2	-3.8	-3.6	#N/A	#N/A

Cluster 10 cont.	Ssc.29424.1.A1_at	-1.5	-1.8	-3.6	NM_019012	pleckstrin homology domain containing; family A member 5
	Ssc.94.1.A1_at	-1.0	-2.9	-3.6	NM_004999	myosin VI
	Ssc.2589.1.S1_at	-1.5	-5.9	-3.5	NM_000363	troponin I; cardiac
	Ssc.1600.3.S1_at	1.0	-2.5	-3.5	NM_020734	KIAA1238 protein
	Ssc.10624.1.S1_at	-1.0	-2.0	-3.5	NM_014033	DKFZP586A0522 protein
	Ssc.29837.1.A1_at	-1.1	-1.7	-3.5	#N/A	#N/A
	Ssc.2925.2.S1_a_at	1.1	-4.2	-3.5	NM_017797	BTB
	Ssc.10082.1.A1_at	-1.3	-2.1	-3.4	NM_024312	MGC4170 protein
	Ssc.23539.1.S1_at	-1.2	-2.1	-3.4	NM_152911	polyamine oxidase
	Ssc.1764.1.A1_at	1.0	-2.2	-3.4	NM_002906	radixin
	Ssc.18261.1.S1_at	-1.2	-2.3	-3.4	NM_024430	proline-serine-threonine phosphatase interacting protein 2
	Ssc.10534.3.A1_a_at	-1.2	-3.3	-3.4	NM_006506	RAS p21 protein activator 2
	Ssc.83.1.S1_at	-1.2	-2.6	-3.4	NM_001977	glutamyl aminopeptidase
	Ssc.25450.1.S1_at	-1.1	-2.0	-3.4	#N/A	#N/A
	Ssc.5793.1.S1_at	-1.6	-3.1	-3.3	#N/A	#N/A
	Ssc.2760.1.A1_at	1.1	-2.2	-3.3	NM_018841	guanine nucleotide binding protein
	Ssc.19553.1.A1_at	-1.4	-3.6	-3.3	NM_206862	transforming; acidic coiled-coil containing protein 2
	Ssc.14425.1.A1_at	-1.0	-2.0	-3.3	NM_020921	ninein
	Ssc.17377.1.S1_a_at	-1.1	-1.8	-3.3	#N/A	#N/A
	Ssc.6342.1.S1_at	-1.5	-1.6	-3.3	NM_153613	PLSC domain containing protein
	Ssc.10534.2.S1_at	-1.1	-2.1	-3.3	NM_006506	RAS p21 protein activator 2
	Ssc.6699.1.A1_at	-1.3	-2.9	-3.3	NM_000252	myotubularin 1
	Ssc.29750.1.A1_at	1.2	-7.8	-3.2	NM_033285	tumor protein p53 inducible nuclear protein 1
	Ssc.30871.1.A1_at	1.2	-6.3	-3.2	NM_033285	tumor protein p53 inducible nuclear protein 1
	Ssc.24375.1.S1_at	-1.1	-2.9	-3.2	NM_024109	hypothetical protein MGC2654
	Ssc.1868.1.S1_at	1.1	-2.6	-3.2	NM_000901	nuclear receptor subfamily 3; group C; member 2
	Ssc.24978.2.S1_at	-1.4	-6.2	-3.2	#N/A	#N/A
	Ssc.30316.1.A1_at	-1.2	-1.9	-3.2	NM_001007794	cholineethanolamine phosphotransferase 1
	Ssc.12650.1.A1_at	1.1	-2.5	-3.2	NM_014616	ATPase; Class VI; type 11B
	Ssc.27573.1.S1_at	-1.3	-1.3	-3.1	NM_001001132	intersectin 1
	Ssc.19478.1.S1_at	-1.3	-1.6	-3.1	#N/A	#N/A
	Ssc.2795.2.S1_at	-1.4	-3.1	-3.1	NM_004059	cysteine conjugate-beta lyase; cytoplasmic
	Ssc.26084.1.S1_at	-1.2	-2.8	-3.1	NM_001001323	ATPase; Ca++ transporting; plasma membrane 1

Cluster 10 cont.	Ssc.27137.1.A1_at	-1.2	-2.0	-3.1	#N/A	#N/A
	Ssc.13508.1.A1_at	-1.3	-2.0	-3.0	NM_016048	isochorismatase domain containing 1
	Ssc.24396.1.S1_at	1.1	-2.7	-3.0	NM_014216	inositol 1;3;4-triphosphate 56 kinase
	Ssc.1525.1.S1_at	1.0	-1.8	-3.0	NM_032219	hypothetical protein FLJ22269
	Ssc.4641.1.A1_at	-1.4	-2.9	-3.0	NM_017771	PX domain containing serinethreonine kinase
	Ssc.12099.1.A1_at	-1.0	-2.1	-3.0	#N/A	#N/A
	Ssc.16937.1.A1_at	-1.1	-3.1	-3.0	NM_021202	tumor protein p53 inducible nuclear protein 2
	Ssc.21033.2.S1_at	-1.0	-1.7	-3.0	NM_006319	CDP-diacylglycerol--inositol 3-phosphatidyltransferase
	Ssc.428.12.A1_at	1.0	-2.0	-3.0	#N/A	#N/A
	Ssc.17458.1.S1_at	-1.1	-2.8	-3.0	#N/A	#N/A
	Ssc.428.23.A1_at	-1.1	-4.6	-3.0	#N/A	#N/A
	Ssc.6342.1.S1_a_at	-1.6	-1.2	-3.0	NM_153613	PLSC domain containing protein
	Ssc.1623.1.S1_at	-1.1	-3.0	-2.9	NM_004415	desmoplakin
	Ssc.21192.3.S1_at	1.1	-2.5	-2.9	NM_145687	mitogen-activated protein kinase kinase kinase kinase 4
	Ssc.11670.3.A1_at	1.0	-2.6	-2.9	XM_496093	similar to PERP; TP53 apoptosis effector; p53-i
	Ssc.9719.1.S1_at	-1.4	-1.5	-2.9	NM_018330	KIAA1598
	Ssc.8355.1.A1_at	-1.4	-2.1	-2.9	NM_018330	KIAA1598
	Ssc.3578.1.S1_at	-1.0	-2.3	-2.9	NM_020533	mucolipin 1
	Ssc.22089.1.A1_at	-1.0	-1.9	-2.9	#N/A	#N/A
	Ssc.18404.1.A1_at	-1.1	-2.4	-2.9	#N/A	#N/A
	Ssc.27052.1.A1_at	-1.3	-5.7	-2.9	#N/A	#N/A
	Ssc.2925.3.S1_a_at	1.1	-3.9	-2.9	#N/A	#N/A
	Ssc.5314.1.S1_at	-1.2	-2.5	-2.8	NM_006149	lectin; galactoside-binding; soluble; 4
	Ssc.16485.1.S1_at	-1.3	-2.4	-2.8	NM_004252	solute carrier family 9
	Ssc.9334.1.S1_at	-1.1	-1.4	-2.8	NM_144563	ribose 5-phosphate isomerase A
	Ssc.7034.2.S1_at	-1.1	-2.6	-2.8	NM_016297	prenylcysteine oxidase 1
	Ssc.16333.1.S1_at	-1.5	-6.1	-2.8	NM_000927	ATP-binding cassette; sub-family B
	Ssc.24795.1.A1_at	-1.4	-1.1	-2.8	#N/A	#N/A
	Ssc.4671.1.A1_at	-1.2	-2.5	-2.8	#N/A	#N/A
	Ssc.14180.1.A1_at	1.0	-2.3	-2.8	NM_015458	myotubularin related protein 9
	Ssc.54.1.A1_at	-1.0	-2.1	-2.8	NM_001769	CD9 antigen
	Ssc.6677.1.S1_at	-1.2	-1.7	-2.8	NM_003379	villin 2
	Ssc.6441.1.A1_at	-1.1	-2.5	-2.7	NM_016029	dehydrogenasereductase

Cluster 10 cont.	Ssc.15515.1.A1_at	-1.0	-2.0	-2.7	#N/A	#N/A
	Ssc.19041.2.S1_at	-1.1	-1.7	-2.7	NM_005689	ATP-binding cassette; sub-family B
	Ssc.15578.1.A1_at	1.1	-2.6	-2.7	NM_018205	leucine rich repeat containing 20
	Ssc.8501.1.S1_at	-1.1	-1.6	-2.7	NM_006407	ADP-ribosylation-like factor 6 interacting protein 5
	Ssc.26169.1.S1_at	-1.2	-2.8	-2.7	#N/A	#N/A
	Ssc.1957.1.A1_at	-1.1	-2.3	-2.7	NM_000259	myosin VA
	Ssc.8501.2.A1_at	-1.2	-2.0	-2.7	NM_006407	ADP-ribosylation-like factor 6 interacting protein 5
	Ssc.14173.1.S1_at	-1.1	-5.5	-2.7	#N/A	#N/A
	Ssc.6783.1.S1_at	1.1	-2.6	-2.7	NM_012338	tetraspanin 12
	Ssc.2672.1.S1_at	-1.3	-2.5	-2.7	NM_012156	erythrocyte membrane protein band 4.1-like 1
	Ssc.26275.1.S1_at	-1.2	-2.1	-2.7	NM_015600	chromosome 20 open reading frame 22
	Ssc.18208.1.S1_at	-1.3	-2.1	-2.7	#N/A	#N/A
	Ssc.2070.1.S1_at	-1.1	-3.4	-2.6	NM_012156	erythrocyte membrane protein band 4.1-like 1
	Ssc.17760.1.S1_at	-1.2	-2.9	-2.6	NM_002886	RAP2B; member of RAS oncogene family
	Ssc.3832.1.S1_at	-1.5	-6.1	-2.6	NM_004925	aquaporin 3
	Ssc.1732.1.S1_at	-1.2	-1.8	-2.6	NM_006407	ADP-ribosylation-like factor 6 interacting protein 5
	Ssc.1285.1.S1_at	-1.1	-2.7	-2.6	#N/A	#N/A
	Ssc.15621.1.A1_at	1.0	-2.4	-2.6	#N/A	#N/A
	Ssc.3255.1.S1_at	-1.1	-2.8	-2.6	NM_024071	zinc finger; FYVE domain containing 21
	Ssc.24390.1.A1_at	-1.4	-2.7	-2.6	XM_370777	Similar to Lysophospholipase
	Ssc.1126.1.A1_at	1.0	-3.6	-2.6	NM_006714	sphingomyelin phosphodiesterase; acid-like 3A
	Ssc.7985.1.S1_at	-1.4	-3.0	-2.6	NM_001682	ATPase; Ca++ transporting; plasma membrane 1
	Ssc.30785.1.S1_at	-1.1	-2.4	-2.6	NM_007063	TBC1 domain family; member 8
	Ssc.24403.1.S1_at	-1.3	-1.2	-2.6	NM_002040	GA binding protein transcription factor; alpha subunit 60k
	Ssc.7084.1.A1_at	-1.8	-2.3	-2.6	#N/A	#N/A
	Ssc.19229.3.A1_at	-1.1	-2.0	-2.6	NM_014857	RAB GTPase activating protein 1-like
	Ssc.4833.1.S1_at	-1.0	-2.2	-2.6	NM_002881	v-ral simian leukemia viral oncogene homolog B
	Ssc.5887.1.A1_at	1.0	-4.6	-2.6	#N/A	#N/A
	Ssc.8612.1.A1_at	-1.1	-2.0	-2.5	#N/A	#N/A
	Ssc.2925.1.S1_at	-1.0	-3.2	-2.5	NM_017797	BTB
	Ssc.30491.1.A1_at	-1.1	-1.9	-2.5	NM_004483	glycine cleavage system protein H
	Ssc.11670.1.A1_at	1.0	-2.0	-2.5	NM_022121	PERP; TP53 apoptosis effector
	Ssc.7818.1.A1_at	-1.0	-1.8	-2.5	NM_012089	ATP-binding cassette; sub-family B

Cluster 10 cont.	Ssc.541.1.S1_at	-1.3	-1.9	-2.5	NM_033553	guanylate cyclase activator 2A
	Ssc.27292.1.S1_at	-1.5	-7.7	-2.5	#N/A	#N/A
	Ssc.7238.1.A1_at	-1.1	-1.9	-2.5	#N/A	#N/A
	Ssc.22275.1.S1_at	-1.3	-1.7	-2.5	NM_003580	neutral sphingomyelinase
	Ssc.5879.4.S1_a_at	1.0	-3.0	-2.5	NM_172171	calciumcalmodulin-dependent protein kinase
	Ssc.12693.1.S1_at	-1.0	-2.0	-2.5	NM_198402	protein tyrosine phosphatase-like
	Ssc.29965.1.A1_at	-1.2	-2.7	-2.5	#N/A	#N/A
	Ssc.23310.1.S1_at	-1.1	-2.6	-2.5	NM_000434	sialidase 1
	Ssc.24831.1.A1_at	-1.1	-2.5	-2.5	NM_133373	phospholipase C; delta 3
	Ssc.21915.3.A1_at	-1.2	-2.3	-2.5	#N/A	#N/A
	Ssc.3278.1.A1_at	-1.1	-1.8	-2.5	NM_012406	PR domain containing 4
	Ssc.4289.1.S1_at	-1.3	-1.3	-2.5	#N/A	#N/A
	Ssc.2795.1.S1_at	-1.4	-3.4	-2.4	NM_004059	cysteine conjugate-beta lyase; cytoplasmic
	Ssc.8317.1.A1_at	-1.1	-2.3	-2.4	NM_019009	toll interacting protein
	Ssc.6792.1.A1_at	-1.6	-1.9	-2.4	NM_001166	baculoviral IAP repeat-containing 2
	Ssc.25412.1.A1_at	-1.0	-4.1	-2.4	#N/A	#N/A
	Ssc.4957.1.S1_at	1.0	-2.1	-2.4	#N/A	#N/A
	Ssc.26491.1.A1_at	-1.2	-1.4	-2.4	NM_006795	EH-domain containing 1
	Ssc.9420.1.A1_at	-1.1	-2.2	-2.4	NM_201281	myotubularin related protein 2
	Ssc.16669.1.S1_at	-1.0	-1.7	-2.4	#N/A	#N/A
	Ssc.25396.1.A1_at	-1.3	-3.6	-2.4	#N/A	#N/A
	Ssc.16392.2.A1_a_at	-1.3	-2.9	-2.4	NM_199054	MAP kinase interacting serinethreonine kinase 2
	Ssc.5085.1.A1_at	-1.1	-2.9	-2.4	NM_006290	tumor necrosis factor; alpha-induced protein 3
	Ssc.16392.2.A1_at	-1.2	-2.5	-2.4	NM_199054	MAP kinase interacting serinethreonine kinase 2
	Ssc.29821.1.A1_at	1.0	-2.4	-2.4	#N/A	#N/A
	Ssc.2306.1.S1_at	-1.0	-2.0	-2.4	NM_015987	heme binding protein 1
	Ssc.6425.1.A1_at	1.1	-3.7	-2.3	#N/A	#N/A
	Ssc.14164.1.A1_at	-1.4	-2.3	-2.3	#N/A	#N/A
	Ssc.16888.1.S1_at	-1.1	-1.6	-2.3	NM_005558	ladinin 1
	Ssc.1600.1.A1_at	-1.3	-2.6	-2.3	NM_020734	KIAA1238 protein
	Ssc.6615.1.S1_at	-1.4	-2.2	-2.3	#N/A	#N/A
	Ssc.19024.1.A1_at	1.0	-2.1	-2.3	NM_139182	centaurin; delta 1
	Ssc.24128.1.A1_at	1.1	-3.9	-2.3	#N/A	#N/A

Cluster 10 cont.	Ssc.7034.1.A1_at	-1.2	-2.0	-2.3	NM_016297	prenylcysteine oxidase 1
	Ssc.2947.1.S1_at	-1.1	-1.7	-2.3	NM_001006665	ribosomal protein S6 kinase; 90kDa; polypeptide 1
	Ssc.15594.1.S1_at	-1.0	-3.3	-2.3	NM_021149	coactosin-like 1
	Ssc.5763.1.A1_at	-1.1	-1.9	-2.3	NM_032936	chromosome 7 open reading frame 35
	Ssc.7460.1.A1_at	-1.5	-1.9	-2.3	NM_006469	influenza virus NS1A binding protein
	Ssc.16147.1.S1_at	-1.0	-1.8	-2.3	NM_001232	calsequestrin 2
	Ssc.19622.1.A1_at	-1.3	-2.3	-2.3	NM_007183	plakophilin 3
	Ssc.8895.1.S1_at	-1.2	-2.5	-2.3	NM_004568	serine
	Ssc.4233.1.S1_at	-1.5	-2.4	-2.3	NM_022776	oxysterol binding protein-like 11
	Ssc.5755.1.S1_at	-1.0	-1.6	-2.3	NM_173823	DnaJ
	Ssc.21187.1.S1_at	-1.0	-2.7	-2.3	#N/A	#N/A
	Ssc.16496.1.S1_at	-1.2	-1.9	-2.3	#N/A	#N/A
	Ssc.4553.1.S1_at	-1.2	-1.5	-2.2	NM_033412	mitochondrial carrier triple repeat 1
	Ssc.23953.1.S1_at	-1.4	-1.0	-2.2	NM_022484	hypothetical protein FLJ13576
	Ssc.30708.1.S1_at	-1.2	-1.8	-2.2	NM_006254	protein kinase C; delta
	Ssc.26027.1.A1_at	-1.2	-1.7	-2.2	#N/A	#N/A
	Ssc.2064.1.A1_at	1.1	-2.5	-2.2	XM_290615	hypothetical protein DKFZp762F0713
	Ssc.12634.1.S1_at	-1.0	-2.3	-2.2	NM_014320	heme binding protein 2
	Ssc.21275.2.S1_at	-1.2	-1.8	-2.2	NM_004703	rabaptin; RAB GTPase binding effector protein 1
	Ssc.5179.1.A1_at	1.1	-2.6	-2.2	NM_006549	calciumcalmodulin-dependent protein kinase kinase 2; beta
	Ssc.22221.1.S1_a_at	-1.5	-3.5	-2.2	NM_000167	glycerol kinase
	Ssc.12633.1.S1_at	-1.1	-1.8	-2.2	#N/A	#N/A
	Ssc.68.1.A1_at	-1.1	-1.5	-2.2	NM_003850	succinate-CoA ligase; ADP-forming; beta subunit
	Ssc.2179.1.S1_at	1.2	-3.9	-2.2	NM_024980	G protein-coupled receptor 157
	Ssc.12938.1.A1_at	1.1	-2.6	-2.2	NM_004841	RAS protein activator like 2
	Ssc.5793.2.S1_at	-1.3	-2.1	-2.2	NM_014698	KIAA0792
	Ssc.5000.1.A1_at	-1.2	-3.8	-2.2	#N/A	#N/A
	Ssc.5353.2.S1_at	-1.1	-2.1	-2.2	NM_016598	zinc finger; DHHC-type containing 3
	Ssc.12282.1.S1_at	-1.2	-2.0	-2.2	NM_006243	protein phosphatase 2; regulatory subunit B
	Ssc.21275.1.A1_at	-1.2	-1.7	-2.2	NM_004703	rabaptin; RAB GTPase binding effector protein 1
	Ssc.24766.1.S1_at	-1.1	-1.8	-2.2	#N/A	#N/A
	Ssc.3623.2.A1_at	-1.5	-1.5	-2.1	NM_001166	baculoviral IAP repeat-containing 2
	Ssc.23132.1.A1_at	-1.1	-1.9	-2.1	NM_198039	nudix

Cluster 10 cont.	Ssc.25008.1.S1_at	-1.3	-1.9	-2.1	#N/A	#N/A
	Ssc.22083.1.S1_at	-1.5	-1.0	-2.1	NM_005746	pre-B-cell colony enhancing factor 1
	Ssc.1746.1.A1_at	-1.1	-2.6	-2.1	NM_138782	FCH domain only 2
	Ssc.31172.3.S1_at	1.1	-3.9	-2.1	NM_001006946	syndecan 1
	Ssc.15316.1.S1_at	-1.2	-2.4	-2.1	NM_001311	cysteine-rich protein 1
	Ssc.4206.1.A1_at	-1.1	-2.3	-2.1	#N/A	#N/A
	Ssc.5353.1.S1_at	-1.1	-1.9	-2.1	NM_016598	zinc finger; DHHC-type containing 3
	Ssc.6441.2.S1_at	-1.0	-1.8	-2.1	NM_016029	dehydrogenasereductase
	Ssc.24193.1.S1_at	-1.1	-1.6	-2.1	NM_024719	growth hormone regulated TBC protein 1
	Ssc.10991.1.A1_at	-1.1	-1.5	-2.1	NM_021160	HLA-B associated transcript 5
	Ssc.1600.1.A1_a_at	-1.2	-2.5	-2.1	NM_020734	KIAA1238 protein
	Ssc.23539.2.S1_at	-1.1	-1.6	-2.1	NM_207125	polyamine oxidase
	Ssc.5158.1.S1_at	-1.1	-2.4	-2.1	NM_024819	hypothetical protein FLJ22955
	Ssc.11910.1.S1_at	1.0	-2.1	-2.1	NM_001981	epidermal growth factor receptor pathway substrate 15
	Ssc.18208.2.S1_at	-1.2	-1.6	-2.1	NM_031436	aldo-keto reductase family 1; member C-like 2
	Ssc.15250.1.S1_at	-1.1	-2.5	-2.1	#N/A	#N/A
	Ssc.21033.1.S1_at	-1.1	-2.0	-2.1	#N/A	#N/A
	Ssc.6771.1.S1_a_at	-1.0	-1.8	-2.1	NM_003130	sorcin
	Ssc.18606.2.A1_at	-1.1	-2.3	-2.1	#N/A	#N/A
	Ssc.27258.1.A1_at	-1.0	-2.0	-2.1	NM_004415	desmoplakin
	Ssc.17318.1.S1_at	-1.1	-1.5	-2.1	NM_003379	villin 2
	Ssc.26747.1.A1_at	-1.3	-1.9	-2.1	XR_000216	cysteine-rich hydrophobic domain 1
	Ssc.17293.1.A1_at	-1.1	-2.1	-2.1	NM_020940	KIAA1600
	Ssc.11077.1.S1_at	-1.1	-1.9	-2.0	NM_003003	SEC14-like 1
	Ssc.18756.1.S1_at	-1.2	-1.2	-2.0	NM_018650	MAPmicrotubule affinity-regulating kinase 1
	Ssc.17918.1.A1_at	-1.1	-2.3	-2.0	#N/A	#N/A
	Ssc.10366.1.A1_at	-1.3	-1.7	-2.0	#N/A	#N/A
	Ssc.6833.1.S1_at	-1.1	-2.7	-2.0	NM_001731	B-cell translocation gene 1; anti-proliferative
	Ssc.22945.1.S1_at	-1.2	-1.9	-2.0	NM_000036	adenosine monophosphate deaminase 1
	Ssc.13891.1.A1_at	-1.5	-3.8	-2.0	NM_152869	regucalcin
	Ssc.3941.1.S1_at	-1.2	-2.2	-2.0	#N/A	#N/A
	Ssc.27835.1.S1_at	-1.1	-2.8	-1.9	NM_020132	1-acylglycerol-3-phosphate O-acyltransferase 3
	Ssc.9953.1.A1_at	-1.5	-2.4	-1.9	#N/A	#N/A

Cluster 10 cont.	Ssc.22732.1.S1_at	-1.1	-2.2	-1.9	#N/A	#N/A
	Ssc.31172.1.S1_at	1.0	-4.5	-1.9	NM_001006946	syndecan 1
	Ssc.20926.1.S1_at	-1.1	-2.1	-1.9	NM_005271	glutamate dehydrogenase 1
	Ssc.29953.1.A1_at	-1.0	-2.7	-1.9	#N/A	#N/A
	Ssc.9908.1.A1_at	-1.2	-2.4	-1.9	#N/A	#N/A
	Ssc.8309.1.A1_at	-1.1	-2.8	-1.9	NM_016245	dehydrogenasereductase
	Ssc.6528.1.S1_at	-1.2	-2.4	-1.9	NM_006412	1-acylglycerol-3-phosphate O-acyltransferase 2
	Ssc.18096.1.A1_at	-1.5	-2.1	-1.8	NM_198353	potassium channel tetramerisation domain containing 8
	Ssc.8061.1.A1_at	-1.2	-2.3	-1.8	#N/A	#N/A
	Ssc.5257.1.S1_at	-1.5	-2.2	-1.8	NM_006577	UDP-GlcNAc:betaGal beta-1;3-N-acetylglucosaminyltransferas
	Ssc.21999.1.S1_a_at	-1.4	-2.2	-1.8	NM_000694	aldehyde dehydrogenase 3 family; member B1
	Ssc.18893.1.A1_at	-1.4	-2.6	-1.7	#N/A	#N/A
	Ssc.10307.1.A1_at	-1.5	-3.9	-1.7	#N/A	#N/A
	n = 364	**-1.1**	**-2.7**	**-3.3**		
Cluster 11	Ssc.18619.1.A1_at	-1.0	1.3	2.9	NM_021183	RAP2C; member of RAS oncogene family
	Ssc.1987.1.S1_at	-1.1	1.1	3.0	NM_004740	TGFB1-induced anti-apoptotic factor 1
	Ssc.19323.1.S1_at	1.2	-1.1	3.0	NM_138389	hypothetical protein BC001096
	Ssc.15674.1.A1_at	-1.2	1.6	3.0	XM_497242	similar to Cathepsin L; preproprotein
	Ssc.2897.1.S1_at	1.1	1.4	3.0	NM_170662	Cas-Br-M
	Ssc.6923.1.A1_at	1.5	1.4	3.0	#N/A	#N/A
	Ssc.27592.2.S1_at	1.1	1.2	3.0	NM_003956	cholesterol 25-hydroxylase
	Ssc.19212.1.S1_at	-1.0	1.1	3.0	NM_000387	solute carrier family 25
	Ssc.6666.1.A1_at	1.2	1.6	3.0	NM_014575	schwannomin interacting protein 1
	Ssc.18578.1.S1_at	-1.3	-1.3	3.1	NM_175842	spermine oxidase
	Ssc.18900.1.A1_at	1.1	1.1	3.1	#N/A	#N/A
	Ssc.7697.1.A1_at	1.3	1.8	3.1	#N/A	#N/A
	Ssc.9279.1.A1_at	-1.0	1.1	3.1	#N/A	#N/A
	Ssc.1798.1.S1_at	1.2	1.4	3.1	NM_003088	fascin homolog 1; actin-bundling protein
	Ssc.2567.2.A1_at	-1.1	1.7	3.2	#N/A	#N/A
	Ssc.8427.1.A1_at	1.1	1.4	3.2	NM_018999	KIAA1128
	Ssc.30667.1.S1_at	-1.3	1.1	3.2	#N/A	#N/A
	Ssc.11251.1.A1_at	1.0	1.1	3.2	#N/A	#N/A
	Ssc.24543.1.S1_at	1.2	1.9	3.2	#N/A	#N/A

Cluster 11 cont.	Ssc.7021.1.A1_at	1.2	1.5	3.3	NM_001431	erythrocyte membrane protein band 4.1-like 2
	Ssc.3321.1.A1_at	1.2	1.8	3.3	NM_001017423	aldehyde dehydrogenase 18 family; member A1
	Ssc.9391.1.A1_at	1.0	1.2	3.3	NM_014734	KIAA0247
	Ssc.12578.1.A1_at	1.6	-1.1	3.3	NM_000618	insulin-like growth factor 1
	Ssc.12842.1.S1_at	1.0	1.1	3.3	NM_001753	caveolin 1; caveolae protein; 22kDa
	Ssc.18540.1.S1_at	1.0	1.0	3.3	#N/A	#N/A
	Ssc.26253.1.S1_at	-1.2	1.0	3.4	#N/A	#N/A
	Ssc.27142.1.A1_at	-2.9	-1.7	3.4	#N/A	#N/A
	Ssc.10859.1.S1_at	-1.1	1.3	3.4	#N/A	#N/A
	Ssc.2642.1.S1_at	1.1	1.3	3.4	NM_003312	thiosulfate sulfurtransferase
	Ssc.1447.1.A1_at	1.1	1.9	3.4	#N/A	#N/A
	Ssc.3021.1.A1_at	1.5	1.2	3.4	#N/A	#N/A
	Ssc.5574.1.S1_at	1.2	1.6	3.4	#N/A	#N/A
	Ssc.5683.1.S1_a_at	-1.2	-1.0	3.4	NM_022371	torsin family 3; member A
	Ssc.26771.1.S1_at	1.0	2.0	3.5	#N/A	#N/A
	Ssc.19873.1.S1_at	1.1	1.2	3.5	NM_194071	cAMP responsive element binding protein 3-like 2
	Ssc.30989.1.A1_at	1.0	1.3	3.5	XM_035299	zinc finger; SWIM domain containing 6
	Ssc.21666.1.S1_at	1.3	1.9	3.5	NM_032562	phospholipase A2; group XIIB
	Ssc.3016.1.S1_at	-1.3	1.1	3.5	#N/A	#N/A
	Ssc.5330.1.A1_at	-1.0	2.0	3.5	#N/A	#N/A
	Ssc.24880.2.S1_at	1.1	1.9	3.5	NM_005385	natural killer-tumor recognition sequence
	Ssc.25121.1.S1_at	1.0	1.2	3.5	#N/A	#N/A
	Ssc.23823.1.A1_at	-1.2	1.5	3.5	NM_005994	T-box 2
	Ssc.18030.1.A1_at	-1.0	-1.1	3.5	#N/A	#N/A
	Ssc.22444.1.A1_at	1.1	1.6	3.5	#N/A	#N/A
	Ssc.11177.1.S1_at	1.2	1.6	3.5	#N/A	#N/A
	Ssc.6394.1.S1_at	1.0	1.5	3.6	NM_198968	DAZ interacting protein 1
	Ssc.2301.1.S1_at	-1.3	1.5	3.6	NM_031283	transcription factor 7-like 1
	Ssc.14914.1.A1_at	1.1	1.2	3.6	NM_002166	inhibitor of DNA binding 2; dominant negative helix-loop-h
	Ssc.9617.1.A1_at	1.5	1.8	3.6	NM_006718	pleiomorphic adenoma gene-like 1
	Ssc.3409.1.A1_at	1.3	1.6	3.6	NM_213662	signal transducer and activator of transcription 3
	Ssc.29038.1.A1_at	-1.1	1.4	3.6	NM_018388	muscleblind-like 3
	Ssc.7149.3.S1_at	-1.0	1.5	3.6	NM_144607	hypothetical protein FLJ32499

Cluster 11 cont.	Ssc.24152.1.A1_at	-1.2	1.2	3.7	NM_005585	SMAD; mothers against DPP homolog 6
	Ssc.24304.2.A1_at	1.3	1.4	3.7	NM_182801	hypothetical protein FLJ39155
	Ssc.31000.1.A1_at	-1.2	1.4	3.7	XM_294353	similar to RIKEN cDNA 6332401O19 gene
	Ssc.183.1.S1_at	1.1	1.9	3.7	NM_004832	glutathione S-transferase omega 1
	Ssc.6352.1.S1_at	1.2	1.7	3.7	NM_000581	glutathione peroxidase 1
	Ssc.2131.1.S1_at	1.3	1.6	3.7	NM_031920	ARG99 protein
	Ssc.2845.1.S1_at	1.0	1.8	3.7	NM_014994	mouse mitogen-activated protein kinase binding protein 1-l
	Ssc.5737.1.S1_at	1.7	-1.2	3.8	NM_078467	cyclin-dependent kinase inhibitor 1A
	Ssc.30029.1.A1_at	-1.2	1.3	3.8	#N/A	#N/A
	Ssc.29435.1.A1_at	1.3	1.4	3.8	NM_003483	high mobility group AT-hook 2
	Ssc.19620.1.S1_at	1.2	1.5	3.8	NM_199262	Sp6 transcription factor
	Ssc.2203.1.A1_at	-1.1	1.7	3.8	#N/A	#N/A
	Ssc.27310.1.S1_at	1.2	1.1	3.8	NM_207361	FRAS1 related extracellular matrix protein 2
	Ssc.26237.1.A1_at	-1.2	-1.1	3.9	NM_006522	wingless-type MMTV integration site family; member 6
	Ssc.18618.1.A1_at	-1.1	-1.0	3.9	#N/A	#N/A
	Ssc.1351.1.S1_at	-1.1	1.3	3.9	NM_006612	kinesin family member 1C
	Ssc.29043.2.A1_at	1.2	1.4	4.0	NM_205860	nuclear receptor subfamily 5; group A; member 2
	n = 69	**1.1**	**1.4**	**3.4**		
Cluster 12	Ssc.4984.1.S1_at	-1.0	1.9	36.7	NM_004887	chemokine
	Ssc.18707.1.A1_at	1.1	2.9	38.7	#N/A	#N/A
	Ssc.8859.1.A1_at	-1.1	4.9	42.2	#N/A	#N/A
	Ssc.5165.1.S1_at	1.1	4.7	42.6	#N/A	#N/A
	Ssc.24584.1.S1_at	1.4	4.8	43.9	#N/A	#N/A
	Ssc.8803.1.A1_at	-1.1	5.9	44.2	NM_016542	Mst3 and SOK1-related kinase
	Ssc.15316.2.S1_at	1.0	1.2	44.7	NM_001311	cysteine-rich protein 1
	Ssc.10389.1.A1_at	-1.0	6.1	49.3	#N/A	#N/A
	Ssc.4815.1.A1_at	1.1	1.4	50.9	#N/A	#N/A
	Ssc.19394.1.A1_at	1.0	1.3	51.9	#N/A	#N/A
	Ssc.8859.1.A1_s_at	-1.1	6.3	54.7	#N/A	#N/A
	n = 11	**1.0**	**3.8**	**45.4**		
Cluster 13	Ssc.17283.3.S1_at	1.0	2.9	10.3	#N/A	#N/A
	Ssc.23766.1.S1_at	1.3	2.3	10.5	NM_015288	PHD finger protein 15
	Ssc.19579.2.S1_at	-1.2	1.7	11.1	#N/A	#N/A

Cluster 13 cont.	Ssc.19587.1.A1_at	1.4	2.4	11.4	NM_205860	nuclear receptor subfamily 5; group A; member 2
	Ssc.10328.1.A1_at	1.1	4.2	11.4	NM_001010000	Rho GTPase activating protein 28
	Ssc.24731.1.A1_at	1.1	4.6	12.0	NM_032246	ring finger and KH domain containing 3
	Ssc.23501.1.S1_s_at	1.4	2.2	12.1	#N/A	#N/A
	Ssc.15695.1.S1_at	1.8	2.4	12.2	NM_006744	retinol binding protein 4; plasma
	Ssc.11131.1.S1_at	1.0	1.5	12.4	NM_003380	vimentin
	Ssc.14258.1.S1_at	1.5	4.7	12.6	NM_000484	amyloid beta
	Ssc.21113.1.A1_at	1.2	1.8	12.7	#N/A	#N/A
	Ssc.20728.1.S1_at	1.5	3.0	12.8	NM_005141	fibrinogen; B beta polypeptide
	Ssc.13284.1.A1_at	1.6	4.7	13.1	NM_001010927	T-cell lymphoma invasion and metastasis 2
	n = 13	**1.3**	**3.0**	**11.9**		
Cluster 14	Ssc.23271.1.S1_at	1.7	8.8	2.1	#N/A	#N/A
	Ssc.16475.1.S1_at	-1.0	7.6	3.2	NM_003489	nuclear receptor interacting protein 1
	Ssc.19413.1.A1_at	1.4	6.9	3.6	NM_003107	SRY
	Ssc.1583.2.S1_at	1.1	6.9	4.0	NM_001624	absent in melanoma 1
	Ssc.22876.1.S1_at	1.9	6.1	4.2	NM_015864	chromosome 6 open reading frame 32
	Ssc.27407.1.A1_at	1.1	5.8	4.2	NM_003489	nuclear receptor interacting protein 1
	Ssc.12565.1.A1_at	1.3	6.4	4.3	NM_005504	branched chain aminotransferase 1; cytosolic
	Ssc.18004.1.A1_at	1.8	7.8	4.5	#N/A	#N/A
	Ssc.9586.2.S1_at	2.0	7.3	4.6	NM_004657	serum deprivation response
	Ssc.19360.1.S1_at	-1.3	5.9	4.8	NM_020379	mannosidase; alpha; class 1C; member 1
	n = 10	**1.4**	**6.9**	**4.0**		
Cluster 15	Ssc.7598.1.A1_at	1.3	9.2	22.1	NM_003711	phosphatidic acid phosphatase type 2A
	Ssc.7399.1.A1_at	1.4	5.8	23.0	#N/A	#N/A
	Ssc.265.1.S3_at	1.1	7.6	24.2	NM_000230	leptin
	Ssc.27522.1.S1_at	1.3	4.0	26.0	NM_015550	oxysterol binding protein-like 3
	Ssc.3668.1.A1_at	-1.1	1.8	26.9	NM_005382	neurofilament 3
	Ssc.7486.1.A1_at	1.6	11.7	30.6	NM_000783	cytochrome P450; family 26; subfamily A; polypeptide 1
	Ssc.5545.1.S1_at	-1.1	3.4	30.9	#N/A	#N/A
	Ssc.6070.1.A1_at	1.5	5.1	34.7	NM_015550	oxysterol binding protein-like 3
	n = 8	**1.3**	**6.1**	**27.3**		
Cluster 16	Ssc.29187.1.A1_at	1.5	24.2	49.1	NM_000165	gap junction protein; alpha 1; 43kDa
	Ssc.942.1.S1_at	1.3	24.6	51.3	NM_000165	gap junction protein; alpha 1; 43kDa

Cluster 16 cont.	Ssc.7484.3.S1_at	-1.6	14.7	59.8	#N/A	#N/A
	Ssc.21874.1.S1_at	1.5	4.2	65.6	NM_015550	oxysterol binding protein-like 3
	Ssc.7588.1.A1_at	1.3	15.9	67.6	#N/A	#N/A
	Ssc.28944.1.S1_at	1.1	3.6	71.6	#N/A	#N/A
	Ssc.22563.1.S1_at	2.1	27.8	72.7	NM_006581	fucosyltransferase 9
	Ssc.10188.1.A1_at	1.1	9.3	73.9	#N/A	#N/A
	Ssc.4193.1.S1_at	-1.1	52.4	75.9	#N/A	#N/A
	n = 9	**1.3**	**19.6**	**65.3**		
Cluster 17	Ssc.29168.1.A1_at	1.2	2.0	2.0	NM_024420	phospholipase A2; group IVA
	Ssc.2877.1.A1_at	-1.0	1.7	2.0	#N/A	#N/A
	Ssc.1340.1.A1_at	1.5	1.9	2.0	#N/A	#N/A
	Ssc.29108.1.S1_at	1.2	1.7	2.1	NM_022845	core-binding factor; beta subunit
	Ssc.27561.2.S1_at	-1.1	1.9	2.1	NM_032636	differential display and activated by p53
	Ssc.4414.1.S1_at	1.0	1.7	2.1	NM_002657	pleiomorphic adenoma gene-like 2
	Ssc.1053.1.S1_at	1.6	1.8	2.1	NM_007361	nidogen 2
	Ssc.6034.2.S1_a_at	1.0	1.9	2.1	NM_033102	prostate cancer associated protein 6
	Ssc.19508.1.S1_at	1.1	1.6	2.1	#N/A	#N/A
	Ssc.19208.2.S1_at	1.3	1.6	2.1	NM_000457	hepatocyte nuclear factor 4; alpha
	Ssc.5073.1.A1_at	1.0	2.1	2.1	NM_004456	enhancer of zeste homolog 2
	Ssc.7712.1.A1_at	1.2	1.6	2.2	#N/A	#N/A
	Ssc.15228.1.A1_at	1.3	1.5	2.2	NM_016824	adducin 3
	Ssc.26216.2.A1_at	1.3	1.7	2.2	NM_003745	suppressor of cytokine signaling 1
	Ssc.30916.1.A1_at	1.2	1.6	2.2	NM_181847	amphoterin induced gene 2
	Ssc.1333.1.A1_at	-1.0	1.9	2.2	NM_001009882	zinc finger; CCHC domain containing 11
	Ssc.4306.1.A1_at	1.3	1.5	2.2	NM_022566	mesoderm development candidate 1
	Ssc.17405.2.A1_at	1.0	1.6	2.2	NM_002537	ornithine decarboxylase antizyme 2
	Ssc.4044.1.A1_at	-1.2	1.8	2.2	#N/A	#N/A
	Ssc.1725.1.S1_at	1.2	1.9	2.2	NM_003705	solute carrier family 25
	Ssc.19801.1.S1_at	1.3	1.7	2.2	NM_033495	kelch-like 13
	Ssc.21326.1.S1_at	1.2	2.2	2.2	#N/A	#N/A
	Ssc.2441.2.A1_at	1.0	1.6	2.2	NM_000341	solute carrier family 3
	Ssc.14340.1.S1_at	1.3	1.9	2.2	NM_004862	lipopolysaccharide-induced TNF factor
	Ssc.1702.2.S1_at	-1.1	1.6	2.2	NM_145290	G protein-coupled receptor 125

Cluster 17 cont.	Ssc.10300.1.S1_at	1.3	1.9	2.3	NM_033495	kelch-like 13
	Ssc.31097.1.A1_at	1.1	2.1	2.3	NM_020774	mindbomb homolog 1
	Ssc.19282.1.S1_at	1.2	1.6	2.3	NM_198530	transmembrane anchor protein 1
	Ssc.9299.1.S1_at	1.4	1.5	2.3	NM_030751	transcription factor 8
	Ssc.21928.1.A1_at	1.0	1.7	2.3	NM_001010853	aminoacylase 1-like 2
	Ssc.384.2.S1_at	1.0	2.0	2.3	NM_002056	glutamine-fructose-6-phosphate transaminase 1
	Ssc.20404.1.S1_at	1.1	2.0	2.3	NM_001618	poly
	Ssc.5157.1.S1_at	1.4	1.7	2.3	NM_022003	FXYD domain containing ion transport regulator 6
	Ssc.26660.1.A1_at	1.1	1.9	2.3	NM_175848	DNA
	Ssc.1097.1.A1_at	1.2	1.8	2.4	#N/A	#N/A
	Ssc.7567.1.S1_at	1.2	2.0	2.4	NM_020774	mindbomb homolog 1
	Ssc.24254.1.S1_at	-1.2	1.6	2.4	NM_138423	H63 breast cancer expressed gene
	Ssc.20239.1.A1_at	1.1	1.6	2.4	#N/A	#N/A
	Ssc.7351.1.S1_at	-1.5	1.7	2.4	NM_014962	BTB
	Ssc.7481.1.A1_at	1.2	1.4	2.4	NM_020200	phosphoribosyl transferase domain containing 1
	Ssc.16609.1.S1_at	-1.1	1.7	2.4	NM_000232	sarcoglycan; beta
	Ssc.25221.1.A1_at	1.2	1.7	2.4	NM_033331	CDC14 cell division cycle 14 homolog B
	Ssc.1084.1.S1_at	1.1	2.4	2.4	NM_016472	chromosome 14 open reading frame 129
	Ssc.8552.3.S1_a_at	1.1	1.5	2.4	NM_182974	glycosyltransferase 6 domain containing 1
	Ssc.23933.1.A1_at	1.1	1.5	2.4	#N/A	#N/A
	Ssc.8905.1.A1_at	-1.1	1.8	2.4	NM_014335	CREBBPEP300 inhibitor 1
	Ssc.5455.1.S1_at	1.1	2.0	2.5	NM_001360	7-dehydrocholesterol reductase
	Ssc.4578.2.S1_at	1.2	1.5	2.5	NM_003567	breast cancer anti-estrogen resistance 3
	Ssc.3990.1.S1_at	-1.1	1.9	2.5	#N/A	#N/A
	Ssc.9037.1.A1_at	1.1	2.1	2.5	#N/A	#N/A
	Ssc.25570.1.S1_at	-1.1	1.5	2.5	NM_024896	KIAA1815
	Ssc.6736.1.S1_at	-1.2	1.8	2.5	NM_002449	msh homeo box homolog 2
	Ssc.15912.1.A1_at	1.2	2.2	2.5	NM_000165	gap junction protein; alpha 1; 43kDa
	Ssc.10906.1.A1_at	1.1	2.2	2.5	#N/A	#N/A
	Ssc.24616.1.S1_a_at	1.7	1.8	2.5	NM_022128	ribokinase
	Ssc.25535.1.S1_at	1.2	1.5	2.5	#N/A	#N/A
	Ssc.1267.1.S1_at	-1.1	1.5	2.5	NM_015554	glucuronyl C5-epimerase
	Ssc.112.1.S1_at	1.0	1.8	2.5	NM_002192	inhibin; beta A

Cluster 17 cont.	Ssc.4159.1.A1_at	-1.1	1.8	2.5	NM_002069	guanine nucleotide binding protein
	Ssc.16704.1.S1_at	1.3	1.9	2.6	NM_006283	transforming; acidic coiled-coil containing protein 1
	Ssc.21860.2.S1_at	-1.1	1.9	2.6	NM_002823	prothymosin; alpha
	Ssc.5735.2.S1_at	1.0	1.4	2.6	NM_022908	hypothetical protein FLJ12442
	Ssc.8407.1.A1_at	-1.1	2.1	2.6	NM_138423	H63 breast cancer expressed gene
	Ssc.12668.1.A1_at	1.3	1.4	2.6	NM_173561	unc-5 homolog C
	Ssc.16996.1.S1_at	1.2	1.4	2.6	NM_006640	septin 9
	Ssc.897.1.S1_at	1.5	2.1	2.6	NM_006307	sushi-repeat-containing protein; X-linked
	Ssc.13844.1.A1_at	1.1	2.0	2.6	NM_032186	zinc finger protein 644
	Ssc.29146.1.A1_at	-1.2	1.5	2.7	#N/A	#N/A
	Ssc.2147.1.A1_at	1.0	1.5	2.7	#N/A	#N/A
	Ssc.2012.1.A1_at	1.2	2.1	2.7	#N/A	#N/A
	Ssc.15592.1.S1_at	1.0	2.2	2.7	NM_020190	olfactomedin-like 3
	Ssc.9914.1.A1_at	-1.0	1.9	2.7	NM_001823	creatine kinase; brain
	Ssc.11844.1.A1_at	1.2	1.6	2.7	#N/A	#N/A
	Ssc.12316.1.S1_at	1.1	1.6	2.7	NM_182565	hypothetical protein MGC29814
	Ssc.17824.1.A1_at	1.0	1.8	2.7	#N/A	#N/A
	Ssc.25405.1.S1_at	1.3	2.2	2.7	NM_145119	praja 1
	Ssc.21154.1.A1_at	1.3	1.7	2.7	NM_005443	3-phosphoadenosine 5-phosphosulfate synthase 1
	Ssc.11694.1.S1_at	1.1	2.1	2.8	NM_002166	inhibitor of DNA binding 2; dominant negative helix-loop-h
	Ssc.24804.1.S1_at	1.1	1.6	2.8	#N/A	#N/A
	Ssc.955.1.S1_at	1.2	1.4	2.8	NM_000769	cytochrome P450; family 2; subfamily C; polypeptide 19
	Ssc.19798.2.A1_at	1.2	1.7	2.8	#N/A	#N/A
	Ssc.6376.1.A1_at	-1.1	2.0	2.8	#N/A	#N/A
	Ssc.7429.1.A1_at	-1.0	1.5	2.8	#N/A	#N/A
	Ssc.27015.1.A1_at	1.0	1.5	2.8	#N/A	#N/A
	Ssc.24083.1.A1_at	1.2	1.5	2.8	NM_017523	XIAP associated factor-1
	Ssc.3128.1.A1_at	1.6	1.4	2.8	#N/A	#N/A
	Ssc.30377.1.A1_at	1.4	1.9	2.9	NM_015271	tripartite motif-containing 2
	Ssc.7712.2.S1_at	1.2	1.8	2.9	NM_006283	transforming; acidic coiled-coil containing protein 1
	Ssc.29090.1.A1_at	1.5	1.7	2.9	NM_015278	SAM and SH3 domain containing 1
	Ssc.12789.1.A1_at	1.2	1.6	2.9	#N/A	#N/A
	Ssc.5832.1.S1_at	-1.1	1.6	2.9	NM_004973	Jumonji; AT rich interactive domain 2

Cluster 17 cont.	Ssc.5663.2.S1_at	1.5	2.0	2.9	#N/A	#N/A
	Ssc.7266.1.A1_at	-1.1	1.9	2.9	NM_006475	periostin; osteoblast specific factor
	Ssc.24911.1.S1_at	-1.0	2.0	2.9	NM_018964	solute carrier family 37
	Ssc.26296.1.S1_at	1.1	1.7	2.9	NM_012288	translocation associated membrane protein 2
	Ssc.6789.1.A1_at	1.2	1.7	2.9	NM_003690	protein kinase; interferon-inducible double stranded RNA d
	Ssc.24304.1.S1_at	1.3	1.5	3.0	NM_152403	hypothetical protein FLJ39155
	Ssc.19208.1.S1_at	1.3	1.7	3.0	#N/A	#N/A
	Ssc.3921.1.S1_at	1.2	1.9	3.0	NM_001430	endothelial PAS domain protein 1
	Ssc.21972.1.A1_at	1.3	2.0	3.1	#N/A	#N/A
	n = 100	**1.1**	**1.8**	**2.5**		
Cluster 18	Ssc.27995.1.A1_at	-1.1	2.7	2.4	NM_013282	ubiquitin-like; containing PHD and RING finger domains; 1
	Ssc.17512.1.S1_at	1.3	2.5	2.6	#N/A	#N/A
	Ssc.1696.1.A1_at	1.4	3.1	2.6	NM_001004417	formin-like 2
	Ssc.5287.1.S1_at	1.3	2.5	2.6	#N/A	#N/A
	Ssc.5039.1.A1_at	1.3	2.6	2.7	NM_178568	reticulon 4 receptor-like 1
	Ssc.30743.1.S1_at	1.5	3.0	2.7	NM_145753	pleckstrin homology-like domain; family B; member 2
	Ssc.4900.2.S1_at	1.2	3.5	2.7	NM_016441	cysteine-rich motor neuron 1
	Ssc.16259.1.S1_at	1.1	2.4	2.8	NM_002069	guanine nucleotide binding protein
	Ssc.1849.1.A1_at	1.2	2.6	2.8	#N/A	#N/A
	Ssc.22297.1.S1_at	-1.1	2.7	2.8	#N/A	#N/A
	Ssc.12340.1.A1_at	2.5	2.2	2.8	#N/A	#N/A
	Ssc.5039.2.S1_at	1.3	2.9	2.8	NM_178568	reticulon 4 receptor-like 1
	Ssc.1638.1.S1_at	-1.4	2.3	2.9	NM_002167	inhibitor of DNA binding 3; dominant negative helix-loop-h
	Ssc.6034.1.S1_at	-1.0	2.6	2.9	NM_033102	prostate cancer associated protein 6
	Ssc.8929.1.S1_at	1.3	2.2	2.9	NM_153333	transcription elongation factor A
	Ssc.23085.2.S1_at	1.1	3.1	3.0	NM_032637	S-phase kinase-associated protein 2
	Ssc.23085.1.S1_at	1.1	2.4	3.0	#N/A	#N/A
	Ssc.9321.1.S1_at	-1.3	3.0	3.0	NM_025078	PQ loop repeat containing 1
	Ssc.18546.1.S1_at	1.3	3.1	3.1	NM_016441	cysteine-rich motor neuron 1
	Ssc.7210.1.A1_at	1.4	2.3	3.1	NM_015271	tripartite motif-containing 2
	Ssc.1969.1.A1_at	-1.2	3.2	3.1	NM_006022	TSC22 domain family; member 1
	Ssc.7881.1.A1_at	1.4	2.5	3.2	NM_145753	pleckstrin homology-like domain; family B; member 2
	Ssc.4214.1.A1_at	1.2	2.9	3.2	#N/A	#N/A

Cluster 18 cont.	Ssc.29264.1.A1_at	1.4	3.1	3.2	#N/A	#N/A
	Ssc.26957.1.S1_at	1.1	2.1	3.3	NM_004172	solute carrier family 1
	Ssc.11796.1.S1_at	1.0	2.4	3.3	NM_031934	RAB34; member RAS oncogene family
	Ssc.24444.1.A1_at	1.1	2.4	3.3	NM_004816	chromosome 9 open reading frame 61
	Ssc.19008.1.A1_at	1.1	2.5	3.3	#N/A	#N/A
	Ssc.27045.1.A1_at	1.2	3.0	3.3	NM_004508	isopentenyl-diphosphate delta isomerase
	Ssc.13537.1.A1_at	1.3	2.2	3.4	NM_005399	protein kinase; AMP-activated; beta 2 non-catalytic subuni
	Ssc.5605.1.A1_at	-1.3	3.2	3.4	NM_002222	inositol 1;4;5-triphosphate receptor; type 1
	Ssc.6474.1.S1_at	-1.1	2.7	3.4	NM_000637	glutathione reductase
	Ssc.25282.1.S1_at	-1.1	2.5	3.5	NM_001018009	SH3-domain binding protein 5
	Ssc.8528.1.A1_at	1.1	2.6	3.7	#N/A	#N/A
	Ssc.12429.1.S1_at	-1.1	2.7	3.7	NM_032790	hypothetical protein FLJ14466
	Ssc.28645.1.A1_at	1.2	3.0	3.8	NM_003045	solute carrier family 7
	Ssc.4503.1.A1_at	-1.2	2.8	3.8	#N/A	#N/A
	Ssc.26270.1.S1_at	-1.6	3.3	3.8	NM_147189	hypothetical protein MGC39325
	Ssc.2864.1.S1_at	1.1	2.8	3.9	NM_006094	deleted in liver cancer 1
	Ssc.7312.1.A1_at	1.7	3.1	4.0	#N/A	#N/A
	n = 40	**1.2**	**2.7**	**3.1**		
Cluster 19	Ssc.13529.1.A1_at	-2.0	1.2	2.0	#N/A	#N/A
	Ssc.3889.1.S1_at	-1.1	1.2	2.0	#N/A	#N/A
	Ssc.7149.2.A1_at	-1.0	1.3	2.0	NM_144607	hypothetical protein FLJ32499
	Ssc.23095.1.A1_at	1.0	1.3	2.0	#N/A	#N/A
	Ssc.12654.2.A1_at	-1.0	1.4	2.0	#N/A	#N/A
	Ssc.3043.1.S1_at	1.1	1.0	2.0	NM_152999	six transmembrane epithelial antigen of the prostate 2
	Ssc.11518.1.A1_at	-1.2	1.1	2.0	#N/A	#N/A
	Ssc.894.1.A1_at	-1.0	1.5	2.0	#N/A	#N/A
	Ssc.4692.1.A1_at	1.0	1.2	2.0	#N/A	#N/A
	Ssc.15840.1.S1_a_at	-1.1	1.3	2.0	NM_022969	fibroblast growth factor receptor 2
	Ssc.8623.1.A1_at	1.1	1.2	2.1	NM_006364	Sec23 homolog A
	Ssc.19161.1.A1_at	-1.3	1.2	2.1	#N/A	#N/A
	Ssc.27462.1.A1_at	1.1	1.1	2.1	NM_015691	KIAA1280 protein
	Ssc.22055.1.A1_at	-1.0	-1.0	2.1	NM_022763	fibronectin type III domain containing 3B
	Ssc.17490.1.S1_at	1.3	1.1	2.1	#N/A	#N/A

Cluster 19 cont.	Ssc.9714.1.S1_at	1.1	1.1	2.1	NM_006769	LIM domain only 4
	Ssc.28930.1.S1_at	-1.2	1.2	2.1	#N/A	#N/A
	Ssc.27539.1.A1_at	-1.0	1.3	2.1	NM_173519	hypothetical protein MGC34646
	Ssc.19763.1.S1_at	1.1	1.4	2.1	#N/A	#N/A
	Ssc.21559.1.S1_at	-1.5	1.1	2.1	NM_017664	ankyrin repeat domain 10
	Ssc.28935.1.S1_at	-1.0	1.3	2.1	NM_182896	ADP-ribosylation factor-like 2-like 1
	Ssc.3570.1.S1_at	1.0	1.3	2.1	#N/A	#N/A
	Ssc.13640.1.A1_at	-1.0	1.4	2.1	#N/A	#N/A
	Ssc.3548.1.S1_at	1.4	-1.9	2.1	#N/A	#N/A
	Ssc.18472.1.S1_at	1.1	1.3	2.1	#N/A	#N/A
	Ssc.1943.1.S1_at	1.1	1.1	2.1	#N/A	#N/A
	Ssc.3799.3.A1_a_at	-1.1	1.3	2.1	NM_001008710	RNA binding protein with multiple splicing
	Ssc.15875.1.S1_at	-1.0	1.5	2.1	NM_021069	ArgAbl-interacting protein ArgBP2
	Ssc.10317.1.A1_at	-1.1	1.5	2.1	NM_024089	KDEL
	Ssc.18674.1.A1_at	-1.2	1.2	2.1	NM_004497	forkhead box A3
	Ssc.16380.1.A1_at	-1.2	1.2	2.1	#N/A	#N/A
	Ssc.17347.1.S1_at	1.1	1.1	2.1	NM_022172	pyruvate carboxylase
	Ssc.15917.1.S1_at	-1.1	1.3	2.1	NM_000546	tumor protein p53
	Ssc.27134.1.A1_at	-1.1	1.1	2.1	#N/A	#N/A
	Ssc.2869.1.S1_at	-1.1	1.5	2.1	NM_017911	chromosome 22 open reading frame 8
	Ssc.4021.1.S1_at	1.0	1.2	2.2	NM_006411	1-acylglycerol-3-phosphate O-acyltransferase 1
	Ssc.16982.1.S1_at	-1.5	-1.2	2.2	NM_014061	melanoma antigen family H; 1
	Ssc.4950.1.S1_at	-1.1	1.3	2.2	#N/A	#N/A
	Ssc.8576.1.A1_at	1.1	1.5	2.2	NM_018847	kelch-like 9
	Ssc.3670.1.S1_a_at	1.2	1.0	2.2	NM_022356	leucine proline-enriched proteoglycan
	Ssc.29043.3.S1_at	-1.0	1.2	2.2	NM_003822	nuclear receptor subfamily 5; group A; member 2
	Ssc.20161.1.S1_at	-1.2	1.5	2.2	XM_059037	WT1-interacting protein
	Ssc.27799.1.S1_at	-1.3	1.2	2.2	NM_004093	ephrin-B2
	Ssc.24239.1.S1_at	1.3	1.2	2.2	NM_031453	chromosome 10 open reading frame 45
	Ssc.23540.3.S1_at	1.1	1.1	2.2	#N/A	#N/A
	Ssc.19798.1.S1_at	1.1	1.5	2.2	NM_152261	hypothetical protein MGC17943
	Ssc.19462.1.S1_at	-1.0	1.1	2.2	NM_005587	MADS box transcription enhancer factor 2; polypeptide A
	Ssc.28226.1.S1_at	1.0	1.4	2.2	#N/A	#N/A

Cluster 19 cont.	Ssc.5966.1.A1_at	-1.5	1.0	2.2	NM_024324	hypothetical protein MGC11256
	Ssc.23073.1.A1_at	1.1	1.1	2.2	NM_015691	KIAA1280 protein
	Ssc.13397.1.S1_at	1.1	1.2	2.2	NM_004311	ADP-ribosylation factor-like 3
	Ssc.6333.1.A1_at	-1.0	1.2	2.2	#N/A	#N/A
	Ssc.23658.1.S1_at	1.0	1.2	2.2	NM_016459	proapoptotic caspase adaptor protein
	Ssc.24596.1.S1_at	1.3	1.1	2.2	#N/A	#N/A
	Ssc.19363.1.S1_at	-1.1	1.3	2.2	NM_032493	adaptor-related protein complex 1; mu 1 subunit
	Ssc.9504.1.A1_at	-1.1	-1.4	2.3	#N/A	#N/A
	Ssc.1896.2.A1_a_at	1.1	-1.1	2.3	NM_000156	guanidinoacetate N-methyltransferase
	Ssc.18253.1.S1_at	-1.3	1.3	2.3	#N/A	#N/A
	Ssc.27354.1.S1_at	-1.3	-1.3	2.3	NM_139244	syntaxin binding protein 5
	Ssc.12524.1.S1_at	1.1	1.3	2.3	NM_016579	CD320 antigen
	Ssc.30788.1.S1_at	-1.1	1.5	2.3	#N/A	#N/A
	Ssc.21857.1.S1_at	-1.0	1.2	2.3	NM_001001555	growth factor receptor-bound protein 10
	Ssc.3799.1.S1_a_at	-1.1	1.4	2.3	NM_001008712	RNA binding protein with multiple splicing
	Ssc.6570.1.S1_at	-1.1	1.4	2.3	NM_000031	aminolevulinate; delta-; dehydratase
	Ssc.272.1.S1_a_at	1.7	1.1	2.3	NM_000574	decay accelerating factor for complement
	Ssc.17824.2.A1_at	-1.0	1.5	2.3	#N/A	#N/A
	Ssc.25051.1.S1_at	1.5	-1.3	2.3	NM_016950	sparcosteonectin; cwcv and kazal-like domains proteoglycan
	Ssc.26363.1.S1_at	-1.2	-1.2	2.3	NM_012262	heparan sulfate 2-O-sulfotransferase 1
	Ssc.13380.1.A1_at	-1.1	-1.2	2.3	#N/A	#N/A
	Ssc.29936.1.A1_at	-1.0	1.4	2.3	#N/A	#N/A
	Ssc.9874.1.S1_at	1.1	1.4	2.3	NM_014764	DAZ associated protein 2
	Ssc.11794.1.A1_at	-1.2	-1.1	2.3	#N/A	#N/A
	Ssc.18072.1.A1_at	1.7	1.3	2.3	#N/A	#N/A
	Ssc.26813.1.S1_at	-1.4	-1.2	2.3	NM_201614	IKK interacting protein
	Ssc.20242.1.A1_at	1.0	1.0	2.3	NM_020119	zinc finger CCCH-type; antiviral 1
	Ssc.12946.1.A1_at	-1.1	-1.8	2.4	#N/A	#N/A
	Ssc.23169.1.S1_at	1.0	-1.2	2.4	NM_002856	poliovirus receptor-related 2
	Ssc.16676.1.A1_at	-1.0	1.5	2.4	NM_173469	hypothetical protein LOC92912
	Ssc.1986.1.S1_at	1.0	1.1	2.4	NM_080591	prostaglandin-endoperoxide synthase 1
	Ssc.15357.1.S1_at	1.2	1.3	2.4	NM_005813	protein kinase D3
	Ssc.21700.1.A1_at	1.1	1.3	2.4	#N/A	#N/A

Cluster 19 cont.	Ssc.19511.1.A1_a_at	-1.0	1.4	2.4	#N/A	#N/A
	Ssc.27556.1.S1_at	1.1	1.3	2.4	NM_017709	family with sequence similarity 46; member C
	Ssc.24233.1.S1_at	1.1	1.1	2.4	NM_015170	sulfatase 1
	Ssc.3714.1.S1_a_at	1.0	1.2	2.4	NM_032621	brain expressed X-linked 2
	Ssc.19591.1.S1_at	1.3	1.3	2.4	NM_000166	gap junction protein; beta 1; 32kDa
	Ssc.12654.1.A1_at	-1.1	1.4	2.4	#N/A	#N/A
	Ssc.7274.1.A1_at	1.1	1.2	2.4	NM_002759	eukaryotic translation initiation factor 2-alpha kinase 2
	Ssc.1308.1.S1_at	-1.3	-1.4	2.4	NM_002081	glypican 1
	Ssc.17312.1.A1_at	1.0	-1.2	2.4	XM_373497	hypothetical LOC387763
	Ssc.16540.1.S1_at	1.2	1.1	2.4	NM_002827	protein tyrosine phosphatase; non-receptor type 1
	Ssc.18306.1.A1_at	-1.0	1.1	2.4	#N/A	#N/A
	Ssc.10777.1.A1_at	-1.3	1.1	2.4	#N/A	#N/A
	Ssc.3588.1.S1_at	1.1	1.3	2.4	NM_002080	glutamic-oxaloacetic transaminase 2; mitochondrial
	Ssc.4578.1.A1_at	1.3	1.3	2.4	NM_003567	breast cancer anti-estrogen resistance 3
	Ssc.23905.1.A1_at	1.2	-1.1	2.4	#N/A	#N/A
	Ssc.22444.2.A1_at	-1.1	1.1	2.5	#N/A	#N/A
	Ssc.12129.1.A1_at	1.0	1.3	2.5	NM_016824	adducin 3
	Ssc.22555.1.A1_at	1.0	1.4	2.5	#N/A	#N/A
	Ssc.11839.1.S1_at	1.2	1.2	2.5	NM_021224	zinc finger protein 462
	Ssc.18610.1.A1_at	-1.2	1.5	2.5	#N/A	#N/A
	Ssc.4228.1.S1_at	-1.1	1.2	2.5	NM_015537	nasal embryonic LHRH factor
	Ssc.29813.1.A1_at	1.1	1.3	2.5	NM_003822	nuclear receptor subfamily 5; group A; member 2
	Ssc.29710.1.A1_at	-1.2	1.1	2.5	#N/A	#N/A
	Ssc.3128.2.S1_at	1.4	1.3	2.5	#N/A	#N/A
	Ssc.5226.1.S1_at	-1.0	1.1	2.6	NM_015252	EH domain binding protein 1
	Ssc.18619.2.A1_at	-1.1	1.2	2.6	NM_021183	RAP2C; member of RAS oncogene family
	Ssc.6988.1.A1_at	1.2	-1.2	2.6	NM_138766	peptidylglycine alpha-amidating monooxygenase
	Ssc.2147.2.A1_at	-1.0	1.2	2.6	#N/A	#N/A
	Ssc.24330.1.S1_at	1.3	1.1	2.6	NM_004820	cytochrome P450; family 7; subfamily B; polypeptide 1
	Ssc.9588.1.A1_at	-1.2	-1.1	2.6	#N/A	#N/A
	Ssc.25410.1.S1_at	1.0	-1.2	2.6	#N/A	#N/A
	Ssc.6430.1.A1_at	1.2	1.1	2.6	#N/A	#N/A
	Ssc.20419.1.S1_at	1.2	1.2	2.6	#N/A	#N/A

Cluster 19 cont.	Ssc.19892.1.A1_at	1.3	1.2	2.6	NM_024408	Notch homolog 2
	Ssc.7434.1.S1_at	-1.2	1.3	2.6	NM_005851	CDK2-associated protein 2
	Ssc.1631.1.S1_at	-1.2	1.1	2.7	NM_002957	retinoid X receptor; alpha
	Ssc.2861.1.A1_at	1.1	1.3	2.7	NM_006010	arginine-rich; mutated in early stage tumors
	Ssc.2197.1.S1_at	-3.0	-5.2	2.7	NM_018004	transmembrane protein 45A
	Ssc.1789.1.S1_at	-1.5	1.2	2.7	#N/A	#N/A
	Ssc.19873.2.S1_at	1.2	1.3	2.7	NM_194071	cAMP responsive element binding protein 3-like 2
	Ssc.22530.1.S1_at	1.2	1.0	2.7	#N/A	#N/A
	Ssc.7610.1.S1_at	1.0	1.4	2.7	NM_014764	DAZ associated protein 2
	Ssc.21188.1.S1_at	1.1	1.0	2.7	NM_021195	claudin 6
	Ssc.265.1.S2_at	-1.1	1.1	2.7	NM_000230	leptin
	Ssc.16312.1.S1_at	-1.0	1.1	2.8	NM_006825	cytoskeleton-associated protein 4
	Ssc.19873.1.S1_a_at	1.1	1.0	2.8	NM_194071	cAMP responsive element binding protein 3-like 2
	Ssc.3479.1.A1_at	-1.2	1.3	2.8	#N/A	#N/A
	Ssc.27248.1.S1_at	-1.1	1.4	2.8	NM_022373	hypothetical protein FLJ22313
	Ssc.19075.1.A1_at	1.1	1.2	2.8	NM_022739	SMAD specific E3 ubiquitin protein ligase 2
	Ssc.18014.1.A1_at	-1.2	-1.4	2.8	NM_052954	cysteine and tyrosine-rich 1
	Ssc.27361.1.A1_at	-1.9	1.2	2.9	#N/A	#N/A
	Ssc.18190.1.A1_at	1.2	-1.2	2.9	NM_182920	a disintegrin-like and metalloprotease
	n = 133	**1.0**	**1.2**	**2.3**		
Cluster 20	Ssc.4255.1.S1_at	1.2	2.2	3.8	#N/A	#N/A
	Ssc.9434.1.A1_at	1.1	2.1	3.8	#N/A	#N/A
	Ssc.1205.1.S1_at	-1.0	2.4	3.8	#N/A	#N/A
	Ssc.5663.1.S1_at	1.5	1.9	3.9	NM_004385	chondroitin sulfate proteoglycan 2
	Ssc.7938.1.A1_at	1.3	1.8	4.0	#N/A	#N/A
	Ssc.19544.1.A1_at	1.2	1.9	4.0	#N/A	#N/A
	Ssc.24138.1.A1_at	1.1	1.8	4.0	#N/A	#N/A
	Ssc.1745.1.A1_at	1.0	2.3	4.0	#N/A	#N/A
	Ssc.5243.1.A1_at	1.2	2.4	4.0	NM_000264	patched homolog
	Ssc.9511.1.A1_at	1.2	1.6	4.0	NM_016073	hepatoma-derived growth factor; related protein 3
	Ssc.18375.1.A1_at	-1.4	1.6	4.1	NM_006378	sema domain; immunoglobulin domain
	Ssc.26651.1.S1_at	1.3	1.8	4.1	NM_016593	cytochrome P450; family 39; subfamily A; polypeptide 1
	Ssc.13476.1.A1_at	-1.1	2.1	4.1	XM_496907	paternally expressed 10

Cluster 20 cont.	Ssc.8084.1.S1_at	1.1	2.5	4.1	NM_006094	deleted in liver cancer 1
	Ssc.24669.1.A1_at	-1.1	1.8	4.1	NM_194317	hypothetical protein MGC52057
	Ssc.16987.1.A1_at	1.2	2.1	4.2	#N/A	#N/A
	Ssc.16453.1.S1_at	-1.1	1.7	4.2	NM_030576	hypothetical protein MGC10986
	Ssc.27110.1.A1_at	2.2	2.2	4.2	#N/A	#N/A
	Ssc.28646.1.A1_at	1.1	2.6	4.2	#N/A	#N/A
	Ssc.12017.1.A1_at	-1.4	2.0	4.2	NM_001010990	homocysteine-inducible; endoplasmic reticulum stress-in
	Ssc.9273.1.A1_at	1.1	2.3	4.3	#N/A	#N/A
	Ssc.29596.1.A1_at	1.3	2.8	4.3	#N/A	#N/A
	Ssc.3129.1.A1_at	-1.1	2.0	4.3	NM_004242	high mobility group nucleosomal binding domain 3
	Ssc.21595.1.S1_at	1.3	2.1	4.3	#N/A	#N/A
	Ssc.2131.2.A1_at	1.4	1.7	4.3	#N/A	#N/A
	Ssc.1125.1.A1_at	1.9	1.5	4.4	NM_000362	tissue inhibitor of metalloproteinase 3
	Ssc.9483.1.A1_s_at	-1.1	1.4	4.4	NM_032523	oxysterol binding protein-like 6
	Ssc.17518.1.S1_at	-1.0	1.2	4.4	NM_000674	adenosine A1 receptor
	Ssc.17140.1.A1_at	1.2	3.0	4.4	NM_003778	UDP-Gal:betaGlcNAc beta 1;4- galactosyltransferase; polype
	Ssc.23921.1.S1_at	1.4	3.0	4.5	#N/A	#N/A
	Ssc.25198.1.A1_at	1.1	2.3	4.5	NM_000274	ornithine aminotransferase
	Ssc.20890.1.S1_at	1.2	1.7	4.5	NM_205860	nuclear receptor subfamily 5; group A; member 2
	Ssc.29275.1.A1_at	1.3	2.1	4.5	#N/A	#N/A
	Ssc.30400.1.A1_at	1.0	2.6	4.6	#N/A	#N/A
	Ssc.9522.1.A1_at	1.1	2.0	4.6	#N/A	#N/A
	Ssc.13553.2.S1_at	1.1	3.1	4.7	NM_004297	guanine nucleotide binding protein
	Ssc.19005.1.A1_at	1.1	2.6	4.7	NM_015009	PDZ domain containing RING finger 3
	Ssc.19579.1.A1_at	-1.0	1.8	4.7	NM_021005	nuclear receptor subfamily 2; group F; member 2
	Ssc.13531.1.A1_at	1.3	1.8	4.7	#N/A	#N/A
	Ssc.22504.1.S1_at	-1.1	1.5	4.8	NM_003619	protease; serine; 12
	Ssc.27249.1.S1_at	-1.3	2.3	4.8	NM_005221	distal-less homeo box 5
	Ssc.7408.1.A1_at	1.5	2.5	4.9	#N/A	#N/A
	Ssc.25002.1.S1_at	-1.7	1.7	4.9	NM_031283	transcription factor 7-like 1
	Ssc.4791.1.S1_at	-1.3	1.9	4.9	#N/A	#N/A
	Ssc.20841.1.S1_at	1.1	1.1	5.0	NM_198291	v-src sarcoma
	Ssc.16346.1.S1_at	-1.4	1.7	5.0	NM_022972	fibroblast growth factor receptor 2

Cluster 20	Ssc.8609.1.A1_at	1.5	1.5	5.0	NM_014456	programmed cell death 4
	n = 47	**1.1**	**2.0**	**4.4**		
Cluster 21	Ssc.7314.1.A1_at	3.4	14.8	2.6	NM_000963	prostaglandin-endoperoxide synthase 2
	Ssc.23994.1.A1_at	2.9	15.6	5.0	#N/A	#N/A
	Ssc.12561.1.A1_at	1.9	10.3	6.3	NM_005504	branched chain aminotransferase 1; cytosolic
	n = 3	**2.7**	**13.6**	**4.6**		
Cluster 22	Ssc.17615.1.S1_at	1.3	8.9	8.7	NM_001677	ATPase; Na+K+ transporting; beta 1 polypeptide
	Ssc.7721.1.A1_at	1.6	8.4	8.8	NM_005032	plastin 3
	Ssc.30064.1.A1_at	-1.1	7.2	9.4	#N/A	#N/A
	Ssc.27388.1.S1_at	1.1	7.7	9.7	NM_020128	Mdm4; transformed 3T3 cell double minute 1; p53 binding pro
	Ssc.6969.1.A1_at	1.0	7.9	11.8	NM_017440	Mdm4; transformed 3T3 cell double minute 1; p53 binding pr
	Ssc.455.1.S1_at	2.0	10.9	12.6	NM_001623	allograft inflammatory factor 1
	Ssc.27508.1.A1_at	-1.3	7.5	12.8	NM_015265	SATB family member 2
	Ssc.4004.1.A1_at	-1.0	11.3	12.9	NM_015180	spectrin repeat containing; nuclear envelope 2
	Ssc.24509.1.A1_at	1.5	7.8	13.6	NM_014211	gamma-aminobutyric acid
	n = 9	**1.3**	**8.6**	**11.1**		
Cluster 23	Ssc.20438.1.S1_at	1.1	-1.4	14.1	NM_000959	prostaglandin F receptor
	Ssc.22354.1.A1_at	1.3	1.6	14.5	NM_018664	Jun dimerization protein p21SNFT
	Ssc.20258.1.S1_at	1.1	3.9	14.8	#N/A	#N/A
	Ssc.23077.1.A1_at	1.8	4.4	15.0	#N/A	#N/A
	Ssc.20578.1.S1_at	-1.0	1.3	15.0	#N/A	#N/A
	Ssc.16886.1.A1_at	1.4	5.4	15.7	NM_003115	UDP-N-acteylglucosamine pyrophosphorylase 1
	Ssc.8698.1.S1_at	1.3	3.5	15.8	NM_033664	cadherin 11; type 2; OB-cadherin
	Ssc.2444.2.A1_a_at	1.8	2.1	15.8	NM_000227	laminin; alpha 3
	Ssc.15906.1.S1_at	-1.3	1.8	15.9	#N/A	#N/A
	Ssc.27738.1.S1_at	-1.4	5.9	16.0	NM_015265	SATB family member 2
	Ssc.27592.1.S1_at	1.1	2.0	18.2	NM_003956	cholesterol 25-hydroxylase
	Ssc.6057.1.A1_at	1.3	2.6	19.4	NM_015550	oxysterol binding protein-like 3
	Ssc.18844.1.S1_at	1.0	1.3	19.5	NM_032510	par-6 partitioning defective 6 homolog gamma
	Ssc.7175.1.S1_at	1.4	3.6	19.6	NM_014375	fetuin B
	n = 14	**1.2**	**2.9**	**16.4**		
Cluster 24	Ssc.21987.2.S1_at	1.3	2.0	-1.3	NM_001550	interferon-related developmental regulator 1
	Ssc.19150.1.S1_at	1.0	2.2	-1.2	NM_197966	BH3 interacting domain death agonist

Cluster 24 cont.	Ssc.26386.2.S1_a_at	1.1	2.4	-1.1	NM_016101	comparative gene identification transcript 37
	Ssc.26446.1.S1_at	-1.1	2.1	-1.0	NM_015143	methionyl aminopeptidase 1
	Ssc.20740.1.S1_at	1.3	2.3	1.1	#N/A	#N/A
	Ssc.29842.1.A1_at	-1.1	2.9	1.1	#N/A	#N/A
	Ssc.26271.2.S1_at	1.1	2.0	1.2	NM_006824	EBNA1 binding protein 2
	Ssc.24556.2.S1_a_at	1.0	2.5	1.2	NM_025181	solute carrier family 35; member F5
	Ssc.27533.1.A1_at	-1.1	2.2	1.2	NM_022473	zinc finger protein 106 homolog
	Ssc.26568.1.A1_s_at	-1.4	2.2	1.2	NM_033671	cyclin B3
	Ssc.27311.1.S1_at	-1.1	2.2	1.2	#N/A	#N/A
	Ssc.27454.1.S1_at	-1.2	2.2	1.2	NM_004044	5-aminoimidazole-4-carboxamide ribonucleotide formyltransf
	Ssc.8582.1.S1_at	1.1	2.1	1.2	NM_031307	pseudouridylate synthase 3
	Ssc.27543.1.S1_at	1.5	2.4	1.2	NM_145693	lipin 1
	Ssc.19326.1.A1_at	-1.2	2.3	1.2	NM_016343	centromere protein F; 350400ka
	Ssc.21179.1.S1_at	1.8	2.4	1.3	#N/A	#N/A
	Ssc.13743.1.S1_at	1.2	2.0	1.3	NM_016472	chromosome 14 open reading frame 129
	Ssc.21965.1.S1_at	1.1	2.1	1.3	NM_138285	nucleoporin 35kDa
	Ssc.7111.1.A1_at	-1.3	2.2	1.3	NM_001034	ribonucleotide reductase M2 polypeptide
	Ssc.19249.2.S1_a_at	-1.0	2.0	1.4	NM_017832	hypothetical protein FLJ20457
	Ssc.6238.3.S1_at	1.2	2.1	1.4	NM_016282	adenylate kinase 3
	Ssc.5082.1.A1_at	1.1	2.2	1.4	#N/A	#N/A
	Ssc.8475.1.A1_at	1.0	2.0	1.4	#N/A	#N/A
	Ssc.25289.1.S1_at	1.9	2.4	1.4	NM_001259	cyclin-dependent kinase 6
	Ssc.18038.1.A1_at	1.0	2.2	1.5	NM_005204	mitogen-activated protein kinase kinase kinase 8
	Ssc.19318.1.S1_at	-1.0	2.0	1.5	#N/A	#N/A
	Ssc.26407.1.S1_at	-1.4	2.0	1.5	NM_020886	ubiquitin specific protease 28
	Ssc.15219.1.S1_at	-1.1	2.4	1.5	NM_012248	selenophosphate synthetase 2
	Ssc.24344.1.S1_at	-1.0	2.4	1.5	NM_001379	DNA
	SscAffx.8.1.S1_s_at	-1.0	2.0	1.5	NM_002467	v-myc myelocytomatosis viral oncogene homolog
	Ssc.7839.1.A1_at	1.2	2.5	1.5	NM_012307	erythrocyte membrane protein band 4.1-like 3
	Ssc.25963.1.A1_at	1.2	2.3	1.5	#N/A	#N/A
	Ssc.8774.2.A1_at	1.2	2.5	1.6	NM_006745	sterol-C4-methyl oxidase-like
	Ssc.24344.1.S1_a_at	-1.1	2.2	1.6	NM_001379	DNA
	Ssc.12845.1.S1_at	1.7	2.3	1.6	NM_001259	cyclin-dependent kinase 6

Cluster 24 cont.	Ssc.25195.1.A1_at	1.2	2.5	1.6	#N/A	#N/A
	Ssc.27520.1.A1_at	1.1	2.7	1.6	XM_086186	hypothetical protein FLJ13815
	Ssc.7554.2.S1_at	-1.0	2.2	1.6	NM_013242	gene trap locus 3
	Ssc.7517.1.A1_at	-1.0	2.4	1.6	NM_024680	likely ortholog of mouse E2F transcription factor 8
	Ssc.5087.1.A1_at	1.0	2.1	1.6	#N/A	#N/A
	Ssc.24556.1.S1_at	-1.1	2.5	1.6	NM_025181	solute carrier family 35; member F5
	Ssc.16693.1.S1_at	-1.1	2.4	1.7	NM_012106	ADP-ribosylation factor-like 2 binding protein
	Ssc.10623.2.S1_at	1.0	2.2	1.7	#N/A	#N/A
	Ssc.16621.1.S1_at	1.5	2.4	1.7	NM_004170	solute carrier family 1
	Ssc.24679.1.S1_at	1.3	2.3	1.7	NM_020774	mindbomb homolog 1
	Ssc.7771.1.A1_at	-1.1	2.3	1.7	XM_034274	v-myb myeloblastosis viral oncogene homolog
	Ssc.12786.1.A1_at	1.0	2.6	1.7	NM_003864	sin3-associated polypeptide; 30kDa
	Ssc.19290.2.A1_at	1.2	2.1	1.7	#N/A	#N/A
	Ssc.14506.1.S1_at	-1.3	2.1	1.7	NM_001067	topoisomerase
	Ssc.30686.1.S1_at	-1.0	2.2	1.7	#N/A	#N/A
	Ssc.23207.1.S1_at	1.1	2.4	1.7	NM_007212	ring finger protein 2
	Ssc.7554.1.S1_at	1.1	2.6	1.7	NM_013242	gene trap locus 3
	Ssc.240.1.S1_at	1.2	2.7	1.7	NM_001147	angiopoietin 2
	Ssc.24852.1.A1_at	1.4	2.1	1.7	NM_018482	development and differentiation enhancing factor 1
	Ssc.4900.1.A1_at	1.2	2.4	1.8	NM_016441	cysteine-rich motor neuron 1
	Ssc.23922.1.A1_at	-1.0	3.0	1.8	NM_018169	hypothetical protein FLJ10652
	Ssc.19011.1.S1_at	1.1	2.1	1.8	NM_003983	solute carrier family 7
	Ssc.2099.1.S1_at	-1.3	2.3	1.8	NM_138555	kinesin family member 23
	Ssc.2056.1.S1_at	1.3	2.3	1.9	NM_022343	chromosome 9 open reading frame 19
	Ssc.15905.1.S1_at	1.2	2.0	1.9	NM_005811	growth differentiation factor 11
	Ssc.24421.1.S1_at	-1.1	2.6	1.9	NM_018169	hypothetical protein FLJ10652
	Ssc.18850.1.S1_at	1.3	2.0	1.9	NM_016548	golgi phosphoprotein 2
	Ssc.28763.1.A1_at	-1.1	2.5	1.9	NM_080743	serine-arginine repressor protein
	Ssc.25441.2.S1_at	-1.1	2.3	1.9	NM_018169	hypothetical protein FLJ10652
	Ssc.25948.1.S1_at	1.0	2.7	1.9	#N/A	#N/A
	Ssc.7570.2.S1_at	1.4	2.1	1.9	NM_004170	solute carrier family 1
	Ssc.11797.1.A1_at	1.1	2.3	1.9	NM_145804	ankyrin repeat and BTB
	Ssc.27842.1.S1_at	-1.0	2.1	1.9	NM_017746	testis expressed sequence 10

Cluster 24 cont.	Ssc.7066.1.S1_at	1.2	2.3	2.0	NM_020774	mindbomb homolog 1
	Ssc.1116.1.S1_at	1.1	2.5	2.0	NM_001304	carboxypeptidase D
	Ssc.6670.2.S1_at	-1.1	2.5	2.0	NM_012319	solute carrier family 39
	Ssc.21060.1.A1_at	1.1	2.5	2.1	NM_014498	golgi phosphoprotein 4
	Ssc.19350.1.S1_at	1.3	2.2	2.1	NM_016545	immediate early response 5
	Ssc.23488.1.S1_at	-1.1	2.4	2.1	NM_000637	glutathione reductase
	Ssc.6418.1.S1_at	1.4	2.7	2.1	#N/A	#N/A
	Ssc.1850.1.A1_at	1.3	2.7	2.2	NM_022343	chromosome 9 open reading frame 19
	n = 76	**1.1**	**2.3**	**1.6**		
Cluster 25	Ssc.7106.1.S1_at	2.7	25.4	11.7	NM_001801	cysteine dioxygenase; type I
	Ssc.9781.1.S1_at	1.5	17.8	14.4	NM_000602	serine
	Ssc.9288.1.A1_at	1.7	20.8	17.6	NM_020799	associated molecule with the SH3 domain of STAM
	Ssc.9991.1.S1_at	1.2	16.9	20.3	NM_198966	parathyroid hormone-like hormone
	Ssc.27300.2.A1_a_at	1.4	19.0	21.5	NM_001001557	growth differentiation factor 6
	Ssc.4425.1.S1_at	1.3	19.3	24.3	#N/A	#N/A
	Ssc.29867.1.A1_at	1.6	19.1	25.5	NM_001001557	growth differentiation factor 6
	n = 7	**1.6**	**19.8**	**19.3**		

[a]This column indicates the 25 clusters generated by the k-means algorithm.
[b]Each gene within a cluster has a specific, non-redundant AffyID that was assigned to a sequence interrogated by a specific probe set.
[c]The fold difference in gene expression is presented for each gene with the relative amount reported in comparison to the expression level of spherical conceptuses. S = spherical; T = tubular; D12F = Day 12 filamentous; and D14F = Day 14 filamentous.
[d]This column represents the human accession number for each gene that had significant homology to human genes that have been annotated and reported in GenBank.
[e]The annotation, as determined by the homology of the porcine sequence similarity to that reported and annotated for the human genome.

Appendix II

Methodology for *In Situ* Hybridization

Tissue Fixation

1. Uterine tissue should be excised and immediately processed. In general, a section of the uterine horn (not greater than 1.0 cm) is placed in 40 ml of freshly 4% paraformaldehyde (w/v) in phosphate buffered saline (PBS). It is important to keep a very high fixative volume to tissue ratio.

2. The section of uterine horn in a fixative should be gently agitated on a rocker or orbital shaker for 24h @ RT.

3. After 24 h, the fixative shall be drained out, and replaced with 40 ml of 70% EtOH (v/v in H_20) and gently agitated overnight at RT.

4. After 24 h, the 70% EtOH should be replaced with fresh 70% EtOH, and tissue permanently stored at RT.

Solution preparations

4% Paraformaldehyde

1. Heat 2/3 final volume to 60 C in fume hood with stir bar.
2. Add granulated paraformaldhyde slowly, add 1 to 2 drops of 1N NaOH (this will help clear solution)
3. When solution is clear, remove from heat
4. Add 1X PBS to make final desired volume
5. After solution is cool, adjust pH to 7.2

10X PBS (1 Liter)
80g NaCl
2g KCl
14.4g Na_2HPO_4 or (11.5g $Na_2HPO_4 \cdot 7\ H_20$)
2.4g KH_2PO_4

Add components to 800 mL of ddH20, adjust pH to 7.6, bring to 1000 mL final volume.

Tissue Sectioning

1. Trim blocks so that they are about 1cm square on the block surface. This is easier to handle in long strips (Ribbons)
    a. Face Blocks to get tissue (Cut at 20 μM) embedded in paraplast
    b. After facing blocks turn the block face down on ice (freeze H_20 in a flat dish). Place 5-6 blocks on the ice at a time.
    c. Use 37°C water (with small amount of gelatin dissolved) to expand sections in the ribbons.
    d. Use positively charged slides to hold sections to slide.

Linearization of Plasmids for *in vitro* Transcription (IVT)

1. Digest 20 μg of DNA with appropriate restriction enzyme for >2h at appropriate temperature.

DNA	20 μg
10X REB	20 μl
Enzyme	10 μl
Water	to 200 μl

2. Extract once with an equal volume of PCI (Phenol:Chloroform:Isoamly alcohol) and once again with chloroform
3. Precipitate DNA with 3 vol 100% EtOH, 1/10 vol 3M NaOAc and 5 λ of Dextrane T500 (10mg/ml)
4. Place at -80 C for 15 min, then spin down for 10 min at MAX speed @ RT
5. Remove EtOH, and wash pellet with 150 μl of 70% EtOH
6. Remove all 70% EtOH and resuspend pellet in 40 λ of Rnase-free water. The DNA is at approximately 0.5 μg/μl

Note: About which enzyme to use with the promoter.

Preparation of Probe

1. Set up probe synthesis reaction (enough for about 10 slides) in a 1.5 mL tube. Use RNAse free tubes and pipet tips.

Order	Solution	10 Slides	20 Slides	40 Slides
1	Water (Ambion DEPC)	4.0 µL	8.0	16.00
2	5X Transfer Buffer (Vortex)	2.5 µL	5.0	10.0
3	100 mM DTT	1.25	2.50	5.0
4	2.5 mM rACG	1.25	2.50	5.0
5	DNA (10mg/ml)	1.0 µγ	2.00	4.0
6	Rnasin (Keep Cold)	0.5 µL	1.00	2.0
7	UTP (^{35}S)-40 mCi/mL	1.25	2.50	5.0
8	Either T7, SP6 or T3 Poly	0.75	1.50	3.0

   Remember you need to know directions of the insert from the plasmid (T7 or SP6) to get antisense or sense gene (Sense is Control!).

2. Vortex tube, Quick spin and then incubate for 2 h at 37 C in heat block

3. Prepare CENTRI-SEP column (Princeton Separations, Inc-CAT# CS-90)
   -Need two columns for 4X reaction. The column can only handle 100 uL of fluid. Need to rehydrate the column at least 1 h before the probe reaction is added to the column.
   a) Add 80 uL Ambion water to the column
   b) Invert and gently vortex
   c) Sit upright for at least 30 min –leave bottom cap on (don't start flow yet).

4. After 2 h incubation add 3uL RQ1-DNAse I (Promega) and 0.5 uL RNasin to tubes. If 4X reaction (40 slides) double the volume-6uL RQ-1-DNase, 1.0 uL RNasin. Vortex, centrifuge briefly and incubate for 15 min at 37^{o}C.

5. After incubation add 20 mL yeast tRNA (10mg/ml) and 40 uL (1-2 X reaction) -Phenol:Chlorofrom:Isoamyl alcohol (Ratio 25:24:1; light sensitive, store at –4^{o}C).
   -For 3-4X Rxn 40 mL yeast tRNA and 80 uL PCI. Vortex well. When pipetting from PCI, make sure to get lower layer where phenol is bottom layer, and water is on top.
   ****Water Saturated Phenol is for RNA, Tris buffered phenol is for DNA****

   a) Centrifuge at full speed on a microcentrifuge (27,000 x g) for 5 min
   b) Remove top layer with a pipet (filtered) and place in a new bullet tube (Don't get bottom layer)

6. Add a volume of chloroform to match PCI
   1X=40uL
   3X=80uL

a. Vortex and spin at full speed for 5 min
   -Complete SEP column preparation: Take top and bottom cap off. Place in tube and use finger to push (top pressure) a drop from the bottom to start flow. After spinning tubes with probe, SEP columns in centrifuged and position the column so the notch on the rim faces out (top of rotor). Centrifuge at 750 x g for 2 min. Use column immediately- do not let it dry out.
b. Add PCI:CI purified probe to Centrisep column (place in middle of matrix and don't touch matrix with pipet tip).
c. Centrifuge column for at 750 x g for 2 min. then discard the column. Purified probe is the flow through remaining in the tube.

7. Precipitate with 60 uL 3M NaOAc (pH 5), 1 uL yeast tRNA, 5uL Dextran T500 (10mg/ml) and 300uL EtOH for 1-2X reactions. Double for 3-4X reactions.

8. Spin bullet tubes at maximum speed for 10 min Pour off liquid in radioactive waste.

9. Wash pellets with 70% EtOH

10. Wash pellets in 50 uL (1X-2X) or 100 uL (3X-4X) of 100 mM DTT. Can use pipet to break-up pellet.

11. Count in β-counter (1-2 uL).

Calculation for probe Hybridization
Antisense -20 slides: 5 X 10^6 cpm/slide
20 slides X 70 uL hybridization soln/slide=1400 uL (may add for 1-2 more slides) + Volume of probe (Need 5 million cpm/slide)

Final solution should be 10% DTT (100 mM DTT) so, divide the amount of hybridization solution + amount of probe and divide the sum by 9 to determine amount of 1M DTT to add.

Need only 1-2 slides for sense Probe.
Vortex, quick spin and incubate at 70 C for 10 min to denature probe.

Summary
cRNA probes (5 X 106 cpm/slide) with hybridization Solution containing 100 mM DTT at 70 C for 10 min. then place in 55^{o}C incubator before until applied to slide.

Preparation of Slides

1. Xylene (CitrSolve CAT# 22-143975) CitriSolve will have a layer on the bottom, so be careful not to pour in the tanks. Make sure tank solvent is clean between runs. Treat for 5 min and agitate every 1-2 min "Critical" repeat 2X. Check to make sure the paraplast is cleared from slides.
2. 100%EtOH fro 1 min -2X (agitate slides through procedure)
3. 95% EtOH 1 min-2X
4. 70% EtOH 3 min- 1X
5. PBS for 5 min-2X
6. Fresh 4% paraformaldhyde (PAF) 20 min-1X
   - Dissolve 4g PAF/100ml of PBS-Need 400-500mL

   To Make: Fill beaker with ddH_20 to about 60% of final volume (Do Not Heat Water). Add PAF (20g/500mL) and about 1.25g NaOH pellets/500 mL. Stir on stir plate in hood until it goes into solution~10 min, then add enough 10X PBS to make final concentration 1X. pH to 7.2 with 12N NaOH "slowly" and bring to volume with ddH_20
7. PBS for 5 min-2X
8. Proteinase K for 7.5 min-1X

   For 500mL:
   25 mL 1M Tris (pH 8.0)
   5 mL 0.5 M EDTA
   1 mL Proteinase K (10mg/mL) stock kept in freezer
   Q.S. with ddH_2O
9. 4% PAF for 15 min 1X(Can reuse the PAF from first wash in step 6)-Dispose PAF in waste bottle
10. ddH2O for 1 min-1X
11. PBS for 5 min-2X
12. 70% EtOH for 3 min-1X
13. 95% EtOH for 1 min-2X
14. 100% EtOH for 1 min-2X
15. Air dry slides at RT (10 min) on paper towels in tray. While drying slides start denaturation of probe.

Probe Hybridizations

1. Following the denaturation of the probe (70 C), add the Hyb soln to the middle of the slide. Set pipetman at 75 μL, but when adding don't blowout last fluid to avoid air bubbles.
2. Put on coverslip
   a. Touch middle soln with coverslip and drawback to edge. Slowly drop cover slip on slide!
3. Place a layer of 3MM paper in a pyrex baking dish that has been wetted with 250 mL of 50% Formamide / 5X SSC

    a. Formamide is stored in freezer as stock! Must thaw out before use. Once thawed keep in the cooler.
4. Cover pyrex dish with plastic wrap and seal. Place in an incubator at 55 C for at least 16 h
5. Make 50% formaldehyde /2X SSC/50 mM BME-*Leave BME out until just before use the next day [make sure BME is not old]
    a. Make 1 liter =500 mL formaldehyde /100 mL 20X SSC=h20 to 1000mL (add 3.5 mL BME next day)
    b. Make 5X SSC/10 mM BME-*Leave BME out until just before use next day. 500 mL=125 mL 20X SSC+H20 to 500 mL (add 350 uL BME Next Day)
    c. Place soln in incubator at 55 C for next day use!!!
6. Add BME to solutions the next day
    a. 50% Formaldhyde/2X SSC/50 mM BME (3.56 mL/liter)
    b. 5X SSC/10 mM BME (350 uL/500 mL) keep in incubator at 55 C
    c. Place the 50% formaldehyde /2X SSC/50 mM BME in 65 C water bath or incubator. Use glass slide holders.
7. Gently remove coverslips by sliding down into radioactive waste container (use empty NaCl container). If coverslip sticks to slide, dip in buffer and slide off. Place slides in rack with 55 C 5X SSC/10 mM BME.
    a. <u>Place in 55 C incubator for 30 min-agitate every 10 min</u>
8. Dump out baking dish (In isotope sink). Wash with 10% Count-off (rinse bottle) then rinse with DDH20. Dry table and rinse large double taped pipets
9. Dump first hybridization wash into radioactive liquid waste [35S]. Add 50% Formaldhyde/2X SSC/50 mM BME and place in 65 C incubator or water bath for 20 min
10. Dump second wash of hybridization in radioactive liquid waste. Add TEN (0.5M NaCl/10mM Tris(pH 8)/5mM EDTA) for 10 min at RT
    a. 10X TEN (1 Liter)
    b. 292.2g NaCL
    c. 10 mL 1M TrisCL (pH 8)
    d. 10 mL 0.5 M EDTA
11. 1X TEN 10 min 37 C. Repeat twice.
12. 1X TEN with RNase A (10ug/mL) -500 mL (0.5 mL Rnase stock 10mg/ml) in the freezer). Incubate 37 C for 30 min.
13. 1X TEN 15 Min at 37 C
14. 50 % Formamide/2X SSC/50 mM BME at 65^{o}C for 20 min.
15. 2X SSC at RT for 15 min
16. 0.1X SSC RT for 12 min
17. 70% EtOH/0.3 M Ammonium Actetate at RT for 5 min. Repeat once.
18. 95% EtOH/0.3 M Ammonium Acetate for RT for 1min.
19. 100% EtOH at RT for 1 min. Repeat once.
20. Air dry and expose to Kodak Biomax Film overnight. Develop next day to estimate length needed to develop slides.
    a. Place slides in order in film case-tape down corners to keep from moving

b. Use Kodak BioMax MR film-packaged in single sheets. Make sure emulsion side down (Non-shiny side)-notched should be in upper left corner. Expose at least 16 hours.

Autoradiography

1. Thaw Kodak NTB2 emulsion vials at 42 C in a light tight container (wrapped in foil).

   -Emulsion is aliquoted in vials (5mL) stored in a box covered in a foil pack in a black plastic bag in the refrigerator. MUST BE LIGHT TIGHT!!!

   -Take strips of foil to wrap two vials in dark room. Don't use safe light, just wrap in total darkness. As an alternative, use orange safe light. Make sure the vials are completely wrapped in foil and the lids are on tight.

   -The slide dipper takes two vials to fill it. This is enough to cover 50-60 slides

   -Make up the slide boxes to holes slides following covering with emulsion. Place a slide about 3-4 notches from the top of the box. Take two kimwipes and cross them. Place some dridrite in the middle and roll up to place above the slide box. Put paper towel cut to the bottom of the box. Wrap up dridrite in paper towels to place in the bread box when slides have been dipped.

2. Need to bring 50 ml conical tube with 10 mL ddH20 placed in 42 C water bath with vials (Make sure light is on). Can get by with as soon as it reaches TEMP./FOR 20 SLIDES. In the dark room with the orange filter, gently mix the emulsion with ddh20 in the conical tube. No air bubbles (rotate tube side to side). Emulsion is 1:1 with water.
3. Fill slide dipper that has been placed in the 42 C H_2O bath.
4. Dip each slide to the bottom of the slide dipper. Wipe off excess, polish back to remove film from edge.
5. After dipping , place towels in light tight box. Leave lids off during this time. Allow to dry for 6 to 8 hours. Rotate slides 3-6 hours.
6. After 3-6 hours drying go to dark room and place lids on slide boxes. Wrap in foil, store at 4C for number of days or weeks based on exposure to X-ray film.
7. To develop allow slides to reach RT
8. Kodak D-19 developer (78.3g / 500 mL) for 4 min-1x
9. ddH2O- 0.5 min-1X
10. Fixer for 5 min-1X

Fixer (Kodak Rapid Fixer with Hardener):

171 mL water
59.5 mL Solution A (Fixer)
6.5 mL Solution B (Hardener)

11. Water for 5 min
12. Hematoxylin (diluted with ddH2O 1:3) for 30 seconds
13. Water for 30 sec
14. Water for 5 min. Repeat until hematoxylin quits leaching into water.
15. 70 EtOH-3 min
16. 95 EtOH-1 min 2X
17. 100 EtOH-1 min 2X
18. Xylene for 3 min 3X
19. Permount and coverslip

Other *In Situ* Hybridization Solutions:

5X SSC/10 mM BME (500mL)
125 mL 20X SSC
350 µl BME
q.s. ddH_2O

50% Formamide/2X SSC/50 mM BME (800 mL)
400 mL Formamide
80 mL 20X SSC
2.72 mL BME
q.s. ddH_2O

20X SSC (1 liter)
175.4 g NaCl
88.2 g Sodium citrate
Dissolve in 800 mL ddH_2O, adjust pH to 7.0 with a few drops of 10N NaOH. Bring to volume with ddH_2O and filter sterilize. DEPC treat and autoclave.

10X TEN (1 Liter)
292.2g NaCL (5M)
10 mL 1M TrisCL (pH 8) – (100 mM)
10 mL 0.5 M EDTA – (50 mM)

50X Denhardt's (500 mL)
5 g Ficoll 400
5 g Polyvinylpyrrolidone
5 g BSA (Pentax Fraction V)
500 mL Water

Hybridization Solution (100 mL)

50 mL Formamide – (50%)
6 mL 5M NaCL – (0.3 M)
2 mL 1M Tris-HCl pH 8.0 - (20mM)
1 mL 0.5 M EDTA pH 8.0 – (5mM)
1 mL 1M Sodium Phosphate pH 8.0 – (10 mM)
2 mL 50X Denhardt's (1X)
10 g Dextran Sulfate (10%)
5 mL of 10 mg/mL Stock Yeast tRNA (0.5 mg/mL)
q.s. H_2O to 20 mL

Store Frozen in -20C

Before use add 1M DTT to a final concentration of 100 mM DTT for probes during hybridization.

VITA

Jason Wayne Ross

Candidate for the Degree of

Doctor of Philosophy

Thesis: CONCEPTUS AND UTERINE FACTORS CONTRIBUTING TO THE ESTABLISHMENT OF PREGNANCY IN PIGS

Major Field: Animal Reproduction

Minor Field: Biochemistry

Biographical:

Personal Information: Born in Grinnell, IA on October 10, 1977, the son of Wayne and Marla Ross

Education: Graduated from Iowa City West High School, Iowa City, Iowa in May of 1996. Earned Bachelor of Science degree from Iowa State University, Ames, Iowa in December 2000. Earned a Master of Science Degree at Oklahoma State University, Stillwater, Oklahoma in May 2003. Completed the requirements for Doctor of Philosophy degree at Oklahoma State University, Stillwater, Oklahoma, in December, 2006.

Experience: Graduate Research Assistant, Oklahoma State University, 2001-2006.

Professional Organizations: Society for the Study of Reproduction, Sigma Xi Scientific Research Society, Animal Science Graduate Student Association.